

In vitro cell culture systems
for the investigation of the morphogen Sonic hedgehog (Shh)

Chiu Wai Kwok

Dissertation
submitted to the
Combined Faculties for the Natural Sciences and for Mathematics
of the Ruperto-Carola University of Heidelberg, Germany
for the degree of
Doctor of Natural Sciences

presented by

Chiu Wai Kwok
born in: Hong Kong
Oral-examination: 16.11.2011

In vitro cell culture systems
for the investigation of the morphogen Sonic hedgehog (Shh)

Referees: Prof. Dr. Uwe Strähle
Prof. Dr. Herbert Steinbeisser

Acknowledgements

I would like to express my gratitude to Prof. Dr. Uwe Strähle for accepting me as one of his graduate students, offering me this challenging but exciting project, and opening up my eyes in different science disciplines. My thanks also go to Dr. Alexander Welle and Dr. Sylwia Sekula for their getting onto the roller-costar with me and keeping me on the track with endless supports and encouragements. Their hard work and contributions to my thesis deserve the biggest claps. Dr. Kay Grobe is graciously appreciated for his constructive comments, discussions and sincere help in the project; and Dr. Tim Schwarnweber for his kindness of abstract translation. I am as well delighted to Cathrin Klumpp, Helga Olinger, Marga Litfin and Simone Weigel for their quality technical assistances.

Finally my appreciations are given to God, my family and friends, and many other unmentioned ones for their love, patience, understanding and acceptance of who I am.

Table of contents

Acknowledgements	i
Table of contents	iii
List of abbreviations	xi
List of figures	xv
List of graphs	xix
List of tables	xxi
Abstract	xxiii
Zusammenfassung	xxv
1. Introduction	1
1.1. Morphogens	1
1.2. The Hedgehog / Sonic hedgehog protein	4
1.2.1. The Hedgehog / Sonic hedgehog signalling pathway	5
1.2.2. Post-translation modifications of the Hedgehog / Sonic hedgehog protein	8
1.2.3. Secretion, transport and concentration gradient formation of the Hedgehog / Sonic hedgehog protein	11
1.3. Current <i>in vitro</i> cell culture system for the investigation of Sonic hedgehog function / role	14
1.4. Surface functionalization and patterning for protein immobilization	17
1.4.1. Physisorption of proteins on extracellular matrices	18
1.4.2. Microcontact printing of proteins onto surfaces	19
1.4.3. UV assisted functionalization of polystyrene surfaces with nickel ions	20
1.4.4. Dip-pen nanolithography of phospholipids for protein immobilization	22
1.4.5. Self assembled monolayer formation of benzylguanine terminated thiols on gold and immobilization of protein via benzylguanine/alkyltransferase covalent binding	24
1.5. Surface analysis techniques	26
1.5.1. Immunofluorescence for the detection of protein adsorption	26

Table of contents

1.5.2.	Enzyme-linked immunosorbent assay for the detection and quantification of adsorbed proteins	27
1.5.3.	Fluorescence recovery after photobleaching for the evaluation of protein motility	29
1.5.4.	Quartz crystal microbalance with dissipation monitoring for the detection and quantification of adsorbed protein on a surface	31
1.5.5.	Time-of-flight secondary ion mass spectroscopy	33
1.6.	Objectives of the thesis	35
2.	Materials and Methods	37
2.1.	Materials	37
2.1.1.	Chemicals	37
2.1.2.	Kits	39
2.1.3.	Buffers and reagents	39
2.1.4.	Enzymes	42
2.1.5.	Bacteria	43
2.1.6.	Bacteria media	43
2.1.7.	Cell lines	44
2.1.8.	Cell culture media and reagents	44
2.1.9.	Zebrafish (<i>Danio rerio</i>)	45
2.1.10.	DNA plasmids	45
2.1.11.	Oligonucleotides	45
2.1.12.	Recombinant proteins and antibodies	46
2.1.13.	RNA probes for <i>in situ</i> hybridization	47
2.1.14.	Phospholipids	47
2.1.15.	Disulfides	47
2.1.16.	Other materials or equipments	48
2.2.	Methods	49
2.2.1.	Peptide sequences of ShhN variants	49
2.2.2.	Polymerase chain reaction	52
2.2.3.	Agarose gel electrophoresis	53
2.2.4.	Purification of DNA from agarose gel	53
2.2.5.	Restriction endonuclease digestion of DNA	54
2.2.6.	DNA ligation	54
2.2.7.	Subcloning of ShhN into pENTR TM 11 and pDEST TM 14 vectors	54
2.2.8.	DNA sequencing	55
2.2.9.	Transformation of <i>Escherichia coli</i>	55

2.2.10.	Protein production in prokaryotic (bacterial) expression system	55
2.2.11.	Extraction and purification of bacterial expressed ShhN	56
2.2.12.	Biotinylation of ShhN-GFP-His, the ShhN variant with a C-terminal biotin acceptor	57
2.2.13.	Immunoprecipitation	57
2.2.14.	SDS-polyacrylamide gel electrophoresis (SDS-PAGE)	58
2.2.15.	Integrity analysis and quantification of bacterial expressed ShhN	59
2.2.16.	Western blot analysis	60
2.2.17.	Subcloning of signal sequence containing ShhN into pcDNA3.1 vector	61
2.2.18.	mRNA preparation	61
2.2.19.	Maintenance and raising of zebrafish (<i>Danio rerio</i>)	61
2.2.20.	Microinjection of mRNA into zebrafish embryos	62
2.2.21.	<i>In situ</i> hybridization	62
2.2.22.	Optical microscopy and image acquisition of zebrafish embryos	64
2.2.23.	Cell culture	65
2.2.23.1.	HEK293 cells for eukaryotic expression of ShhN	65
2.2.23.2.	C3H10T1/2 clone 8 cells for biological activity analysis of ShhN by alkaline phosphatase assays	65
2.2.23.3.	Shh LIGHT II for biological activity analysis of ShhN by Gli-luciferase assay	66
2.2.24.	Propagation, freezing and thawing of cells	67
2.2.25.	Tranfection of HEK293 cells	67
2.2.26.	Treatment of C3H10T1/2 clone 8 and Shh LIGHT II cells	68
2.2.27.	Alkaline phosphatase expression assay and cell counting	69
2.2.28.	Alkaline phosphatase colorimetric assay	70
2.2.29.	Gli-luciferase reporter assay	71
2.2.30.	Immunofluorescence of cells	71
2.2.31.	Microscopy and imaging of cells	72

Table of contents

2.2.32.	UV photopatterning and nickel functionalization of polystyrene surfaces	73
2.2.33.	Immobilization of ShhN on surfaces functionalized via dip-pen nanolithography	75
2.2.33.1.	Immobilization of ShhN-GFP-His via nickel(II)/poly(6)histidine affinity interaction on nickel chelating lipid functionalized surfaces	75
2.2.33.2.	Immunofluorescence of ShhN-GFP-His bound onto nickel functionalized polyethylene glycol surfaces	76
2.2.33.3.	Immobilization of ShhN-GFP-His-Biotin via biotin/streptavidin affinity interaction on biotinylated lipid functionalized glass surfaces	76
2.2.33.4.	Covalent immobilization of ShhN-GFP-His-SNAP by benzylguanine/SNAP TM reaction	77
2.2.33.5.	Immunofluorescence of ShhN-GFP-His-SNAP benzylguanine functionalized polystyrene surfaces	78
2.2.34.	Functionalization of gold surfaces with benzylguanine thiol and immobilization of ShhN-GFP-His-SNAP	79
2.2.35.	Immunofluorescence of ShhN-GFP-His-SNAP on benzylguanine thiol functionalized surfaces	80
2.2.36.	Time-of-flight secondary ion mass spectroscopy (ToF-SIMS) for surface analysis of benzylguanine thiol modified gold substrate	81
2.2.37.	Adsorption of ShhN-His and ShhN-GFP-His on collagen and fibronectin functionalized glass surfaces	81
2.2.38.	Immunofluorescence of ShhN-His and ShhN-GFP-His on collagen and fibronectin functionalized surfaces	82
2.2.39.	Blocking of collagen functionalized surfaces by microcontact printing of bovine serum albumin	83

2.2.40.	Quartz micro gravimetry for quantification of ShhN-GFP-His and ShhN-GFP-His-SNAP on collagen and benzylguanine thiol functionalized surfaces	84
2.2.41.	Enzyme-linked immunosorbent assay (ELISA) for quantity measurement of ShhN-GFP-His adsorbed on collagen coated surfaces	85
2.2.42.	Fluorescence recovery after photobleaching (FRAP) for determination of the protein adsorption efficiency of collagen and fibronectin	86
3.	Results	87
3.1.	Introduction	87
3.2.	Part 1 – Production of biologically active ShhN proteins	88
3.2.1.	Production and purification of <i>E. coli</i> expressed mouse ShhN proteins	88
3.2.2.	Molecular analysis of the <i>E. coli</i> expressed ShhN proteins	91
3.2.3.	Analysis of the biological activity of the <i>E. coli</i> expressed ShhN proteins	94
3.2.3.1.	Detection of Shh signalling induced alkaline phosphatase expression in C3H10T1/2 clone 8 cells and cell counting assay	94
3.2.3.2.	Quantification of Shh signalling induced alkaline phosphatase expression in C3H10T1/2 clone 8 cells by cell lysate based colorimetric assay	99
3.2.3.3.	Enhancement of the biological activity of <i>E. coli</i> expressed ShhN proteins	102
3.2.3.4.	Stability analysis of the <i>E. coli</i> expressed ShhN proteins	103
3.2.3.5.	Analysis of the biological activity of the <i>E. coli</i> expressed ShhN proteins with selective truncation	108
3.2.4.	Potential usage of the <i>E. coli</i> expressed ShhN proteins in functionalized surface development for protein immobilization	117

Table of contents

3.2.5.	Production of ShhN-GFP-His and ShhN-GFP-His-SNAP in a eukaryotic expression system using HEK293 cells	118
3.2.6.	Analysis of the biological activity of ShhN-GFP-His and ShhN-GFP-His-SNAP expressed in the HEK293 cells	122
3.2.6.1.	Functional specificity of the ShhN-GFP-His and ShhN-GFP-His-SNAP expressed in HEK293 cells	123
3.2.6.2.	Dosage dependent analysis of the biological activity of ShhN variants expressed in HEK293 cells by the alkaline phosphatase expression detection and cell counting assay	128
3.2.6.3.	Dosage dependent analysis of the biological activity of ShhN variants expressed in HEK293 cells by alkaline phosphatase colorimetric assay	131
3.2.6.4.	Dosage dependent analysis of the biological activity of ShhN variants expressed in HEK293 cells by Gli-luciferase reporter assay	132
3.2.6.5.	Analysis of the biological activity of ShhN-GFP-His and ShhN-GFP-His-SNAP in zebrafish embryos	134
3.3.	Part 2 – Development of biological compatible interfaces for ShhN immobilization	137
3.3.1.	Immobilization of ShhN-GFP-His on modified polystyrene surfaces via nickel(II)/poly(6)histidine affinity interaction	138
3.3.2.	Immobilization of ShhN by dip-pen nanolithography	141
3.3.2.1.	ShhN immobilization via poly(6)histidine tag on nickel presenting phospholipids	142

3.3.2.2.	ShhN immobilization via biotin/streptavidin affinity interaction on the biotinylated phospholipids	146
3.3.2.3.	ShhN immobilization via benzylguanine/SNAP TM covalent reaction on the benzylguanine functionalized phospholipids	148
3.3.3.	Immobilization of ShhN-GFP-His-SNAP on gold surfaces via benzylguanine thiol/SNAP TM covalent binding	150
3.3.3.1.	Microcontact printing of benzylguanine terminated thiol on gold surfaces	150
3.3.3.2.	UV patterning and ToF-SIMS analysis of BGT SAM, and immobilization of ShhN-GFP-His-SNAP on gold surfaces	152
3.3.3.3.	QCM-D analysis of BGT/ShhN-GFP-His-SNAP binding on gold surfaces	158
3.3.3.4.	Immobilization and immunodetection of the HEK293 cell expressed ShhN-GFP-His-SNAP on gold surfaces	160
3.3.4.	Adsorption of ShhN-His and ShhN-GFP-His on surfaces coated with the extracellular matrix components collagen and fibronectin	162
3.3.4.1.	Detection and quantification of adsorbed ShhN-His and ShhN-GFP-His on collagen and fibronectin coated glass surfaces	162
3.3.4.2.	Analysis of the motility of ShhN-GFP-His on collagen coated glass surfaces by fluorescence recovery after photobleaching	171
3.3.4.3.	Adsorption and biological activity analysis of the HEK293 cell expressed ShhN-GFP-His on collagen coated glass surfaces	175
4.	Discussion	185
4.1.	Expression and detection systems of ShhN variants	185

Table of contents

4.2. Immobilization of ShhN on different substrates for various <i>in vitro</i> studies of protein activities	186
4.2.1. Collagen matrix allows motility and availability of ShhN	188
4.2.2. Supplement of heparin or BSA in the collagen matrix further resembles the <i>in vivo</i> extracellular environment	188
4.2.3. UV irradiated polystyrene surfaces presenting nickel adsorb histidine tagged proteins but provide no sufficient selectivity	190
4.2.4. ShhN immobilization by dip-pen nanolithography retains the motility of the immobilized protein	191
4.2.5. The benzylguanine/SNAP TM system allows for highly selective ShhN immobilization	193
4.3. Immobilization of ShhN with the flexibility for controlled protein motility	194
4.4. Alternative analytical strategies for determination of the biological activity of immobilized ShhN	195
4.4.1. Investigation of cell migration by time lapse imaging	196
4.4.2. Localized study of signal transduction induced by immobilized ShhN with fluorescence labelled Gli reporter cell line	197
4.4.3. Establishment of specific reporter cell lines for investigation of the role of Shh in neural cell fate determination	197
4.5. Conclusions	199
References	203

List of abbreviations

$\Delta m/m$	Change-of-mass to mass ratio
(v/v)	Volume to volume
a.u.	Arbitrary unit
ADAM	A disintegrin and metalloproteinase
AFM	Atomic force microscope
ALP	Alkaline phosphatase
APS	Ammonium persulfate
ATP	Adenosine triphosphate
BA	Biotin acceptor
BCIP	5-bromo-4-chloro-3-indolyl phosphate
BG	Benzylguanine
BGT	Benzylguanine thiol
BME	Basal medium Eagle
BSA	Bovine serum albumin
CM	Conditioned medium
ColX	Collagen X
DMEM	Dulbecco's modified Eagle medium
DMSO	Dimethyl sulfoxide
DOPC	1,2-dioleoyl- <i>sn</i> -glycero-3-phosphocholine
DOPE	Dioleoylphosphatidylethylene
DPN	Dip-pen nanolithography
DTT	Dithiothreitol
ECM	Extracellular matrix
EDC	1-ethyl-3-[3-(dimethylamino)-propyl] carbodiimide
EDTA	Ethylenediaminetetraacetic acid
EG6OH	(11-mercaptoundecyl) hexa(ethylene glycol) alcohol
EG3OMe	(1-mercaptoundec-11-yl) tri(ethylene glycol) monomethylether
ELISA	Enzyme-linked immunosorbent assay
FBS	Fetal bovine serum
FL	Full length
FN	Fibronectin
FRAP	Fluorescence recovery after photobleaching
GFP	Green fluorescence protein
hAGT	O ⁶ -alkylguanine-DNA alkyltransferase
HEK	Human embryonic kidney

List of abbreviations

HEPES	4-(2-hydroxyethyl)-1-piperazineethanesulfonic acid
Hh	hedgehog
HHIP	Hedgehog interacting protein
HI	Heat-inactivated
His	Histidine
HSPG	Heparin sulfate proteoglycan
HYB	Hybridization buffer
IPTG	Isopropyl β -D-1-thiogalactopyranoside
ISH	<i>In situ</i> hybridization
LB	Lysogeny broth
μ Cp	Microcontact printing
min	Minute
mol%	Molar percentage/ratio
MT	Passivating or matrix thiol
NBT	Nitro blue tetrazolium chloride
NHS	N-hydroxysulfo succinimide
Ni-NTA	Nickel(II)-nitrilotriacetic acid
OD405	Optical density at wavelength of 405nm
PBS	Phosphate buffered saline
PBS++	PBS containing Ca^{2+} and Mg^{2+}
PCR	Polymerase chain reaction
PDMS	Polydimethylsiloxane
PEG	Polyethylene glycol
PFA	Paraformaldehyde
PLL-g-PEG	Poly-L-lysine-grafted-polyethylene glycol
pNpp	Para-nitrophenylphosphate
ppm	Parts per million
PA	Peptide amphiphile
PS	Polystyrene
Ptc	Patched
PVDF	Polyvinylidene fluoride
QCM-D	Quartz crystal microbalance with dissipation monitoring
RCmShhN	Recombinant N-terminal signaling domain of mouse Sonic hedgehog
rpm	Revolutions per minute
RT	Room temperature
SAG	Sonic hedgehog agonist
SAM	Self assembled monolayer

SDS	Sodium dodecyl sulfate
SDS-PAGE	Sodium dodecyl sulfate-polyacrylamide gel electrophoresis
sec	Second
Shh	Sonic hedgehog
ShhN	N-terminal signaling domain of Sonic hedgehog
ShhNp	Processed N-terminal signaling domain of Sonic hedgehog
Smo	Smoothed
SOC	Super optimal broth with catabolite repression
STV	Streptavidin
TEMED	N,N,N',N'-tetramethylethylenediamine
TMB	3,3',5,5'-tetramethylbenzidine
ToF-SIMS	Time-of-flight secondary ion mass spectroscopy
U	Unit
UV	Ultraviolet light
WB	Western blot
WT	Wildtype
χ_{BGT}	Molar ratio of BGT to EG6OH
XPS	X-ray photoelectron spectroscopy

List of figures

- Figure 1.1. The French flag model of morphogen concentration gradient, positional cell fate determination, and pattern formation.
- Figure 1.2. Shh and other Hh homologs and their roles in mouse development from an embryo to an adult.
- Figure 1.3. Model of vertebrate Shh signal transduction pathway.
- Figure 1.4. Maturation of Sonic hedgehog (Shh) signaling domain.
- Figure 1.5. Model illustrating the formation of Hh concentration gradients with the contribution of HSPG in the extracellular matrix (ECM), and the resulting signal strength of unprocessed (Hh-N) and processed signaling domains of Hh (Hh-Np).
- Figure 1.6. Biomolecules inside the cells may react differently when the morphogen is applied in a constant concentration or is distributed in a gradient. introduction of Shh to embryonic stem cells with different gradients via hydrogel triggered differentiation and graded expression of neural transcription factors
- Figure 1.7. Principle of microcontact printing (μ Cp) of protein molecules onto a glass surface.
- Figure 1.8. Substrate-bound gradient fabricated by microcontact printing of ephrin.
- Figure 1.9. Applications of UV irradiated polystyrene surfaces.
- Figure 1.10. Schematic diagram illustrating dip-pen nanolithography of phospholipids.
- Figure 1.11. Schematic representation of protein-coupling strategies to spatially patterned lipid supports, and the chemical structures of the used phospholipids.
- Figure 1.12. Covalent immobilization of a hAGT (SNAPTM) fusion protein on a BG modified surface.
- Figure 1.13. Schematic depiction of direct and indirect immunofluorescence.
- Figure 1.14. Schematic diagram demonstrating the typical procedure of ELISA.
- Figure 1.15. Schematic depiction of FRAP experiment on cell surface.
- Figure 1.16. An idealized plot of a FRAP recovery curve.
- Figure 1.17. Illustration of a QCM setup.
- Figure 1.18. Schematic diagram describing the production of secondary ions by a focused, pulsed primary ion beam in the ToF-SIMS system.
- Figure 2.1. Expression of alkaline phosphatase by C3H10T1/2 clone 8 cells.

List of figures

- Figure 2.2. Procedure of immobilizing ShhN-GFP-His on UV irradiated and nickel functionalized polystyrene surfaces.
- Figure 2.3. Scheme of immobilizing biotinylated and poly(6)histidine-tagged Shh protein on biotin-streptavidin and nickel functionalized surfaces by DPN.
- Figure 2.4. Molecular structures of the used disulfides.
- Figure 2.5. Diagram illustrating microcontact printing of BSA on collagen coated surface.
- Figure 3.1. Quantification of *E. coli* expressed ShhN proteins.
- Figure 3.2. The Shh N-terminal signaling domain is present in the *E. coli* expressed proteins.
- Figure 3.3. The Shh N-terminal signaling domain is present in the *E. coli* expressed proteins.
- Figure 3.4. The N-terminal Cardin-Weintraub sequence of the *E. coli* expressed ShhN variants was available.
- Figure 3.5. The *E. coli* expressed ShhN variants contained the histidine tag.
- Figure 3.6. The SNAPTM tag is present in the *E. coli* expressed ShhN-GFP-His-SNAP protein.
- Figure 3.7. The *E. coli* expressed ShhN-His-C25M_{del26-34}, ShhN-GFP-His-C25M_{del26-34} and ShhN-GFP-His-SNAP-C25M_{del26-34} possessed the Shh signaling domain, the N-terminal Cardin-Weintraub sequence and the C-terminal histidine tag.
- Figure 3.8. *E. coli* expressed ShhN variants stimulated expression of the chondrocyte differentiation marker ColX.
- Figure 3.9. Expression of ShhN-GFP-His and ShhN-GFP-His-SNAP in HEK293 cells. The HEK293 cells were transiently transfected with the constructs of ShhN-GFP-His and ShhN-GFP-His-SNAP.
- Figure 3.10. Biological activity of the HEK293 expressed ShhN variants revealed from staining for ALP expression in C3H10T1/2 clone 8 cells.
- Figure 3.11. Alignment of the N-terminal signaling domains of the mouse ShhN and zebrafish shh (shhN).
- Figure 3.12. Expansion of *nkx2.2* and *pax2a* expression patterns by overexpression of ShhN variants in zebrafish embryos.
- Figure 3.13. ShhN-GFP-His immobilization on polystyrene surfaces after masked UV irradiation and nickel modification.
- Figure 3.14. Immobilization of *E. coli* expressed ShhN-GFP-His on nickel presenting phospholipids patterns printed by DPN.

- Figure 3.15. Immobilization of HEK293 expressed ShhN-GFP-His on the nickel chelating phospholipid patterns produced by DPN.
- Figure 3.16. Immobilization of *E. coli* expressed ShhN-GFP-His-Biotin on biotinylated phospholipid patterns with streptavidin as the linker between the lipids and the protein.
- Figure 3.17. Immobilization of ShhN-GFP-His-SNAP on the biotin functionalized lipids via covalent binding between the BG and the SNAPTM tag.
- Figure 3.18. Immobilization of ShhN-GFP-His-SNAP on gold surface.
- Figure 3.19. Molecular structures of the applied disulfides that form a self-assembled monolayer on gold surfaces for the immobilization ShhN-GFP-His-SNAP.
- Figure 3.20. ToF-SIMS images of photo patterned EG6OH SAM.
- Figure 3.21. ToF-SIMS images of photo patterned EG6OH sample with 60min UV exposure after backfill with BGT/EG6OH 1:5.
- Figure 3.22. Immunofluorescence of the HEK293 cell expressed ShhN-GFP-His-SNAP on 1:10 BGT/EG6OH functionalized gold surfaces.
- Figure 3.23. Immunofluorescence detection of ShhN-His and ShhN-GFP-His adsorption on collagen coated surfaces.
- Figure 3.24. Immunofluorescence detection for adsorption of ShhN-His and ShhN-GFP-His on fibronectin coated surfaces.
- Figure 3.25. ShhN-GFP-His adsorption on collagen coated surfaces.
- Figure 3.26. Induction of Shh signaling specific ALP expression in C3H10T1/2 clone 8 cells by the HEK293 expressed ShhN-GFP-His.
- Figure 3.27. Induction of ALP expression in C3H10T1/2 clone 8 cells by the HEK293 cell expressed ShhN-GFP-His immobilized on collagen functionalized surface.

List of graphs

- Graph 3.1. Biological activity of *E. coli* expressed ShhN variants recorded by BCIP/NBT staining for the expressed ALP in C3H10T1/2 clone 8 cells and cell counting.
- Graph 3.2. Biological activities of *E. coli* expressed ShhN variants measured by ALP colorimetric assay.
- Graph 3.3. Inhibition of the biological activity of the HEK293 expressed ShhN variants by 5E1 blocking of the Ptc binding pseudo-active site analyzed by ALP colorimetric assay.
- Graph 3.4. Specificity of the HEK293 expressed ShhN variants on Gli activity induction shown by 5E1 inhibition of the biological activity of the HEK293 expressed ShhN variants.
- Graph 3.5. Dose dependent biological activity of the HEK293 expressing ShhN variants analyzed by BCIP/NBT detection of ALP expression in C3H10T1/2 clone 8 cells.
- Graph 3.6. Dose dependent induction of ALP expression in C3H10T1/2 clone 8 cells by the HEK293 expressed ShhN variants measured by ALP colorimetric assay.
- Graph 3.7. Dose dependent induction of Gli-luciferase activity in Shh LIGHT II cells by the HEK293 ShhN variants.
- Graph 3.8. QCM-D measurement of the deposition of BSA and FBS on UV irradiated polystyrene surfaces.
- Graph 3.9. Negative secondary ion spectrum from a pristine EG6OH self assembled monolayer.
- Graph 3.10. Negative secondary ion spectrum from a pristine BGT self assembled monolayer.
- Graph 3.11. QCM-D measurement of adsorption of BSA and ShhN-GFP-Hi-SNAP on BGT modified gold surfaces with different χ_{BGT} .
- Graph 3.12. ELISA response curve showing the surface densities (ng/cm^2) of ShhN-GFP-His deposited on collagen coated surfaces.
- Graph 3.13. Comparison of ShhN-GFP-His motility on surfaces coated with different concentrations of collagen.
- Graph 3.14. Comparison of the motility of ShhN-GFP-His immobilized on collagen functionalized surfaces.

List of graphs

- Graph 3.15. ALP expression induction in C3H10T1/2 clone 8 cells by RCmShhN immobilized on collagen coated surfaces.
- Graph 3.16. Induction of ALP expression in C3H10T1/2 clone 8 cells by the HEK293 cell expressed ShhN-GFP-His.
- Graph 3.17. Induction of ALP expression in C3H10T1/2 clone 8 cells by the HEK293 cell expressed ShhN-GFP-His immobilized on collagen surfaces.
- Graph 4.1. Immobilization of His-SNAP-GFP on gold surface via the Ni-NTA thiol.

List of tables

- Table 2.1. Peptide sequence of ShhNp, RCmShhN and different versions of ShhN designed for bacterial expression and immobilization on nickel(II)-nitrilotriacetic acid (Ni-NTA), biotin-streptavidin (biotin-STV) and benzylguanine (BG) functionalized surfaces.
- Table 2.2. Peptide sequence information of the eukaryotic expressed ShhN.
- Table 3.1. Schematic drawings showing the amino acid sequences of the ShhN variants expressed in *E. coli*. ShhN-His, ShhN-GFP-His and ShhN-GFP-His-SNAP were designed based on the peptide sequence of RCmShhN
- Table 3.2. Comparison of the peptide sequences and the biological activities of the *E. coli* expressed ShhN-His, ShhN-GFP-His and ShhN-GFP-His-SNAP variants analyzed by the ALP assays.
- Table 3.3. Scheme of peptide sequences of the mutated variants of the *E. coli* expressed ShhN proteins: ShhN-His-C25M_del26-34, ShhN-GFP-His-C25M_del26-34 and ShhN-GFP-His-SNAP-C25M_del26-34.
- Table 3.4. Summary of the biological activity of the *E. coli* expressed ShhN variants in ALP assays and chondrocyte differentiation assay.
- Table 3.5. Schematic drawing of the amino acid sequences of the ShhN variants expressed in the eukaryotic HEK293 cells.
- Table 4.1. Summary of different approaches used for ShhN immobilization.

Abstract

Sonic hedgehog (Shh) plays an important role in embryogenesis. It acts as a morphogen that diffuses to form a concentration gradient and works in a temporally and spatially controlled manner. Shh not only regulates organogenesis, such as formation of digits on limbs and organization of the brain, but also controls cell division of stem cells. Perturbations in Shh signaling have been implicated in developmental disorders and development of some cancers. However, owing to the dynamic *in vivo* environment and the high degree of complexity of the molecular processes and transports, there are challenges of investigating the cell-Shh interactions.

Controlled immobilization of proteins like cell adhesion proteins, immunoglobulins, hormones, morphogens, including Shh, is an essential step for a large set of applications in biology, medicine and biotechnology ranging from developmental biology to tissue engineering and biosensing. Reliable attachment of biomolecules on solid man-made substrates opens routes for many new key experiments, allowing studies of the biomolecules in simplified and thus controllable conditions.

By taking advantage of the immobilization models for studying complicated biological events, the objective of the current project was to organize Shh *in vitro* in a way mimicking the *in vivo* microenvironment, in which the morphogen is distributed with a concentration gradient extracellularly. The immobilization processes have to show selective binding chemistry, provide control of the positioning and orientation of Shh on the substrate, and need to allow access of Shh to its receptor.

In the presented project, biologically active Shh protein variants were synthesised *in vitro*. Plasmids of Shh with different tags or linker groups for immobilization were made. Production of sufficient amount of Shh for immobilization and surface analysis was performed in the *E. coli* expression system; while the determination of biological activity of Shh was carried out with the proteins obtained from the HEK293 cell culture system. The C3H10T1/2 clone 8 and the Shh LIGHT II cells demonstrated that the *in vitro* expressed Shh proteins are biologically active. The Shh induced cellular responses are dosage dependent.

Adsorption or immobilization of Shh on substrates by a variety of physical and chemical interactions was then developed and tested. These interactions include collagen matrix networking; nickel(II)/poly(6)histidine affinity; biotin/streptavidin affinity; and benzylguanine (BG)/SNAPTM covalent binding. Each of them exhibits different binding strength. Surface analysis illustrated that all of the applied systems are capable of immobilizing Shh by physisorption or chemical binding. Collagen permits motility of the adsorbed Shh. The biological activity of the protein is maintained to induce Shh signal specific cellular responses. The nickel(II)/poly(6)histidine and biotin/streptavidine systems facilitate Shh binding with high selectivity. The BG/SNAPTM approach promotes specific and irreversible immobilization of Shh. Further experiments are under progression for the establishment of a tailor-made platform for the *in vitro* investigation of the interaction of irreversibly bound Shh with the responsive cells.

Zusammenfassung

Das Signalprotein "Sonic hedgehog" (Shh) spielt eine bedeutende Rolle in der Embryogenese. Es fungiert als Morphogen: Das von einer lokalen Quelle aus diffundierende Molekül bildet einen Konzentrationsgradienten aus, dessen räumliche und zeitliche Ausprägung die Zellentwicklung steuert. Shh steuert nicht nur die Organentwicklung wie beispielsweise die Ausbildung von Gliedmaßen und die Organisation des Gehirns, sondern auch die Zellteilung von Stammzellen. Störungen des Sonic hedgehog Signalwegs führen zu Fehlbildungen in der Embryonalentwicklung und werden mit dem Auftreten bestimmter Krebsarten in Zusammenhang gebracht. Aufgrund der großen Dynamik im lebenden Organismus und der hohen Komplexität der Prozesse auf molekularer Ebene, ist die Untersuchung der Wechselwirkung zwischen Zellen und Shh oft schwierig.

Die kontrollierte Immobilisierung von Proteinen wie Zelladhäsionsproteine, Immunoglobuline, Hormone, Morphogene wie Shh ist ein essentieller Schritt in zahlreichen und ganz verschiedenen biologischen, medizinischen oder biotechnologischen Anwendungen wie beispielsweise Entwicklungsbiologie, Tissue Engineering und Biosensorik. Eine gezielte Anbindung von Biomolekülen an feste, künstliche Substrate ermöglicht viele neue Schlüsselexperimente, die es erlauben Biomoleküle unter einfachen – und daher kontrollierbaren – Bedingungen zu untersuchen. Gemäß diesem Ansatz war es das Ziel dieser Arbeit einen Konzentrationsgradienten wie ihn das Morphogen Shh in seiner Mikroumgebung *in vivo* ausbildet *in vitro* nachzubilden. Dafür muss der chemische Immobilisierungsprozess selektiv sein und es erlauben Position und Orientierung von

Zusammenfassung

Shh auf dem Substrat zu steuern, so dass eine Bindung zwischen Shh und seinem Rezeptor möglich ist.

In diesem Projekt wurde biologisch aktives Shh *in vitro* hergestellt. Dazu wurden Plasmide erzeugt, deren Sequenz Shh mit verschiedenen Tags und Linkern zur Immobilisierung enthält. Größere Mengen an Shh für Immobilisierungsversuche und Experimente zur Quantifizierung immobilisierten Proteins wurden in *E. coli* exprimiert. Versuche zur Bestimmung der biologischen Aktivität des Proteins wurden mit Shh durchgeführt, das mit Hilfe des HEK293 Kultursystems erhalten worden war. Zwei verschiedene Zellkultursysteme wurden herangezogen, um die biologische Aktivität des exprimierten Proteins zu verifizieren: C3H10T1/2 Klon 8 und Shh LIGHT II. Die durch Shh induzierten Zellantworten waren dosisabhängig.

Anschließend wurden verschiedene Verfahren zur Adsorption oder Immobilisierung von Shh auf künstlichen Substraten mittels physikalischer bzw. chemischer Methoden entwickelt und getestet. Zu den untersuchten Immobilisierungsstrategien gehörte Adsorption an vernetzte Kollagenmatrix, Affinitätsbindung über Ni^{2+} /Poly(6)histidin bzw. Biotin/Streptavidin und kovalente Bindung von Benzylguanin (BG) an SNAPTM-tragende Moleküle. Die Bindungsstärke variiert je nach Methode. Mittels Oberflächenanalyse konnte gezeigt werden, dass alle verwendeten Systeme in der Lage waren Shh zu adsorbieren bzw. zu binden. Die Kollagenmatrix erlaubt eine gewisse Mobilität des adsorbierten Shh. Die biologische Aktivität des Proteins blieb erhalten: Das Shh-Signal war in der Lage spezifische Zellantworten zu induzieren. Sowohl das Ni^{2+} /Poly(6)histidin als auch das Biotin/Streptavidin System ermöglichen eine hochselektive Bindung. Die Kopplung mit BG/SNAP führt zu spezifischer und irreversibler Immobilisierung von Shh. Weitere Experimente zielen

auf die Entwicklung einer maßgeschneiderten Plattform ab, welche die Grundlage für die *in vitro* Untersuchung der Wechselwirkungen von immobilisierten Shh mit Shh-sensitiven Zellsystemen sein wird.

1. Introduction

Embryonic development is the result of a series of signaling events. Morphogens, which are represented by a number of signaling molecules, contribute to the developmental events and are key players of proper tissue patterning. Because of their significance in embryonic development, there is a large interest in studying morphogens in detail. While some studies focus on *in vivo* approaches based e.g. on transgenic animals etc., other aspects of morphogens functions are more conveniently studied *in vitro* using cell culture set-ups allowing for precise morphogen gradients and reducing the interferences with other factors present in the *in vivo* situation.

1.1. Morphogens

Morphogens are substances that govern pattern formation and growth in development (Ashe and Briscoe, 2006; Gallet and Therond, 2004; Mehlen et al., 2005; Torroja et al., 2004). Particularly, morphogens work in a dose dependent manner to determine locally the differentiation of cells (Ashe and Briscoe, 2006; Gallet and Therond, 2004; Mehlen et al., 2005; Torroja et al., 2004). Depending on the rate of production, the rates of the transport and self-enhanced ligand degradation, morphogens are able to form different slopes of concentration gradients (Torroja et al., 2004). Regarding the terms of transport there have been experimental studies illustrating that morphogens achieve gradient formation by diffusion through extracellular matrix (ECM), while others have proposed that morphogens spread in vesicles through repeated cycles of endocytosis and exocytosis. These processes ultimately shape the concentration and thus extent of morphogen activity (Torroja et al., 2004). Furthermore, recent studies

have shown that receptors of morphogens are capable of regulating endocytic trafficking (Han et al., 2004; Torroja et al., 2004). This lead to the hypothesis that also the receptors play an important role in morphogen gradient formation (Torroja et al., 2004).

The French flag model (Figure 1.1), a renowned and conceptual definition of morphogen spreading / gradient formation, was introduced by Lewis Wolpert in the 1960s (Dessaud et al., 2008). In this model, the effects of different morphogen concentrations on cellular responses were illustrated by the different colors of the French flag. Morphogens are rigorously regarded as secreted signaling molecules that emanate from a localized source and spread through the positional fields (Mehlen et al., 2005). Positional values would then be specified by the local concentration of the morphogen, which would decrease with distance from the source. When the morphogen reaches its target cells, it acts directly on the cells to produce specific cellular activities in regard to morphogen concentration (Dessaud et al., 2008). In other words, morphogens affect cell states based on concentrations and these states are represented by the different colors of the French flag (Dessaud et al., 2008). Tissues are then subdivided into domains of different gene expression that correspond to these colors. For instance, high concentrations activate "blue" genes, lower concentrations activate "white" genes, with "red" serving as the default state in cells below the necessary concentration threshold.

In this view, morphogens are defined to carry two distinctive features. On one hand, they act on cells at a distance from their sources, namely the signaling ranges. On the other hand, they induce differential gene expression in a concentration-dependent manner.

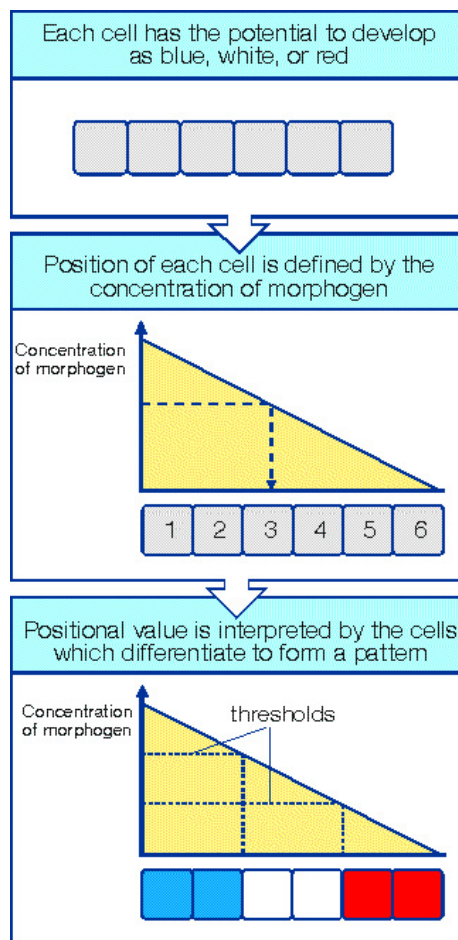


Figure 1.1. The French flag model of morphogen concentration gradient, positional cell fate determination, and pattern formation. The morphogen is secreted from a localized source of expression. After secretion, the morphogen is transported over several cell distances by means of diffusion and/or through interactions with carrier molecules, thereby establishing a concentration gradient. Cells located along the distance from the source of expression are exposed to different morphogen concentrations and respond by differentiating into corresponding cell types. (Adapted from Kerszberg and Wolpert, 2007).

The earliest and best-studied morphogens are some transcription factors that diffuse in early *Drosophila melanogaster* (fruit fly, denoted as *Drosophila* in the rest of the text) embryos. Other examples are the secreted intercellular signaling factors decapentaplegic (Dpp) / Transforming Growth Factor beta (TGF β); hedgehog (Hh) / Sonic hedgehog; wingless / Wnt; Epidermal Growth Factor (EGF); and Fibroblast

Growth Factor (FGF) (Mehlen et al., 2005) that mediate communication between cells. Apart from these proteins, also small organic molecules like retinoic acid can be regarded as morphogens. In summary, morphogens are defined conceptually and not by their molecular structure (White et al., 2007).

1.2. The Hedgehog / Sonic hedgehog protein

The Hedgehog (Hh) signaling pathway plays a crucial role in determining cell fate and patterning during development. It starts with the Hedgehog gene, which was first discovered in *Drosophila*, and is required for multiple development processes such as embryonic segmentation, imaginal disc formation, eye and appendage development, and cell fate specification in wings (Heemskerk and DiNardo, 1994; Hidalgo, 1991; Ingham, 1993, 1995; Lee et al., 1992; Mohler, 1998; Robbins et al., 1997; Tabata et al., 1992).

In vertebrates, three homologs of the *Drosophila* Hh gene have been identified to be expressed in a tissue specific manner and are responsible for the morphogenesis of various organs such as neural tube, limbs, somites and pharyngeal arches and cartilage and male germinal cell differentiations (Monnier et al., 2002). These three homologs are Sonic hedgehog (Shh), Desert hedgehog (Dhh) and Indian hedgehog (Ihh) (Ågren et al., 2004). Among them, Shh shows the best similarity to *Drosophila* Hh (Chang et al., 1994; Chiang et al., 1996; Echelard et al., 1993; Johnson and Tabin, 1995; Krauss et al., 1993; Riddle et al., 1993; Robbins et al., 1997; Roelink et al., 1994). Shh is also the most broadly expressed member of the hedgehog family and is probably responsible for the major effects in the development of brain, spinal cord, axial skeleton and limbs (Figure 1.2; Chiang et al., 1996).

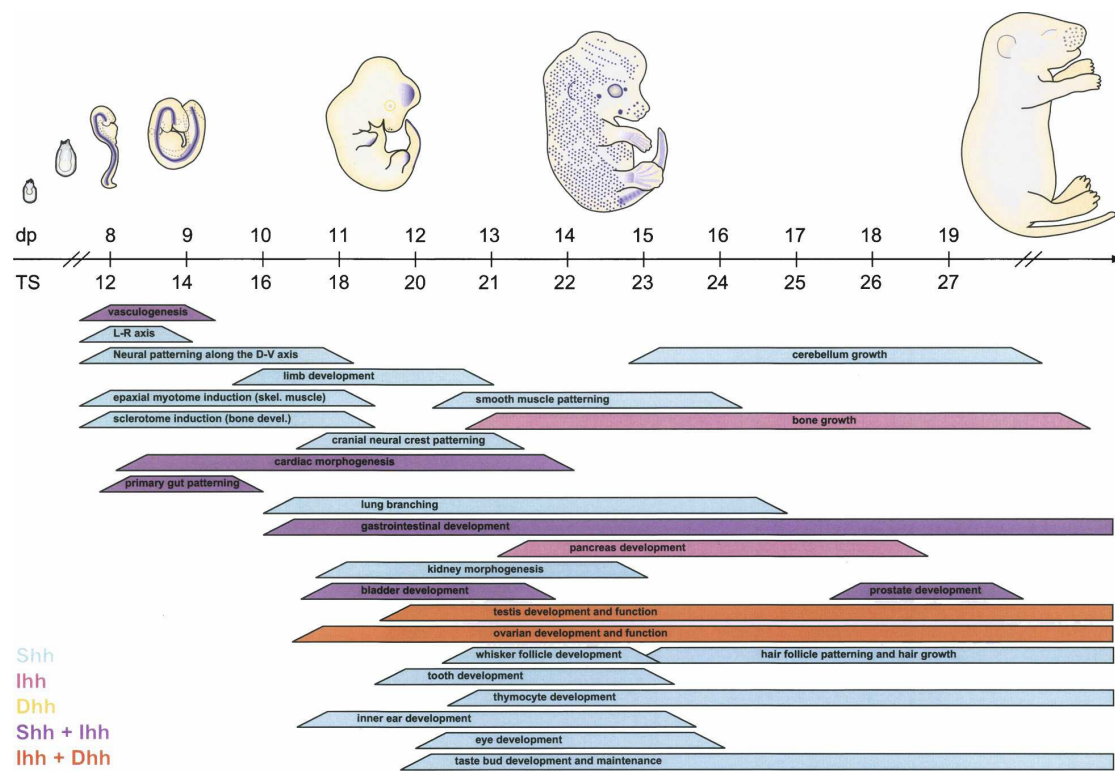


Figure 1.2. Shh and other Hh homologs and their roles in mouse development from an embryo to an adult. (Top) The embryo cartoons show aspects of expression of the Hh target gene *patched* (blue) during mouse embryonic development. (Bottom) Bars show approximate embryonic stages when Shh, Ihh, and/or Dhh (color code in bottom left) control developmental processes in the indicated tissues or cell types. The approximate embryonic stage is indicated by dpc and Theiler stage (TS) (Theiler 1989). (Adapted from Varjosalo and Taipale, 2008)

1.2.1. The Hedgehog / Sonic hedgehog signaling pathway

At the plasma membrane of Hh / Shh responsive cell, there is a receptor complex composed of Patched (Ptc) and Smoothed (Smo) proteins. Ptc is a 12-span transmembrane protein and binds directly to the ligand. It serves as the primary receptor for Hh / Shh (Martín et al., 2001). At the same time, Ptc is also a negative regulator of Hh / Shh signaling by suppressing the signal transmitter Smo at the cell membrane and the subsequent signal transduction (Ågren et al., 2004; Karpen et al.,

2001; Martín et al., 2001). Smo is a 7-span transmembrane protein with strong resemblance to a G-protein coupled receptor (Ågren et al., 2004; Martin et al., 2001). It orchestrates the Hh / Shh pathway signaling and controls transcription factor activation by transducing the Hh / Shh signal via a multiprotein complex (Ayers and Thérond et al., 2010). The multiprotein complex, which contains the serine-threonine kinase Fused (Fu), Suppressor of Fused [Su(Fu)], and the zinc finger containing transcription factor Cubitus interruptus (Ci) in *Drosophila* or the vertebrate homolog Gli, is associated with the microtubule (Ågren et al., 2004).

In the absence of Hh / Shh, Smo is suppressed by Ptc (Ågren et al., 2004; Karpen et al., 2001; Martín et al., 2001). No Hh / Shh signal is transmitted from Smo to the multiprotein complex. The transcription factor Ci / Gli is cleaved to the repressor form. The Su(Fu) regulated cytoplasmic-nuclear shuttling of Ci / Gli does not take place (Ågren et al., 2004). There is no transcription of any downstream target genes of the Hh / Shh signaling.

Upon binding of the Hh / Shh ligand to Ptc, the suppression of Smo by Ptc is relieved (Robbins et al., 1997; Sisson et al., 1997). This relief of inhibition of Smo leads to the accumulation of Smo to the primary cilia (Corbit et al., 2005) and the dissociation of the multiprotein complex from microtubules (Ågren et al., 2004). Transport of the full length activated form of Ci / Gli into the nucleus activates transcription of the Hh / Shh signaling downstream target genes such as Wingless (Wg), the TGF β family member Decapentaplegic (Dpp), and Ptc (Ågren et al., 2004; Lefers et al., 2001; Taipale et al., 2000; Wang and Holmgren, 2000). In the mouse mesenchymal cells, Shh signalling induces the expression of alkaline phosphatase (ALP) as an early indicator of chondrogenic differentiation. In this project, the mouse pluripotent mesenchymal cell

line, C3H10T1/2 clone 8, was used for the determination of Shh biological activity. In addition, gene transcription driven by the Gli promoter is also an indicator of the activation of Shh signal transduction. The Shh LIGHT II cell line, which is stably transfected with the Gli-luciferase fusion DNA construct and expresses luciferase upon the activation of Gli promoted transcription, was also used for Shh activity analysis in this project.

A detailed illustration of the vertebrate Shh signaling pathway is shown in figure 1.3.

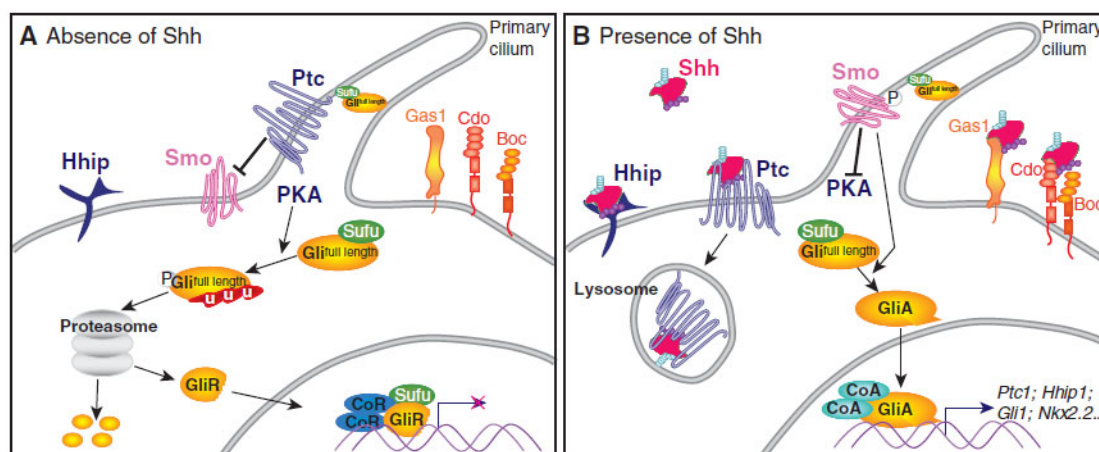


Figure 1.3. Model of vertebrate Shh signal transduction pathway. (A) In the absence of Shh, Ptc inhibits Smo activity at the cell membrane. No Shh signal is transferred to the multiprotein complex of Fu, Su(Fu) and the transcription factor Gli. Gli exists as a cleaved repressor form. No transcription of any downstream target genes takes place. (B) After the Shh ligand binds to its receptor Ptc, the suppression of Smo by Ptc is relieved. Smo is relocated to the microtubule. There the multiprotein complex is dissociated. Gli remains in the full length activator form, and is transported into the nucleus and triggers transcription of the target genes of Shh signaling. (Modified from Ribes and Briscoe, 2009).

1.2.2. Post-translation modifications of the Hedgehog / Sonic hedgehog protein

Shh is initially produced as a 45kDa premature precursor (Wang et al., 2007). After translation, like other Hedgehog homologs, Shh undergoes multiple processing steps in the endoplasmic reticulum (Goetz et al., 2002; Heussler and Suri, 2003; Peters et al., 2004; Varjosalo and Taipale, 2008; Wang et al., 2007). Since the mechanisms for Hh processing and secretion are evolutionarily conserved (Varjosalo and Taipale, 2007, 2008), the modification of Shh was taken as an example for all homologs in the family (Figure 1.4).

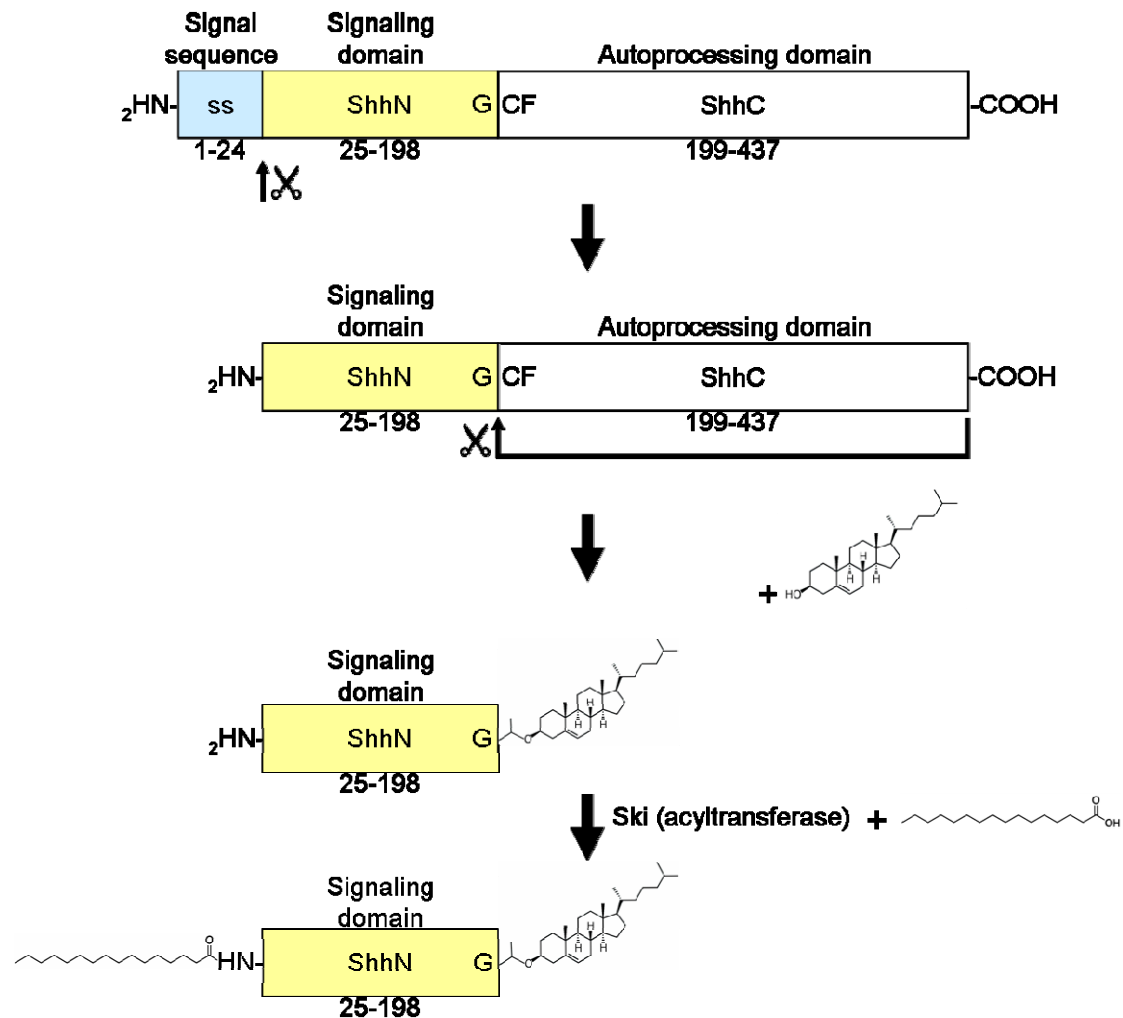


Figure 1.4. Maturation of Sonic hedgehog (Shh) signaling domain. Firstly, the full length premature Shh precursor is translated and transported to the endoplasmic reticulum. There the N-terminal signal sequence (ss), which is encoded by the first 24 amino acids of the full length Shh and is responsible for the release of the processed signaling domain (ShhN) from the expressing cell, is removed. Secondly, the autoprocessing domain (ShhC) is cleaved off from the C terminus of ShhN. A cholesterol modification then takes place at the exposed glycine residue and facilitates association of ShhN to the plasma membrane to get ready for ShhN secretion. With the catalysis by the acyltransferase Skinny hedgehog (Ski), palmitate is attached to the N terminus of ShhN. After this final processing step, ShhN is matured and regarded as ShhN_p, where p denotes processed.

After the signal sequence (or signal peptide) at the N terminus of the 45kDa Shh precursor is removed, an autoproteolytic cleavage is performed at the C terminus to generate an N-terminal fragment of Shh protein of about 19kDa (Chen et al., 2004;

Heussler and Suri, 2003; Miura and Treisman, 2006; Peters et al., 2004; Varjosalo and Taipale, 2008; Wang et al., 2007). This separation of the N- and C-terminals is catalyzed by the C-terminal autoprocessing domain and takes place between the conserved glycine and cysteine residues (Chen et al., 2004; Varjosalo and Taipale, 2008). During the cleavage, the cholesterol modification occurs simultaneously. First, the peptide bond between the glycine and cysteine residues is rearranged to form a thioester. Subsequently, cholesterol attacks the carbonyl of the thioester, covalently displacing the sulfur and cleaving the Shh protein into two parts (Heussler and Suri, 2003; Miura and Treisman, 2006; Peters et al., 2004; Varjosalo and Taipale, 2008). The C-terminal autoprocessing domain appears to carry no function, while the N-terminal Shh signaling domain (ShhN) that contains an ester-linked cholesterol at its C terminus is further processed to gain full protein activity (Peters et al., 2004; Varjosalo and Taipale, 2008).

The cholesterol modification facilitates the association of ShhN with the plasma membrane and spatially restricts the activity zone and diffusion of ShhN from the site of secretion (Heussler and Suri, 2003; Peters et al., 2004; Varjosalo and Taipale, 2008), resulting in controlled release of protein from the membrane regions of the producing cells to form stable gradients (Peters et al., 2004). The hydrophobicity and membrane anchoring ability of ShhN are further enhanced by the addition of palmitate, a 16-carbon saturated fatty acid that is required for ShhN activity, at its N terminus by the acyltransferase Skinny hedgehog (Ski) (Chen et al., 2004; Heussler and Suri, 2003; Miura and Treisman, 2006; Peters et al., 2004; Varjosalo and Taipale, 2007, 2008).

The resulting mature and fully active form of ShhN signaling molecule is thus modified by cholesterol at its C terminus and palmitate at its N terminus, and is denoted as ShhN_p, where p indicates processed (Chen et al., 2004; Varjosalo and Taipale, 2008).

1.2.3. Secretion, transport and concentration gradient formation of the Hedgehog / Sonic hedgehog protein

Despite its tight membrane association due to the C-terminal cholesterol modification and N-terminal palmitoylation, the Hh / Shh protein is able to affect patterning of distal tissues, acting directly over a long range of many cell diameters in a time- and concentration-dependent manner (Figure 1.5; Varjosalo and Taipale, 2007, 2008; Wang et al., 2007). The distance over which Hh has been shown to act is ~50µm in the *Drosophila* wing imaginal disc formation (Varjosalo and Taipale, 2008; Zhu And Scott, 2004). In vertebrate limb bud formation, Shh can travel up to ~300µm, which is up to 20 cell diameters, from its source of secretion (Saha and Schaffer, 2005; Varjosalo and Taipale, 2008; Zhu and Scott, 2004). The formation of the gradient of Hh / Shh activity emanating from the secreting cells is facilitated by multiple macromolecules such as heparin sulfate proteoglycans (HSPGs), which control release, transport and sequestration of Hh / Shh (Dierker et al., 2009a, b; Lin, 2004; Varjosalo and Taipale, 2007; Zhu and Scott, 2004).

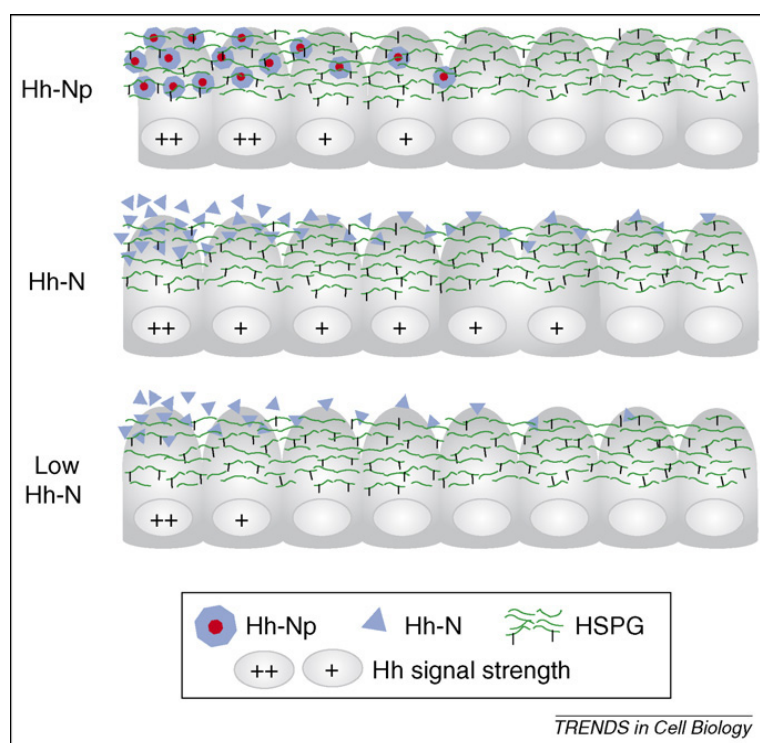


Figure 1.5. Model illustrating the formation of Hh concentration gradients with the contribution of HSPG in the extracellular matrix (ECM), and the resulting signal strength of unprocessed (Hh-N) and processed signaling domains of Hh (Hh-Np). Processed Hh-Np associates with HSPG and exhibits a controlled concentration gradient in the ECM. Unprocessed Hh-N, on the contrary, demonstrates a more diffused pattern of morphogen distribution without close contact with HSPG. (Adapted from Guerrero and Chiang, 2006)

In both *Drosophila* and vertebrates, hedgehog proteins are trafficked and anchored to the cell surface and released from the producing cells as lipoprotein (LP)-associated oligomers in a process mediated by the 12-span transmembrane protein Dispatched (Disp) (Saha and Schaffer, 2005; Varjosalo and Taipale, 2008). Disp, like Ptc, belongs to the bacterial Resistance-Nodulation-Division (RND) family of transport proteins by virtue of their sequence similarity (Varjosalo and Taipale, 2007, 2008; Wang et al., 2007). Loss of Disp leads to accumulation of Hh in the producing cells and failure of long-range signaling in *Drosophila* (Burke et al., 1999; Varjosalo and Taipale, 2008).

After the secretion of Hh from the producing cells, several molecules and mechanisms are used to control the shape and size of the Hh gradient (Wang et al., 2007). For instance, ECM proteins have been found to regulate Shh transport. High affinity binding of Shh to vitronectin in the neural tube has been suggested to aid in the proper presentation of Shh to differentiating motoneurons (Saha and Schaffer, 2005). The effective transport of *Drosophila* Hh depends upon the activity of HSPG. Shh has also been shown to bind to HSPG, as indicated by the failure of Hh transport in embryos lacking heparan sulfate-synthesizing enzymes of the EXT/tout velu (ttv) family (Saha and Schaffer, 2005; Varjosalo and Taipale, 2007). There is also evidence indicating that Hh oligomers travel from Hh producing cells to Hh responsive cells via interactions with both, glypicans and megalin (Wang et al., 2007).

At the plasma membrane of Hh responsive cells, Hh is capable of inducing the expression of its receptor Patched (Ptc). Ptc restricts the range of action of Hh in all species analyzed by sequestering and internalizing Hh, and targeting it to lysosomes for degradation (Varjosalo and Taipale, 2007, 2008). In addition to Ptc, vertebrates have an additional transmembrane glycoprotein, the Hh-interacting protein (Hhip), which is also induced by Hh signaling. It binds to Hh with high affinity, and reduces its range of movement by modulating Hh signaling activity (Saha and Schaffer, 2005; Varjosalo and Taipale, 2007, 2008).

While the *in vivo* secretion and transportation of Hh have been widely studied in *Drosophila*, there is a growing number of works for Shh in vertebrates. Previously, Shh transport via diffusion was modeled in the vertebrate limb bud, using a simple signal transduction mechanism without consideration of any of the accessory transport mechanisms described above (Dillon et al., 2003; Saha and Schaffer, 2005). Based on

the proposed mechanism of Shh signal transduction with the active and inactive Smo, the model was developed to study the Ptc-Smo interaction and effects of the post-translationally modified and unmodified ShhN. Bead- and tissue-implant experiments can be monitored by using the model without postulating different diffusivities for the two forms of Shh; and the difference in other parameters such as the rate of release of Shh from the bead or transplant can explain the Shh diffusion mechanism equally well.

1.3. Current *in vitro* cell culture system for the investigation of Sonic hedgehog function / role

With reference to the significance of Shh in cell fate determination during tissue development and the severity of developmental defects resulting from malfunction of Shh or interruption of its signal transduction, many *in vivo* studies of Shh signaling were performed. However, studies of Shh function *in vivo* are complicated by the high complexity of its signaling pathway and the involvement and interactions of many other molecules in the signaling network. Moreover, the post-translational modifications that the protein undergoes in its maturation procedure *in vivo* hinders researchers from examining some Shh functions at the basic level. The establishment of an *in vitro* cell culture system would therefore be helpful in eliminating the contribution of other *in vivo* factors and provide a simplified platform for the investigation of the Shh modes of action.

Like other morphogens, Shh can be transported by various mechanisms to generate a concentration gradient (Kang et al., 2007; Morales et al., 2006; Wilson and Chuang, 2010). In an *in vitro* system, the formation of concentration gradient and restriction of

local availability of the morphogen can be achieved by immobilization of the morphogen on a functionalized surface. With the assumption that the Shh responsive cells are initially of the same type, would they react and differentiate into different cell types according to the sensed morphogen concentration gradient? If yes, it would provide information, in addition to the current knowledge on the effect of Shh on cell fate determination at certain levels of concentrations, on the contribution of the steepness of gradient slope to the definition of morphogens.

In 2010, Amadi and colleagues demonstrated that the Shh gradient in a Resistor-Capacitor (RC) device is capable of inducing graded expression of the neuronal transcription factors Olig2 and Nkx2.2 in mouse embryonic stem cells (Figure 1.6; Amadi et al, 2010). Nevertheless, using hydrogel to "immobilize" Shh does not allow irreversible binding of the protein to the substrate. The work of Amadi's group was thus unable to fully restrict the motility of Shh. Immobilization of Shh with more stringent condition, on the other hand, could raise the possibility in solving the problem.

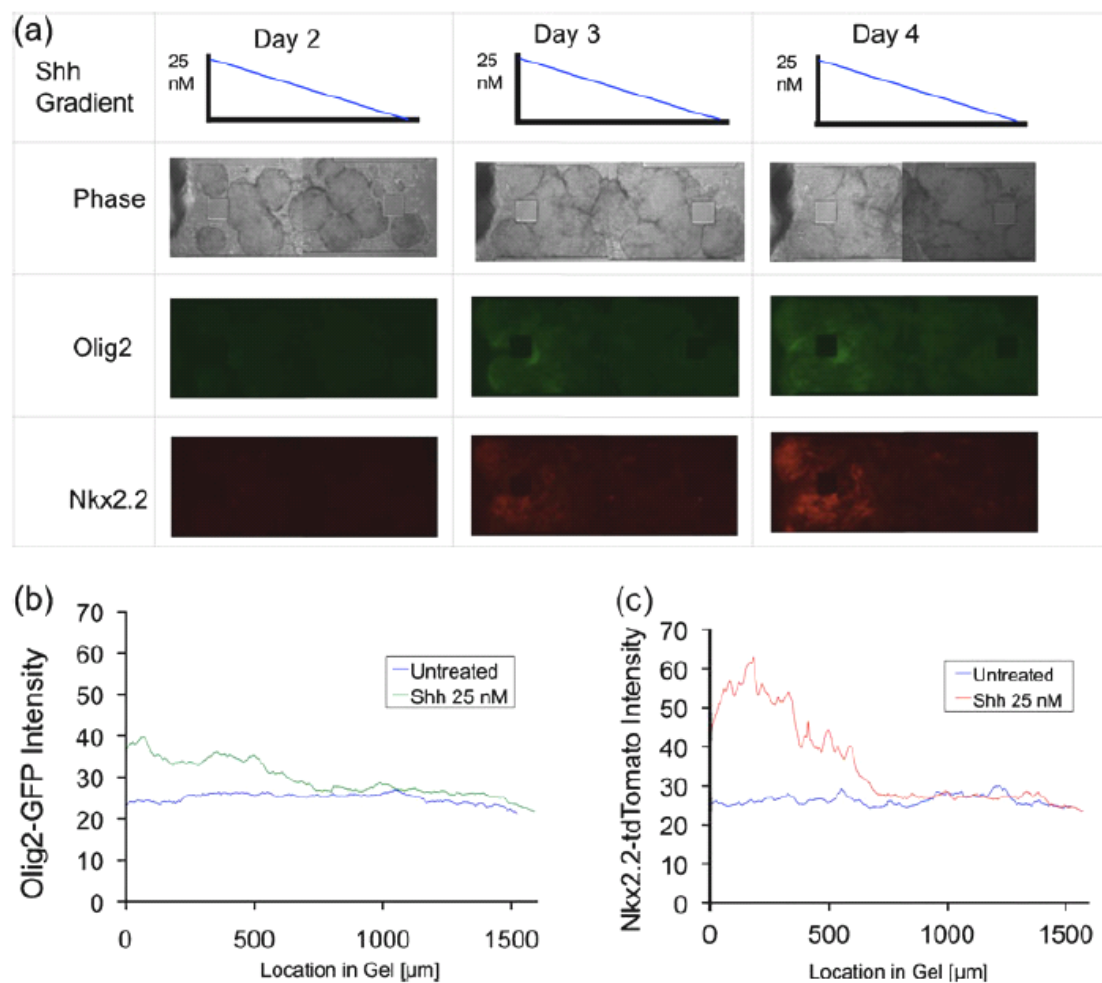


Figure 1.6. Biomolecules inside the cells may react differently when the morphogen is applied in a constant concentration or is distributed in a gradient. Introduction of Shh to embryonic stem cells with different gradients via hydrogel triggered differentiation and graded expression of neural transcription factors (Adapted from Amadi et al., 2010).

In the last decades, a variety of strategies have been established for surface modifications and patterning for organizing cell cultures and biomolecules such as nucleotides and proteins in a defined and controlled manner, probably by virtue of the expanding demand for more realistic *in vitro* tissue models to get closer to the *in vivo* situation (Welle et al., 2002). Taking proteins as an example, once proteins are adsorbed onto a biomaterial surface, they serve as mediators between the surface features and the biological microenvironment in touch with them (Willumeit et al., 2007). The *in vitro* assemble of cellular networks offering control over positions,

connectivities and activities of cells by patterned culture substrates is a valuable tool for researches in cell biology (Chen et al., 1998; Ostuni et al., 2009). Such an approach not only gives the advantage of simplification of systems for fundamental understanding of biological metabolisms, but also enhances the resolution in viewing complicated cellular reactions / responses.

In the case of Shh, patterning Shh in a controlled system may provide information on how Shh works as a morphogen: Are the absolute amounts of the protein provided and received governing the strength of signaling? Or are the slopes of varying protein concentrations more critical in modulating cellular behaviours? These questions can be addressed using tailor made systems for Shh immobilization and specific cell based assays. Taken together, substrate patterning for protein immobilization and investigation may reveal the most basic mechanisms of protein action.

1.4. Surface functionalization and patterning for protein immobilization

There are numerous possibilities of immobilizing proteins on functionalized surfaces (You et al., 2009). In the current project, immobilization of Shh was conducted by making use of functional group interactions such as the affinity binding between nickel ion and polyhistidine; biotin and streptavidin; and the benzylguanine (BG) and SNAPTM tag covalent bonding system. Physisorption of Shh on collagen and fibronectin coated surfaces were also performed to mimick Shh distribution in the extracellular matrix. With respect to properties of the interactions, three surface substrates with distinct physical properties: polystyrene (PS), glass and gold were used. To optimize each surface for ShhN immobilization and maximal protein activity,

designated methods of improving protein adsorption properties of surfaces, introducing active functional groups, patterning and coating of materials were tested.

The following subsections provide general introduction to each of the surfaces and modifications employed for protein immobilization, and elucidate their advantages and applications.

1.4.1. Physisorption of proteins on extracellular matrices

The extracellular matrix (ECM) is a biological structure that provides structural support with their properties of forming connection networks. The well-known components in the ECM include collagen and fibronectin. They assist in migration of cells and transportation of biomaterials and information for effective protein-cell and cell-cell communications. Based on the results of Guerrero and Chiang (2006), also collagen and fibronectin should have an impact on ShhN distribution and bioavailability. If the ShhN/collagen or ShhN/fibronectin adsorption are fully or partially reversible ShhN endocytosis can take place (Jarov et al., 2003).

By coating different amounts of collagen or fibronectin on glass surfaces, different amounts of Shh can be adsorbed. As collagen and fibronectin are ready in attaching themselves on glass surfaces, the two extracellular matrix substances provide a favorable platform for protein adsorption and cell adhesion, mimicking the *in vivo* environment.

1.4.2. Microcontact printing of proteins onto surfaces

Microcontact printing (μ CP) is a soft lithography method. It utilizes a polydimethylsiloxane (PDMS) stamp for parallel deposition of molecules on a target surface through conformal contact with the substrate (Figure 1.7; Thibault et al., 2005). μ Cp is simple, reproducible and, cost-effective (Thibault et al., 2005). Previous work demonstrated that proteins and self resembled monolayers (SAMs) can be deposited on a substrate surface by μ CP (Malaquin et al., 2003; Michel et al., 2001; Thibault et al., 2005). Since μ CP can provide patterns at the micro- and nano-scales, it allows investigation of cell-protein interaction at subcellular length scales (Renault et al., 2003; Thibault et al., 2005). μ Cp can be used to generate special patterns with different local densities of protein forming a protein gradient. An example of gradient generation by μ Cp is shown in figure 1.8.

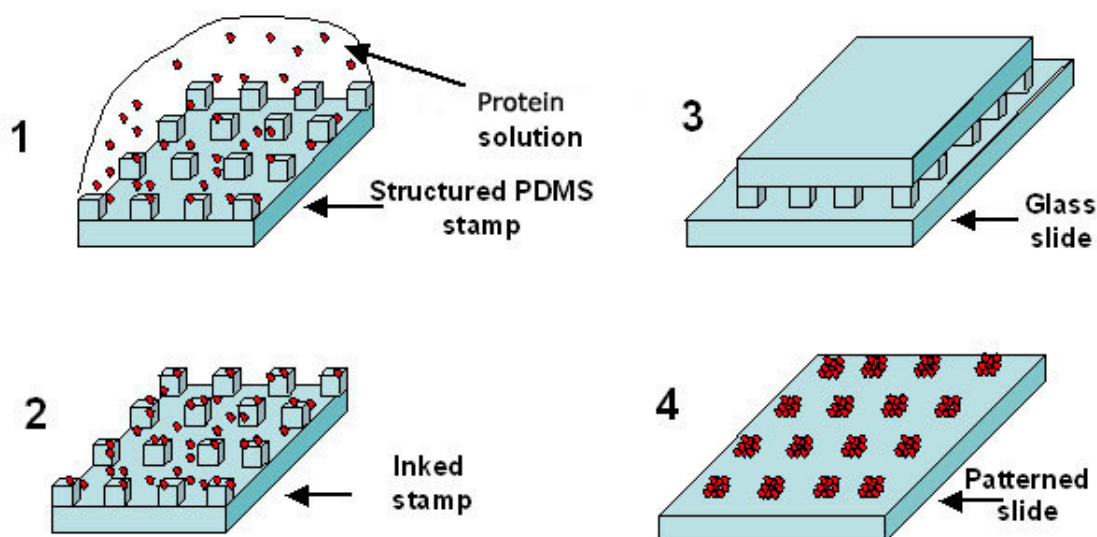


Figure 1.7. Principle of microcontact printing (μ Cp) of protein molecules onto a glass surface. (1) Inking of the stamp with the protein solution. (2) Drying of the stamp under nitrogen stream. (3) Manual contact between the inked PDMS stamp and the glass slide. (4) Protein molecules were transferred on the surface along the patterns that correspond to the relief structures of the PDMS stamp. (Modified from Thibault et al., 2005)

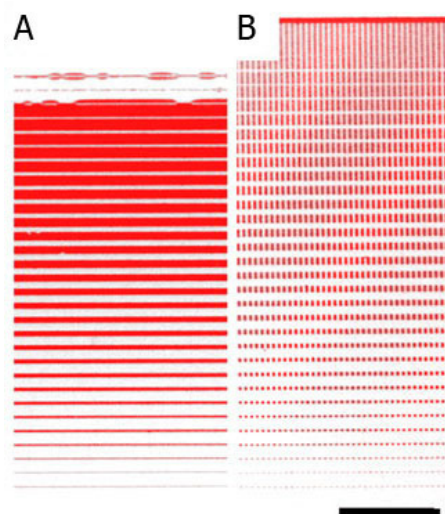


Figure 1.8. Substrate-bound gradient fabricated by microcontact printing of ephrin. (A) A steep gradient built by an array of stripes and (B) a shallow gradient built by dots. Scale bar: 50 μm . (Modified from von Philipsborn et al., 2006).

1.4.3. UV assisted functionalization of polystyrene surfaces with nickel ions

Polystyrene (PS) was originally used in the form of sterile, non-functionalized petri dishes for bacterial culture (Welle et al., 2002). Irradiation of polystyrene surfaces with ultraviolet light of $\lambda = 185\text{nm}$ for more than 5 minutes leads to the formation of carboxylic groups and negative surface charges (Welle et al., 2002). The resulting hydrophilic surfaces favor binding of certain adhesion proteins such as collagen, fibronectin and laminin (Welle et al., 2002, 2005). By using chromium/quartz masks during UV irradiation, and different irradiation times or a proximity gap between the mask and substrate, one can establish different densities of carboxylic groups, hence different densities of adsorbed proteins on the PS surface (Figure 1.9).

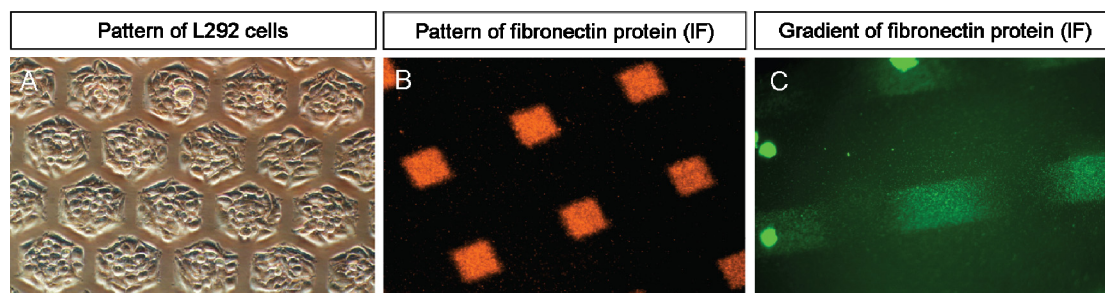


Figure 1.9. Applications of UV irradiated polystyrene surfaces. (A) Phase contrast micrography of L929 cells on UV patterned polystyrene surface. Irradiation of the PS surface with ultraviolet light of $\lambda = 185\text{nm}$ gives rise to the formation of a hydrophilic surface, which favors cell adhesion. (B, C) The change of hydrophilicity of the UV irradiated PS surfaces allows adsorption of fibronectin on the surfaces with sharp or graded density profiles along the patterns. Fibronectin was detected by immunofluorescence (IF) using the anti-fibronectin antibody conjugated with Cy3 (B) or green fluorescence (C) labeled secondary antibodies. (Courtesy of Dr. S. Engin, KIT, Karlsruhe, Germany)

UV modified polystyrene is usually applied for direct cell adhesion and protein immobilization. In addition, the produced carboxylic acid groups at the irradiated PS surface can be further reacted with nickel(II)-nitrilotriacetic acid (Ni-NTA) containing compounds which in turn bind to poly(6)histidine tagged proteins. When six histidine molecules are continuously arranged, they bear a high affinity of binding to the metal nickel (Hochuli, 1988). The nickel-histidine binding affinity is strong and has the dissociation constant (K_d) of 10^{-13}M (Schmitt et al., 1993). Such affinity is not only beneficial in purifying polyhistidine tagged proteins by column chromatography but also provides a strong and stable intermediate for protein immobilization on functionalized surfaces (Sigal et al., 1996).

1.4.4. Dip-pen nanolithography of phospholipids for protein immobilization

Dip-pen nanolithography (DPN) is an alternative approach for biomaterial immobilization. It is a scanning probe lithography technique where an atomic force microscope (AFM) tip is used as an ultra-sharp pen for direct and micro- and nanoscale deposition of materials onto a surface via a water meniscus (Figure 1.10; Echelard et al., 1993; Ginger et al., 2004).

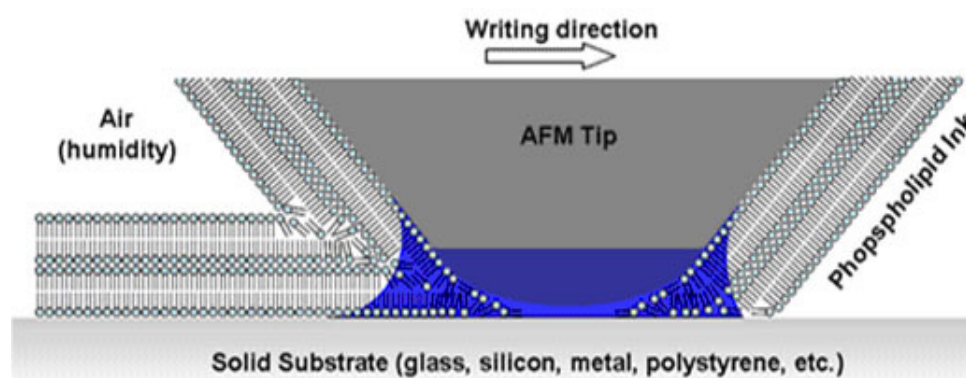


Figure 1.10. Schematic diagram illustrating dip-pen nanolithography of phospholipids. On a solid substrate, an AFM tip is used to deliver phospholipids ink onto the surface via a water meniscus in an atmosphere surrounded with optimized humidity. (Courtesy of Dr. S. Lenhart, Florida State University, USA)

DPN of phospholipids with a nickel chelating head group can be used for selective adsorption of polyhistidine-tagged proteins (Agarwal et al., 2003). Similarly, biotin terminated phospholipids can also be used to immobilize a biotinylated protein with a streptavidin linked between the biotin head group in the lipids and the biotin fused with the protein (Sekula et al., 2008). Biotin is a vitamin found in all cells while streptavidin, a bacterial homologous protein to avidin purified from chicken egg white, is isolated from the actinobacterium *Streptomyces avidinii* (Holmberg et al.,

2005). The biotin/streptavidin system is the strongest non-covalent interaction known in nature, having a dissociation constant (K_d) of $4 \times 10^{-14} \text{M}$ (Holmberg et al., 2005; Livnah et al., 1993). The high affinity and specificity are due to the high shape complementarity as well as the extensive network of hydrogen bonds formed between biotin and the binding pocket of streptavidin. Biotinylation of the protein of interest and the phospholipids used for DPN, and connecting the two with streptavidin as the intermediate layer can therefore facilitate immobilization of the protein on a designated surface. Because of the small size of biotin, the biological activity of the immobilized protein is most likely unaffected.

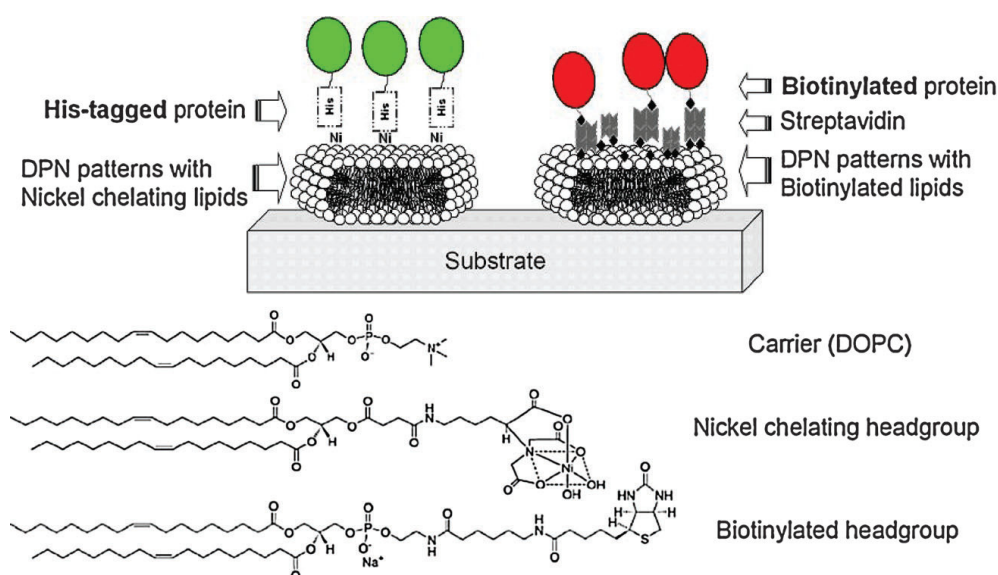


Figure 1.11. Schematic representation of protein-coupling strategies to spatially patterned lipid supports (Top), and the chemical structures of the used phospholipids (Bottom) (Adapted from Sekula et al., 2008)

1.4.5. Self assembled monolayer formation of benzylguanine terminated thiols on gold and immobilization of protein via benzylguanine/alkyltransferase covalent binding

Apart from functionalized phospholipids deposited by DPN, SAMs of thiols or disulfides on gold are also important building blocks for surface functionalization used in many disciplines (Mrksich and Whitesides, 1996). For example, a thiol SAM on gold can be used for protein immobilization (Kim et al., 2008). A thiol group is a sulfhydryl (-SH) group. It is itself a head group that can form an alkanethiol with an alkyl chain ((CH₂)_n) as a backbone and a tail group, which usually is a tag for binding of the protein of interest (Love et al., 2005). An alkanethiol strongly binds to noble metal substrates, like gold and silver, by virtue of the high affinity of sulfur in the sulfhydryl group to the metal. The sulfur-gold interaction is semi-covalent with a binding energy of 50kcal/mol (Love et al., 2005). Over a long enough period of time, a SAM of the alkanethiol would form on the gold surface with the sulfhydryl group assembling together on the gold substrate and the tail group far from it for protein binding. Generation of SAMs of an alkanethiol with an appropriate tail group could therefore be applied for immobilizing proteins on gold surfaces.

While different tail groups can be associated with the alkanethiol for the immobilization of relevantly tagged proteins on gold, the SNAPTM system was discovered to be appropriate for covalent immobilization of proteins (Kindermann et al., 2003). In nature, the human DNA repair protein O⁶-alkylguanine-DNA alkyltransferase (hAGT) transfers the alkyl group from its substrate, O⁶-alkylguanine-DNA, to one of its cysteine residues, resulting in a covalent bond at the site of reaction (Kindermann et al., 2003; Pegg, 2000). Previously,

O⁶-benzylguanine (BG) was found to exhibit similar properties as O⁶-alkylguanine-DNA. It could react with and form covalent bonding with hAGT, and thus could be used for specific labelling of hAGT fusion proteins *in vivo* and *in vitro* (Keppler et al., 2003; Kindermann et al., 2003). The coupling of BG and hAGT is covalent and is commercialized under the trade name SNAPTM. By attaching a BG group at the tail of an alkanethiol and substituting it, a SNAPTM tagged protein could be covalently immobilized on gold surface (Figure 1.12). Thus, the SNAPTM system can strictly control protein immobilization *in vitro*.

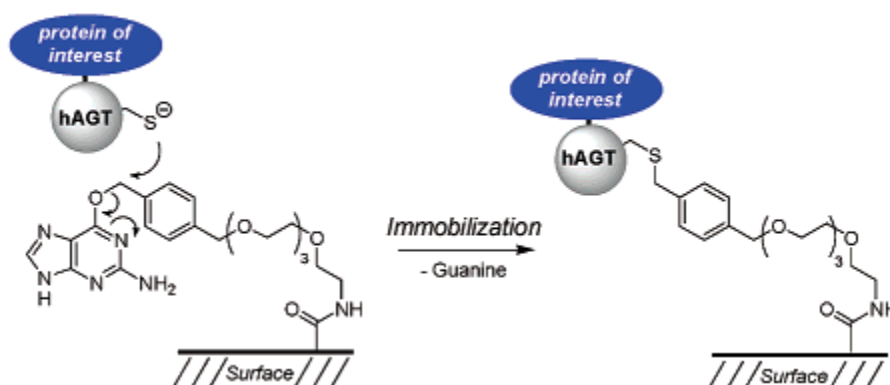


Figure 1.12. Covalent immobilization of a hAGT (SNAPTM) fusion protein on a BG modified surface.

(Adapted from Kindermann et al., 2003)

In addition to direct protein immobilization on a BG terminated SAM on gold, benzylguanine terminated phospholipid pattern can be generated via DPN lithography on other substrates than gold, e.g. polystyrene.

1.5. Surface analysis techniques

It is important not only to immobilize target proteins on designated surfaces, but also to evaluate the efficiency of protein adsorption. There are a variety of choices for surface analysis. The following subsections introduce the techniques used in this project.

1.5.1. Immunofluorescence for the detection of protein adsorption

Immunofluorescence (IF) is a common laboratory technique widely used for specific detection of proteins in cells and tissues. In IF, antibodies are chemically conjugated to fluorescent dyes such as fluorescein isothiocyanate (FITC) (Robinson et al., 2009) and bind directly or indirectly to the antigen of interest (Figure 1.13). Antigen detection is performed with a flow cytometer, an array scanner or automated imaging instrument, or by a fluorescence or confocal microscope (Robinson et al., 2009).

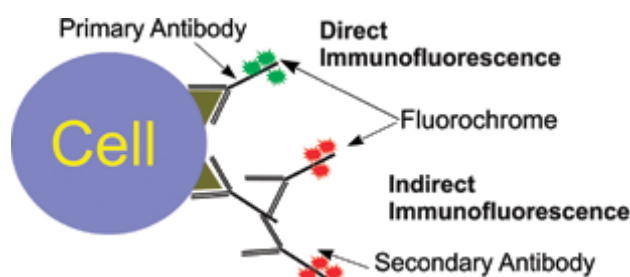


Figure 1.13. Schematic depiction of direct and indirect immunofluorescence. The primary antibody detects the antigen or protein of interest. A secondary antibody, which is conjugated with a fluorophore, binds to the primary antibody and thereby indicates the presence of the targeted antigen or protein. (Adapted from Robinson et al., 2009)

1.5.2. Enzyme-linked immunosorbent assay for the detection and quantification of adsorbed proteins

Enzyme-linked immunosorbent assay (ELISA), also known as enzyme immunoassay (EIA), is a biochemical technique conceptualized and developed by Engvall and Perlmann in 1971 at Stockholm University, Sweden (Lequin, 2005). Similar to immunofluorescence, ELISA is used mainly in immunology to detect the presence of an antibody or an antigen (or simply a protein of interest). Typically, a specific detection antibody is applied over the sample surface of an unknown amount of antigen or protein of interest affixed to the surface. The antibody forms a complex with the antigen or protein and is detected by a secondary antibody linked to an enzyme through bioconjugation. Finally an enzyme substrate is added and enzymatic conversion results in detectable signal, most commonly a color change in a chemical substrate, which indicates the quantity of the antigen or protein of interest in the sample (Figure 1.14).

Introduction

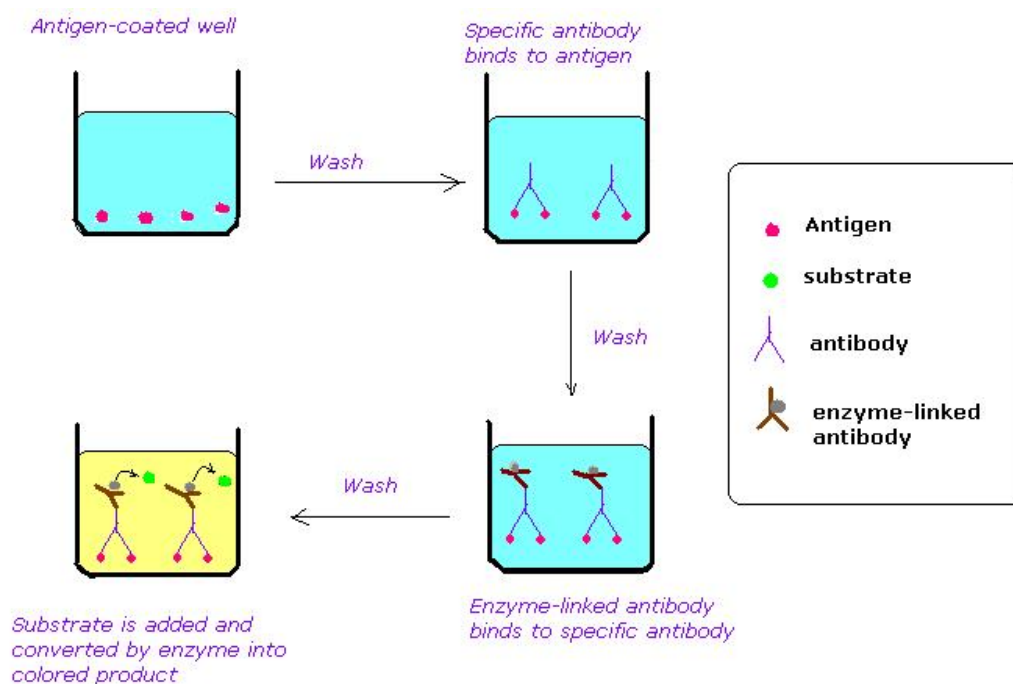


Figure 1.14. Schematic diagram demonstrating the typical procedure of ELISA. (Adapted from <http://en.wikibooks.org>)

By measuring the color intensity of known amounts of a protein, a standard curve can be plotted for quantification of the protein. In this project, ELISA was applied to determine the amount of Shh adsorbed on collagen surfaces.

1.5.3. Fluorescence recovery after photobleaching for the evaluation of protein motility

Fluorescence recovery after photobleaching (FRAP), also termed fluorescence photobleaching recovery (FPR), denotes a method for measuring two-dimensional lateral translational dynamics of molecules based on the diffusion of fluorescent particles (Axelrod et al., 1976; Koppel et al., 1979; Soumpasis et al., 1983). To initiate FRAP, a small area of fluorescence labeled molecules on a surface is first chosen. The fluorescence of the molecules is photobleached by a brief exposure to an intense focused laser beam (Axelrod et al., 1976; Koppel et al., 1976; Soumpasis et al., 1983). The subsequent recovery of the fluorescence, which occurs by replenishment of intact fluorophores in the bleached spot by diffusion from the surroundings, is monitored by fluorescence microscopy (Axelrod et al., 1976). By measuring the kinetics and the intensity of the fluorescence recovery, the motility of the molecules on the surface can be determined. Figures 1.15 and 1.16 illustrate the typical redistribution of a fluorescently labeled molecule on a cell surface in a FRAP experiment and an ideal FRAP recovery curve, respectively.

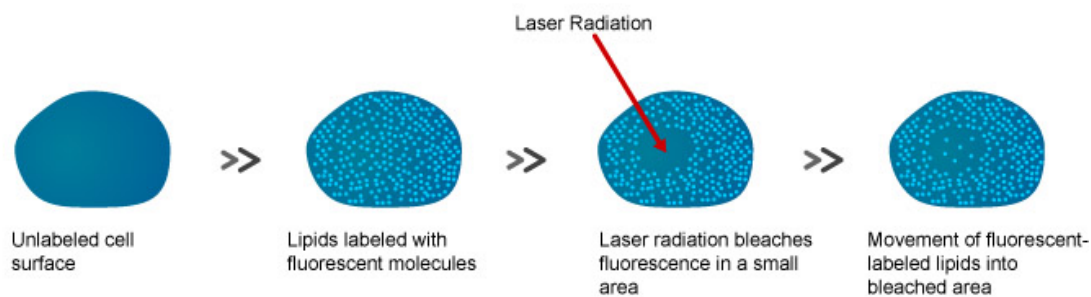
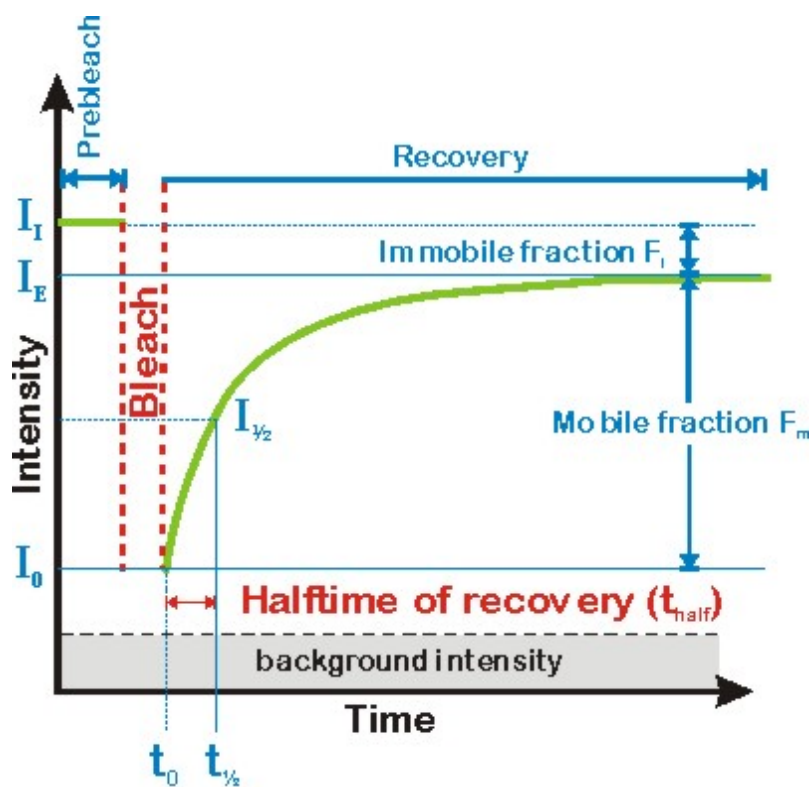


Figure 1.15. Schematic depiction of FRAP experiment on cell surface. An intense focused laser beam with the corresponding wavelength of the fluorophore used for molecule labeling is applied to photobleach the spot of interest. While the laser intensity is always kept constant during the following analysis, the fluorescence intensity in the illuminated region changes as molecules in the unbleached surroundings move into the photobleached area. (Adapted from Biology 230 Tutorials, The Pennsylvania State University, USA)



- I_i : initial intensity
- I_0 : intensity at timepoint t_0 (first postbleach intensity)
- $I_{1/2}$: half recovered intensity ($I_{1/2} = (I_E - I_0) / 2$)
- I_E : endvalue of the recovered intensity
- t_{half} : Halftime of recovery corresponding to $I_{1/2}$ ($t_{1/2} - t_0$)
- Mobile fraction $F_m = (I_E - I_0) / (I_i - I_0)$
- Immobile fraction $F_i = 1 - F_m$

Figure 1.16. An idealized plot of a FRAP recovery curve. The emitted fluorescence from the illuminated region is measured as a continuous function of time. Transport dynamics are measured by monitoring the transient behavior of an inhomogeneous distribution of fluorescently labeled molecules. An exposure with a high laser power bleaches the fluorophore within the beam, producing spatial distributions of the fluorophore. As molecules in the unbleached surroundings move into the photobleached area, a photo recovery occurs and the fluorescence intensity in the bleached area increases until equilibrium is reached. In ideal case, the recovered intensity (I_E) should be the same as the initial intensity (I_I). Due to different association and dissociation coefficient of molecule binding, there can be retardation of recovery rate and the immobile fraction (F_i) cannot be replenished by diffusion. (Adapted from EAMNET FRAP online teaching module, EMBL, Germany)

In this work FRAP was used to quantify the diffusion of GFP labeled Shh in collagen or fibrinectrin matrices.

1.5.4. Quartz crystal microbalance with dissipation monitoring for the detection and quantification of adsorbed protein on a surface

A quartz crystal microbalance (QCM) is an electro acoustic device for mass and viscoelastic analysis of adsorbed layers at a solid/liquid or solid/air interface (Chang and Zhao, 2008). The system consists of a megahertz piezoelectric quartz crystal resonator sandwiched between two gold electrodes, an oscillator, a frequency counter and a computer (Figure 1.17). When an alternating current (AC) is applied, the quartz crystal will oscillate at a certain resonance frequency (Spetz, 2006). By measuring the change in frequency, the mass of the adsorbed materials on the crystal can be determined. In this work, Shh adsorption on collagen surfaces and immobilization on benzylguanine thiol (BGT) SAMs were analyzed by quartz crystal microgravimetry with dissipation monitoring (QCM-D), which is a special kind of QCM.

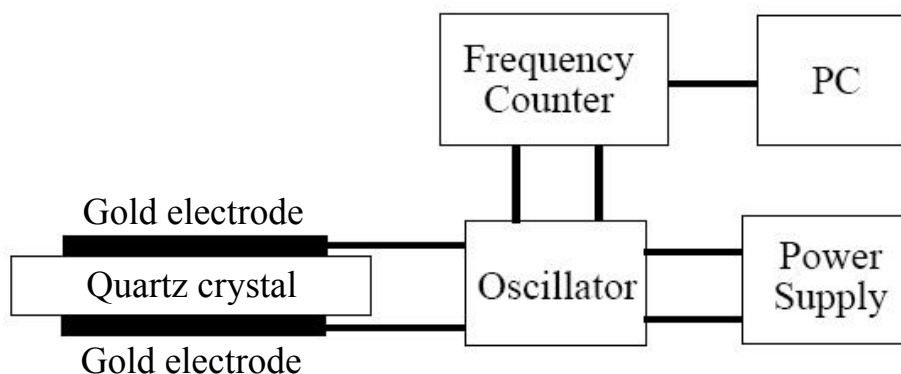


Figure 1.17. Illustration of a QCM setup. A resonant oscillation is generated in the quartz crystal by the application of an AC current. The resonant frequency is then measured by the frequency counter (Sauerbrey, 1959). (Diagram adapted from Chang and Zhao, 2008)

QCM-D is developed by Q-Sense AB, Sweden. QCM-D enables real-time, label free measurements of molecular adsorption and/or interactions on various surfaces. In addition to the adsorbed mass (ng/cm^2 sensitivity) measured as changes in the frequency of the quartz crystal, the dissipation parameter (D) provides insights regarding viscoelastic properties and hydrodynamic conductivity of the adsorbed layers. Dissipation occurs when the driving voltage to the crystal is shut off and the energy from the oscillating crystal dissipates from the system. QCM-D technology can be used to characterize the formation of thin films (nm) such as polymers, cells and proteins on surfaces (Chang and Zhao, 2008).

1.5.5. Time-of-flight secondary ion mass spectroscopy

Time-of-flight secondary ion mass spectroscopy (ToF-SIMS) is a powerful surface-sensitive analytical technique. It is able to determine the composition, structure, orientation, and spatial distribution of molecules and chemical structures on a surface through both spectral analysis and direct chemical state imaging (Belu et al., 2003). A focused, pulsed primary ion beam is scanned in a raster pattern over a sample surface to charge and dislodge particles from the surface of the sample. These secondary ions are then accelerated into a flight path and their mass is determined by measuring the exact time at which they reach the detector (i.e. time-of-flight) (Figure 1.18). Because ToF-SIMS is capable of measuring the "time-of-flight" of particles on a scale of nanoseconds, a mass resolution down to a few ppm $\Delta m/m$ can be achieved. By quasi-continuously collecting a large number of mass spectra, a "molecular map" of a sample area can be generated for any compound that produces a diagnostic ion in the spectrum.

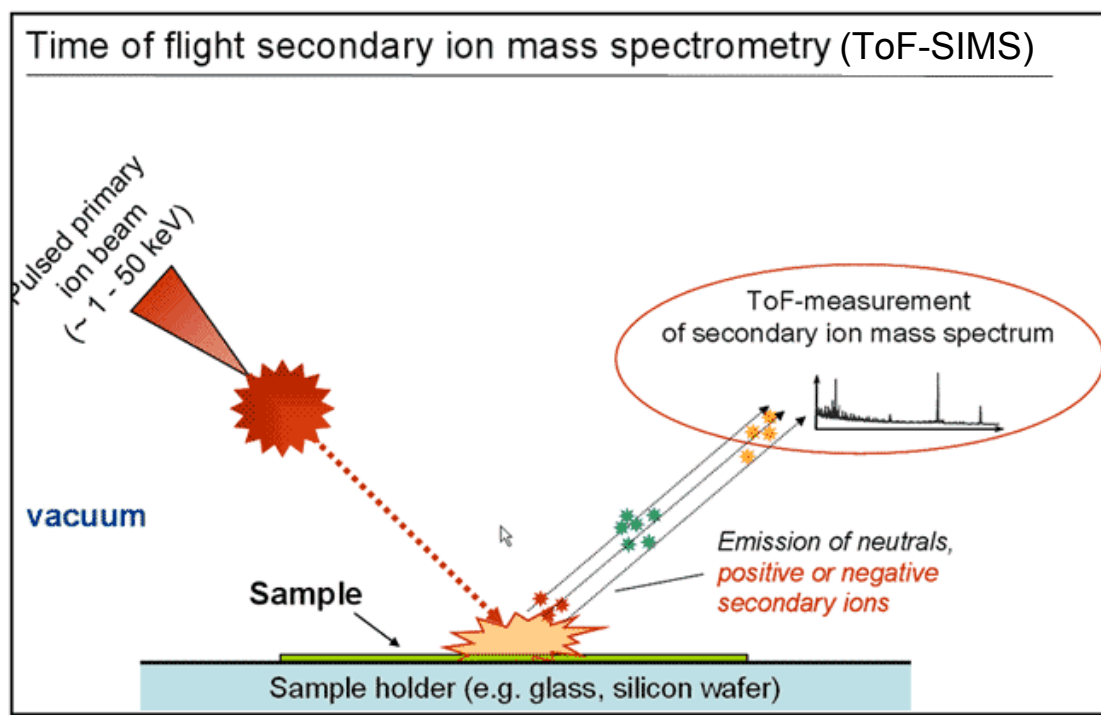


Figure 1.18. Schematic diagram describing the production of secondary ions by a focused, pulsed primary ion beam in the ToF-SIMS system. A pulsed primary ion beam is scanned in a raster pattern over the sample surface to charge and dislodge the outermost particles. The secondary ions are then accelerated into a flight path and their mass is determined by measuring the exact time at which they reach the detector. (Adapted from http://www.geomuseum.uni-göttingen.de/people/vthiel/tof_sims.shtml)

1.6. Objectives of the thesis

Sonic hedgehog (Shh) is an essential morphogen to study. However, investigation of the transport and signal transduction of the protein is difficult to perform *in vivo*. As mentioned in sections 1.3 and 1.4, it is necessary to eliminate the *in vivo* factors interfering with the modes of action of Shh so as to uncover the basic characters of the protein. Published literature provides invaluable information on the morphogenic property of Shh, especially on how cell fate determination is controlled by different concentration gradients of Shh. Nevertheless, it failed to give details on the roles of the tested cells regarding their sensing and recruitment of the morphogen. Whether endocytosis of the Shh ligand is required for proper induction of Shh signaling is another issue to be addressed. During molecule distribution, some portion of the diffusing substance would be immobilized by reversibly binding to the fixed polymer (Thorne et al., 2008). It therefore becomes meaningful to develop novel *in vitro* tools which mimick this *in vivo* situation and allow for investigations of the cellular responses to Shh in this advanced setup.

The objectives of this project are to express the biologically active signaling domain of Shh (ShhN), and develop methodologies of immobilizing ShhN on defined functionalized surfaces making use of the advantages of several immobilization approaches as described afore. The thesis will stress the evaluation of the efficiency of the immobilization techniques, observations of the effects of immobilization on the accessibility and biological activity of the Shh protein, as well as the induced signal transduction in Shh responsive reporter cell lines. The findings may provide a reference for future studies of Shh in *in vitro* cell culture systems.

2. Materials and Methods

2.1. Materials

2.1.1. Chemicals

Chemical	Supplier
1kb plus DNA ladder	Fermentas, St. Leon-Rot, Germany
Acrylamide, 30%	Carl Roth, Karlsruhe, Germany
Ammonia (28 – 30% in water)	Merck, Darmstadt, Germany
Ampicillin	Sigma-Aldrich, Munich, Germany
APS	Carl Roth, Karlsruhe, Germany
ATP	Sigma-Aldrich, Munich, Germany
Bacto-agar	Carl Roth, Karlsruhe, Germany
BCIP	Roche, Mannheim, Germany
Bromophenoblu	Merck, Darmstadt, Germany
BSA	PAA, Linz, Austria
BSA (albumin fraction V) for QCM	Merck, Darmstadt, Germany
Coelenterazin (Renilla luciferin)	Biosynth AG, Staad, Switzerland
Collagen (rat tail)	Roche, Mannheim, Germany
Complete tablets, EDTA free	Roche, Mannheim, Germany
Coomassie brilliant blue R-250	Merck, Darmstadt, Germany
DMSO	Fluka (Sigma-Aldrich), Munich, Germany
dNTPs	Promega, Mannheim, Germany
DTT	Carl Roth, Karlsruhe, Germany
EDTA	Carl Roth, Karlsruhe, Germany
EGTA	Carl Roth, Karlsruhe, Germany
Ethanol, analytical grade	Sigma, Steinheim, Germany
Ethidium bromide (EtBr)	Carl Roth, Karlsruhe, Germany
Fibronectin	Sigma-Aldrich, Munich, Germany
Firefly luciferin	Biosynth AG, Staad, Switzerland
Glycerol	Carl Roth, Karlsruhe, Germany
Glycine	Carl Roth, Karlsruhe, Germany
Heparin	Sigma-Aldrich, Munich, Germany

Materials and Methods

HEPES	Sigma-Aldrich, Munich, Germany
Hydrogen peroxide (30% in water, no Sn stabilizers)	EMSURE, Merck, Darmstadt, Germany
Imidazole	Carl Roth, Karlsruhe, Germany
IPTG	Carl Roth, Karlsruhe, Germany
Lysozyme	Sigma-Aldrich, Munich, Germany
NBT	Roche, Mannheim, Germany
PageRuler™ prestained protein ladder	Fermentas, St. Leon-Rot, Germany
PFA	Carl Roth, Karlsruhe, Germany
PLL-g-PEG	Dr. S. Sekula, INT, KIT, Karlsruhe, Germany
Proteinase K	Sigma-Aldrich, Munich, Germany
SAG	Axxora, Lörrach, Germany
SDS	Carl Roth, Karlsruhe, Germany
TEMED	Carl Roth, Karlsruhe, Germany
TMB tablets	Sigma-Aldrich, Munich, Germany
Tris	Carl Roth, Karlsruhe, Germany
Triton X-100	Carl Roth, Karlsruhe, Germany
Tween-20	Carl Roth, Karlsruhe, Germany
ZnCl ₂	Carl Roth, Karlsruhe, Germany

All other chemicals were purchased from Carl Roth GmbH + Co. KG (Karlsruhe, Germany) or Sigma-Aldrich Co. (Munich, Germany) unless otherwise stated.

2.1.2. Kits

Kit	Supplier
Alkaline phosphatase colorimetric assay kit	Abcam, Cambridge, UK
Biotin protein ligase	GeneCopoeia, Rockville, MD, USA
Gateway [®] LR Clonase [™] II enzyme mix	Invitrogen, Darmstadt, Germany
mMessage Machine [®] T7 kit	Ambion, Austin, TX, USA
Ni-NTA agarose	Qiagen, Hilden, Germany
Ni-NTA purification system	Invitrogen, Darmstadt, Germany
Passive lysis buffer 5X	Promega, Mannheim, Germany
peqGold gel extraction kit	Peqlab, Sarisbury Green, UK
Plasmid maxi kit	Qiagen, Hilden, Germany

2.1.3. Buffers and reagents

Buffer or reagent	Supplier / Composition
Alkaline phosphatase (ALP) staining buffer, pH9.5	100mM Tris 50mM MgCl ₂ 100mM NaCl 0.1% Tween-20
BCIP/NBT in ALP staining buffer	7µl of 50mg/ml BCIP 4.5µl of 100mg/ml NBT in 1ml ALP staining buffer
BT-fix, pH7.4	4% paraformaldehyde 4% sucrose 0.12mM CaCl ₂ 0.1M NaPi
CertiPUR buffer solution di sodium hydrogen phosphate / potassium hydrogen phosphate pH 6.88, 50mM	Merck, Darmstadt, Germany

Materials and Methods

Coomassie blue protein staining solution	0.2% Coomassie brilliant blue R-250 7.5% acetic acid 50% EtOH
Coomassie gel destaining solution	50% MeOH 10% acetic acid
Firefly luciferin assay solution	20% firefly luciferin stock solution in GlyGly stock buffer
Firefly luciferin stock solution	1mM (0.28mg/ml) firefly luciferin in GlyGly stock buffer
Glycylglycine (GlyGly) buffer	Sigma-Aldrich, Munich, Germany
Glycylglycine (GlyGly) assay buffer	2mM ATP 1mM DTT in GlyGly stock buffer
Glycylglycine (GlyGly) stock buffer	25mM glycylglycine (GlyGly) 15mM MgSO ₄ 4mM EGTA
Hybridization buffer (HYB)	50% formamide 5X SSC 500µg/ml yeast RNA 50µg/ml heparin 0.1% Tween-20 9mM citric acid
<i>In situ</i> hybridization (ISH) Blocking buffer	0.1% Tween-20 0.2% (2mg/ml) BSA 1% DMSO in 1X PBS
Lämmli sample buffer 2X, pH6.8	2% SDS 10% glycerol 60mM Tris

	0.001% bromophenol blue 100mM DTT
MilliQ H ₂ O	Purified and deionized at 18.5MΩ·cm by Millipore water purification system
Ni-NTA purification cell lysis buffer	1% TritonX-100 100μM ZnCl ₂ 1mM EDTA 1 Complete tablet, EDTA free 5 spatula of lysozyme Fill up to 50 ml with 1X PBS
Ni-NTA purification washing buffer, pH7.4	8.77ml of 200mM NaH ₂ PO ₄ 1.23ml of 200mM Na ₂ HPO ₄ 0.5M NaCl 20mM imidazole Fill up to 100ml with H ₂ O
Ni-NTA purification elution buffer, pH7.4	8.77ml of 200mM NaH ₂ PO ₄ 1.23ml of 200mM Na ₂ HPO ₄ 0.5M NaCl 500mM imidazole Fill up to 100ml with H ₂ O
PBS	Invitrogen, Darmstadt, Germany
PBT 1X	0.1% Tween-20 in 1X PBS
Phosphate-citrate buffer, pH5.0	25.7ml of 0.2M Na ₂ HPO ₄ ·2H ₂ O 24.3ml of 0.1M citric acid·H ₂ O Fill up to 50ml with H ₂ O
Renilla luciferase reaction mix 1	108.75ml of 0.4M K ₂ HPO ₄ 16.25ml of 0.4M KH ₂ PO ₄ 50ml of 5M NaCl 1ml of 0.5M EDTA

Materials and Methods

	Fill up to 500ml with H ₂ O
Renilla luciferase reaction mix 2	125mM Coelenterazin (Renilla luciferin) in Renilla luciferase reaction mix 1
SDS electroblotting buffer 1X, pH8.3	30mM Tris 200mM glycine 20% MeOH
SDS-PAGE running buffer 1X, pH8.3	25mM Tris 197.5mM glycine 0.1% SDS
SSC 1X, pH7.0	150mM NaCl 15mM sodium citrate
TAE 1X, pH7.8	40mM Tris 5mM acetic acid 1mM EDTA
TBST 1X, pH7.6	2mM Tris 14mM NaCl 0.2% Tween-20
Western blot (WB) blocking buffer	5% BSA in 1X TBST

The pH values of all buffers and reagents were adjusted with 37% hydrochloric acid (HCl) and 1N sodium hydroxide (NaOH).

2.1.4. Enzymes

All restriction endonucleases, PCR enzymes and other modifying enzymes were purchased from Fermentas GmbH (St. Leon-Rot, Germany) unless otherwise stated

2.1.5. Bacteria

Bacteria	Strain	Usage
<i>E. coli</i>	BL-21	Expression of ShhN variants
<i>E. coli</i>	<i>ccdB</i> Survival T1 ^R	Propagation of empty pDEST TM 14 vector
<i>E. coli</i>	DB3.1 TM	Propagation of empty pENTR TM 11 vector
<i>E. coli</i>	DH5 α	Propagation of DNA of ShhN variants in pDEST TM 14 vector
<i>E. coli</i>	TOP10	Propagation of DNA of ShhN variants in pENTR TM 11 vector
<i>E. coli</i>	XL1-Blue	General propagation of plasmids

2.1.6. Bacteria media

Medium	Composition
LB	10g tryptone 5 g yeast extract 5 g NaCl Fill up to 1L with H ₂ O
SOC	2% bacto-tryptone 0.5% bacto-yeast extract 10mM NaCl 2.5mM KCl 10mM MgSO ₄ 10mM MgCl ₂ 20mM glucose

2.1.7. Cell lines

Cell line	Origin	Source	Medium
HEK293	Human embryonic kidney cells	M. Litfin, ITG, KIT, Karlsruhe, Germany	DMEM 10% FBS
C3H10T1/2 clone 8	Mouse pluripotent mesenchymal cells	American Type Culture Collection (ATCC) (LGC Standards), Wesel, Germany	BME 10% HI FBS 2mM L-glutamine
Shh LIGHT II	NIH/3T3 stably transfected with Gli responsive firefly luciferase reporter	Dr. Anita Büttner, University of Leipzig, Germany	DMEM (ATCC) 10% FBS 0.15mg/ml zeocin 0.4mg/ml G-418

2.1.8. Cell culture media and reagents

Cell culture medium or reagent	Supplier
BME	Invitrogen, Darmstadt, Germany
DMEM	Invitrogen, Darmstadt, Germany
DMEM (American Type Culture Collection (ATCC))	LGC Standards, Wesel, Germany
FBS	PAA, Linz, Austria
Geneticin (G418 sulfate)	Invitrogen, Darmstadt, Germany
L-glutamine	Invitrogen, Darmstadt, Germany
PolyPlus jetPEI transfection reagent	Polyplus-transfection, New York, NY, USA
Trypsin	Invitrogen, Darmstadt, Germany
Zeocin	Invitrogen, Darmstadt, Germany

2.1.9. Zebrafish (*Danio rerio*)

Wildtype zebrafish (strain AB₂O₂) were maintained in fish water at 28°C in the fish facility at Karlsruhe Institute of Technology (KIT) Campus North.

2.1.10. DNA plasmids

DNA plasmid	Supplier
pcDNA3.1:Shh (ShhNp)	Dr. K. Grobe, Westfälische Wilhelms-Universität Münster, Germany
pcDNA3.1:ShhN-Myc-His (ShhN ^{6×his})	Dr. K. Grobe, Westfälische Wilhelms-Universität Münster, Germany
pBlueScript KSII:mouse Shh	Dr. A. McMahon, Harvard University, MA, USA
pCS2:GFP	Prof. Dr. U. Strähle, ITG, KIT, Karlsruhe, Germany
pDEST TM 14	Invitrogen, Darmstadt, Germany
pENTR TM 11	Invitrogen, Darmstadt, Germany
pSS26m	Covalys, Witterswil, Switzerland

2.1.11. Oligonucleotides

All oligonucleotides for PCR were purchased from Metabion (Martinsried, Germany) unless otherwise stated.

Oligonucleotide	Sequence (5' – 3')
EcoRIStartShhNF	5'-gaattcatgtgtgggcccgagg-3'
KpnISalIStartShhNF	5'-aattgggtaccgtcgacatgtgtgggcccgagggtttggaaagagg-3'
SalIStartShhNG35F	5'-aattcgtcgacatgcggcaccceaaaagctgacccc-3'
NotIStopHisShhNR	5'-aattggcggccgcctaatgatgatgatgatggccgccgatttgccgccacg g-3'

XhoIShhNR	5'-aattcctcgagcgcgccggattggccgccacgg-3'
NotIStopHisGFPR	5'-aattcgcggccgcctaataatgatgatgatgatgtttgtatagttcatccatgcc-3'
NotStopBAR	5'-aattggcggccgcctattcatgccattcaattttctgtgc-3'
Hind3HisGFPR	5'-aattgaagcttatgatgatgatgatgtttgtatagttcatccatgccatg-3'
NotIStopSNAPR	5'-aattggcggccgcctagcccagcccaggcttggccagtctgtggcc-3'

2.1.12. Recombinant proteins and antibodies

Recombinant protein	Supplier	
Recombinant mouse Sonic hedgehog, amino-terminal peptide (RCmShhN)	Neuromics, Edina, MN, USA	
	Species	Supplier
Primary antibody		
Anti-GFP antibody	Mouse	Cell signaling, Danvers, MA, USA
Anti-SNAP antibody	Rabbit	Prof. Dr. D. Wedlich, KIT, Karlsruhe, Germany
Monoclonal anti-Shh antibody 5E1	Mouse	Developmental Studies Hybridoma Bank (DSHB), Iowa City, IA, USA
Qiagen Penta-his antibody BSA-free	Mouse	Qiagen, Hilden, Germany
Shh (N-19):sc1194	Goat	Santa Cruz, Santa Cruz, USA
Shh antibody #2287	Rabbit	Cell signaling, Danvers, MA, USA
Secondary antibody	Supplier	
Alexa Fluor® 488 goat anti-mouse IgG	Invitrogen, Darmstadt, Germany	
Alexa Fluor® 546 donkey anti-goat IgG	Invitrogen, Darmstadt, Germany	
Alexa Fluor® 546 goat anti-mouse IgG	Invitrogen, Darmstadt, Germany	
Alexa Fluor® 546 goat anti-rabbit IgG	Invitrogen, Darmstadt, Germany	
Alexa Fluor® 591 goat anti-mouse IgG	Invitrogen, Darmstadt, Germany	
Alexa Fluor® 680 donkey anti-goat IgG	Invitrogen, Darmstadt, Germany	
Alexa Fluor® 680 goat anti-mouse IgG	Invitrogen, Darmstadt, Germany	
Alexa Fluor® 680 goat anti-rabbit IgG	Invitrogen, Darmstadt, Germany	
Anti-digoxigenin-AP, Fab fragments	Roche, Mannheim, Germany	
Anti-goat IgG peroxidase conjugate	Sigma-Aldrich, Munich, Germany	

2.1.13. RNA probes for *in situ* hybridization

Probe	Origin	Supplier
<i>nkx2.2b</i>	Zebrafish (wildtype)	Dr. L. Yang, ITG, KIT, Karlsruhe, Germany
<i>pax2a</i>	Zebrafish (wildtype)	Dr. L. Yang, ITG, KIT, Karlsruhe, Germany

2.1.14. Phospholipids

Phospholipids	Supplier
Biotinylated lipids	Dr. S. Sekula, INT, KIT, Karlsruhe, Germany
BG terminated lipids	Dr. A. Welle, IBG, KIT, Karlsruhe, Germany
DOPC	Dr. S. Sekula, INT, KIT, Karlsruhe, Germany
DOPE	Dr. S. Sekula, INT, KIT, Karlsruhe, Germany
Nickel chelating lipids	Dr. S. Sekula, INT, KIT, Karlsruhe, Germany

2.1.15. Disulfides

Compound	Supplier
BGT (C ₄₈ H ₈₂ N ₆ O ₉ S ₂) ¹ , FW: 951.3 g/mol	SensoPath, Bozeman, MT, USA
EG6OH (C ₄₆ H ₉₄ O ₁₄ S ₂), [913836-40-5], FW: 935.4 g/mol	Prochimia, Sopot, Poland

¹ This compound is not assigned a CAS-number (chemical abstract service). Its molecular structure is shown in figure 2.4.

2.1.16. Other materials or equipments

Material or equipment	Supplier
Gold coated sensor crystals (gold on chromium adhesion layer)	Q-Sense, Frölunda, Sweden
Immobilon™ PVDF transfer membranes	Millipore, Schwalbach/Ts., Germany
Lab-Tek™ II Chamber Slides™	Nunc, Wiesbaden, Germany
Low pressure mercury NNQ 8/18 lamp	Heraeus Noblelight, Kleinostheim, Germany
PD MiniTrap G25	GE Healthcare, Munich, Germany
Poly-Prep columns	Bio-Rad, Munich, Germany
Protein A Sepharose™ CL-4B	GE Healthcare, Munich, Germany
QCM-D	Q-Sense AB, Västra Frölunda, Sweden
Rotilabo®-syringe filters, pore size 0.22µm	Carl Roth, Karlsruhe, Germany
Silicon wafers with a 20nm chromium adhesion layer and a 200nm gold layer	Dr. M. Bruns, IAM-WPT, KIT, Karlsruhe, Germany
TOF.SIMS5	ION-TOF GmbH, Münster, Germany
UV/Ozone ProCleaner Plus	BioForce Nanosciences, Inc., Ames, IA, USA

2.2. Methods

2.2.1. Peptide sequences of ShhN variants

With reference to the peptide sequences of the biologically active ShhNp (p means processed) and the recombinant ShhN (referred as RCmShhN) purchased from Neuromics (Edina, MN, USA), and the poly(6)histidine sequence provided by the supplier, peptide sequences of different ShhN variants for bacterial expression were designed and are presented in table 2.1.

Name of protein	Size (kDa)	Schematic drawing (not to scale)
Shh-FL		
ShhNp	19.314	
RCmShhN	19.980	
ShhN-His	20.202	
ShhN-GFP-His	46.953	
ShhN-GFP-His-BA	48.840	
ShhN-GFP-His-SNAP	67.710	
ShhN-GFP-His-C25M_del26-34	45.843	
ShhN-GFP-His-SNAP-C25M_del26-34	66.600	

Table 2.1. Peptide sequence of ShhNp, RCmShhN and different versions of ShhN designed for bacterial expression and immobilization on nickel(II)-nitrilotriacetic acid (Ni-NTA), biotin-streptavidin (biotin-STV) and benzylguanidine (BG) functionalized surfaces.

ShhN encoded from amino acid residues C25 to G198 were fused with different tags for immobilization on nickel(II)-nitrilotriacetic acid (Ni-NTA), biotin-streptavidin (biotin-STV) or benzylguanine (BG) functionalized surfaces. Methionine (M) served as the starting site of translation. The poly(6)histidine tag was used for purification by immobilized metal affinity chromatography (IMAC) or immobilization of ShhN on Ni-NTA surfaces. Biotin adaptor (BA) was for biotin fusion to ShhN prior to immobilization of ShhN by biotin-streptavidine affinity. The benzylguanine transferase (SNAPTM) tag was for covalent binding of ShhN to benzylguanine thiol (BGT) for immobilization on gold surfaces. Green fluorescence protein (GFP) was for detection and visualization of ShhN. The number after the amino acid symbol represents the position of the amino acid in Shh-FL.

Similarly, variants of ShhN for eukaryotic expression were designed according to the peptide sequences of ShhNp and RCmShhN (Table 2.2). ShhNp and ShhN^{6×his} were biologically active ShhN. The DNA constructs were kindly provided by Dr. K. Grobe, Westfälische Wilhelms-Universität Münster, Germany.

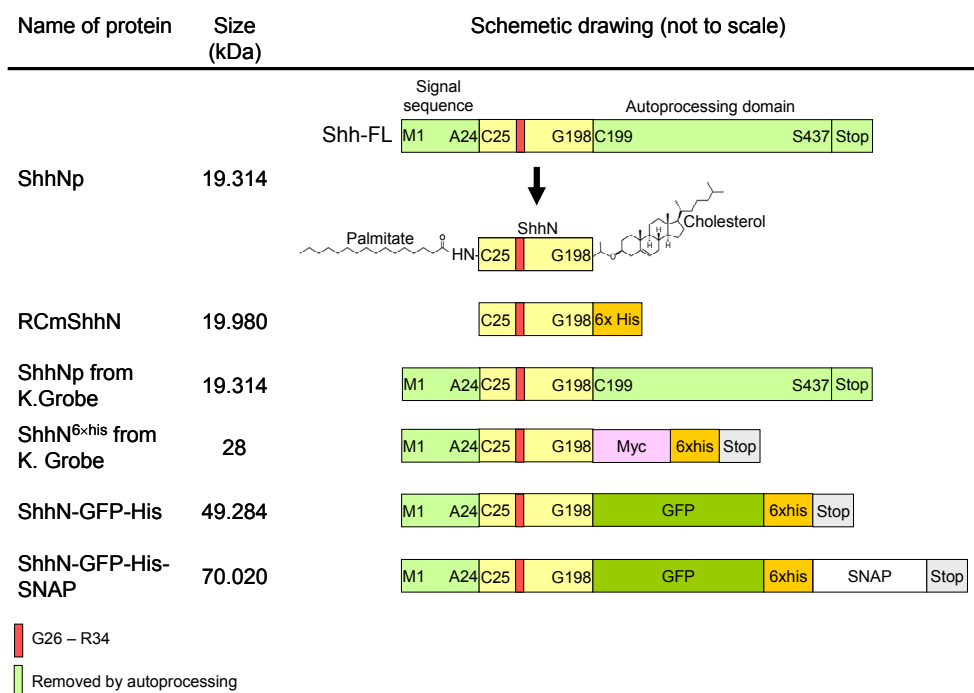


Table 2.2. Peptide sequence information of the eukaryotic expressed ShhN.

Eukaryotic expressed ShhN encoded from amino acid residues C25 to G198 were fused different tags for immobilization on Ni-NTA or BG functionalized surfaces. Methionine served as the starting site of translation. The signal sequence (M1 to A24) was responsible for ShhN secretion from the expressing cells. The poly(6)histidine tag was used for immobilization of ShhN on Ni-NTA surfaces. The SNAPTM tag was for covalent binding of ShhN to BGT for immobilization on gold surfaces. GFP was for detection and visualization of ShhN. The number after the amino acid symbol represents the position of the amino acid in Shh-FL.

ShhN proteins were prepared based on the sequences designed.

2.2.2. Polymerase chain reaction

DNA fragments of ShhN were amplified by polymerase chain reaction (PCR) with the plasmids shown in section 2.1.10 as templates; and the primers in section 2.1.11.

Reaction mixtures with the components described below were prepared in a total volume of 25 μ l.

10X polymerase buffer with MgSO ₄	2.5 μ l
25mM dNTPs	1 μ l
DNA template	100ng
10pmol/ μ l forward primer	1 μ l
10pmol/ μ l reverse primer	1 μ l
<i>Pfu</i> DNA polymerase	1U
H ₂ O	Fill up to 25 μ l

PCR reactions were conducted in GeneAmp® PCR System 9700 (Applied Biosystems, Carlsbad, CA, USA) with the following parameters.

94°C	45 sec	}	1 cycle	
94°C	30 sec		}	35 cycles
60°C – 68°C	1 min			
72°C	1 – 2 min			
72°C	10 min			1 cycle

The PCR products were stored at 4°C or subjected directly to agarose gel electrophoresis.

2.2.3. Agarose gel electrophoresis

1.5g of powder agarose was dissolved in 100ml of 1X TAE buffer by heating in the microwave oven. 0.5 μ g/ml of ethidium bromide (EtBr) was added to the melted agarose. The agarose was then poured into a gel casting tray equipped with a comb and was allowed to set at room temperature (RT). The comb was removed after the gel was set. Next agarose gel was placed in the electrophoresis chamber filled with 1X TAE buffer.

5 μ l of 6X DNA loading buffer was mixed into the 25 μ l PCR products and loaded into the gel wells. GeneRulerTM 1kb Plus DNA Ladder (Fermentas, St. Leon-Rot, Germany) was used as a size reference. The electrophoresis chamber was connected to the power supply. The gel was run at 130 Volts.

After electrophoresis the gel was exposed to UV light at $\lambda = 185\text{nm}$ in the Gel Doc system (Bio-Rad, Munich, Germany). DNA separation was recorded by photography.

2.2.4. Purification of DNA from agarose gel

DNA with correct size was cut from the agarose gel with a razor blade. The DNA was extracted and purified using the peqGold gel extraction kit (Peqlab, Sarisbury Green, UK) according to the manufacturer's instruction.

2.2.5. Restriction endonuclease digestion of DNA

Reaction mixture with the manufacturer recommended buffer (Fermentas, St. Leon-Rot, Germany) was set up as the following:

10X buffer	2 μ l
DNA	1 μ g
Restriction endonuclease	1U
H ₂ O	Fill up to 20 μ l

Reaction was allowed to take place at 37°C for 1 to 3 hours.

Digested DNA fragments were examined by agarose gel electrophoresis.

2.2.6. DNA ligation

DNA ligation reaction was carried out with T4 DNA ligase (Fermentas, St. Leon-Rot, Germany) according to the manufacturer's instruction.

2.2.7. Subcloning of ShhN into pENTRTM11 and pDESTTM14 vectors

DNA fragments of ShhN were subcloned into pENTRTM11 and pDESTTM14 with Gateway® LR ClonaseTM II enzyme mix (Invitrogen, Darmstadt, Germany) according to the manufacturer's instructions.

2.2.8. DNA sequencing

DNA plasmids were sent to either GATC Biotech AG (Konstanz, Germany) or Qiagen Sequencing Services (Hilden, Germany) for sequencing.

2.2.9. Transformation of *Escherichia coli*

For all *Escherichia coli* (*E. coli*) strains used, including BL-21, *ccdB* Survival T1^R, DB3.1TM, DH5 α , TOP10, and XL1-Blue, 50 μ l of the competent bacteria was taken out from -80°C freezer and thawed on ice. 1 μ g DNA plasmid was added to the thawed competent *E. coli*, incubated on ice for 10 to 30 minutes and heat-shocked at 42°C for 2 minutes. 500 μ l LB or SOC medium without antibiotics was added to the bacteria. Next, the transformed bacteria was grown at 37°C for 1 hour with aeration. The propagated bacteria was spread on bacto-agar plate with antibiotics and incubated at 37°C overnight for colony formation.

2.2.10. Protein production in prokaryotic (bacterial) expression system

DNA construct for protein expression was transformed into the *E. coli* strain BL-21. Single bacterial colony was picked for an overnight culture at 37°C in LB medium. The overnight culture was diluted to OD₆₀₀ = 0.1 in LB medium to 100ml and was allowed to grow at 37°C until the OD₆₀₀ reached 0.4 to 0.6. Protein expression was induced by addition of 0.5mM isopropyl β -D-1-thiogalactopyranoside (IPTG) into the bacterial culture. The culture was incubated at 37°C with aeration for 2.5 hours and then harvested.

2.2.11. Extraction and purification of bacterial expressed ShhN

Bacterially expressed protein was extracted by lysis and purified either using the Ni-NTA purification system (Invitrogen, Darmstadt, Germany) according to the manufacturer's instruction or by immobilized metal affinity chromatography (IMAC) with Ni-NTA agarose (Qiagen, Hilden, Germany).

Reagents for protein extraction and purification were stored at 4°C. The extraction and purification procedures were conducted on ice in 4°C cold room unless otherwise stated.

Bacterial pellet was obtained by centrifugation at 4000rpm at 4°C for 30 minutes. The pellet was washed with 10ml ice cold 20mM Tris, pH8.0. The washed pellet was stored at -20°C or directly homogenized and lysed in 10ml Ni-NTA purification cell lysis buffer. The homogenized pellet was incubated on ice for 30 minutes and then subjected to sonication for 3 minutes with pulses for complete bacterial cell lysis. Next, bacteria was centrifuged at 4000rpm at 4°C for 30 minutes. Supernatant was collected in a new 50ml centrifuge tube. 2ml of 50% Ni-NTA agarose slurry (Qiagen, Hilden, Germany) was added to the supernatant. The supernatant was rocked at 4°C for 1 hour. The protein bound agarose was spinned down by centrifugation at 1000rpm at 4°C for 2 minutes and washed 3 times with 8ml Ni-NTA purification washing buffer. The agarose was then transferred to a vertically equipped Poly-Prep column (Bio-Rad, Munich, Germany) and washed for another 3 times by gravity with 8ml Ni-NTA purification washing buffer. Protein was eluted from the column with 500µl Ni-NTA purification elution buffer and collected in a 1.5ml microcentrifuge tube on ice.

Buffer exchange for bacterial expressed and purified protein to 1X phosphate buffered saline (PBS) (Invitrogen, Darmstadt, Germany) supplemented with 0.5mM DTT was performed on ice at 4°C with PD MiniTrap G25 (GE Healthcare, Munich, Germany) according to the manufacturer's instruction.

2.2.12. Biotinylation of ShhN-GFP-His, the ShhN variant with a C-terminal biotin acceptor

Biotinylation was done at the biotin acceptor, which was composed of a 15-mer peptide sequence of GLNDIFEAQKIEWHE (Staszczak, 2007), at the C-terminal of bacterial expressed ShhN-GFP-His-BA, using biotin protein ligase (GeneCopoeia, Rockville, MD, USA) according to the manufacturer's instruction. The resulting biotinylated protein was ShhN-GFP-His-Biotin.

2.2.13. Immunoprecipitation

25mg of protein A SepharoseTM CL-4B (GE Healthcare, Munich, Germany) was immersed in 1.5ml 1X TBS and was rocked at 4°C for 2 days. 250µl of the monoclonal anti-Shh antibody 5E1 (Developmental Studies Hybridoma Bank (DSHB), Iowa City, IA, USA) was added to the fully soaked sepharose beads. The sepharose-antibody mixture was rocked at 4°C overnight. The antibody bounded sepharose beads were spinned down by centrifugation at 1000rpm at 4°C for 3 minutes, washed with 1.5ml 1X TBS, and resuspended in 100µl 1X TBS. The beads were either stored at 4°C or used directly for immunoprecipitation.

100µl of the purified bacterial expressed protein after buffer exchange was mixed with 1.5ml 1X TBS and 10µl of the 5E1 bound sepharose beads. The mixture was rocked at 4°C overnight. The beads were spinned down by centrifugation at 1000rpm at 4°C for 3 minutes, washed with 1.5ml 1X TBS and resuspended in 15µl Lämmli sample buffer. Shh-5E1 binding was analyzed by SDS-PAGE and Western blot.

2.2.14. SDS-polyacrylamide gel electrophoresis (SDS-PAGE)

A large glass with 0.75mm thick spacers on both sides and a small glass were slipped in a polyacrylamide gel casting stand (Bio-Rad, Munich, Germany). Leakage was checked by applying EtOH in between the glasses.

Polyacrylamide gel was prepared as the followings.

5% Stacking gel	H ₂ O	1.4ml
	1M Tris pH6.8	250µl
	30% acrylamide	330µl
	10% SDS	20µl
	10% APS	20µl
	TEMED	2µl
15% separation gel	H ₂ O	1.1ml
	1.5M Tris pH8.8	1.3ml
	30% acrylamide	2.5ml
	10% SDS	50µl
	10% APS	50µl
	TEMED	2µl

The 15% separation gel was poured into the glass sandwich. A layer of isopropanol was added above the gel to prevent from drying. The isopropanol was removed and

the space was loaded with the 5% stacking gel. A comb with 10 wells was inserted at the upper edge of the stacking gel. The gel was allowed to set at room temperature.

The set gel was placed in a SDS-PAGE chamber (Bio-Rad, Munich, Germany) fully filled with 1X SDS-PAGE running buffer. Lämmli buffer mixed protein samples were loaded into the wells generated with the combs. The SDS-PAGE chamber was connected to the power supply and the gel was run at 80 Volts per 10 cm gel length.

2.2.15. Integrity analysis and quantification of bacterial expressed ShhN

Protein gel obtained after SDS-PAGE was stained with Coomassie blue protein staining solution at room temperature for 15 minutes to 1 hour. The stained gel was then washed with Coomassie gel destaining solution several times until bands of the purified ShhN proteins were clearly visible on the gel. The Coomassie staining was recorded by scanning the gel by Odyssey[®] infrared imaging system (LI-COR[®], Lincoln, NE, USA).

Known concentration of bovine serum albumin (BSA) loaded for SDS-PAGE was used as a standard for protein quantification.

2.2.16. Western blot analysis

Protein gel obtained after SDS-PAGE was situated on 2 pieces of Whatmann filter paper and a piece of sponge, which were wetted in advance with 1X SDS electroblotting buffer. A piece of MeOH activated PVDF transfer membrane (Millipore, Schwalbach/Ts., Germany) was placed on top of the gel and covered with another 2 pieces of Whatmann filter paper and a piece of sponge. The sandwich was fitted in a cassette and chamber was filled with 1X SDS electroblotting buffer with the gel facing to the negative electrode and the membrane to the positive electrode. The cassette was connected to the power supply and the transfer was run at 100 Volts at room temperature for 1 hour.

The membrane after transfer was blocked overnight in Western blot blocking buffer at 4°C with rocking. The membrane was then incubated with primary antibody solution in blocking buffer at room temperature with rocking for 1 hour. Next membranes were rinsed 2 times with 1X TBST, each for 5 minutes. The membrane was exposed to secondary antibody (dilution 1:5000) solution in blocking buffer in dark at room temperature with rocking for 1 hour. The membrane was washed 3 times with 1X TBST, each for 5 minutes and analyzed by Odyssey[®] infrared imaging system (LI-COR[®], Lincoln, NE, USA).

Western blot with Shh antibody #2287 (dilution 1:1000; Cell Signaling, Danvers, MA, USA), Shh (N-19):sc1194 (dilution 1:20; Santa Cruz, Santa Cruz, USA), Penta-his (dilution 1:500; Qiagen, Hilden, Germany) and anti-SNAP antibody (dilution 1:1000; kindly provided by Prof. Dr. D. Wedlich, KIT, Karlsruhe, Germany) antibodies were conducted for the 5E1 immunoprecipitated ShhN.

2.2.17. Subcloning of signal sequence containing ShhN into pcDNA3.1 vector

DNA fragment of the Shh signal sequence (M1 to A24) and ShhN was cut out from the ShhNp construct (Dr. K. Grobe, Westfälische Wilhelms-Universität Münster, Germany) at the restriction endonuclease digestion sites of HindIII and SphI. DNA fragments encoding GFP, poly(6)histidine, SNAPTM and stop codon were cut out from the pENTRTM11 construct at the SphI and NotI sites. The DNA fragments obtained from both constructs were then subcloned into the HindIII and NotI sites of the pcDNA3.1 vector.

2.2.18. mRNA preparation

mRNA was prepared using the mMessage Machine® T7 kit (Ambion, Austin, TX, USA) according to the manufacturer's instruction with pcDNA3.1 empty vector, and constructs of ShhNp (kindly provided by Dr. K. Grobe, Westfälische Wilhelms-Universität Münster, Germany), ShhN-GFP-His and ShhN-GFP-His-SNAP (Table 2.2) as templates.

2.2.19. Maintenance and raising of zebrafish (*Danio rerio*)

Adult zebrafish were maintained in fish water at 28°C in the fish facility at Karlsruhe Institute of Technology (KIT) Campus North.

Embryos were obtained by mating adult zebrafish (AB₂O₂ strain) in pairs. Laid embryos was collected and washed with fish water in a mesh. Next washed embryos

were kept in Petri dishes at 28°C in fish water supplemented with 0.01% methylene blue to prevent fungal growth. 5-day-old larvae were transferred to fish tanks. Feeding was started.

2.2.20. Microinjection of mRNA into zebrafish embryos

Wildtype (AB₂O₂ strain) adult zebrafish were mated in pairs. Embryos were collected and washed with fish water in a mesh right after they were laid. Embryos were maintained in fish water at 28°C.

Microinjection of 600ng/μl mRNA of the full length zebrafish *shh* (*shh*-FL) or 1μg/μl mRNA of eukaryotic expressed *ShhN*-GFP-His and *ShhN*-GFP-His-SNAP was performed when the embryos were at 1-cell stage with Eppendorf FemtoJet[®] microinjector (Eppendorf, Hauppauge, NY, USA).

2.2.21. *In situ* hybridization

In situ hybridization (ISH) of the sonic hedgehog (*shh*) target genes *nkx2.2b* and *pax2a* was done for the zebrafish embryos at 18-somite stage.

On the day before ISH, zebrafish embryos at 18-somite stage after mRNA microinjection were washed with 1X PBS and fixed in 4% BT-fix at 4°C overnight to maintain the injected embryos at the desired developmental stage and preserve the mRNA for detection by RNA probes.

On day 1, the zebrafish embryos were rinsed once with 1X PBT and washed 4 times with 1X PBT, each for 5 minutes. The embryos were then incubated in 10µg/ml Proteinase K in 1X PBT at room temperature for 6 minutes. The Proteinase K was removed and replaced by 4% BT-fix. The embryos were incubated at room temperature for 20 minutes, washed 5 times with 1X PBT, each for 5 minutes and next rinsed once in hybridization buffer (HYB) at room temperature. The embryos were then prehybridized in HYB at 70°C for at least 4 hours to homogenize the *in vivo* microenvironment. The embryos were hybridized overnight with the DIG-labeled RNA probes of *nkx2.2b* and *pax2a* (dilution 1:400) in HYB at 70°C. Two or three embryos were used for overnight preabsorption of the anti-digoxigenin-AP, Fab antibody fragments (Roche, Mannheim, Germany) in blocking buffer at 4°C.

On day 2, hybridized embryos were washed twice in solution 50% formamide with 50% (2X SSC/0.1% Tween-20) at 70°C, each for 30 minutes; next washed once with 2X SSC/0.1% Tween-20 at 70°C for 15 minutes; and twice in 0.2X SSC/0.1% Tween-20 at 70°C, each for 30 minutes. Finally embryos were rinsed with solution 50% (0.2% SSC/0.1 Tween20) / 50% 1X PBT at 70°C. The embryos were washed in ISH blocking buffer at room temperature for 5 minutes and incubated in new blocking buffer at room temperature for 3 to 4 hours. Next embryos were incubated overnight in the preabsorbed anti-digoxigenin-AP, Fab antibody fragment (dilution 1:4000) solution in the blocking buffer at 4°C.

On day 3, embryos were rinsed twice with 1X PBT at room temperature. They were next washed 6 times in 1X PBT at room temperature, each for 15 minutes and twice in alkaline phosphatase (ALP) staining buffer at room temperature, each for 5 minutes. The embryos were transferred to a 24-well plate and stained in

5-bromo-4-chloro-3-indolyl phosphate (BCIP) / nitro blue tetrazolium chloride (NBT), toluidine salt in 67% dimethyl sulfoxide (DMSO) (v/v) (Roche, Mannheim, Germany) in the ALP staining buffer at room temperature until signal revealing the target gene expression was observed. The staining reaction was stopped by removing the ALP staining buffer. The stained embryos were washed 5 times in 1X PBT at room temperature, each for 5 minutes and fixed in 4% BT-fix at room temperature for 1 hour. Next fixed embryos were rinsed twice with 1X PBT at room temperature and washed 4 times in 1X PBT at room temperature, each for 5 minutes. Stained embryos were kept overnight in 1X PBT in dark at room temperature in order to dilute the background formed by unspecific probe and antibody binding . After that step the embryos were ready for microscopic imaging.

For long term storage, the stained embryos were kept in 70% glycerol/1X PBT in dark, at room temperature.

2.2.22. Optical microscopy and image acquisition of zebrafish embryos

Zebrafish embryos after ISH were visualized under a stereomicroscope (model MZ16F, Leica, Solms, Germany) equipped with a CCD digital camera (model DFC320). Images revealing gene expression patterns were taken and processed using Adobe Photoshop CS3.

2.2.23. Cell culture

2.2.23.1. HEK293 cells for eukaryotic expression of ShhN

The HEK293 cell line was derived from human embryonic kidney cells.

It was maintained at 37°C with 5% CO₂ in Dulbecco's modified Eagle's medium (DMEM) (Invitrogen, Darmstadt, Germany) supplemented with 10% fetal bovine serum (FBS) (PAA, Linz, Austria).

To express ShhN, the cells were seeded in 6-well tissue culture plate, 2×10^4 cells/cm², 24 hours prior to transfection. 24 hours later the cells were transfected as described in section 2.2.25.

2.2.23.2 C3H10T1/2 clone 8 cells for biological activity analysis of ShhN by alkaline phosphatase assays

C3H10T1/2 clone 8, a murine pluripotent mesenchymal cell line, was purchased from American Type Culture Collection (ATCC) (LGC Standards) (Wesel, Germany). Cells were expressing alkaline phosphatase (ALP), a marker of chondrogenic differentiation induced by Shh.

The cell line was cultivated at 37°C with 5% CO₂ with a density of 2,000 cells/cm² in basal medium Eagle (BME) (Invitrogen, Darmstadt, Germany) supplemented with 2mM L-glutamine (Invitrogen, Darmstadt, Germany) and 10% heat-inactivated FBS (PAA, Linz, Austria). Cells were split after reaching 70% confluency.

For biological activity analyses of ShhN, the cells were cultured in Dulbecco's modified Eagle's medium (DMEM) (Invitrogen, Darmstadt, Germany) supplemented with 0.5% FBS and the soluble ShhN (i.e. non-immobilized form of ShhN) or the Shh agonist SAG; or immobilized ShhN or SAG on modified surfaces (details can be found in section 2.2.26). Treated cells were incubated at 37°C with 5% CO₂ for 5 days. After 5 days, ALP assay was carried out as described in sections 2.2.27 and 2.2.28.

2.2.23.3 Shh LIGHT II for biological activity analysis of ShhN by Gli-luciferase assay

The Shh LIGHT II cell line was kindly provided by Dr. A. Büttner, University of Leipzig, Germany. This cell line is derived from the NIH/3T3 cells stably transfected with the Gli responsive firefly luciferase reporter gene (Sasaki et al., 1997). In the presence of Shh, the cells responded by producing firefly luciferase, a light generating enzyme, the activity of which can be measured with a luminometer after addition of Shh or the Shh agonist SAG.

For routine maintenance, Dulbecco's modified Eagle's medium (DMEM) (American Type Culture Collection (ATCC) (LGC Standards), Wesel, Germany) was used with a supplement of 10% FBS, 0.15mg/ml zeocin (Invitrogen, Darmstadt, Germany) and 0.4mg/ml geneticin (G-418) (Invitrogen, Darmstadt, Germany).

DMEM (ATCC (LGC Standards), Wesel, Germany) supplemented with 0.5% FBS was used for treatment of the cells with ShhN expressed in *E. coli* or the HEK293 cells.

2.2.24. Propagation, freezing and thawing of cells

For propagation of the HEK293, C3H10T1/2 clone 8 and Shh LIGHT II cell lines in T-75 cell culture flasks, cells at 80 – 90% confluency were washed twice with 1X PBS, trypsinized with 1ml trypsin for 5 minutes at 37°C, resuspended in 10ml medium and collected by centrifugation. Cells were resuspended at dilution 1:10 in complete medium and cultured at 37°C with 5% CO₂.

For freezing, cells were washed twice with 1X PBS, trypsinized and collected by centrifugation. Complete medium supplemented with 5% DMSO (Fluka (Sigma-Aldrich), Munich, Germany) was used to resuspend the cells. Resuspended cells (3×10^6 cells/ml for HEK293; 1.5×10^5 cells/ml for C3H10T1/2 clone 8; and 4×10^5 cells/ml for Shh LIGHT II) were transferred to cryotubes in the cryogenic freezing container and kept at -80°C overnight. Frozen cells were next transferred to cryobox in liquid nitrogen container for long term storage.

For thawing, frozen cells were taken out from the liquid nitrogen container and thawed quickly in 37°C water bath. The thawed cells were inoculated in fresh medium without antibiotics. After 24 hours the medium was replaced with fresh complete medium with antibiotics.

2.2.25. Transfection of HEK293 cells

pcDNA3.1 empty vector, and constructs of ShhNp (from Dr. K. Grobe), ShhN-GFP-His and ShhN-GFP-His-SNAP (Table 2.2) were transfected into HEK293 cells with PolyPlus jetPEI transfection reagent in fresh complete medium, which is

composed of Dulbecco's modified Eagle's medium (DMEM) and 10% FBS, according to the manufacturer's instruction.

Transfected cells were further cultured at 37°C with 5% CO₂ for 48 hours. Conditioned medium from each transfection was collected and filtered through 22µm syringe filters (Carl Roth, Karlsruhe, Germany) to get rid of any cell debris. The collected conditioned medium was stored at 4°C and used for ShhN treatment on C3H10T1/2 clone 8 or Shh LIGHT II cells, or ShhN immobilization on modified surfaces within 24 hours.

2.2.26. Treatment of C3H10T1/2 clone 8 and Shh LIGHT II cells

Different concentrations of the Shh agonist SAG, RCmShhN or bacterially expressed ShhN, or different volume ratios of conditioned media of eukaryotic expressed ShhN were added to the C3H10T1/2 clone 8 cells or Shh LIGHT II cells with the medium conditions described in sections 2.2.23.2 and 2.2.23.3.

The treated C3H10T1/2 clone 8 and Shh LIGHT II cells were maintained at 37°C with 5% CO₂ for 5 days and 48 hours, respectively. Alkaline phosphatase assays were then carried out for cellular response analysis in C3H10T1/2 clone 8 cells. Shh LIGHT II cells were used for Gli-luciferase assay.

For determining the presence of ShhN in the conditioned media of the HEK293 cells transfected with ShhN DNA constructs, the filtered conditioned media were added to the C3H10T1/2 clone 8 or Shh LIGHT II cells together with the Shh antibody 5E1, which prevents Shh from binding to its receptor Patched (Ptc), at dilution 1:5. The

recombinant ShhN signaling domain was fused with green fluorescent protein (GFP). Anti-GFP antibody (dilution 1:250; Cell Signaling) was used to test GFP effect on the ligand binding to Ptc.

2.2.27. Alkaline phosphatase expression assay and cell counting

After 5 days incubation of C3H10T1/2 clone 8 cells with soluble or immobilized ShhN, the cells were fixed with 4% paraformaldehyde (PFA) at room temperature for 20 minutes, washed 6 times with 1X PBS and detected with the BCIP/NBT substrate in dark at room temperature for ALP expression, which acts as a read-out of chondrogenic differentiation of the C3H10T1/2 clone 8 cells in response to Shh induced signaling. Figure 2.1 illustrates response of the C3H10T1/2 clone 8 cells to 50nM RCmShhN (Neuromics, Edina, MN, USA), which serves as the positive control for ALP expression in response to Shh induced signaling.

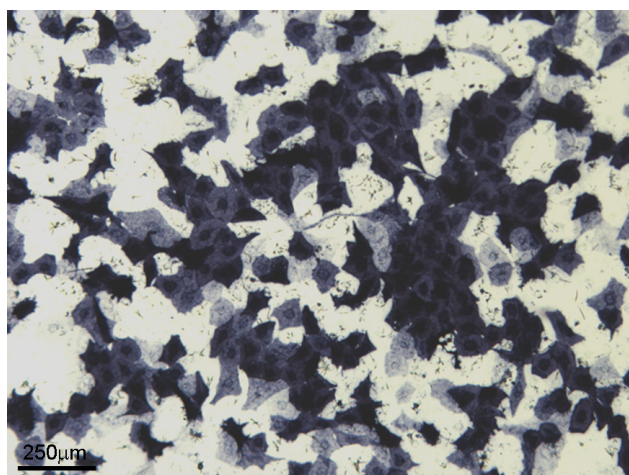


Figure 2.1. Expression of alkaline phosphatase by C3H10T1/2 clone 8 cells. Cells were treated with 50nM RCmShhN. Cell staining indicates the cellular response to Shh induced signaling and cell differentiation.

To analyze the biological activity of soluble ShhN, staining for ALP in the C3H10T1/2 clone 8 cells was done. Cells were seeded on a 4- or 8-chambered slide (Nunc, Wiesbaden, Germany) with the density of 5×10^3 cells/cm² 24 hours prior to the addition of ShhN to the medium. After protein addition, the cells were cultivated for 5 days at 37°C with 5% CO₂. Staining for ALP and cell counting for ALP expressing cells were done.

For functional analysis of immobilized ShhN, C3H10T1/2 clone 8 cells were cultured on the functionalized protein surface for 5 days as described. Staining for ALP and cell counting were performed.

For the eukaryotic expressed ShhN, all measurements were normalized by converting the quantity of ShhN to volume ratios of the ShhN containing conditioned medium to the differentiation medium composed of DMEM and 0.5% FBS.

2.2.28. Alkaline phosphatase colorimetric assay

To quantify the biological activity of soluble ShhN in the C3H10T1/2 clone 8 cells, cells were seeded on 24-well tissue culture plates, 5×10^3 cells/cm². For the functionalized protein surfaces, the area of cultivation was restricted to 1cm² to standardize the cell number and volume of medium. All treatments and quantifications of ALP expression were conducted in triplicates.

After 5 days of treatment, the ShhN treated C3H10T1/2 clone 8 cells were washed twice with 1X PBS on ice. The assay was conducted with the alkaline phosphatase

colorimetric assay kit (Abcam, Cambridge, UK) according to the manufacturer's instruction.

2.2.29. Gli-luciferase reporter assay

Three days before ShhN treatment, the Shh LIGHT II cells were cultivated with the density of 5×10^4 cells/cm² in a 24-well plate format. Different volume ratios of the ShhN conditioned medium to the assay medium, DMEM, 0.5% FBS and 5mM 4-(2-hydroxyethyl)-1-piperazineethanesulfonic acid (HEPES) (pH7.4), were added to the wells accordingly. Treated cells were kept at 37°C with 5% CO₂ for 48 hours.

On the day of luciferase assay, treated cells were gently washed twice with 1X PBS. 100µl 1X passive lysis buffer (Promega, Mannheim, Germany) was added to the cleaned cell layer on ice. Cell lysis progress was monitored regularly for about 1 hour, visible individual nuclei observed under stereomicroscope. The cell layer was scraped to facilitate further lysis. 20µl of the cell lysate was transferred to a white 96-well plate. Firefly luciferase activity was measured with Wallac 1420 luminescence counter (Perkin Elmer, Waltham, MA, USA) and was normalized to *Renilla* luciferase activity (*Ubi-Renilla*).

2.2.30. Immunofluorescence of cells

Cells were washed once with cell culture medium without FBS and twice with 1X PBS containing Ca²⁺ and Mg²⁺ (PBS⁺⁺). Next cells were fixed in 4% PFA at room temperature for 20 minutes. The fixed cells were rinsed 3 times with PBS⁺⁺ and permeabilized with 0.2% Triton X-100 solution in PBS⁺⁺ at room temperature for 10

minutes. Next cells were rinsed 3 times with PBS++ and blocked in 1% BSA in PBS++ solution at room temperature for 15 minutes. The blocked cells were rinsed twice with PBS++ and incubated in 100µl primary antibody in 1% BSA in PBS++ solution at room temperature for 1 hour. The cells were rinsed three times with PBS++, blocked in 1% BSA in PBS++ at room temperature for 15 minutes and rinsed twice with PBS++. 100µl of secondary antibody solution carrying a fluorescence label (dilution 1:500) in 1% BSA in PBS++ was added to the cells. The cells were incubated in dark at room temperature for 1 hour. Next cells were rinsed 3 times with PBS++ at room temperature, mounted with 96% glycerol and imaged under fluorescence microscope.

Immunofluorescence of transfected HEK293 cells were performed with the Shh antibody #2287 as the primary antibody (dilution 1:50) in 1% BSA in PBS++ and Alexa Fluor® 488 goat anti-rabbit IgG (dilution 1:500) as the secondary antibody.

2.2.31. Microscopy and imaging of cells

Cells were visualized under an upright compound microscope (model DM5000B, Leica, Solms, Germany) equipped with DIC optics and different fluorescence channels. Images were taken with the DFC300FX digital camera and processed using Adobe Photoshop CS3.

2.2.32. UV photopatterning and nickel functionalization of polystyrene surfaces

Glass slides were spin-coated applying a solution of 5% polystyrene in toluene at 3,000rpm. They were then irradiated with UV from a low pressure mercury NNQ 8/18 lamp (Heraeus Noblelight, Kleinostheim, Germany). This lamp has a 254nm, quartz tube, 10W, providing a UV irradiation density of $200\mu\text{W}/\text{cm}^2$ at $\lambda = 185\text{nm}$ as measured with a calibrated UV power meter (traceable to NIST USA) (C8026, Hamamatsu Photonics K.K., Japan). It emits mainly the two sharp mercury UV spectral lines, nearly no visible light and no infra red, therefore sample heating during irradiation is negligible. After 20 minutes of UV irradiation, carboxyl (COOH) groups were formed at the polymer surfaces. The polymer surfaces were functionalized to provide a nickel chelating moiety. The COOH groups on the polystyrene surface obtained by deep UV lithography were activated with an EDC/NHS reactive ester and reacted with N_2,N_2 -bis (carboxymethyl)-lysine forming the nickel chelating group. Activated surfaces were loaded with Ni^{2+} ions from an aqueous 40mM NiSO_4 solution. The slides could be kept dry in air until protein coating or incubation directly with 50nM ShhN-GFP-His in PBS at 37°C for 24 hours (Figure 2.2).

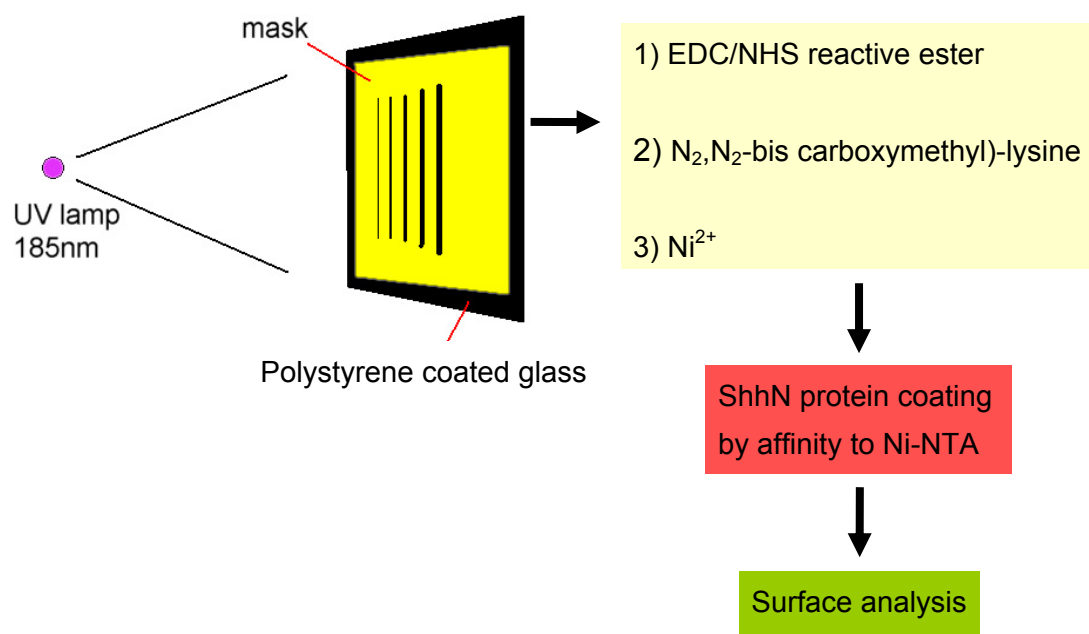


Figure 2.2. Procedure of immobilizing ShhN-GFP-His on UV irradiated and nickel functionalized polystyrene surfaces.

2.2.33. Immobilization of ShhN on surfaces functionalized via dip-pen nanolithography

By functionalizing surfaces with nickel, biotin and benzylguanine modified phospholipids with dip-pen nanolithography (DPN), ShhN proteins fused with poly(6)histidine, biotin and SNAPTM tags were immobilized.

2.2.33.1 Immobilization of ShhN-GFP-His via nickel(II)/poly(6)histidine affinity interaction on nickel chelating lipid functionalized surfaces

Glass slides were coated with 1mg/ml poly(L-lysine)-graft-poly(ethylene glycol) (PLL-g-PEG) (surface solution) for 30 minutes, washed with Milli Q water and blown dry with nitrogen. The polyethylene glycol (PEG) compound possesses biomaterial repulsive properties when applied on untreated (hydrophilic) glass surfaces and prevents protein or cell adhesion, thereby minimizing unspecific binding (Deglau et al., 2006; Tessmar and Göpferich, 2007). Dioleoylphosphatidylcholine (DOPC) lipids were found to be a suitable ink for DPN (Lenhert et al., 2007). It was mixed with different molar percentage/ratio (mol%) of nickel chelating lipids and used for DPN on the PEG coated glass surfaces. The substrates were then blocked with 0.5% BSA at room temperature for 30 minutes, washed twice with PBS and exposed to either 1 μ M *E. coli* expressed ShhN-GFP-His solution or undiluted conditioned medium collected from the HEK293 cells transfected with the DNA construct of ShhN-GFP-His. The adsorption of protein took place at room temperature for 30 minutes (Figure 2.3).

2.2.33.2 Immunofluorescence of ShhN-GFP-His bound onto nickel functionalized polyethylene glycol surfaces

After protein binding the functionalized surfaces were blocked in 0.5% BSA in PBS at room temperature for 30 minutes. Next substrates were washed twice with PBS at room temperature, each for 5 minutes and were incubated in the solution of Shh antibody 5E1 (dilution 1:10) in PBS at room temperature for 1 hour. The surfaces were washed twice with PBS at room temperature, each for 5 minutes and were incubated with the Alexa Fluor® 488 goat anti-mouse IgG antibody solution (dilution 1:500) in PBS at room temperature for 1 hour. After two washes in PBS at room temperature, each for 5 minutes, the surfaces were examined by fluorescence microscopy.

2.2.33.3 Immobilization of ShhN-GFP-His-Biotin via biotin/streptavidin affinity interaction on biotinylated lipid functionalized glass surfaces

Glass slides were coated with 1mg/ml PLL-g-PEG (surface solution) for 30 minutes, washed with Milli Q water and dried with nitrogen. DOPC lipids admixed with 0 to 8mol% of biotinylated lipids were used for DPN on the PEG coated glass surfaces. The patterned substrates were blocked with 0.5% BSA at room temperature for 30 minutes, washed twice with PBS and coated with 5µg/ml streptavidin at room temperature for 30 minutes. Next samples were washed three times and finally exposed to 1µM ShhN-GFP-His-Biotin solution at room temperature for 30 minutes.

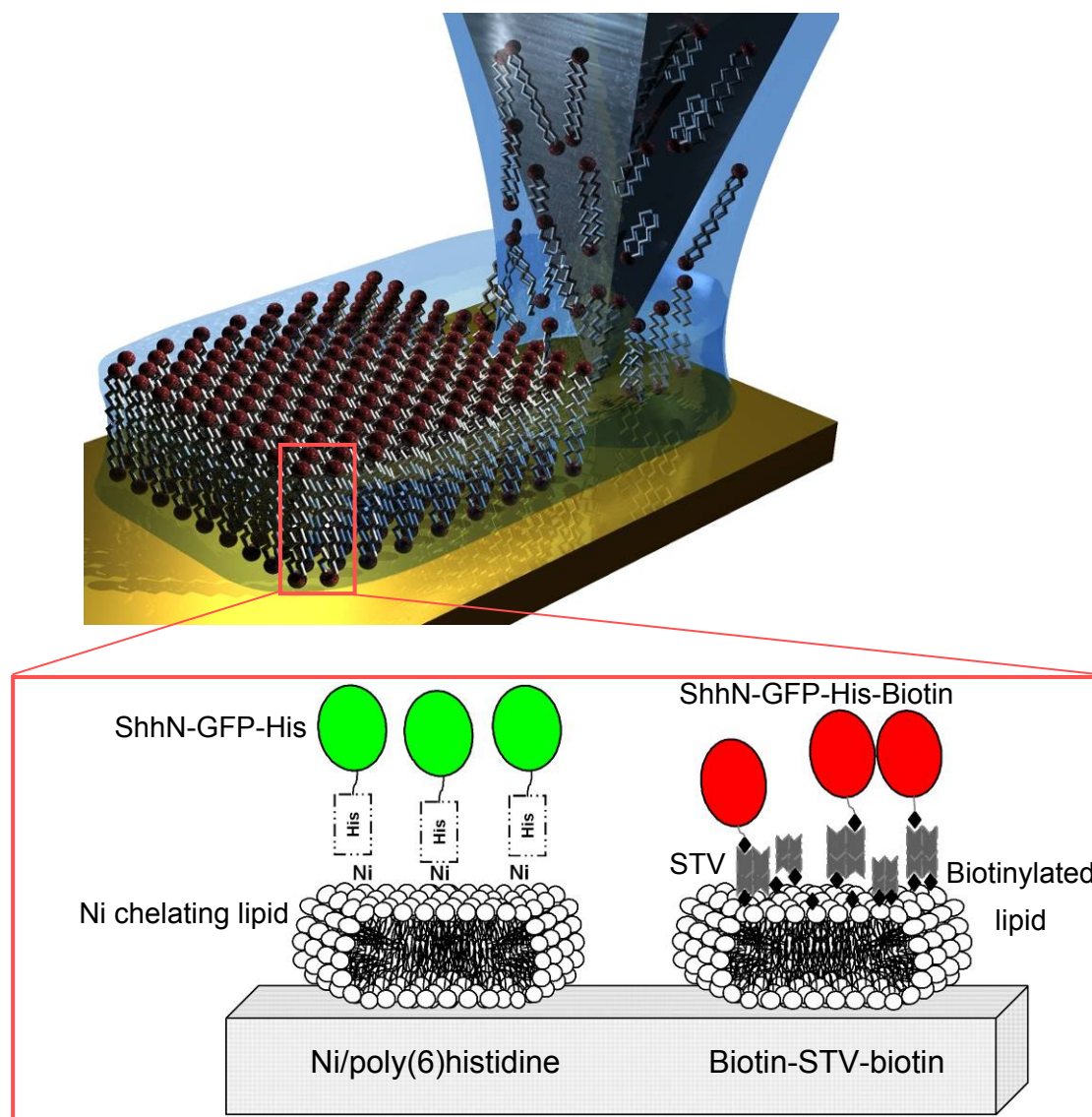


Figure 2.3. Scheme of immobilizing biotinylated and poly(6)histidine-tagged Shh protein on biotin-streptavidin and nickel functionalized surfaces by DPN (Adapted from Sekula et al., 2008)

2.2.33.4 Covalent immobilization of ShhN-GFP-His-SNAP by benzylguanine/SNAPTM reaction

DOPC lipids mixed with BG terminated dioleoylphosphatidylethylene (DOPE) lipids at the ratio 1:1 were deposited via DPN on polystyrene coated glass surfaces. The substrates were blocked with 0.5% BSA at room temperature for 30 minutes, washed

three times with PBS and then exposed to 1 μ M ShhN-GFP-His-SNAP protein solution at room temperature for 30 minutes.

2.2.33.5 Immunofluorescence of ShhN-GFP-His-SNAP on benzylguanine functionalized polystyrene surfaces

For immunodetection of the SNAPTM tag, the anti-SNAP antibody (kindly provided by Prof. Dr. D. Wedlich, KIT, Karlsruhe, Germany) was used as the primary antibody, dilution of 1:50 and Alexa Fluor® 546 goat anti-rabbit IgG (dilution 1:500) as the secondary antibody. To detect the poly(6)histidine tag, a combination of Penta-his antibody (dilution 1:50) and Alexa Fluor® 591 goat anti-mouse IgG (dilution 1:500) was used.

To start the immunofluorescence staining, the functionalized surfaces were blocked in 0.5% BSA in PBS at room temperature for 30 minutes, washed twice with PBS at room temperature, each for 5 minutes and incubated in the primary antibody solution in PBS at room temperature for 1 hour. Next the surfaces were washed twice with PBS at room temperature, each for 5 minutes and incubated in the solution of the secondary antibody (dilution 1:500) in PBS at room temperature for 1 hour. After 2-time washes in PBS at room temperature, each for 5 minutes, the surfaces were examined with fluorescence microscopy.

2.2.34. Functionalization of gold surfaces with benzylguanine thiol and immobilization of ShhN-GFP-His-SNAP

BGT and the passivating thiol EG6OH (Figure 2.4), being waxy solids, were dissolved in analytical grade ethanol (Sigma, Steinheim, Germany) in 0.1mM concentrations. Stock solutions (0.1 and 1mM) were sealed in all-glass vials for storage at -80°C up to 6 months. Aliquots were kept up to 3 weeks at -20°C in screw cap glass vials.

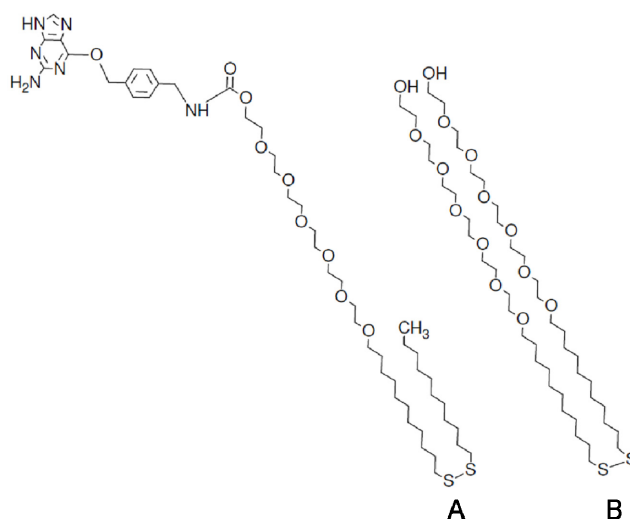


Figure 2.4. Molecular structures of the used disulfides. (A) benzylguanine terminated, active disulfide (BGT); (B) passivating disulfide EG6OH.

Silicon wafers having a 20nm chromium adhesion layer and a 200nm gold layer were provided by Michael Bruns, IAM-WPT, KIT. For QCM-D measurements standard gold coated sensor crystals were used. These sensors were recycled for subsequent experiments by boiling used crystals in a mixture of 1:1:5 volumes of hydrogen peroxide (30% in water, no Sn stabilizers, EMSURE, Merck, Darmstadt, Germany), ammonia (28-30% in water, Merck, Darmstadt, Germany) and distilled water. Prior to SAM formation these substrates were subjected to a UV cleaning step, 20 min in an

UV/Ozone ProCleaner Plus (BioForce Nanosciences, Inc., Ames, IA, USA). This treatment effectively removed airborne contaminations from gold. Immediately after this cleaning step the substrates were immersed in solutions mixed from the stock solutions of BGT or EG6OH. Afterwards the substrates were rinsed with pure ethanol and used for surfaces analysis or protein binding.

Patterning was achieved by photo degradation of a deposited EG6OH SAM. Therefore, the samples were covered with a quartz/chromium mask having transparent squares of $50\mu\text{m}\times 50\mu\text{m}$ spaced by $100\mu\text{m}$. This sandwich was exposed to UV irradiation as described in section 2.2.32. Following irradiation, the sample was washed with pure ethanol and water and exposed to the second, BGT containing, disulfide solution to fill the exposed areas on the sample surface. Finally, samples were rinsed with ethanol.

2.2.35. Immunofluorescence of ShhN-GFP-His-SNAP on benzylguanine thiol functionalized surfaces

The functionalized surfaces were washed twice with PBS at room temperature, each for 5 minutes and incubated in the Shh antibody 5E1 (dilution 1:10) in PBS at room temperature for 1 hour for the detection of the pseudo-active site of ShhN. The surfaces were washed twice again with PBS at room temperature, each for 5 minutes and were incubated in the solution of the Alexa Fluor® 488 goat anti-mouse IgG antibody (dilution 1:2500) in PBS at room temperature for 1 hour. After two washes in PBS at room temperature, each for 5 minutes, the surfaces were examined under fluorescence microscope.

2.2.36. Time-of-flight secondary ion mass spectroscopy (ToF-SIMS) for surface analysis of benzylguanine thiol modified gold substrate

ToF-SIMS was performed on a TOF.SIMS5 instrument of ION-TOF GmbH, Münster, Germany. This instrument is equipped with a Bi cluster liquid metal primary ion source and a non-linear time of flight analyzer. Dynamic emittance matching in the analyzer allows high mass resolution at large scanning areas. The primary ion source was operated in the "bunched" mode to produce ultra short primary Bi_1^+ or Bi_3^+ ion pulses at 25keV, optimized for spectroscopy. Therefore, the lateral resolution is limited to approx 5 μm . Pictures with high lateral resolution were taken in "burst alignment" mode. This primary ion gun operation mode allows for a precisely focussed beam to the disadvantage of limitation to nominal mass resolution. Spectrometry was performed in static SIMS mode by limiting the primary ion dose to $<10^{11}$ impingent ions/cm². No charge compensation was required. Spectra were calibrated on the omnipresent C^- , C_2^- , C_3^- , C_3H^- , C_4H^- peaks. Deviations from the theoretical mass were usually $< 10\text{ppm}$.

2.2.37. Adsorption of ShhN-His and ShhN-GFP-His on collagen and fibronectin functionalized glass surfaces

Glass slides were sterilized with 70% ethanol or isopropanol, rinsed with MilliQ H₂O, and either air dried or blown dry with nitrogen. The surfaces were then exposed to 25 to 240 $\mu\text{g/ml}$ collagen or fibronectin solution at room temperature for 1 hour. The protein binding substrates were washed twice with H₂O. Next, solutions of the Shh agonist SAG, *E. coli* expressed ShhN-His or ShhN-GFP-His; or the conditioned

medium collected from ShhN-GFP-His transfected HEK293 cells was applied on the surfaces at room temperature for 1 hour. The protein coated surfaces were finally rinsed twice with PBS.

2.2.38. Immunofluorescence of ShhN-His and ShhN-GFP-His on collagen and fibronectin functionalized surfaces

For immunodetection of the pseudo-active site of ShhN, the Shh antibody 5E1 1 was used as the primary antibody with the dilution of 1:10 and Alexa Fluor® 488 or 591 goat anti-mouse IgG (dilution 1:2500) as the secondary antibody. For ShhN in general, Shh (N-19):sc1194 (dilution 1: 20) and Alexa Fluor® 546 donkey anti-goat IgG (1:2500) were used. In the case of detection of the poly(6)histidine tag, a combination of Penta-his antibody (dilution 1:100) and Alexa Fluor® 488 or 546 goat anti-mouse IgG (dilution 1:2500) was used.

The functionalized surfaces were washed twice with PBS at room temperature, each for 5 minutes and were incubated in solutions of the primary antibodies mentioned above in PBS at room temperature for 1 hour. The surfaces were washed twice again with PBS at room temperature, each for 5 minutes and were incubated in the solutions of the fluorescence labelled secondary antibodies mentioned (dilution 1:2500) in PBS at room temperature for 1 hour. After 2-time washes in PBS at room temperature, each for 5 minutes, the surfaces were examined with fluorescence microscopy.

2.2.39. Blocking of collagen functionalized surfaces by microcontact printing of bovine serum albumin

Glass surfaces were coated with collagen as described in section 2.2.37. BSA was applied on patterned polydimethylsiloxane (PDMS) stamps at a concentration of 1mg/ml at room temperature for 15 minutes. The stamp was blown dry with nitrogen stream and was then pressed onto the collagen coated surfaces. The stamp was in contact with the surface for 1 minute and was removed carefully. This procedure is depicted schematically in Figure 2.5.

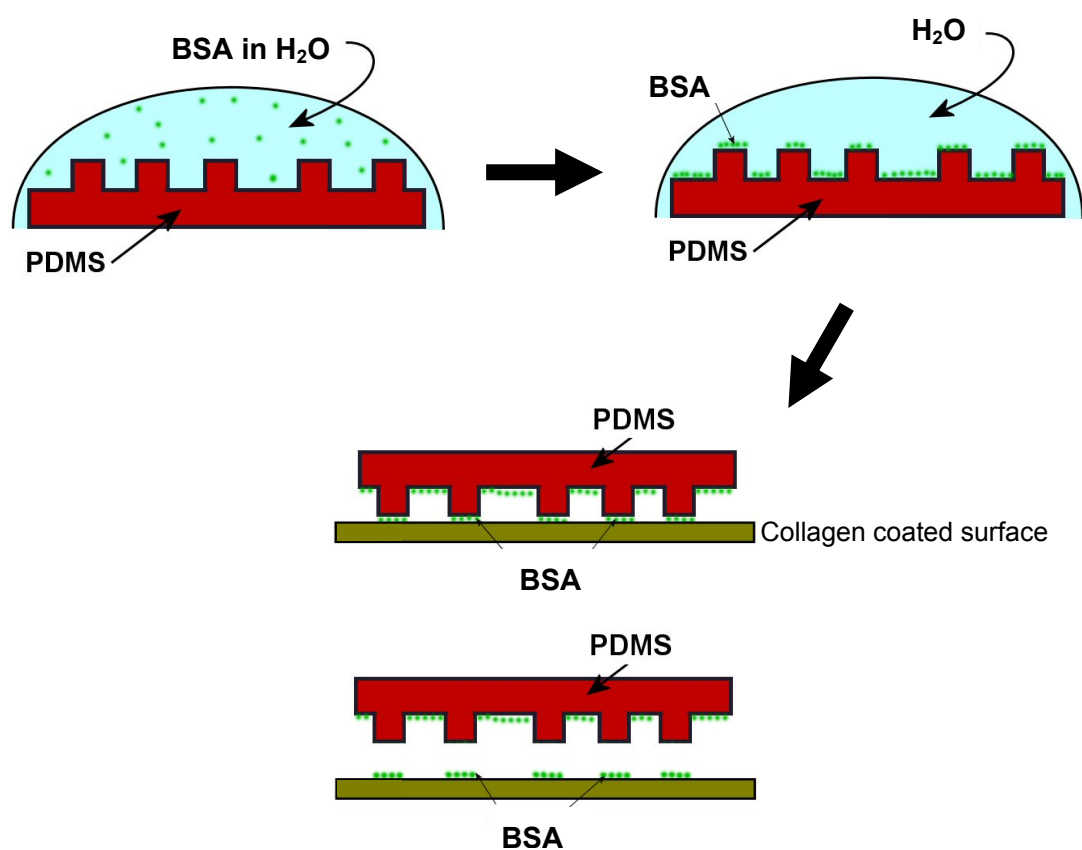


Figure 2.5. Diagram illustrating microcontact printing of BSA on collagen coated surface. 1mg/ml BSA was applied on a patterned PDMS stamp. The setup was kept at room temperature for 15 minutes. The stamp was blown dry with nitrogen stream and was then inverted and pressed onto the collagen coated surfaces. The stamp was allowed to stand on the surface for 1 minute and was removed carefully.

Next, the BSA stamped collagen or fibronectin modified surfaces were exposed to solutions of *E. coli* expressed ShhN-GFP-His with different concentrations for at room temperature for 2 hours. The surfaces were then ready for microscopy and FRAP experiments.

2.2.40. Quartz micro gravimetry for quantification of ShhN-GFP-His and ShhN-GFP-His-SNAP on collagen and benzylguanine thiol functionalized surfaces

A quartz crystal microbalance with dissipation monitoring (QCM-D) (Q-Sense AB, Västra Frölunda, Sweden) was employed to determine the amount of ShhN-GFP-His or ShhN-GFP-His-SNAP adsorbed on the collagen or BGT functionalized surfaces prepared as described in section 2.2.34.

The applied instrument uses the ac output of the damped oscillation of an AT-cut quartz crystal at 15, 25 and 35MHz to extract the resonance frequencies and energy dissipations. Measurements were performed with an ‘axial flow chamber’ having a very small exchange volume of the measurement chamber (0.05ml), a central inflow towards the crystal surface, and an internal temperature controlled loop of approximately 0.5ml volume. The presented data was measured in a stopped flow mode. The temperature in the measurement chamber was kept at $25 \pm 0.02^\circ\text{C}$. The sample was equilibrated in phosphate buffer (CertiPUR buffer solution di-sodium hydrogen phosphate / potassium hydrogen phosphate, pH6.88, Merck, Darmstadt, Germany). In the case of the BGT adsorption of ShhN-GFP-His-SNAP, an additional step of flushing of a BSA solution (1mg/ml in afore mentioned buffer; Albumin fraction V, Merck, Darmstadt, Germany) into the measurement chamber was

performed. After the signals had stabilized after 30min, the chamber was flushed with buffer and the solution of ShhN-GFP-His or ShhN-GFP-His-SNAP ($5\mu\text{M}$ in buffer) was injected. Finally, after another hour the chamber was rinsed with buffer. Readings of both adsorption steps were taken in the buffer steps to avoid effects of reversibly bound proteins.

Data handling was performed with the manufacturers' software allowing modeling the protein adsorbate as a viscoelastic solid with a frequency dependent complex shear modulus according to the Voight model. Here, it was sufficient to rely on the straight forward model of Sauerbrey to quantify the protein adsorption. The density, ρ , of all protein adsorbates was fixed to $1.15 \times 10^6 \text{g/m}^3$ corresponding to a densely packed low hydrated protein film. Film thickness values, d , scale nearly linear with $1/\rho$. Results are presented as average \pm standard deviation.

2.2.41. Enzyme linked immunosorbent assay (ELISA) for quantity measurement of ShhN-GFP-His adsorbed on collagen coated surfaces

After each QCM-D experiment, the crystals coated with collagen and ShhN-GFP-His were subjected to an ELISA assay, an alternative approach for protein quantification and cross-checking with the measurement made by QCM-D.

An ELISA response curve with different concentrations of RCmShhN (Neuromics, Edina, MN, USA) was established by coating the protein onto a 96-well ELISA microplate at room temperature for 1 hour. The plate was washed 5 times with PBS and blocked with 0.5%BSA in PBS at room temperature for 1 hour. The RCmShhN

was detected by 10µg/ml Shh (N-19) antibody (Santa Cruz, Santa Cruz, USA). After one hour incubation at room temperature, the plate was washed three times with PBS. The anti-goat IgG peroxidase conjugate (Sigma-Aldrich, Munich, Germany) for coupling Shh (N-19) was added at a dilution of 1:40,000 at room temperature for 30 minutes. The plate was washed 7 times with PBS with 30-second intervals. Substrate solution reacting with the peroxidase conjugate was prepared by mixing 11ml phosphate-citrate buffer, pH 5.0, 2µl 30% H₂O₂ and a TMB tablet (Roche, Mannheim, Germany). 100µl of the prepared substrate solution was added to each well of the microplate. The reaction was allowed to take place at room temperature for 30 minutes in dark and stopped with 50µl 2M H₂SO₄. The plate was then read by an ELISA microplate reader at 450nm. An ELISA response curve was plotted.

The corresponding procedure was applied to the QCM-D crystals coated with ShhN-GFP-His for the quantification of this protein by ELISA.

2.2.42. Fluorescence recovery after photobleaching (FRAP) for determination of the protein adsorption efficiency of collagen and fibronectin

Glass surfaces were exposed to collagen or fibronectin solutions with concentrations of 25 to 240µg/ml, and 500nM ShhN-GFP-His protein solution was bound as described in section 2.2.37. After washing twice with H₂O, the surfaces were analyzed by FRAP with the Leica SP2 confocal microscopic system. The surfaces were photobleached at 488nm with 800Hz for 3 seconds. The fluorescence recovery was measured every 1 second after bleaching. Graphs illustrating the fluorescence intensity recovery of the photobleached area against time were plotted.

3. Results

3.1. Introduction

Recombinant mouse ShhN (denoted as RCmShhN in the rest of the text; ShhN – the signaling domain of the Sonic hedgehog protein (amino acid residues C25 to G198), RC – the recombinant, m – mouse source of the ShhN sequence) was purchased from Neuromics (Edina, MN, USA). Unlike the wildtype ShhNp, which is derived from full length mouse Shh and possesses post-translational modifications – palmitoylation at the N-terminus and lipidation with cholesterol at the C-terminus, the commercially available RCmShhN is produced in an *E. coli* expression system and does not undergo post-translational processing. RCmShhN is therefore incapable of forming multimeric complex like ShhNp and remains monomeric (Chen et al., 2004). Despite the absence of these modifications, RCmShhN is biologically active. Palmitate and cholesterol is not necessary for the biological activity of ShhN in *in vitro* system. The modifications are responsible for the secretion and diffusion of ShhNp in *in vivo* environments (Heussler and Suri, 2003; Peters et al., 2004; Varjosalo and Taipale, 2008).

To engineer substrates with immobilized ShhN, two major research and development issues arose. The first issue was the production of biologically active ShhN in sufficient quantity with reference to the information obtained from RCmShhN cloning and expression. However, since RCmShhN lacks functional groups for the attachment and detection of ShhN on surfaces, relevant linker groups and fluorescence molecules were fused to the proteins. The second issue was then the development of efficient strategies to attach ShhN on surfaces in a spatially controlled manner.

Parameters for these two critical issues were investigated in parallel, however the results show firstly the protein production step and secondly the surface immobilization approaches.

3.2. Part 1 – Production of biologically active ShhN proteins

3.2.1. Production and purification of *E. coli* expressed mouse ShhN proteins

Bacterial expression systems are commonly utilized for mass production of functional proteins, since growth of bacteria on a large scale does not require sophisticated equipment, is economic and can be repeated routinely with stable performance. Moreover, protocols for bacterial culture and purification of biologically active ShhN from bacteria are well established with a wide variety of developed extraction methods from bacterial lysates (Williams et al., 1999). Although it is clear that in bacteria the Shh protein will not undergo post-translational modifications (cholesterol lipidation and palmytoylation) as it happens in mammalian cells, there is evidence that the recombinant ShhN expressed in bacteria is also highly active (Williams et al., 1999).

The design of the commercially available mouse RCmShhN was closely imitated (Table 3.1). This protein also served as a positive control. However, as mentioned before, this protein does not possess any functional groups to attach or detect ShhN on surfaces. The cloning of a number of variants that contained additional sequences was therefore embarked on. ShhN-His contained the same sequence as RCmShhN with the

exception of an additional methionine at the N-terminus (Table 3.1). This protein was intended as a control of my purification procedure. In addition, constructs of different ShhN variants for *E. coli* expression were designed.

Table.3.1 illustrates the peptide information of ShhNp and RCmShhN as reference. Details of the ShhN variants, with included additional tags sequences used for purification, immobilization and visualization of the proteins are shown. ShhN-His was designed based on the sequence of RCmShhN protein with modifications including: addition of the ATG codon, which encodes methionine, at the N-terminus for initiation of translation; addition of the poly(6)histidine tag at the C-terminus for purification on Ni-NTA agarose (Qiagen, Hilden, Germany) and immobilization of the protein on nickel functionalized surfaces; and addition of the stop codon for termination of translation. For visualization of immobilized ShhN-His on surfaces green fluorescence protein (GFP) was fused at the C-terminus and ShhN-GFP-His was produced. Another variant of ShhN, ShhN-GFP-His-SNAP possessed the SNAPTM tag included at the C-terminus of the peptide. The SNAPTM tag is derived from the human alkylguanine transferase and can covalently bind to benzylguanine (BG). ShhN-GFP-His-SNAP can therefore be immobilized on nickel functionalized surfaces as well as on BG modified surfaces.

Results

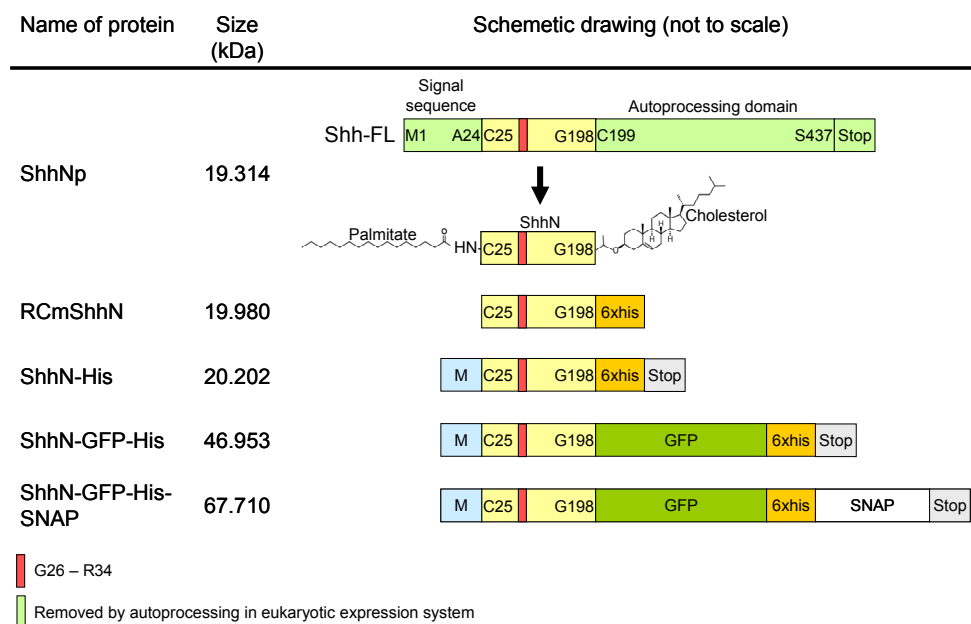


Table 3.1. Schematic drawings showing the amino acid sequences of the ShhN variants expressed in *E. coli*. ShhN-His, ShhN-GFP-His and ShhN-GFP-His-SNAP were designed based on the peptide sequence of RCmShhN (Neuromics, Edina, MN, USA). ShhNp is shown as a reference for the biologically active ShhN. The ShhN is encoded from the amino acid residues C25 to G198. The ATG start codon (methionine; M) and stop codon (Stop) were included in the two termini of the peptide for initiation and termination of translation. The poly(6)histidine tag was added for purification with Ni-NTA columns and immobilization of ShhN-GFP-His on nickel functionalized surfaces. The SNAPTM tag was added for covalent binding of ShhN-GFP-His-SNAP onto benzylguanine (BG) modified surfaces. GFP was fused to the protein sequence for detection and visualization of the expressed ShhN. Owing to the absence of the signal sequence (amino acids M1 to A24) and the autoprocessing domain (C199 to S437), and that the production was conducted in bacterial expression system, ShhN, ShhN-GFP-His and ShhN-GFP-His-SNAP do not undergo post-translational modifications. The number after the amino acid symbol corresponds to the position of the amino acid in Shh-FL.

The ShhN sequence in different ShhN variants was obtained from the pBlueScript KSII:mouse Shh plasmid (gift from Dr. A. McMahon, Harvard University, MA, USA). The start and stop codons, and the poly(6)histidine tag were cloned by the polymerase chain reaction (PCR). The sequence of the poly(6)histidine tag was provided by Neuromics. For ShhN-GFP-His, the ShhN fragment was subcloned into the

pCS2:GFP plasmid in fusion with the GFP protein. The pSS26m vector (Covalys, Witterswil, Switzerland) was employed to fuse the SNAPTM tag at the C-terminus of ShhN-GFP-His-SNAP. All of the ShhN variants were subcloned into the pENTRTM11 vector (Invitrogen, Darmstadt, Germany), resulting in entry clones for the Gateway[®] cloning system, which were sent to Qiagen Sequencing Services (Hilden, Germany). Correct ShhN-His, ShhN-GFP-His and ShhN-GFP-His-SNAP fragments were then cloned to the pDESTTM14 vector (Invitrogen) for plasmid propagation and protein expression in *E. coli*.

The ShhN variants in the pDESTTM14 vector were then expressed in the *E. coli* strain BL-21 with IPTG as the inducing agent of expression. The expressed proteins were extracted by lysing the bacteria and were purified with Ni-NTA agarose. During the Ni-NTA chromatographic purification, green fluorescence was visualized from the ShhN-GFP-His and ShhN-GFP-His-SNAP proteins.

3.2.2. Molecular analysis of the *E. coli* expressed ShhN proteins

After purification from the bacterial lysates, the amount and purity of the isolated ShhN proteins were analyzed. The ShhN proteins were resolved by sodium dodecyl sulfate-polyacrylamide gel electrophoresis (SDS-PAGE). The quantity was assessed by running in parallel bovine serum albumin (BSA) standards of known concentrations. Comparison of the band intensities allowed to quantify the purified ShhN proteins.

Figure 3.1 illustrates an example of protein quantification using a BSA standard of known concentrations and the purified ShhN proteins loaded into the same

Results

SDS-PAGE gel. The run gel was Coomassie stained, and images of the stained bands were captured. The intensity of the BSA and ShhN bands were measured using the software provided by the manufacturer. A standard curve of the BSA intensity against the known BSA concentration was plotted, and was used to estimate the amount of ShhN proteins purified from *E. coli*.

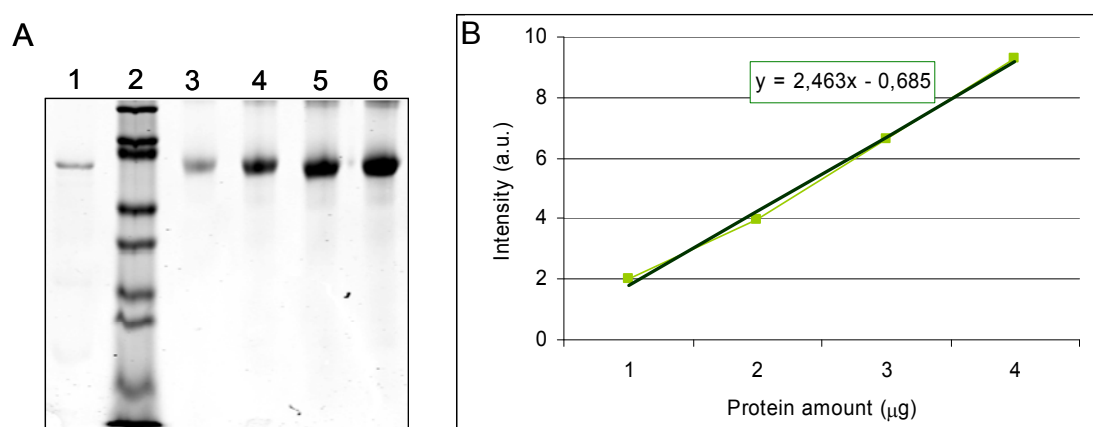


Figure 3.1. Quantification of *E. coli* expressed ShhN proteins. (A) ShhN-GFP-His-SNAP was loaded on the SDS-PAGE gel together with the BSA standard solutions with known concentrations. Lanes 1: ShhN-GFP-His-SNAP; 2: protein marker; 3 – 6: 1, 2, 3 and 4µg BSA. (B) A standard curve was plotted with the intensity obtained from the BSA standard solutions. The intensity of the ShhN-GFP-His-SNAP band was measured, and the protein amount was determined from the BSA standard curve.

Next, Western blot was carried out to probe the Shh N-terminal signaling domain of the isolated proteins. For enrichment of the ShhN proteins before WB, immunoprecipitation step was done with the monoclonal antibody 5E1 (Maun et al., 2010a). This antibody competes with the Shh receptor Patched (Ptc) and blocks Shh activity by occupying the pseudo-active site involving the five histidine residues at positions 133, 134, 140, 180 and 182 of biologically active Shh (Bosanac et al., 2009). 5E1 antibody was bound to protein A sepharose and Shh proteins were immunoprecipitated, subjected to SDS-PAGE and immunoblotted.

Figure 3.2 shows the Western blot results of the *E. coli* expressed ShhN proteins using the Shh (N-19):sc1194 antibody after 5E1 immunoprecipitation. Markers for protein size reference are illustrated in the lane on the left. The untransformed BL21 lysate and supernatant purified from the GFP-His transformed *E. coli* acted as the negative controls for Shh (N-19):sc1194 detection, while the 19kDa RCmShhN served as positive control. Bands, indicated by arrows, with the sizes of about 20, 47 and 68 kDa are observed for the purified supernatants from the *E. coli* transformed with the ShhN-His, ShhN-GFP-His and ShhN-GFP-His-SNAP constructs, respectively, indicating the presence of the proteins with the expected sizes. Successful 5E1 immunoprecipitation of the ShhN proteins demonstrates that the pseudo-active site, where Shh binds to its receptor Ptc, is available.

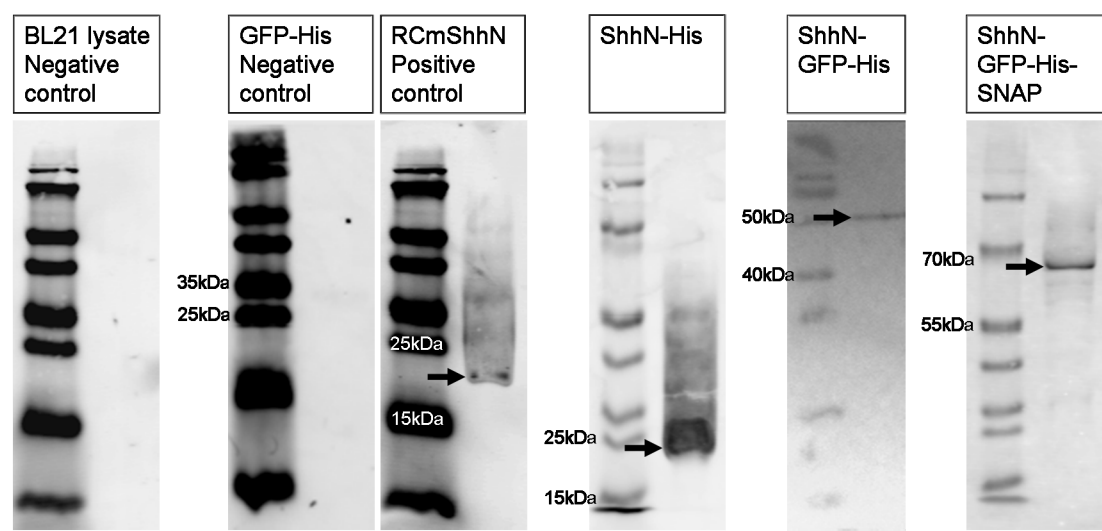


Figure 3.2. The Shh N-terminal signaling domain is present in the *E. coli* expressed proteins. Proteins were resolved on SDS-PAGE gel and blotted. Membranes were incubated with Shh (N-19):sc1194 antibody. Bands, indicated by arrows, visualized on the membranes illustrated the presence of ShhN purified from the lysates of *E. coli* transformed with the DNA expression constructs of the ShhN variants.

3.2.3. Analysis of the biological activity of the *E. coli* expressed ShhN proteins

Supernatants from *E. coli* cultures of ShhN-GFP-His and ShhN-GFP-His-SNAP showed green fluorescence indicating the correct folding of the GFP peptide fused to the ShhN proteins. Next step was to test if the ShhN proteins are biological active. Assays for the detection of alkaline phosphatase (ALP) expression of the Shh responsive cells were employed.

3.2.3.1. Detection of Shh signaling induced alkaline phosphatase expression in C3H10T1/2 clone 8 cells and cell counting assay

C3H10T1/2 clone 8 cells are mouse mesenchymal cells capable of expressing ALP as a marker of differentiation induced by Shh signaling (Kinto et al., 1997). To confirm that the ShhN variants induced specific ALP expression, the Sonic hedgehog agonist SAG (Axxora, Lörrach, Germany) and the *E. coli* expressed RCmShhN (Neuromics, Edina, MN, USA) were used as the positive controls together with the purified ShhN proteins. GFP-His served as the negative control of Shh signaling.

Different concentrations of SAG, RCmShhN, GFP-His or the *E. coli* expressed ShhN variants were applied to the C3H10T1/2 clone 8 cells, which were pre-cultured in 8-well chamber slides for 24 hours. After addition of proteins, the cells were cultivated for 5 days at 37°C with 5% CO₂. Next the cells were fixed and stained for ALP expression with BCIP/NBT substrates in the ALP staining buffer. Draq5 was used to stain the nuclei for cell number counting. Alternatively, the treated cells were

lysed and analyzed with the alkaline phosphatase colorimetric assay kit (Abcam, Cambridge, UK).

Images of ALP expression detection in the C3H10T1/2 clone 8 cells are illustrated in figure 3.3. In the negative controls with no Shh proteins or with 100nM GFP-His, no ALP expression was detected. On the other hand, ALP expression indicated by the blue stained cells, was detected in cells treated with 100nM SAG or RCmShhN. These observations suggested that the C3H10T1/2 clone 8 cells differentiate and express ALP in response to the presence of Shh signaling. In the case of treatment with 100nM of the *E. coli* expressed ShhN-His, ShhN-GFP-His and ShhN-GFP-His-SNAP variants, ALP expression was detected in a small number of C3H10T1/2 clone 8 cells. Quantification of ALP expressing cells are shown in graph 3.1.

Results

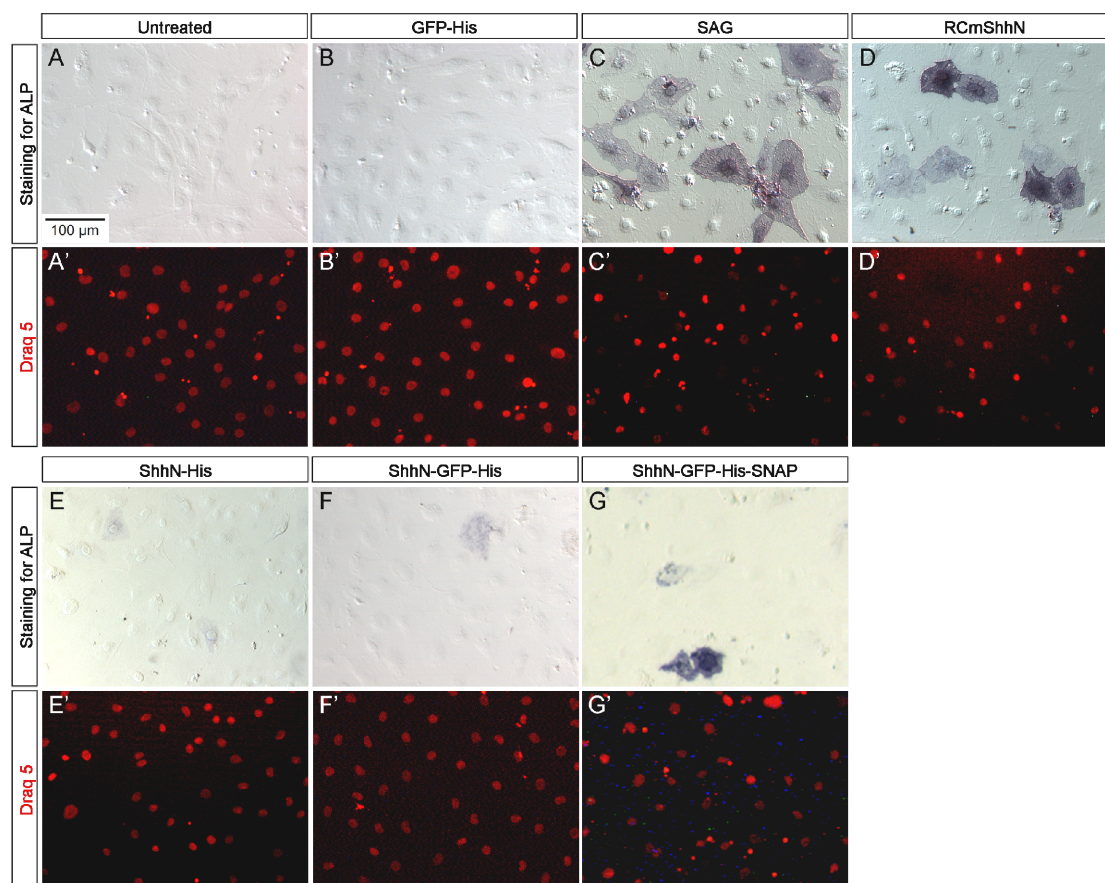


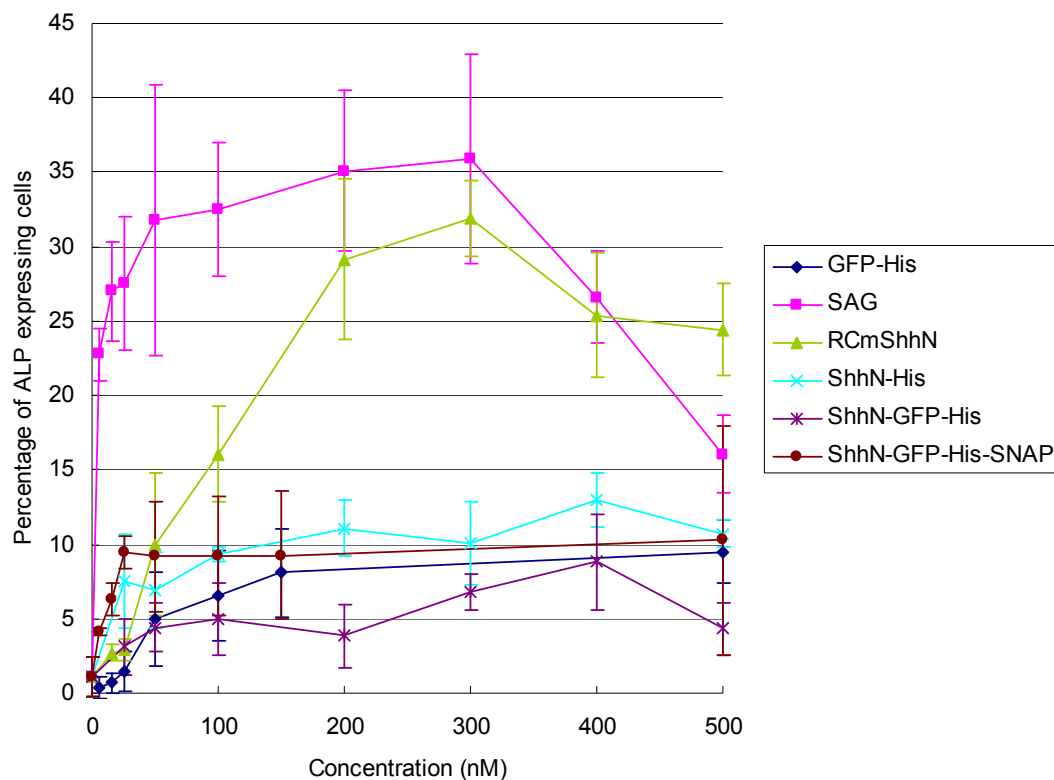
Figure 3.3. Staining for ALP expressed in C3H10T1/2 clone 8 cells treated with *E. coli* expressed ShhN variants. C3H10T1/2 clone 8 cells were treated for 5-day with 100nM of *E. coli* expressed ShhN variants: ShhN-His, ShhN-GFP-His or ShhN-GFP-His-SNAP, and with GFP-His, SAG, RCmShhN as controls. In the no-Shh (A) and GFP-His (B) negative controls, no ALP expression was detected. SAG (C) and RCmShhN (D) served as positive controls for Shh signaling and ALP expression. Treatment of C3H10T1/2 clone 8 cells with ShhN-His (E), ShhN-GFP-His (F) or ShhN-GFP-His-SNAP (G) resulted in ALP expression only in a small population of the cells. Quantification of ALP expressing cells is shown in graph 3.1.

A concentration dependent ALP expression was triggered in C3H10T1/2 clone 8 cells after treatment of cells with SAG and the *E. coli* expressed ShhN variants (Graph 3.1). A concentration series of 0 to 500nM of proteins was tested. SAG and RCmShhN were the positive controls for Shh signaling and ALP expression, while GFP-His served as the negative control.

With the increasing concentration of the SAG and RCmShhN, from 0 to 300nM, an increased percentage of the ALP expressing cells was observed. The highest percentages of ALP expressing cells were noticed for SAG (36%) and RCmShhN (32%) at the concentration of 300nM. Application of higher concentration of SAG and RCmShhN led to a decrease of the number of ALP expressing cells.

GFP-His induced unspecific ALP expression in a small population of the C3H10T1/2 clone 8 cells. 9% of the cells expressed ALP in the culture medium containing 500nM GFP-His. ShhN treated C3H10T1/2 clone 8 cells responded similarly as the GFP-His treated cells. 10% of the cells expressed ALP when 400 to 500nM of ShhN-His, ShhN-GFP-His or ShhN-GFP-His-SNAP was applied onto the cells. These findings suggested that the *E. coli* expressed ShhN protein variants could not trigger specific ALP expression in the C3H10T1/2 clone 8 cells thus were biologically inactive.

Results



Graph 3.1. Biological activity of *E.coli* expressed ShhN variants recorded by BCIP/NBT staining for the expressed ALP in C3H10T1/2 clone 8 cells and cell counting. C3H10T1/2 clone 8 cells were specifically responsive to the positive controls Sonic hedgehog agonist SAG and RCmShhN. The percentage of ALP expressing cells increased with an increasing concentration of SAG and RCmShhN and reached the saturation point of 36% with 300nM SAG and 32% with 300nM RCmShhN. GFP-His induced unspecific ALP expression. The percentages of ALP expressing cells treated with ShhN-His, ShhN-GFP-His and ShhN-GFP-His-SNAP remained low and were comparable to that of the GFP-His treated ones.

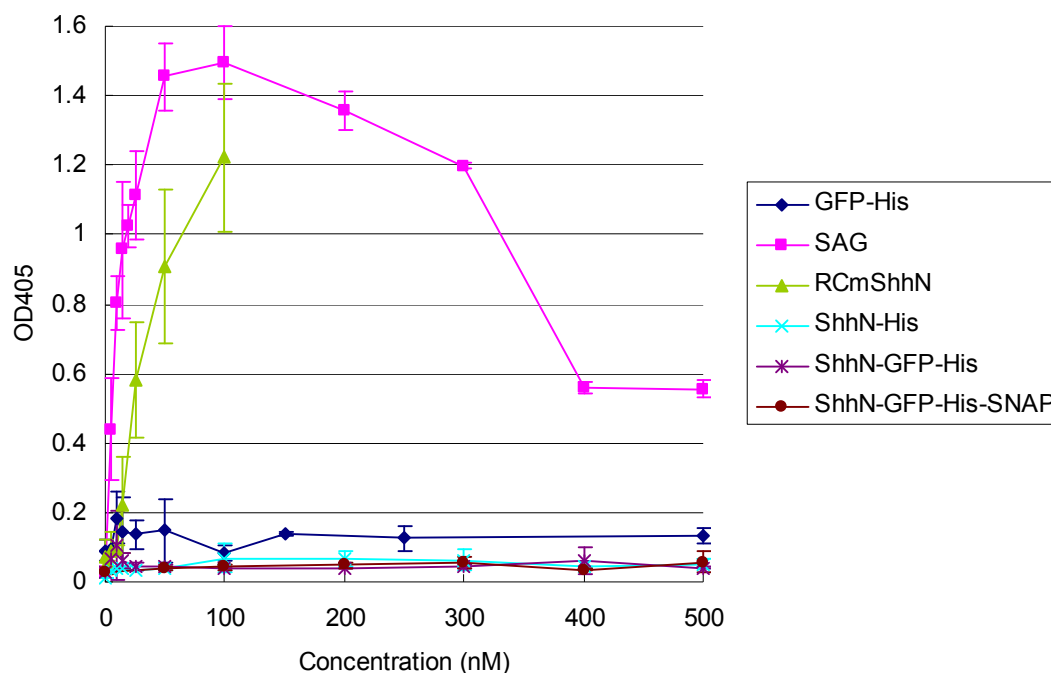
3.2.3.2. Quantification of Shh signaling induced alkaline phosphatase expression in C3H10T1/2 clone 8 cells by cell lysate based colorimetric assay

The ALP expressing cell counting assay provided qualitative information on cellular responses to Shh signaling. Nevertheless, it could be subjective in quantifying and comparing the cellular responses. Individual cells were not stained to the same intensity and normalization of the staining is challenging. The colorimetric assay, based on cell lysate analysis, for the quantification of ALP expression can compensate for the bias.

As revealed from the ALP colorimetric assay, ALP expression in C3H10T1/2 clone 8 cells was triggered by the positive controls SAG and RCmShhN in a concentration dependent manner (Graph 3.2). Cells treated with 100nM SAG showed the highest level of ALP expression: optical density measured at $\lambda = 405\text{nm}$ (OD₄₀₅) of about 1.5. An OD₄₀₅ of 1.2 was measured when 100nM RCmShhN was used. Owing to the limited supply of RCmShhN, higher concentrations of RCmShhN were not tested in this assay.

GFP-His served as the negative control and the OD₄₀₅ value remained at 0.1 in all concentrations applied. Cells treated with the *E. coli* expressed ShhN-His, ShhN-GFP-His and ShhN-GFP-His-SNAP showed even lower values of OD₄₀₅, implying that Shh variants were incapable of inducing ALP expression in C3H10T1/2 clone 8 cells and were biologically inactive.

Results



Graph 3.2. Biological activities of *E. coli* expressed ShhN variants measured by ALP colorimetric assay. The positive controls SAG and RCmShhN induced concentration dependent ALP expression in the C3H10t1/2 clone 8 cells. An OD405 of 1.5 was noted when 100nM SAG was added to the cells. 100nM RCmShhN also induced a substantial level of ALP expression (OD405 of 1.2). Concentrations higher than 100nM were not investigated for RCmShhN due to source limitation of RCmShhN. The negative control GFP-His gave a low OD405 value of around 0.1 for all concentrations tested. ShhN-His, ShhN-GFP-His and ShhN-GFP-His-SNAP did not show any OD405 value higher than that of GFP-His for all applied concentrations, indicating that the *E. coli* expressed ShhN proteins did not induce ALP expression at all in the C3H10T1/2 clone 8 cells.

Table 3.2 summarizes the peptide sequences and biological activities of ShhNp, RCmShhN and the different *E. coli* expressed ShhN variants. Despite the availability of the Ptc binding site detected by 5E1 immunoprecipitation, the *E. coli* expressed ShhN proteins were biologically inactive. The constructs encoding ShhN were sequenced again and the differences between RCmShhN and ShhN were compared. The DNA and the inferred peptide sequences of ShhN (C25 to G198) were identical to the corresponding amino acid sequence of Shh. The poly(6)histidine tag at the N-terminus of ShhN did not affect the biological activity of RCmShhN, suggesting

that fusions at the C-terminus, including the poly(6)histidine, GFP, SNAPTM tag and the stop codon, should not interfere with the biological activity of *E. coli* expressed ShhN. The only concern remains the addition of a methionine residue, the ATG codon encoding which is required for the start of translation, at the N-terminus of ShhN. This N-terminal methionine forms disulfide bonds by oxidation and hydrolysis (Lemke, 2003). It changes the electric properties and destabilizes the native state of the recombinant protein through a conformational entropy effect, thereby altering the biological and physicochemical properties of the protein (Chaudhuri et al., 1999).

Name of protein	Size (kDa)	Schematic drawing (not to scale)	Biological activity
Shh-FL			
ShhNp	19.314		+
RCmShhN	19.980		+
ShhN-His	20.202		-
ShhN-GFP-His	46.953		-
ShhN-GFP-His-SNAP	67.710		-

G26 – R34
 Removed by autoprocessing in eukaryotic expression system

Table 3.2. Comparison of the peptide sequences and the biological activities of the *E. coli* expressed ShhN-His, ShhN-GFP-His and ShhN-GFP-His-SNAP variants analyzed by the ALP assays. The peptide sequence of ShhN (C25 to G198) was identical to that of RCmShhN. The major difference of the *E. coli* expressed ShhN variants and the biologically active RCmShhN was the methionine residue at the N-terminus of the ShhN. The ATG codon, which encodes methionine, is responsible for the initiation of translation but yet the methionine produced can adversely affect the biological activity of the *E. coli* expressed proteins.

3.2.3.3. Enhancement of the biological activity of *E. coli* expressed ShhN proteins

The ATG codon encoding methionine was required to start translation and therefore could not be omitted for protein expression. In order to produce biologically active ShhN in bacterial expression system, the protocol for extraction and purification of ShhN from *E. coli* was modified with regard to the unique properties of ShhN. Modifications included addition of 0.5mM DTT to eliminate ShhN dimerization; and substitution of Zn²⁺ ions in the ShhN pseudo-active site to stabilize the Ptc binding groove.

During ShhN expression, a dimeric form of ShhN is formed spontaneously by the formation of disulfide bonds (Hochman et al., 2006; Kellner et al., 2002). The ShhN dimer is ten times less active than the monomeric form (Kellner et al., 2002). By applying proteins on the SDS-PAGE gel one is not able to distinguish the monomeric and dimeric ShhN, since the disulfide bonds are broken by 50mM dithiothreitol (DTT), a reducing agent in the Lämmli sample buffer and by heat denaturation prior to gel loading.

To get rid of dimeric ShhN, 0.5mM DTT was included in all buffers used for extraction and Ni-NTA chromatography. This DTT concentration was low enough to reduce ShhN without interfering with the nickel(II)/poly(6)histidine interaction. Purified ShhN was eluted and stored under reducing condition in DTT containing PBS to ensure that the ShhN proteins were in monomeric form in all cell treatment experiments.

In biologically active Shh the pseudo-active site is comprised of five histidine residues at positions 133, 134, 140, 180 and 182 of the peptide (Bosanac et al., 2009). It is those positions where Shh/Ptc binding takes place (Bosanac et al., 2009; Maun et al., 2010a, b) and also coordination of the Zn^{2+} ion in the groove comprised of His141, Asp148 and His183 of Shh (Maun et al., 2010a) occurs. In the presence of Zn^{2+} , the affinity of Shh to Ptc receptor increases 10 to 20 folds (Maun et al., 2010b).

To stabilize the Shh/Ptc binding pseudo-active site and improve the receptor affinity of the *E. coli* expressed ShhN, purified ShhN was dialyzed against 100 μ M $ZnCl_2$ for Zn^{2+} coordination to the Zn^{2+} containing groove of ShhN. However, dialysis resulted in enormous loss and contamination of the protein. Alternatively, 100 μ M $ZnCl_2$ was added to the bacterial cell lysis buffer and ShhN is expected to coordinate the Zn^{2+} ions from the $ZnCl_2$ solution. The anti-Shh monoclonal antibody 5E1, which competes with Ptc for the Shh pseudo-active site, was used to immunoprecipitate the ShhN variants. The results of the Western blots after 5E1 immunoprecipitation suggested that the ShhN variants bind to Ptc. The Western blot images are shown in figures 3.4 to 3.6.

3.2.3.4. Stability analysis of the *E. coli* expressed ShhN proteins

Shh is capable of binding to heparin sulfate proteoglycan (HSPG) for effective transportation *in vivo* (Saha and Schaffer, 2005; Varjosalo and Taipale, 2007). The ability of Shh to recognize and interact with HSPG or heparin depends on the Cardin-Weintraub sequence at the amino acid residues Lys33 to Lys39 (Cardin and Weintraub, 1989). ShhN protein variants sequence starts at Cys25 and the Cardin-Weintraub sequence is located close to its N-terminus. Since *E. coli* proteases

Results

could unspecifically cleave the N-terminus of a protein during protein expression, it is plausible that ShhN may be truncated at the N-terminus or Cardin-Weintraub sequence and became biologically inactive.

To test if the peptide sequence of bacterially expressed ShhN was complete, Shh antibody #2287 (Cell Signaling, Danvers, MA, USA) was used to detect the Cardin-Weintraub sequence at the N-terminus (Figure 3.4). Penta-his (Qiagen, Hilden, Germany) and anti-SNAP (D. Wedlich, KIT, Germany) antibodies were employed to detect the corresponding tags at the C-terminus of ShhN (Figures 3.5, 3.6). Immunoprecipitation with 5E1 was done to enrich the ShhN protein variants before Western blot, and to detect the pseudo-active site.

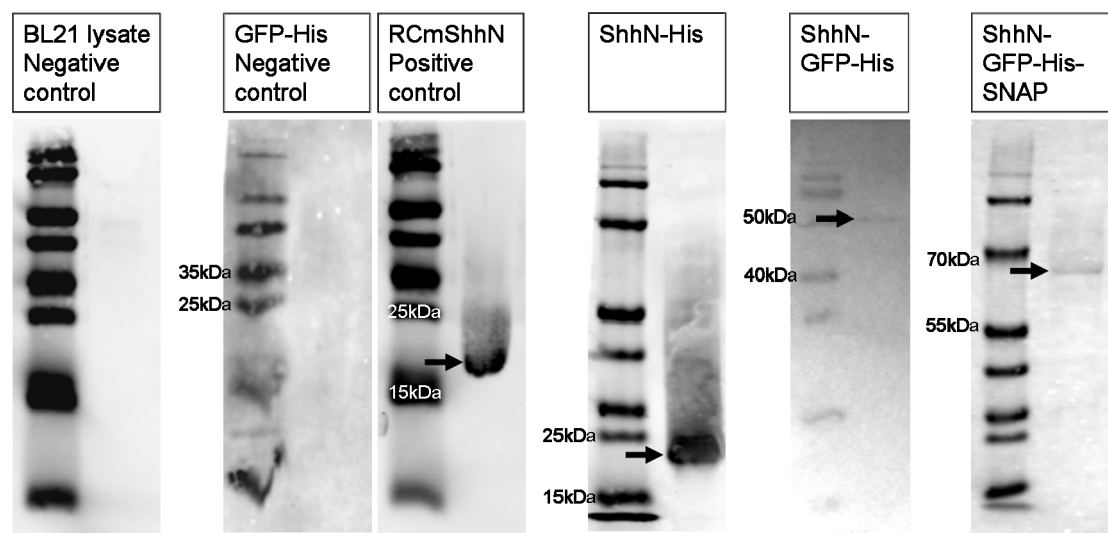


Figure 3.4. The N-terminal Cardin-Weintraub sequence of the *E. coli* expressed ShhN variants was available. The *E. coli* expressed ShhN variants were immunoprecipitated by 5E1 and probed with Shh antibody #2287 (indicated by arrows). The untransformed BL21 lysate and GFP-His served as the negative controls, illustrating that 5E1 and Shh antibody #2287 detections were ShhN specific.

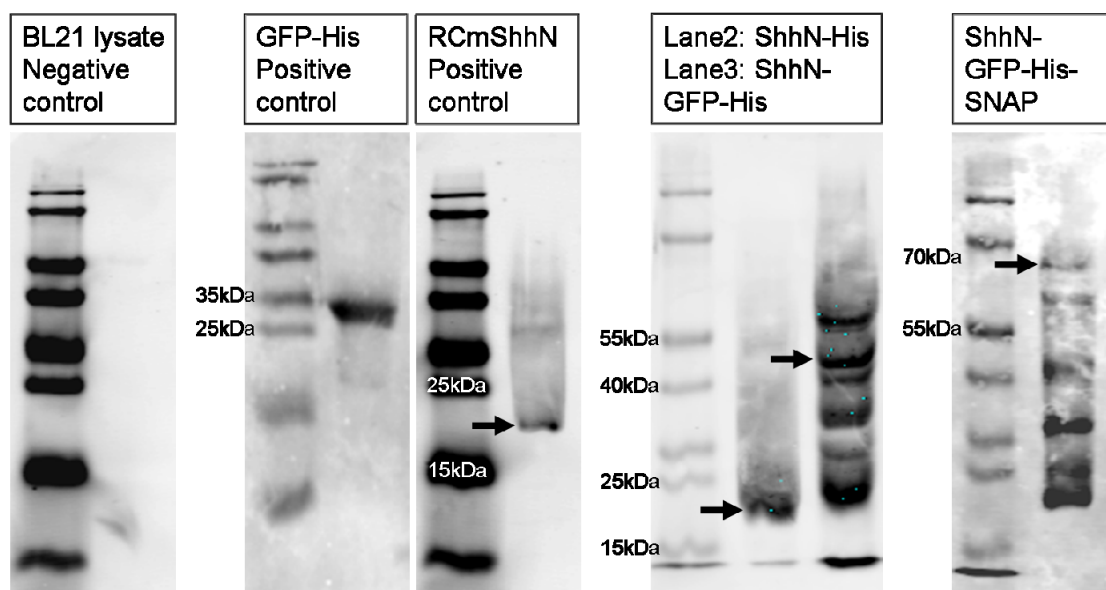


Figure 3.5. The *E. coli* expressed ShhN variants contained the histidine tag. The poly(6)histidine tag at the N-terminus of the purified ShhN variants were detected by the Penta-his antibody after 5E1 immunoprecipitation. Detected bands are indicated by arrows. The untransformed BL21 lysate served as the negative control ; while GFP-His was the positive control, illustrating that 5E1 immunoprecipitation and Penta-his detection were histidine specific. The multiple bands observed for ShhN-GFP-His and ShhN-GFP-His-SNAP may be due to unspecific antibody detection.

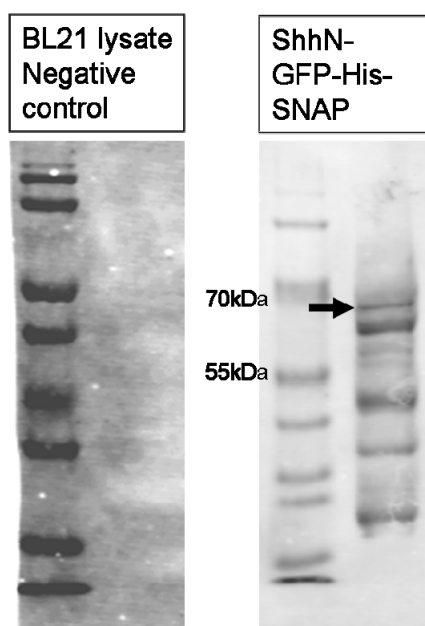


Figure 3.6. The SNAPTM tag is present in the *E. coli* expressed ShhN-GFP-His-SNAP protein. The purified ShhN-GFP-His-SNAP was 5E1 immunoprecipitated and probed with the anti-SNAP antibody. The probed band corresponding to ShhN-GFP-His-SNAP is shown by an arrow. The BL21 lysate served as the negative control. The multiple bands observed may be due to unspecific antibody detection.

Probing the membranes with the Shh antibody #2287 showed the presence of the N-terminal Cardin-Weintraub sequence in the *E. coli* expressed ShhN variants (Figure 3.4). The bands visualized on the membranes incubated with the Penta-his antibody demonstrated that the C-terminal poly(6)histidine tag was fused with the ShhN variants (Figure 3.5). And the anti-SNAP antibody was able to detect the C-terminally fused SNAPTM tag ShhN-GFP-His-SNAP (Figure 3.6). All of these observations implied that the peptide sequences of the *E. coli* expressed ShhN variants detected by the antibodies with expected sizes (as indicated by the arrows) were complete.

The multiple bands in the samples after probing with Penta-his and anti-SNAP antibodies may be a result of unspecific antibody detection. Histidine rich proteins from the *E. coli* genome may be isolated from the Ni-NTA column purification along with the ShhN variants. Since the ATG codons of the GFP and SNAP were not

removed from the expression plasmids, translation starting at the GFP or SNAP may give rise to the production of Shh free peptides and contribute to the multiple band detection with the Penta-his and anti-SNAP antibodies. Nevertheless, these "contaminants" were not detected by the Shh specific antibodies. There was one and specific band detected for both ShhN-GFP-His and ShhN-GFP-His-SNAP with the Shh (N-19):sc1194 antibody (Figure 3.2) and the Shh antibody #2287 (Figure 3.4) but not in the case when Penta-his or anti-SNAP antibody was applied. Detection of the multiple bands may also be a result of degraded peptide residues. Degradations were not detected by the anti-Shh antibodies because they may occur at the Shh (N-19):sc1194 recognition site or at the Cardin-Weintraub sequence, where degradation can interrupt the binding of the Shh (N-19):sc1194 antibody and Shh antibody #2287 to these target sites.

In spite of the presence of contaminants and degradations, substantial amounts of the *E. coli* expressed ShhN variants with expected sizes were obtained as detected by the anti-Shh antibodies (Figures 3.2, 3.4). Experiments of ShhN immobilization, which are described in later sections, also showed that ShhN-GFP-His and ShhN-GFP-His-SNAP were immobilized on nickel and BG functionalized surfaces, respectively.

3.2.3.5. Analysis of the biological activity of the *E. coli* expressed ShhN proteins with selective truncation

Regardless of the DTT and Zn^{2+} supplementation of protein extracts, the *E. coli* expressed ShhN variants still showed no biological activity as tested in the ALP assays (data not shown).

According to Chaudhuri et al. (1999), the methionine at the N-terminus blocks the biological activity of bacterially expressed proteins. Therefore it is plausible that the biological activities of the *E. coli* expressed ShhN variants were inhibited by methionine (M24). However, since methionine is important for the initiation of translation, it has to be retained at the N-terminus of the peptide sequence. Recently it was found by the collaborator K. Grobe (Westfälische Wilhelms-Universität Münster, Germany) that removal of the amino acid residues G26 to A34 rescued the biological activity of the eukaryotic expressed mutant ShhN-C25S. In ShhN-C25S, cysteine (C25), which is the first amino acid at the N-terminus, is replaced by serine. This C25S replacement perturbs the biological activity of the mutated Shh. For the G26 – A34 removal helps ShhN-C25S regain its biological activity, it is plausible that in the *E. coli* system, biologically active ShhN proteins can be expressed with C25 substituted with methionine (i.e. C25M), provided that the amino acids G26 to A34 is removed.

In light of the findings by K. Grobe, the variant of ShhN-His with the mutation C25M_del26-34, was produced in the *E. coli* expression system. C25 was replaced by methionine instead of serine for the start of translation. The amino acid residues G26 to A34 were removed. Since the C-terminal tags did not interfere with the biological

activity of ShhN (as demonstrated by ShhN^{6×his}, the autoprocessing domain of which is replaced by a Myc tag and a poly(6)histidine tag (Dierker et al., 2009a); sequence detail in table 2.2), the poly(6)histidine tag was retained for purification by Ni-NTA chromatography. Schematic description illustrating the Shh variants with mutations is presented in table 3.3. ShhN-His-C25M_del26-34 was expected to have properties similar to the eukaryotic expressed variant ShhN-C25S_del26-34, which is biologically active.

Results

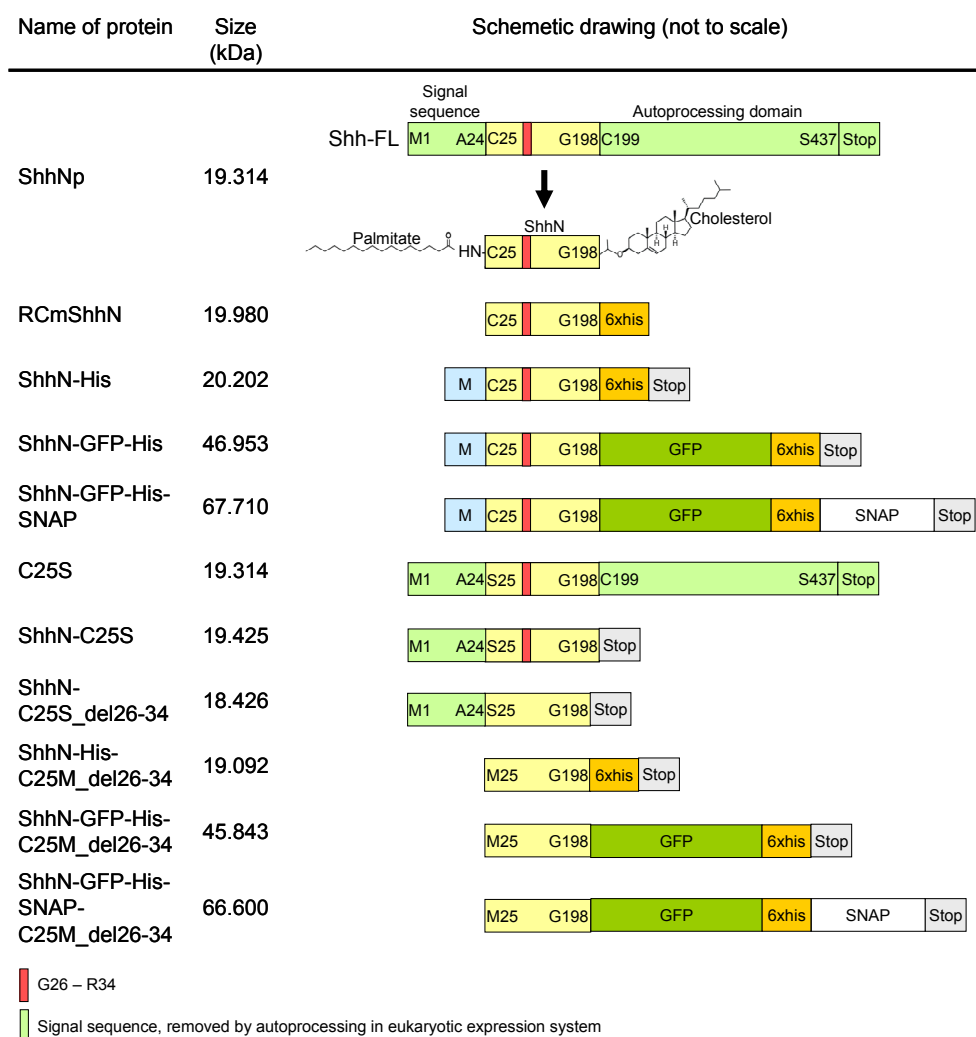


Table 3.3. Scheme of peptide sequences of the mutated variants of the *E. coli* expressed ShhN proteins: ShhN-His-C25M_del26-34, ShhN-GFP-His-C25M_del26-34 and ShhN-GFP-His-SNAP-C25M_del26-34. Peptide sequences of the mutants were designed with reference to modifications made in the eukaryotic expressed Shh-C25S_del26-34. C25 was replaced by methionine for the start of translation. G26 to R34 were removed. GFP fusion, poly(6)histidine and SNAP tags were remained at the C-termini of ShhN.

After extraction and purification from *E. coli*, ShhN-His-C25M_del26-34, ShhN-GFP-His-C25M_del26-34 and ShhN-GFP-His-SNAP-C25M_del26-34 were subjected to 5E1 immunoprecipitation and Western blot analysis in order to test for the presence of the Ptc binding pseudo-active site, the N-terminal Cardin-Weintraub sequence, and the C-terminal poly(6)histidine and SNAPTM tags.

The mutated ShhN variants were first immunoprecipitated by 5E1 and detected by Shh (N-19):sc1194 antibody. The bands visualized from the probed membrane illustrated the presence of the Shh signaling domain (Figure 3.7). Detection of Cardin-Weintraub sequence by Shh antibody #2287 and poly(6)histidine by Penta-his antibody indicated that the ShhN were produced with complete peptide sequences (Figure 3.7). The multi bands noticed for ShhN-GFP-His-C25M_del26-34 and ShhN-GFP-His-SNAP-C25M_del26-34 with Penta-his antibodies may be because of unspecific antibody detection.

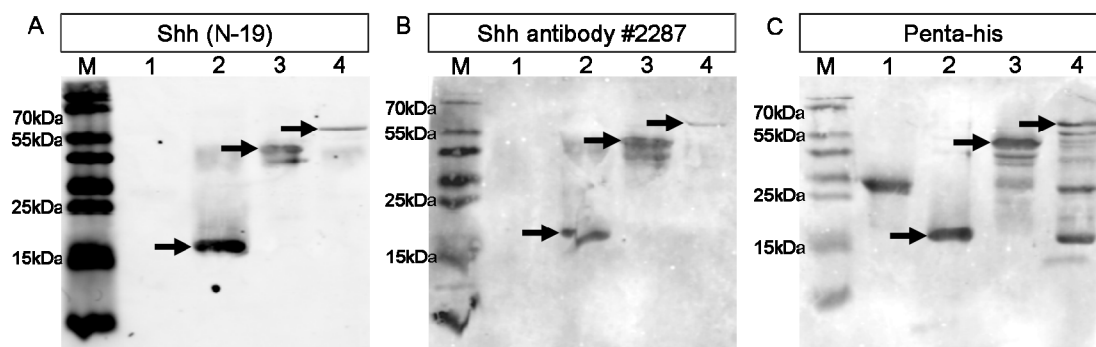


Figure 3.7. The *E. coli* expressed ShhN-His-C25M_del26-34, ShhN-GFP-His-C25M_del26-34 and ShhN-GFP-His-SNAP-C25M_del26-34 possessed the Shh signaling domain (A), the N-terminal Cardin-Weintraub sequence (B) and the C-terminal histidine tag (C). The purified proteins were immunoprecipitated with 5E1 and probed with Shh (N-19):sc1194 antibody, ShhN antibody #2287 and Penta-his antibody for the detections of the Shh signaling domain, Cardin-Weintraub sequence, and histidine, respectively. Probed bands were indicated by arrows. GFP-His served as the negative controls for the Shh (N-19):sc1194 antibody and Shh antibody #2287, and as the positive control for the Penta-his antibody.

Results

Shh has diverse functions in embryo development. Induction of alkaline phosphatase expression is only one of the many parameters that can be used to verify the biological activity of Shh. Therefore, the activity of the newly expressed ShhN mutants, as well as the other ShhN variants, was tested with a chondrocyte differentiation system instead of the ALP assays. The chondrocyte differentiation assay is a very sensitive system for investigating the biological activity of Shh by detecting the expression of the chondrogenic marker Collagen X (ColX), which is responsive to Shh signaling (Dreier et al., 2008). This assay however was conducted by the collaborator K. Grobe, where the facilities and experienced man power for culturing and analysis of the chondrocyte progenitor cells were available. All the *E. coli* expressed ShhN variants were produced in house and then sent to K. Grobe for analysis after purification.

To do the chondrocyte differentiation assay, the chondrocyte progenitor cells were cultivated in serum free medium. Next the *E. coli* expressed ShhN-GFP-His, ShhN-GFP-His-C25M_del26-34, ShhN-GFP-His-SNAP and ShhN-GFP-His-SNAP-C25M_del26-34 were added to the cells in two concentrations: 2.848 μ g (5 μ l) and 28.48 μ g (50 μ l). Then the cells were allowed to undergo differentiation for 2 weeks, after which they were lysed and the cell lysates were resolved by SDS-PAGE. Western blot was then performed with the radioactively labeled anti-ColX antibody with an exposure time of 2 to 3 weeks until signals were detected.

Figure 3.8 shows a Western blot image illustrating the expression of ColX in the chondrogenic progenitor cells after the cells were treated with the *E. coli* expressed ShhN-GFP-His, ShhN-GFP-His-C25M_del26-34, ShhN-GFP-His-SNAP and ShhN-GFP-His-SNAP-C25M_del26-34.

When a lower dose (2.848 μ g (5 μ l)) of ShhN-GFP-His, ShhN-GFP-His-C25M_del26-34, ShhN-GFP-His-SNAP and ShhN-GFP-His-SNAP-C25M_del26-34 was applied, only weak induction of ColX expression in the chondrocyte progenitor cells was detected. When the dosage of the ShhN proteins was increased by 10 times to 28.48 μ g (50 μ l), the expression of ColX became clearly detectable. Taken together, these results suggested that the *E. coli* expressed ShhN proteins, whether with or without C25S mutation and the removal of the amino acid residues G26 to A34, were biologically active. They stimulated the Shh induced expression of the chondrogenic marker ColX and triggered differentiation of the chondrocyte progenitor cells.

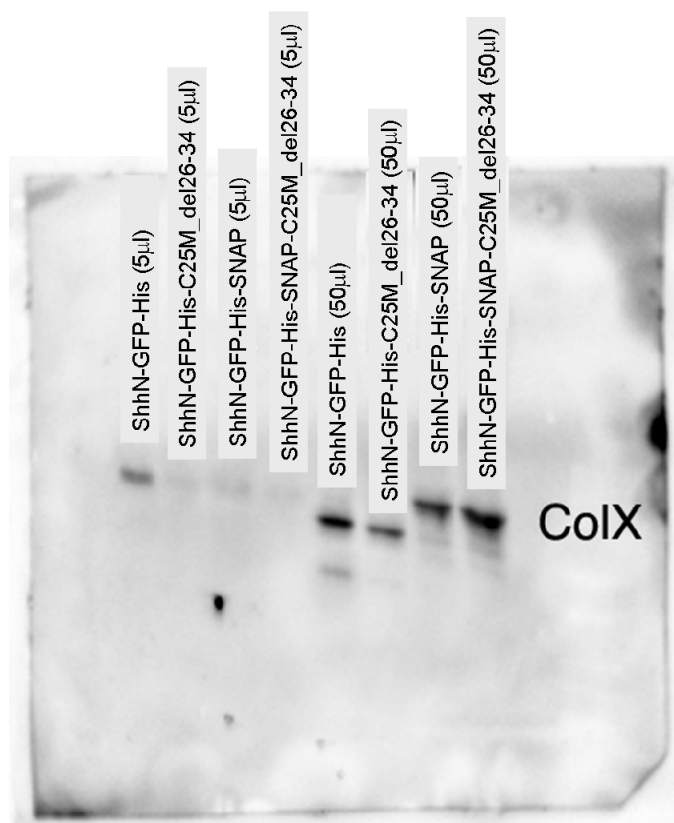


Figure 3.8. *E. coli* expressed ShhN variants stimulated expression of the chondrocyte differentiation marker ColX. The four ShhN variants: ShhN-GFP-His, ShhN-GFP-His-C25M_del26-34, ShhN-GFP-His-SNAP and ShhN-GFP-His-SNAP-C25M_del26-34 were applied to the chondrocyte progenitor cells with the doses of 2.848 µg/5 µl or 28.48 µg/50 µl. The cells were allowed to differentiate for 2 weeks. SDS-PAGE was performed for the cell lysates. The expression of ColX was immunodetected by the radioactively labeled anti-ColX antibody. The bands visualized on the blot demonstrate ColX expression. All of the tested proteins were noticed to induce ColX expression, implying that they are biologically active in chondrocyte differentiation assay. Weak expression of ColX was observed when 2.848 µg/5 µl of the proteins was used for cell treatment (left 4 lanes). A 10-time higher dosage (28.48 µg/50 µl) resulted in higher expression level of ColX (right 4 lanes).

Unlike RCmShhN, the biological activity of the *E. coli* expressed ShhN variants: ShhN-His, ShhN-GFP-His and ShhN-GFP-His-SNAP, was not detected by the ALP assays, which are based on the differentiation of pluripotent mesenchymal cells. However, it was visualized in the chondrocyte differentiation assay, no matter if there are C25S mutation and deletion of the amino acids G26 to A34. These findings demonstrated that ShhN-His, ShhN-GFP-His and ShhN-GFP-His-SNAP are biologically active but the intensity of activity from the tested dosages is not high enough to induce differentiation of the mesenchymal cells. On the contrary, they were capable of stimulating differentiation of the chondrocytic progenitor cells when used in high dosages (i.e. 2.848 μ g/5 μ l and 28.48 μ g/50 μ l).

Table 3.4 summarizes the biological activity of all the *E. coli* expressed ShhN variants. The black + or – indicate if the proteins were tested biologically active in the ALP assays. The red + shows the positive biological activity of the protein in the chondrocyte differentiation assay.

Results

Name of protein	Size (kDa)	Schematic drawing (not to scale)	Biological activity
Shh-FL			
ShhNp	19.314		+
RCmShhN	19.980		+
ShhN-His	20.202		+
ShhN-GFP-His	46.953		+
ShhN-GFP-His-SNAP	67.710		+
C25S	19.314		-
ShhN-C25S	19.425		-
ShhN-C25S_del26-34	18.426		+
ShhN-GFP-His-C25M_del26-34	45.843		+
ShhN-GFP-His-SNAP-C25M_del26-34	66.600		+

G26 – R34
 Signal sequence, removed by autoprocessing in eukaryotic expression system

Table 3.4. Summary of the biological activity of the *E. coli* expressed ShhN variants in ALP assays (black + or –) and chondrocyte differentiation assay (red +). Removal of the amino acid residues G26 to R34 rescued the biological activity of eukaryotic expressed ShhN-C25S. In the case of bacterially expressed ShhN, the tested ShhN-GFP-His, ShhN-GFP-His-C25M_del26-34, ShhN-GFP-His-SNAP and ShhN-GFP-His-SNAP-C25M_del26-34 were all found to be biologically active in the chondrocyte differentiation assay, regardless of the presence or absence of the G26-R34 residues.

3.2.4. Usage of the *E. coli* expressed ShhN proteins in functionalized surface development for protein immobilization

The *E. coli* expressed ShhN proteins were detected biologically active with the chondrocyte differentiation assay. Nevertheless, it takes altogether 4 to 5 weeks for the activity verification of the proteins. On the other hand, the ALP assays take a comparatively shorter time for ALP detection. But it was incapable to detect the biological activity of the *E. coli* expressed ShhN variants used in the current project. In light of the time consumption of the protein activity detection assay, the *E. coli* expressed ShhN variants were not used for biological analysis on functionalized surfaces.

However, because of the capability of *E. coli* to produce enormous amount of proteins in a routine basis, the bacterial expression system was still employed in the project in order to provide a feasible amount of ShhN variants for protein immobilization on functionalized surfaces, and surface-protein binding analysis. The green fluorescence visualized from the GFP fusion proteins ShhN-GFP-His and ShN-GFP-His-SNAP offered a hand for surface analysis after protein immobilization.

3.2.5. Production of ShhN-GFP-His and ShhN-GFP-His-SNAP in a eukaryotic expression system using HEK293 cells

In parallel to the efforts made to produce biologically active ShhN in *E. coli*, a eukaryotic expression system was set up.

Bacterially expressed ShhN do not have the post-translational modifications such as lipidation by the addition of cholesterol at the C-terminus and palmitoylation at the N-terminus. On the other hand, the ShhNp expressed in the eukaryotic Bosc23 cells is lipidated by cholesterol and membrane-tethered with the added palmitate, and is also processed by metalloprotease-mediated ectodomain shedding at the N-terminus prior to being released from the expressing cells (Dierker et al., 2009a). Bosc23 expressed ShhNp is thus considered to be biologically active (Dierker et al., 2009a).

In order to produce biologically active ShhN-GFP-His and ShhN-GFP-His-SNAP, the HEK293 cell line, which is derived from human embryonic kidney cells and is a derivative of the Bosc23 cell line, was employed.

Constructs of ShhN-GFP-His and ShhN-GFP-His-SNAP for protein expression in HEK293 cells were cloned. Consistent with the constructs for *E. coli* expression, the expression plasmids possessed the DNA fragment encoding the amino acids of the Shh signaling domain (C25 to G198) (i.e. ShhN). They are fused with the DNA encoding GFP for detection and visualization, the poly(6)histidine tag for purification via Ni-NTA columns and immobilization on nickel functionalized surfaces, and the SNAPTM tag for immobilization on BG functionalized surfaces. To ensure protein secretion from the expressing cells, the signaling sequence was integrated at the

N-terminus of ShhN (amino acids M1 to A24). This signaling sequence was automatically cleaved off after translation and right before the post-translational modifications (refer to figure 1.4 for details). The autoprocessing domain (amino acids C19 to S437) was not included in the ShhN-GFP-His and ShhN-GFP-His-SNAP constructs, since the absence of cholesterol modification at the C-terminus of ShhN does not adversely influence the cellular response to ShhN, as indicated by the biological activity of ShhN^{6×his} (Dierker et al., 2009a). Detailed information on the DNA plasmid constructs is shown in table 3.5. The pcDNA3.1 vector was used as the backbone of all constructs.

The ShhNp and ShhN^{6×his} constructs were kindly provided by K. Grobe (Westfälische Wilhelms-Universität Münster, Germany). The biological activity of the proteins expressed by Bosc23 cells was confirmed by ALP induction in C3H10T1/2 cells (Dierker et al., 2009a). ShhNp and ShhN^{6×his} therefore served as the positive controls for expression in the HEK293 cells.

Results

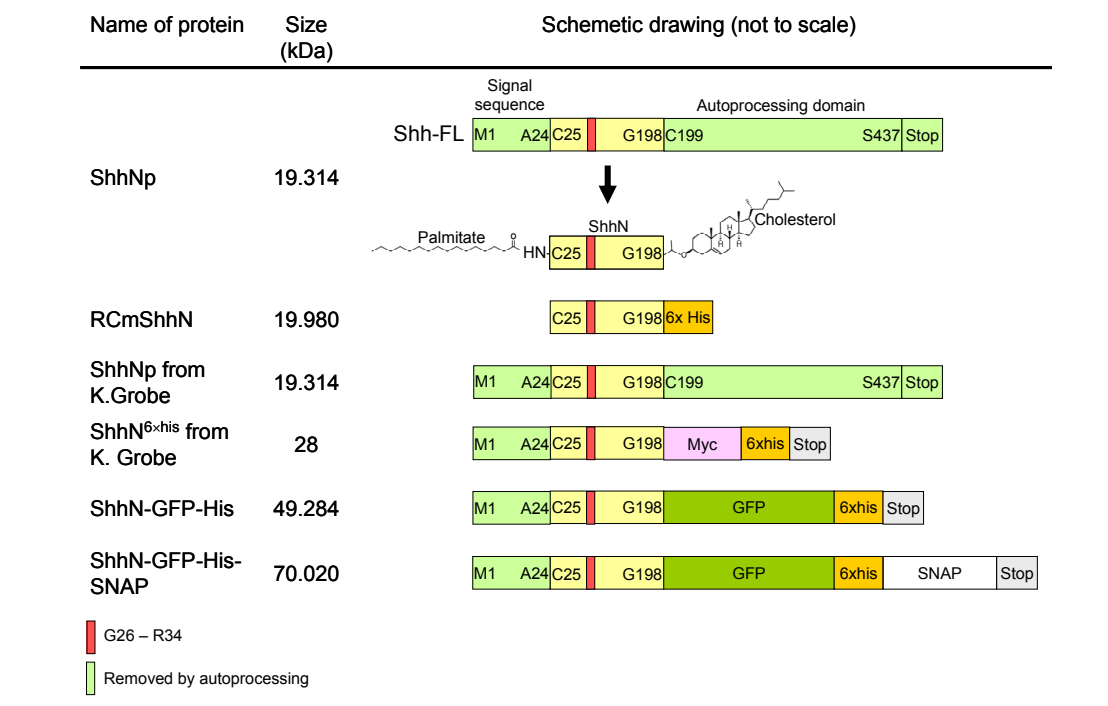


Table 3.5. Schematic drawing of the amino acid sequences of the ShhN variants expressed in the eukaryotic HEK293 cells. The N-terminal signal sequence of ShhN was composed of amino acid residues M1 to A24 required for secretion of ShhN from the expressing cells. The poly(6)histidine tag was added for purification with Ni-NTA columns or immobilization of ShhN-GFP-His on nickel functionalized surfaces. The SNAPTM tag was used for covalent binding of ShhN-GFP-His-SNAP to BGT for immobilization on gold surfaces. GFP was used for visualization of the expressed ShhN.

Transfection of the ShhN plasmids was performed in 6-well tissue culture plates. 24 hours prior to transfection, HEK293 cells were seeded with the density of 2×10^4 cells/cm². 2ml of the culture medium (DMEM supplemented with 10% FBS) was added in each well. Cells were cultivated at 37°C with 5% CO₂. On the day of transfection, the culture medium was replaced with 2ml of the fresh DMEM medium, supplemented with 10% FBS. Transfection of the cells was conducted with PolyPlus jetPEI transfection reagent (Polyplus-transfection, New York, NY, USA) according to the manufacturer's instruction. Transfected HEK293 cells were cultured at 37°C with 5% CO₂ for the following 48 hours in order to achieve protein expression. Conditioned medium from the transfected cells was collected and filtered through

22 μ m syringe filters (Carl Roth, Karlsruhe, Germany) to remove cell debris. The collected conditioned medium was stored at 4°C and used within 24 hours.

Since the ShhN-GFP-His and ShhN-GFP-His-SNAP were fused with GFP, their expression in the HEK293 cells was visualized under the green fluorescence channel with the upright compound fluorescence microscope (model DM5000B, Leica, Solms, Germany). Figure 3.9 shows the images taken 48 hours post transfection. Tissue culture surface filled with culture medium (DMEM and 10% FBS) alone does not show a fluorescence signal. No GFP signal was detected from the untransfected HEK293 cells and HEK293 cells transfected with the empty vector pcDNA3.1, which is the backbone of the ShhN-GFP-His and ShhN-GFP-His-SNAP constructs. The green fluorescence observed therefore indicates the expression of ShhN-GFP-His and ShhN-GFP-His-SNAP in HEK293 cells (Figure 3.9).

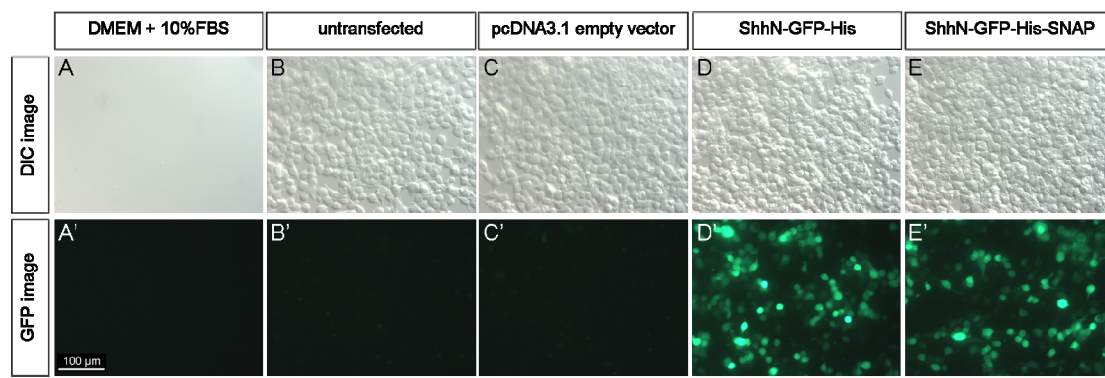


Figure 3.9. Expression of ShhN-GFP-His and ShhN-GFP-His-SNAP in HEK293 cells. The HEK293 cells were transiently transfected with the constructs of ShhN-GFP-His and ShhN-GFP-His-SNAP. Images were taken 48 hours post transfection. The green fluorescence indicates expression of ShhN-GFP-His and ShhN-GFP-His-SNAP in the transfected HEK293 cells (D', E'). Tissue culture surface with culture medium (DMEM and 10% FBS) alone does not show a fluorescence signal and was used as the negative control. (A'). Untransfected HEK293 cells and HEK293 cells transfected with the empty vector pcDNA3.1 were used as the negative control., respectively (B', C').

3.2.6. Analysis of the biological activity of ShhN-GFP-His and ShhN-GFP-His-SNAP expressed in the HEK293 cells

In contrast to the *E. coli* expression system, expression of the ShhN variants in the HEK293 cells resulted in barely detectable amounts of the proteins. None of the expressed proteins from the HEK293 cells was detected in Western blot using the Shh (N-19):sc1194 antibody (Santa Cruz, Santa Cruz, USA) and the Shh antibody #2287 (Cell signaling, Danvers, MA, USA). The biological activity of the HEK293 expressed ShhN variants were therefore directly examined by ALP staining, colorimetric assays, and Gli-luciferase reporter assay.

For the ALP assays, the conditioned medium of individual ShhN variants collected from the transfected HEK293 cells was applied onto the mouse mesenchymal C3H10T1/2 clone 8 cells, which are capable of expressing ALP as a marker of cell differentiation in response to Shh signaling. The cells were cultivated in the conditioned medium at 37°C with 5% CO₂ for 5 days. Next, the cells were either fixed and stained for ALP expression with the BCIP/NBT substrates in the ALP staining buffer or lysed and analyzed with the alkaline phosphatase colorimetric assay kit (Abcam, Cambridge, UK) according to the manufacturer's instruction.

In the case of the Gli-luciferase reporter assay, the conditioned medium of individual ShhN variants collected from the transfected HEK293 cells was applied to the Shh LIGHT II cells, stably transfected with the Gli responsive firefly luciferase reporter (Sasaki et al., 1997). Those cells respond to the Shh signaling via production of the firefly luciferase enzyme. Shh LIGHT II cells were treated for 48 hours in standard

cell culture conditions. Luciferase assay was then conducted by lysing the cells and measuring the firefly luciferase activity normalized to Ubi-*Renilla* luciferase activity.

Since the amount of the ShhN variants expressed in HEK293 cells could not be determined via Western blot, dosage dependent response analyses were done by applying the conditioned media containing the expressed proteins in ratios. For instance, a conditioned medium to fresh medium ratio of 1:1 implies that 500 μ l of the protein containing conditioned medium was mixed with 500 μ l of the fresh medium. The final volume is therefore 1ml. The fresh medium is composed of DMEM and 0.5% FBS for the C3H10T1/2 clone 8 cells, and DMEM supplemented with 0.5% FBS and 5mM HEPES, pH 7.4 for the Shh LIGHT II cells..

3.2.6.1. Functional specificity of the ShhN-GFP-His and ShhN-GFP-His-SNAP expressed in HEK293 cells

BCIP/NBT staining for the ALP expressed from the C3H101/2 clone 8 cells treated with the conditioned media collected from the HEK293 cells transfected with ShhN-GFP-His and ShhN-GFP-His-SNAP showed that the HEK293 expressed ShhN proteins were biologically active (Figure 3.10). When the same ratio of conditioned medium to fresh medium (1:1) of the ShhN variants and the positive control ShhNp was applied, the two ShhN variants: ShhN-GFP-His and ShhN-GFP-His-SNAP demonstrated a comparable intensity of ALP expression to ShhNp. The Shh agonist SAG is another positive control showing Shh signaling specific induction of ALP expression in C3H10T1/2 clone 8 cells. The untreated C3H10T1/2 clone 8 cells and the cells treated with conditioned medium of untransfected HEK293 cells were the negative controls for transfection; while those treated with conditioned medium from

Results

HEK293 transfection of the empty vector of pcDNA3.1 (mock transfection) were the negative control of ShhN expression.

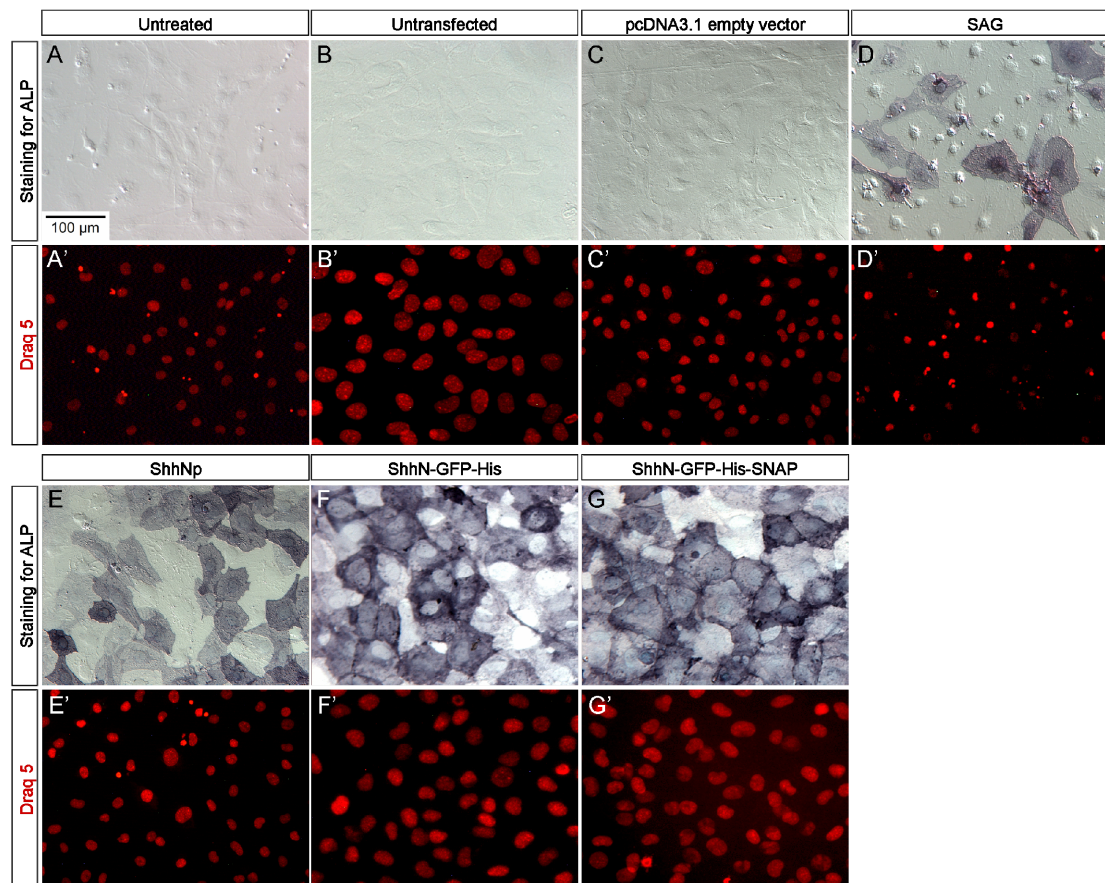


Figure 3.10. Biological activity of the HEK293 expressed ShhN variants revealed from staining for ALP expression in C3H10T1/2 clone 8 cells. 500 μ l of the conditioned medium was collected from the HEK293 cells of different transfections and mixed with 500 μ l of fresh medium (i.e. DMEM and 0.5% FBS). The mixed medium (with the conditioned medium to fresh medium ratio of 1:1) was added to the C3H10T1/2 clone 8 cells for a 5-day treatment. The C3H10T1/2 clone 8 cells treated with the conditioned media of HEK293 cells transfected with ShhN-GFP-His and ShhN-GFP-His-SNAP plasmids showed ALP expression (F, G). In the untreated C3H10T1/2 clone 8 cells (A), and the negative controls with the conditioned media from untransfected HEK293 cells (B) and mock transfection (empty vector of pcDNA3.1) (C), no ALP expression was detected. 100nM SAG (D) and the conditioned medium from HEK293 cells transfected with the construct of ShhNp (E) served as the positive control for Shh signaling and ALP expression. Nuclei were stained with Draq 5 (A' to G').

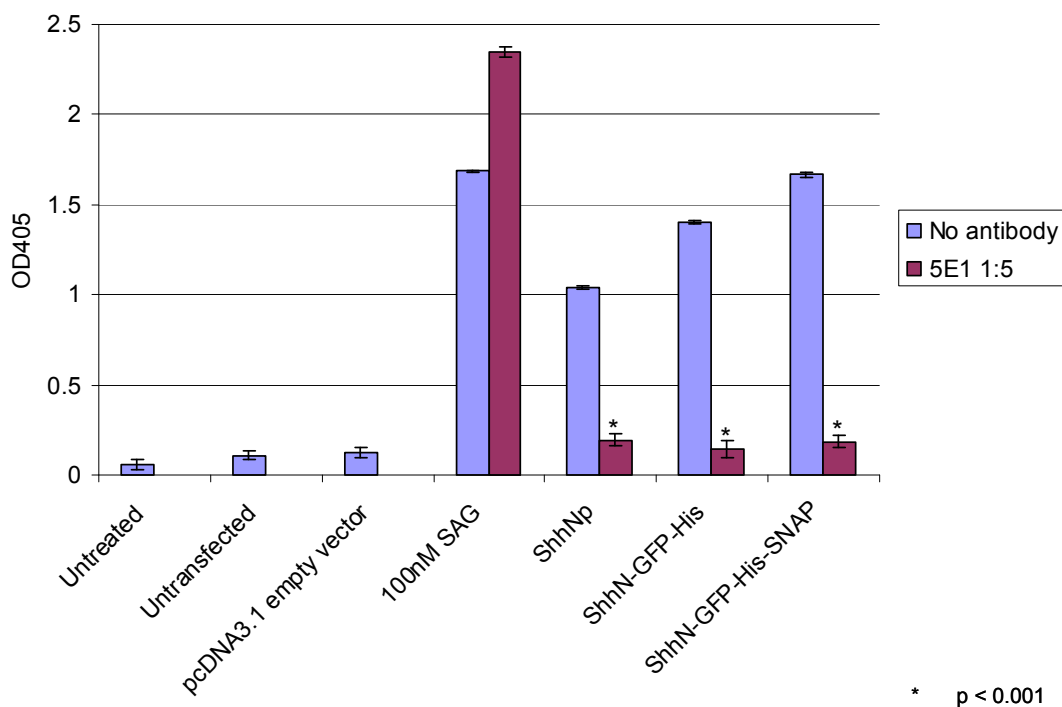
The high-affinity, neutralizing anti-Shh monoclonal antibody 5E1 can disrupt Shh activity by competing with the Shh receptor Ptc for the pseudo-active site of Shh (Bosanac et al., 2009; Maun et al., 2010a, b). As the HEK293 cell expressed ShhN-GFP-His and ShhN-GFP-His-SNAP could not be detected by Western blot, blockage of the Shh activity by 5E1 is an alternative approach to determine the functional specificity of these ShhN variants. The 5E1 antibody was used to block Shh signaling in the C3H10T1/2 clone 8 and Shh LIGHT II cells treated with the conditioned media from the HEK293 cells transfected with the constructs of ShhN-GFP-His and ShhN-GFP-His-SNAP. The effects of 5E1 antibody treatment on the biological activity of the proteins were examined by ALP colorimetric and Gli-luciferase reporter assays.

For the ALP colorimetric assay, 500 μ l of the conditioned medium collected from the HEK293 cells transfected with the constructs of ShhN-GFP-His or ShhN-GFP-His-SNAP, and 500 μ l of fresh medium (i.e. DMEM with 0.5% FBS) were added to the C3H10T1/2 clone 8 cells. The 5E1 antibody with the dilution of 1:5 (Gulacsi and Lillien, 2003) was then applied onto the cells. The cells were incubated at 37°C with 5% CO₂ for 5 days. Next cells were lysed and ALP expression was detected as the optical density at the wavelength of 405nm (OD405).

For the Gli-luciferase assay, Shh LIGHT II cells were treated the same way with the conditioned medium as for ALP assay but were incubated for 48 hours prior to the measurement of luciferase activity.

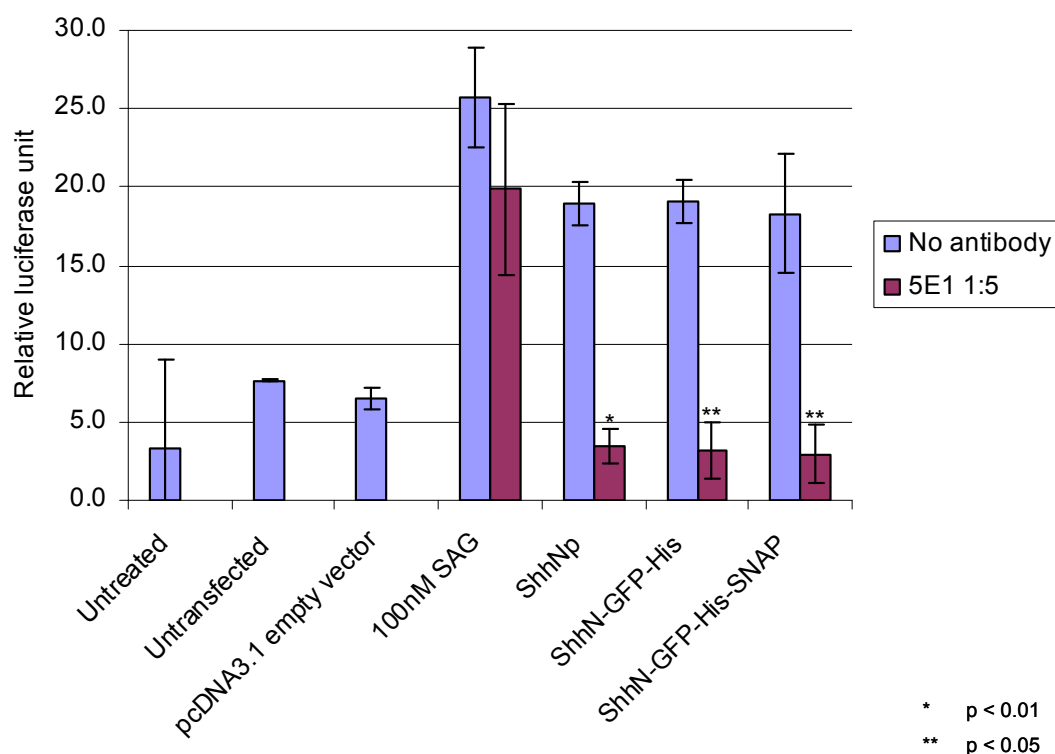
Graphs 3.3 and 3.4 summarize the results of Shh signaling blockage by the 5E1 antibody in the ALP colorimetric and Gli-luciferase reporter assays.

Results



Graph 3.3. Inhibition of the biological activity of the HEK293 expressed ShhN variants by 5E1 blocking of the Ptc binding pseudo-active site analyzed by ALP colorimetric assay. ALP expression induced by the treatment with ShhNp, ShhN-GFP-His and ShhN-GFP-His-SNAP in C3H10T1/2 cells was reduced after treatment with the anti-Shh antibody 5E1. The ShhNp conditioned medium was the positive control of Shh signaling and ALP expression. 100nM SAG was both a positive control of Shh signaling and ALP expression, and a negative control of 5E1 blocking.

The blockage of ALP expression by 5E1 was specific only in the cells treated with the conditioned media of ShhNp, ShhN-GFP-His and ShhN-GFP-His-SNAP (Graph 3.3). This result indicated that the ALP expression detected in the C3H10T1/2 clone 8 cells was specifically induced by and only due to the presence of the ShhN variants in the conditioned media of the transfected HEK293 cells.



Graph 3.4. Specificity of the HEK293 expressed ShhN variants on Gli activity induction shown by 5E1 inhibition of the biological activity of the HEK293 expressed ShhN variants. The Gli-luciferase activity induced by the ShhNp, ShhN-GFP-His and ShhN-GFP-His-SNAP variants was reduced in in Shh LIGHT II cells treated with 5E1 antibody. The untreated Shh LIGHT II cells, the cells treated with the conditioned media of the untransfected HEK293 cells and the empty vector mock transfection served as negative controls of Shh signaling and luciferase activity. The ShhNp conditioned medium was the positive control of Shh signaling and luciferase activity. 100nM SAG was both a positive control of Shh signaling and luciferase activity, and a negative control of 5E1 blocking.

Similar to the ALP expression in the C3H10T1/2 clone 8 cells, the Gli-luciferase activity in ShhNp, ShhN-GFP-His and ShhN-GFP-His-SNAP treated Shh LIGHT II cells was blocked by the 5E1 antibody. It illustrated that the activation of Gli transcription was specific to the HEK293 expressed ShhN variants.

Efficient blockage of Shh signal transduction by 5E1 (Graphs 3.3, 3.4) showed that the activities recorded in both ALP colorimetric and Gli-luciferase assays resulted

from ShhN-GFP-His or ShhN-GFP-His-SNAP activity and not from metabolites or contaminants from the expressing cells or culture medium. The ALP colorimetric assay and the Gli-luciferase reporter assay showed comparable results of the biological activity of ShhN variants and its blockage by the 5E1 antibody.

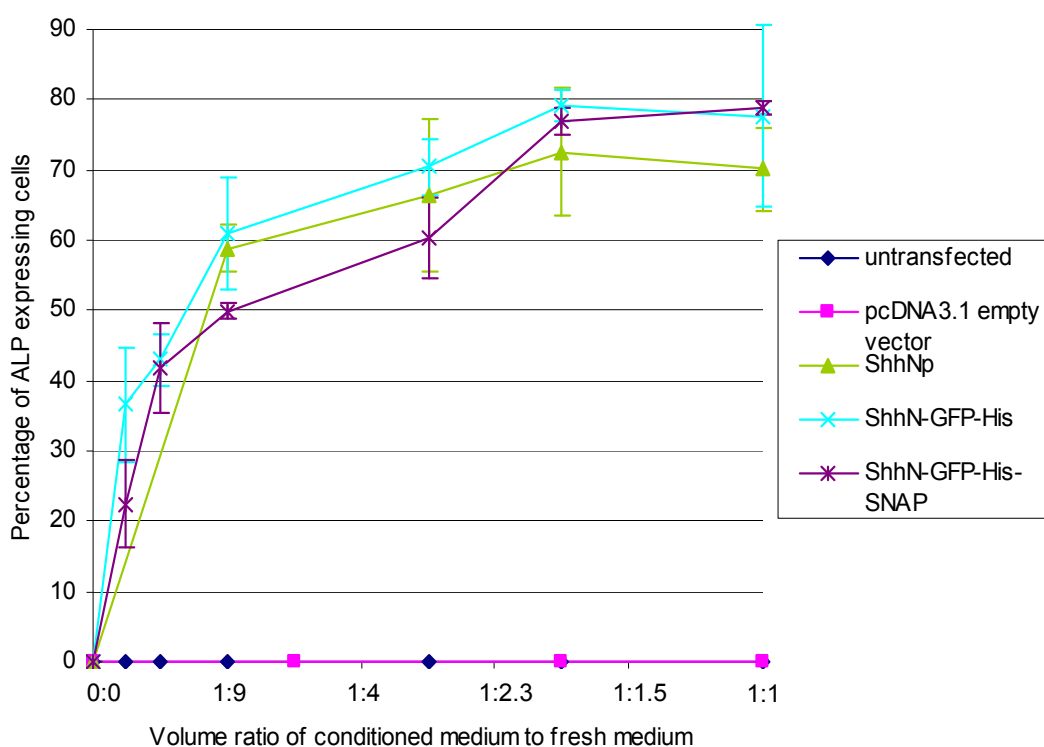
3.2.6.2. Dosage dependent analysis of the biological activity of ShhN variants expressed in HEK293 cells by the alkaline phosphatase expression detection and cell counting assay

After confirming the biological activity and specificity of the HEK293 cell expressed ShhN-GFP-His and ShhN-GFP-His-SNAP, the dosage effect of the proteins on cellular responses was determined by applying different ratios of the ShhN-GFP-His and ShhN-GFP-His-SNAP containing conditioned media onto the Shh responsive cell. ALP expression detection and colorimetric assays, and Gli-luciferase reporter assay were employed again for dosage dependent analysis of the ShhN variants.

Different volume ratios of the ShhN-GFP-His or ShhN-GFP-His-SNAP conditioned medium were mixed with the fresh medium (i.e. DMEM supplemented with 0.5% FBS). The C3H10T1/2 clone 8 cells were then treated with the mixed medium and incubated for 5 days at 37°C with 5% CO₂. Next, cells were fixed and stained for ALP expression with the BCIP/NBT substrate. The number of cells expressing ALP was counted.

Graph 3.5 shows the dose response curves of the C3H10T1/2 clone 8 cells to the HEK293 expressed ShhN variants. Treatment with the conditioned medium from the untransfected HEK293 cells or from the HEK293 cells transfected with the empty

vector of pcDNA3.1 (mock transfection) did not induce ALP expression. The percentage of the ALP expressing C3H10T1/2 clone 8 cells increased with the increasing volume ratios of the applied conditioned media with ShhNp, ShhN-GFP-His and ShhN-GFP-His-SNAP variants. 70 to 80% of the C3H10T1/2 clone 8 cells were expressing ALP when the ShhNp, ShhN-GFP-His or ShhN-GFP-His-SNAP conditioned medium was applied at the volume ratio of 1:1.5 to 1:1. This result shows that the induction of ALP expression was specific to Shh induced signaling.



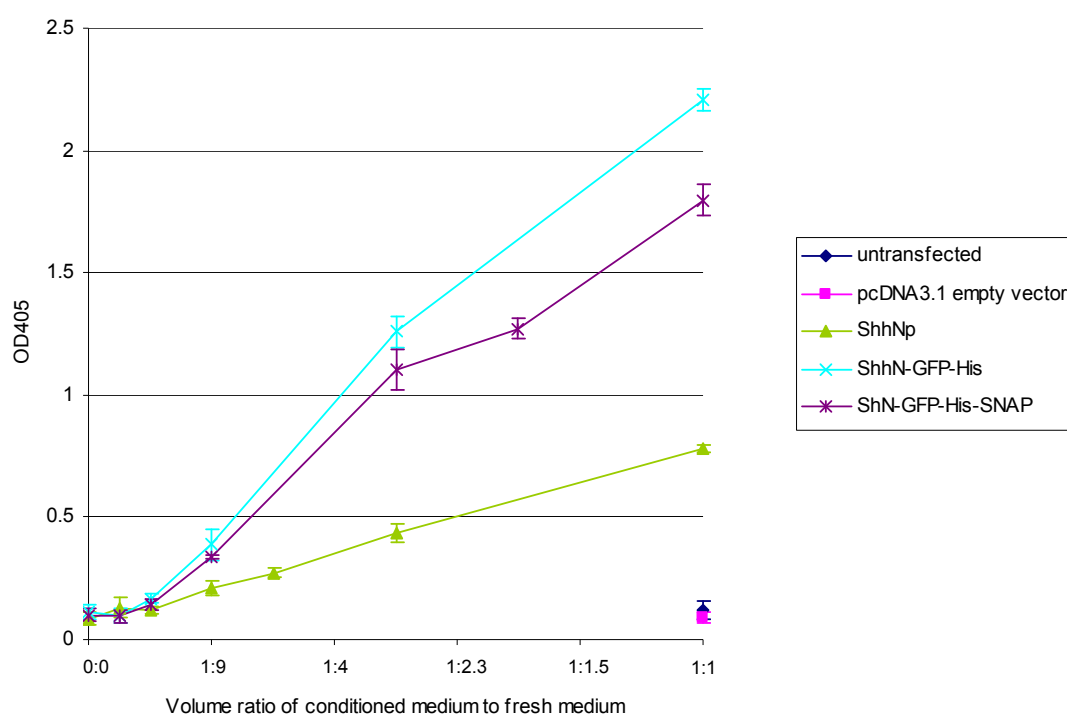
Graph 3.5. Dose dependent biological activity of the HEK293 expressing ShhN variants analyzed by BCIP/NBT detection of ALP expression in C3H10T1/2 clone 8 cells. The percentages of ALP expressing C3H10T1/2 clone 8 cells after 5-day treatment with the conditioned media of untransfected HEK293 cells, mock transfection (empty vector of pDNA3.1) and HEK293 cells transfected with the constructs of ShhNp, ShhN-GFP-His and ShhN-GFP-His-SNAP are shown.

Results

The percentage of the ALP expressing cells increased in a dosage dependent manner with the volume ratios of the conditioned media applied (Graph 3.5). While SAG and RCmShhN gave rise to a maximal percentage of ALP expressing cells (about 32 to 36%) with the concentration of 300nM and showed a declination of biological activity in higher concentrations (Graph 3.1), the ShhN variants expressed in HEK293 cells showed a steady increase in ALP expression up to 80% with an increase in the conditioned medium ratio.

3.2.6.3. Dosage dependent analysis of the biological activity of Shh variants expressed in HEK293 cells by alkaline phosphatase colorimetric assay

ALP colorimetric assay was employed to test the dose dependent biological activity of the ShhN-GFP-His and ShhN-GFP-His-SNAP variants.



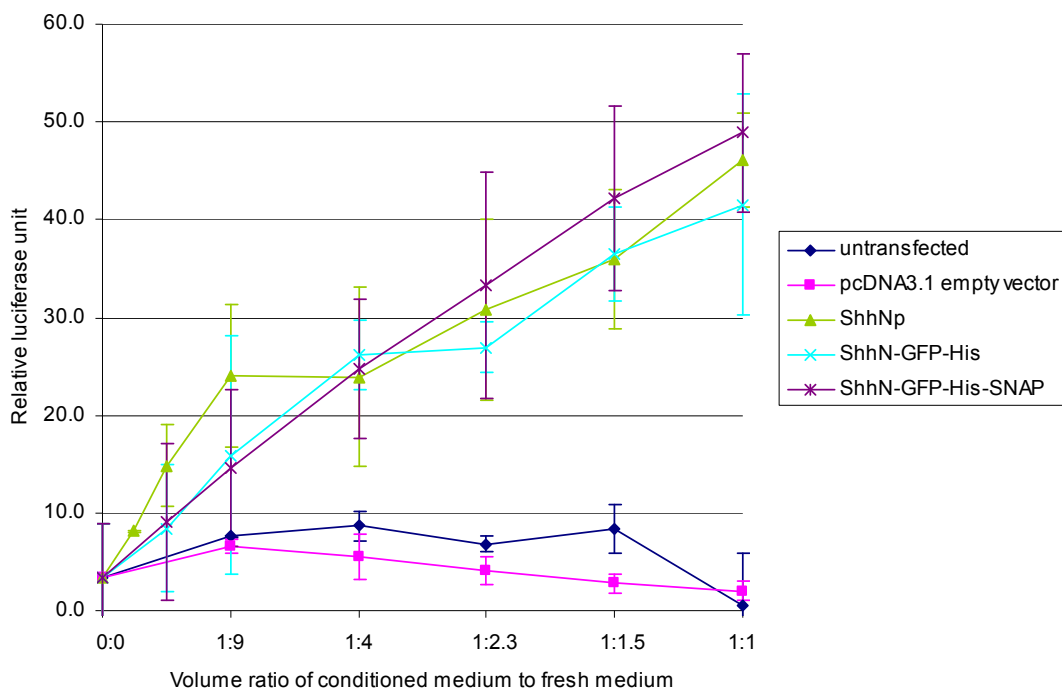
Graph 3.6. Dose dependent induction of ALP expression in C3H10T1/2 clone 8 cells by the HEK293 expressed ShhN variants measured by ALP colorimetric assay. Different volume ratios of the conditioned media collected from the HEK293 cells transfected with the constructs of ShhNp, ShhN-GFP-His and ShhN-GFP-His-SNAP were added to the C3H10T1/2 clone 8 cells and incubated for 5 days. The optical density revealing the ALP activity was measured at the wavelength of 405nm (OD405).

The highest ALP activity was noticed at the ShhN variant containing conditioned medium to fresh medium ratio of 1:1 (Graph 3.6). However, although there was a general increase in ALP expression in the C3H10T1/2 clone 8 cells with an increasing

dosage of the Shh variants, it was observed that ShhN fused with different tags gave rise to different intensities of cellular response. This is quite different from what was observed in the ALP expression detection and cell counting assay (Graph 3.5), in which all ShhN variants showed comparable intensity of cellular responses. In the ALP colorimetric assay (Graph 3.6), ShhNp, which is 19kDa and does not possess any tags, shows a dosage dependent response curve with a shallow slope. ShhN-GFP-His and ShhN-GFP-His-SNAP are 49 and 70kD, respectively and show steeper dosage dependent response curves. These variations in cellular responses detected may be due to the different detection limits of the two assays. The BCIP/NBT staining of ALP expression is based on the substrate interaction with the intracellular ALP. The color intensity as well as the number of cells stained are dependent on the reaction between the BCIP/NBT substrate and alkaline phosphatase enzyme in the cells. On the other hand, the ALP colorimetric assay relies on cell lysis and the release of the expressed ALP for the detection by the ALP specific substrate para-nitrophenylphosphate (pNpp) for color development.

3.2.6.4. Dosage dependent analysis of the biological activity of ShhN variants expressed in HEK293 cells by Gli-luciferase reporter assay

In the Gli-luciferase reporter assay, induction of the luciferase activity, which dependent on Shh signaling, was done in Shh LIGHT II cells. Graph 3.7 illustrates the dosage dependent response curves of the Shh LIGHT II cells treated with the conditioned media containing ShhNp, ShhN-GFP-His and ShN-GFP-His-SNAP variants.



Graph 3.7. Dose dependent induction of Gli-luciferase activity in Shh LIGHT II cells by the HEK293 ShhN variants. Different volume ratios of the conditioned media collected from the HEK293 cells transfected with the constructs of ShhNp, ShhN-GFP-His and ShhN-GFP-His-SNAP were added to the Shh LIGHT II cells and incubated for 48 hours. Firefly luciferase activity revealing the Gli response to Shh signaling was measured and normalized with the constitutive *Renilla* luciferase activity to give the relative luciferase units. The response curve showed that Shh LIGHT II cells were specifically responsive to the conditioned media collected from the HEK293 cells transfected with the constructs of ShhNp, ShhN-GFP-His and ShhN-GFP-His-SNAP. The luciferase activity increased in a dosage dependent manner. Conditioned media from the untransfected HEK293 cells and mock transfection (empty vector of pcDNA3.1) served as negative controls of transfection and Shh signaling, indicating the luciferase activity detected from the ShhNp, ShhN-GFP-His and ShhN-GFP-His-SNAP conditioned media was specifically induced by Shh signaling.

The highest luciferase activity (40 to 50%) was observed when the conditioned media with the ratio of 1:1 to the fresh medium were applied (Graph 3.7). While the luciferase activity of the Shh LIGHT II cells treated with the conditioned media of untransfected HEK293 cells and the HEK293 cells transfected with the empty vector of pcDNA3.1 was low and could be considered as a background, the cells treated with

the ShhNp, ShhN-GFP-His and ShhN-GFP-His-SNAP conditioned media demonstrated a dosage dependent increase in luciferase activity. These findings were comparable with results obtained in the ALP assays (Graph 3.6).

3.2.6.5. Analysis of the biological activity of ShhN-GFP-His and ShhN-GFP-His-SNAP in zebrafish embryos

Owing to the high homology of the peptide sequences of ShhN in mouse and *Danio rerio* (zebrafish) (95% homology) (Figure 3.11), it was speculated that mouse ShhN protein may maintain its biological activity in zebrafish. Therefore zebrafish was employed as another eukaryotic assay system for determining the biological activity of the ShhN-GFP-His and ShhN-GFP-His-SNAP proteins, the ShhN sequence of which was the same as that of the signaling domain of mouse Shh. *In vitro* transcription of the constructs of ShhN-GFP-His and ShhN-GFP-His-SNAP plasmids was done with the mMessage Machine® T7 kit (Ambion, Austin, TX, USA). The transcribed mRNAs were injected into 1-cell stage zebrafish embryos. The injected embryos were raised and collected at 18-somite stage for *in situ* hybridization for *nkx2.2b* and *pax2a*, which are target genes of shh induced signaling in zebrafish.

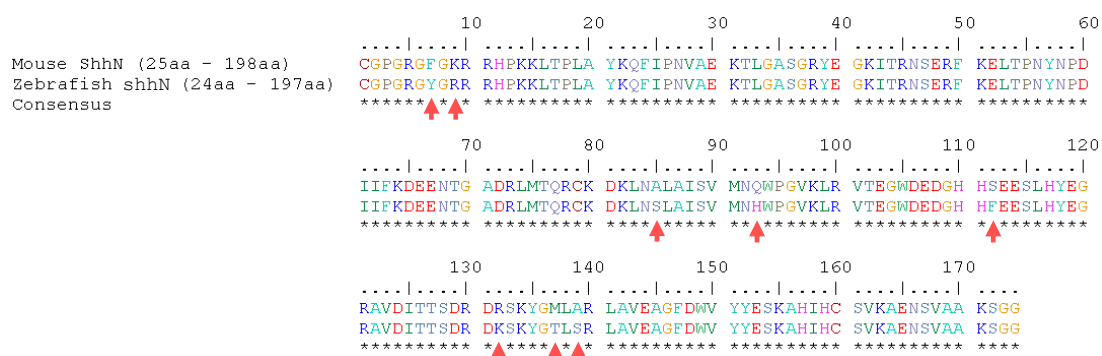


Figure 3.11. Alignment of the N-terminal signaling domains of the mouse ShhN and zebrafish shhN (shhN). The amino acid sequence alignment shows that the mouse ShhN and zebrafish shhN share a sequence homology of 95% with 8 amino acids different (indicated by red arrows),

600ng/ μ l mRNA of the full length zebrafish shh (shh-FL) or 1 μ g/ μ l mRNA of ShhN-GFP-His and ShhN-GFP-His-SNAP were injected into zebrafish embryos. 600ng/ μ l zebrafish shh-FL was found enough to induce Shh signaling; while a higher concentration of the mouse ShhN variants was used to ensure the induction of Shh signaling. The ShhN sequences in mouse and zebrafish are very similar, but there are still 8 amino acids different in the 174 residue containing peptide sequences. In addition, the mouse ShhN protein variants expressed would lack the C-terminal cholesterol modification, which is important for the extracellular diffusion of morphogens. Higher dosage of mouse ShhN may be required to compensate the slight sequence difference as well as the transport inefficiency for generating the same phenotype induced by zebrafish shh signaling. The mRNA of zebrafish shh-FL, and mouse ShhN-GFP-His and ShhN-GFP-His-SNAP protein variants injected led to expanded expression pattern of and the shh target gene *pax2a* at 18-somite stage (Figure 3.12). A very mild up-regulation of *nkx2.2b* was detected in the telencephalon of the embryos injected with zebrafish shh-FL and ShhN-GFP-His-SNAP mRNA.

Results

The mRNA of full length zebrafish *shh* gene served as the positive control of *shh* signaling in the injected zebrafish embryos. The similar results obtained after injection of the mRNA of ShhN-GFP-His and ShhN-GFP-His-SNAP variants, and the mRNA of full length zebrafish *shh* indicated that ShhN-GFP-His and ShhN-GFP-His-SNAP were biologically active.

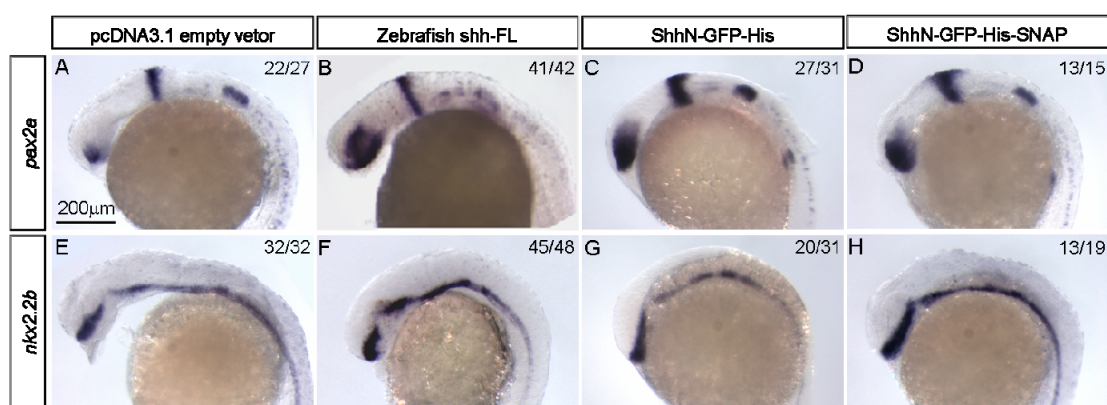


Figure 3.12. Expansion of *pax2a* expression pattern (A – D) and weak up-regulation of *nkx2.2b* (E – H) by overexpression of ShhN variants in zebrafish embryos. *In situ* hybridization of 18-somite stage zebrafish embryos injected with mRNA of full length zebrafish *shh*, ShhN-GFP-His and ShhN-GFP-His-SNAP was done. Numbers at the right hand upper corner indicated the numbers of embryos with the phenotypes shown in the image and the total numbers of embryos counted, respectively.

Taken together, the biological activity of the HEK293 cell expressed ShhN variants was found to be consistent in assays with different read out systems.

3.3. Part 2 – Development of biological compatible interfaces for ShhN immobilization

To immobilize ShhN protein on functionalized surfaces for cellular response analysis *in vitro*, it is essential not only to know if ShhN is available to the responsive cells but also to understand how ShhN recognizes and interacts with its receptor at the membrane of the responsive cells. The tag or linker group used for protein immobilization on a surface should not block the accessibility of the receptor to the protein. In the case of ShhN, the poly(6)histidine, biotin and SNAPTM tags were fused at the C-terminus of the protein. The 5E1 immunoprecipitation experiments suggested the availability of the pseudo-active site (Figures 3.2, 3.4 to 3.6). Further, the immobilization technologies have to provide exceptional selectivity for ShhN to allow specific binding of ShhN to the target molecule from a complex mixture of other proteins. This is of special importance for immobilizations directly from the HEK293 cell supernatant without any purification step like e.g. affinity chromatography.

For binding to its receptor Ptc, the availability of the binding groove of ShhN is essential. The pseudo-active site of Shh is comprised of five histidine residues at positions 133, 134, 140, 180 and 182 of the ShhN peptide (Bosana et al., 2009). In the tertiary structure of the biologically active ShhN, those 5 histidine residues are in close vicinity in the binding pocket for Ptc (Bosana et al., 2009; Maun et al., 2010a, b). Since this pseudo-active site is located in the middle of the ShhN peptide, both N- and C-termini of ShhN can serve as immobilization sites. Published literature does not indicate involvements of both termini of ShhN for ShhN/Ptc binding, hence immobilization of ShhN via its C-terminus was tested.

The ShhN variants expressed in *E. coli* were used for development and optimization of the immobilization conditions unless otherwise stated. The convenient large scale production using *E. coli* guaranteed the availability and required quantities of the proteins. The fusion with GFP provided easy visualization.

3.3.1. Immobilization of ShhN-GFP-His on modified polystyrene surfaces via nickel(II)/poly(6)histidine affinity interaction

Irradiation of polystyrene surfaces with ultraviolet light of $\lambda = 185\text{nm}$ leads to formation of hydrophilic surfaces rich in carboxylic acid (COOH) groups (Welle et al., 2002; Welle et al., 2005). These surface properties affect strongly the adsorption of proteins from single protein solutions or from complex mixtures like fetal calf serum. It was found that native, hydrophobic polystyrene preferentially adsorbs albumin, whereas UV irradiated polystyrene favored the adsorption of cell attractive proteins from serum containing media (Welle et al., 2002, 2005). To allow selective binding of ShhN-GFP-His via the nickel(II)/poly(6)histidine interaction the polymer surface was functionalized to provide a nickel chelating moiety.

The first step was to introduce the COOH groups on the polystyrene surface by deep UV lithography followed by a wet chemical activation of the COOH groups with an EDC to form a NHS reactive ester. The following coupling of N₂,N₂-bis (carboxymethyl)-L-lysine via the terminal amino group formed the nickel chelating groups at the polymer surface. Finally the surfaces were loaded with nickel (Ni²⁺) ions from a 40mM NiSO₄ solution (Ashe and Briscoe, 2006; Ekblad and Liedberg, 2010; Gallet and Therond, 2005; Wong et al., 2009). To examine if the C-terminally poly(6)histidine tagged ShhN could be immobilized on the obtained nickel

functionalized polystyrene surfaces, ShhN-GFP-His was used. ShhN-GFP-His fused with GFP is easily detectable under a fluorescence microscope if bound onto the surfaces.

After 24 hours of incubation in 500nM ShhN-GFP-His solution at 4°C, GFP signal was observed on the UV photopatterned polystyrene surfaces modified with Ni²⁺ ions (Figure 3.13). Fluorescence micrographs demonstrate the successful immobilization of ShhN-GFP-His on nickel modified polystyrene surfaces.

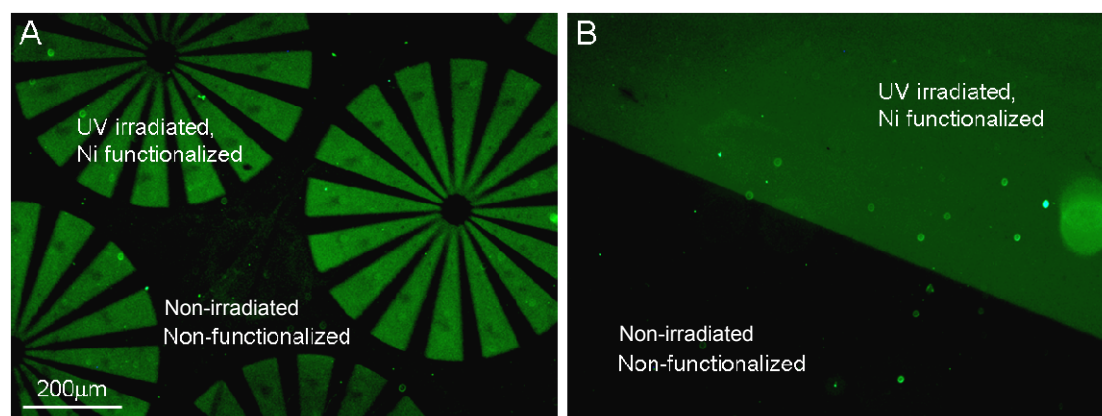
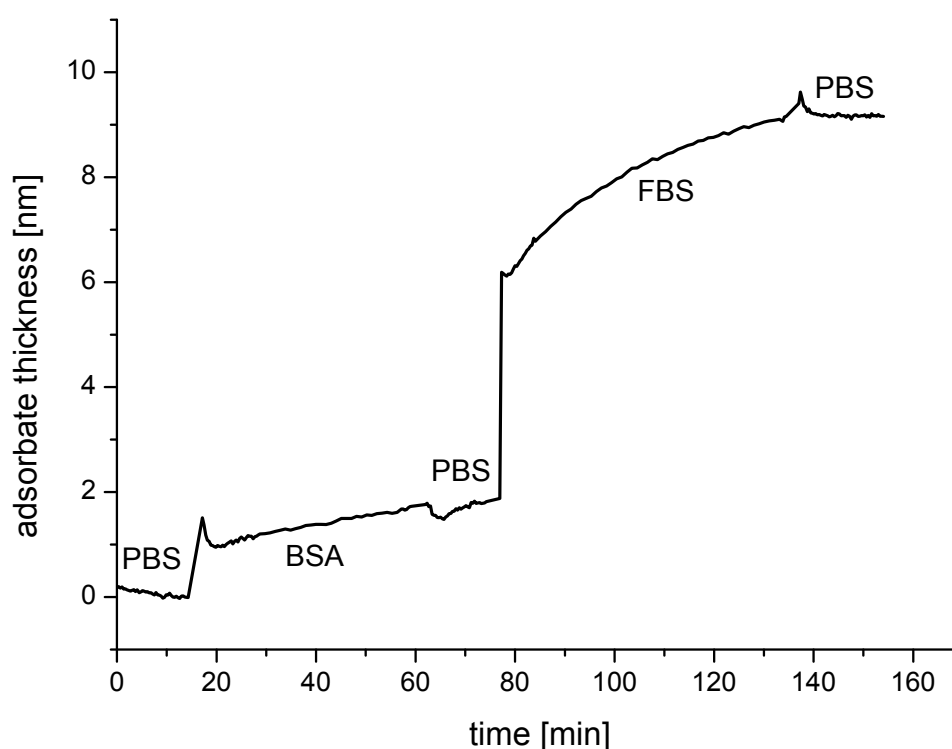


Figure 3.13. ShhN-GFP-His immobilization on polystyrene surfaces after masked UV irradiation and nickel modification. Ni-NTA was coupled exclusively to the photo modified areas. (A, B) ShhN-GFP-His was immobilized only in the UV irradiated and nickel functionalized areas, as revealed by the green fluorescence.

However, it is known that UV induced surface hydrophilization yields not exclusively carboxylate groups on the PS surface but also some intermediates and by products affecting protein binding on polystyrene surfaces. Regardless of the presence of nickel, the applied UV lithography based preprocessing step results in random adsorption of non-histidine tagged proteins onto the UV irradiated surface (figure 1.9). Apart from the possibility of some randomly oriented ShhN molecules which might not be functional, a sample of this type might exhibit unwanted effects in the

cell culture experiment due to the adsorption of some unknown proteins from the cell culture medium. Therefore it was tested if BSA preadsorbed onto the patterned samples can act as blocking agent against unspecific adsorption. To prove this possibility, a QCM-D measurement of the deposition of BSA and FBS on non-nickel functionalized UV irradiated polystyrene surfaces was performed (Graph 3.8). Adsorption of both BSA and FBS on the surfaces is irreversible as they could not be washed away with PBS. The thicknesses of BSA and FBS measured indicate that UV modified polystyrene surfaces adsorb protein unselectively.



Graph 3.8. QCM-D measurement of the deposition of BSA and FBS on UV irradiated polystyrene surfaces. All protein adsorption experiments were performed by exposing the polymer coated quartz crystals to the following solutions: 15 min, PBS; 60 min, 50 $\mu\text{g/ml}$ BSA in PBS; 75 min, PBS; 135 min, 1 vol% FCS in PBS; 135 min, PBS. Changes of the resonant frequencies and dissipation values were recorded, and converted to adsorbate thicknesses as indicated in the graph.

As shown in graph 3.8. BSA blocking of UV irradiated PS does not provide an inert surface with respect of unspecific adsorption of other proteins from FBS containing media. Other experiments, data not shown, however, demonstrated that BSA is indeed passivating a pristine PS surface with respect of deposition of other proteins from FBS. Because the UV irradiated polystyrene, with or without further nickel modification, can induce unspecific protein absorption, it was not possible to quantify the amount of ShhN-GFP-His, being actually immobilized via the specific nickel(II)/poly(6)histidine interaction on the UV irradiated areas.

To minimize unspecific adsorption of ShhN-GFP-His and to reduce effects of possibly co-adsorbed proteins, the development of protein repellent surfaces and application of highly selective protein anchoring head groups were critical.

3.3.2. Immobilization of ShhN by dip-pen nanolithography

In order to ensure immobilization of ShhN only on specific areas of the functionalized surfaces, dip-pen nanolithography (DPN) was employed. Nickel chelating as well as biotinylated phospholipids were used to immobilize the ShhN-GFP-His and ShhN-GFP-His-BA variants on polyethylene glycol (PEG) modified surfaces via nickel(II)/poly(6)histidine and biotin/streptavidin affinity interactions, respectively. BG terminated DOPE lipids were delivered on polystyrene surfaces for ShhN-GFP-His-SNAP immobilization via BG/SNAPTM covalent binding.

3.3.2.1. ShhN immobilization via poly(6)histidine tag on nickel presenting phospholipids

As shown, UV irradiated polystyrene surfaces exhibited unspecific protein adsorption which could interfere with the immobilization of ShhN-GFP-His via nickel(II)/poly(6)histidine interaction and possibly affect the specific ShhN/Ptc receptor binding or introduce other unwanted side effects during the in vitro experiment. However, if the unspecific protein binding could be eliminated, the nickel(II)/poly(6)histidine interaction would be reliable and convenient for protein immobilization on functionalized surfaces.

Unlike polystyrene, PEG does not favor protein adsorption (Huang et al., 2001). Therefore, PEG modified surfaces can allow for selective protein immobilization on designated areas where a specific functionalization was introduced. Nickel chelating lipids were printed in 10 μ m \times 10 μ m square patterns by DPN on a PEG coated glass surface. The surfaces were then exposed to 1 μ M solution of *E. coli* expressed ShhN-GFP-His at room temperature for 30 minutes.

As shown in figure 3.14, green fluorescence signal from ShhN-GFP-His was detectable on the square patterns where the nickel presenting lipids were printed but not on the non-functionalized PEG areas. On control patterns, where pure DOPC (no nickel chelating lipids admixed to DOPC) were printed, no signal from ShhN-GFP-His was detected. The green fluorescence signal intensity, which was measured by ImageJ, increased with the increasing molar ratio of the nickel chelating lipids in DOPC and reached a maximum at 30mol% (Figure 3.14). With reference to the applied range of molar ratio of nickel chelating lipids in DOPC, different amounts

of ShhN-GFP-His could be immobilized via nickel(II)/poly(6)histidine interaction on PEG coated glass surfaces with high specificity.

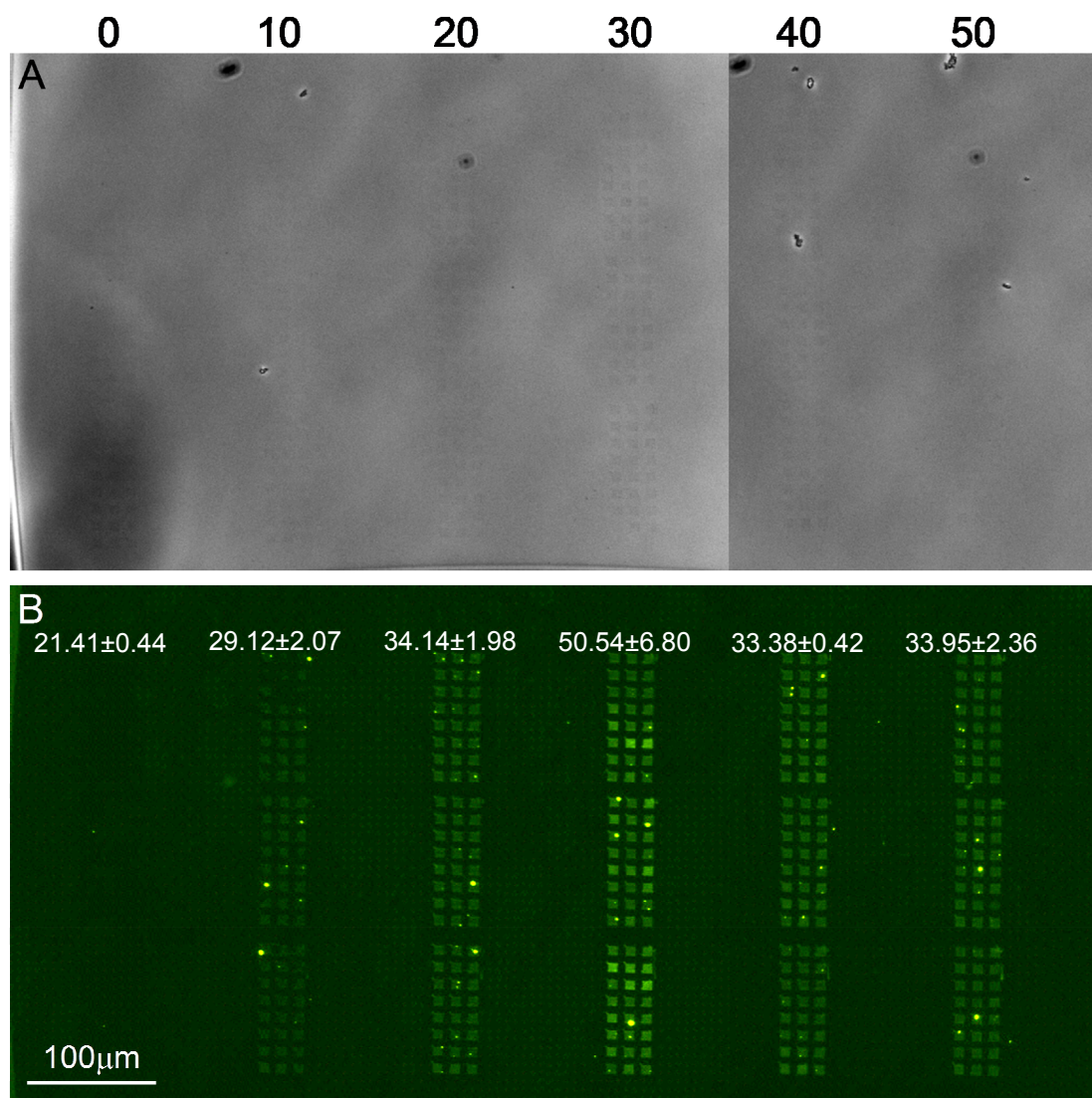


Figure 3.14. Immobilization of *E. coli* expressed ShhN-GFP-His on nickel presenting phospholipids patterns printed by DPN. Phospholipid patterns were deposited on PEG coated glass surfaces to form supported lipid multilayers. DOPC was admixed with 0, 10, 20, 30, 40, and 50 mol% nickel chelating lipids. Bright field image was taken immediately after printing (A). The numbers at the top of this figure represent the mol% of nickel chelating lipids in DOPC. 1µM ShhN-GFP-His solution was applied on the surfaces and incubated at room temperature for 30 minutes. Fluorescence image was taken and GFP fluorescence intensity was quantified (B). The highest green fluorescence intensity was observed for 30mol% nickel chelating lipids in DOPC.

Results

After testing the *E. coli* expressed ShhN-GFP-His binding to the nickel chelating lipids, glass surfaces with the same PEG modification and DPN patterns of 30mol% nickel chelating lipids in DOPC were used to immobilize the HEK293 expressed ShhN-GFP-His. HEK293 cells were first transfected with the DNA construct of ShhN-GFP-His. The conditioned medium containing the expressed ShhN-GFP-His protein was then collected after 48 hours and applied on the PEG modified glass surfaces, on which 30mol% nickel chelating lipids admixed with DOPC and rhodamine was printed in 50 μ m \times 50 μ m square patterns, prepared in advance. The adsorption and availability of the pseudo-active site of the immobilized ShhN-GFP-His was detected by the anti-Shh antibody 5E1. Figure 3.15 shows the immunofluorescence images of the surfaces exposed to the HEK293 expressed ShhN-GFP-His. The green fluorescence detected suggests that the ShhN-GFP-His was immobilized on the surfaces and that the pseudo-active site of ShhN was available. There was no signal detected from the pure PEG coated glass or the one incubated with the conditioned medium from untransfected HEK293. The poor lipid pattern quality was due to some printing error. Nonetheless, the rhodamine signal indicates the locations of the nickel chelating lipids. The signal was correspondent to the green fluorescence signal, where the anti-Shh antibody 5E1 detected the HEK293 expressed ShhN-GFP-His protein.

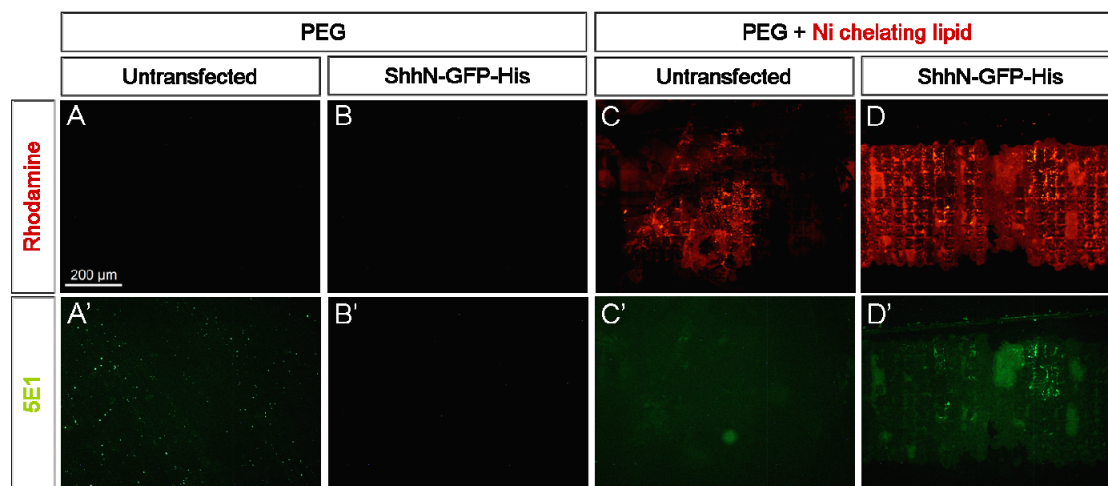


Figure 3.15. Immobilization of HEK293 expressed ShhN-GFP-His on the nickel chelating phospholipid patterns produced by DPN. Phospholipids were admixed with 30mol% nickel chelating lipids and rhodamine labelled lipids (red fluorescence). These phospholipids were then deposited on the PEG treated glass surfaces in $50\mu\text{m}\times 50\mu\text{m}$ square patterns to form supported lipid multilayers. The surfaces were incubated with the conditioned medium containing HEK293 expressed ShhN-GFP-His at room temperature for 2 hours. Immunodetection of the immobilized protein with the anti-Shh antibody 5E1 shows the green fluorescence signal (D'). Conditioned medium from untransfected HEK293 cells and pure PEG surfaces served as the negative controls for protein binding (A' to C').

Apart from the poly(6)histidine tag at the C-terminus, there are another 6 individual histidine residues at different positions in the ShhN peptide. Five of these histidine residues get into close vicinity as a result of tertiary peptide folding ending up with the formation of the pseudo-active site, the binding pocket to the Shh receptor Ptc (Bosana et al., 2009; Maun et al., 2010a, b). This binding pocket coordinates with a zinc (Zn^{2+}) ion for Ptc binding. That means for identical ionic charge and similar ion sizes, the pseudo-active site of ShhN may also strongly interact with Ni^{2+} ion. Therefore, a nickel immobilization would not just couple ShhN-GFP-His via the poly(6)histidine tag but also potentially block the pseudo-active site of ShhN, hindering the ShhN/Ptc binding and its biological activity. The weaker green fluorescence signal detected and the smaller area coverage by 5E1 than the rhodamine

may indicate partial blockage of the pseudo-active site by the Ni²⁺ ions. Therefore another tagging system was employed for ShhN immobilization.

3.3.2.2. ShhN immobilization via biotin/streptavidin affinity interaction on the biotinylated phospholipids

To ensure that ShhN could only be immobilized via the C-terminus without disturbing the histidine rich pseudo-active site, the specificity and position of the tag are crucial. Therefore the well known biotin/streptavidin system was also tested for ShhN immobilization on the DPN printed biotinylated lipids. The biotin/streptavidin binding is remarkably strong with a dissociation constant (K_d) of 4×10^{-14} M (Holmberg et al., 2005; Livnah et al., 1993). A biotin, which recognizes and binds to streptavidin, was fused at the C-terminus of ShhN. The resulting protein was ShhN-GFP-His-Biotin with GFP for visualization and the histidine tag for Ni-NTA column purification. By introducing streptavidin to the biotin functionalized surfaces, the biotinylated ShhN-GFP-His-Biotin could be adsorbed onto the surfaces with streptavidin as an intermediate substrate in a "sandwich system" of biotin-streptavidin-biotin.

Biotinylated lipids were deposited in $10\mu\text{m} \times 10\mu\text{m}$ square patterns by DPN on PEG coated glass surface. The surfaces were then incubated in $5\mu\text{g/ml}$ streptavidin solution at room temperature for 30 minutes, washed twice with PBS and then exposed to $1\mu\text{M}$ *E. coli* expressed ShhN-GFP-His-Biotin solution at room temperature for 30 minutes.

As expected, ShhN-GFP-His-Biotin (sequence information in table 2.1) was immobilized on the biotinylated lipids via streptavidin. The maximal amount of ShhN-GFP-His-Biotin, with quantified GFP fluorescence intensity of 30.38 ± 2.64

arbitrary units, was immobilized on the biotinylated phospholipid patterns via binding with 4 mol% biotinylated lipids in DOPC (Figure 3.16).

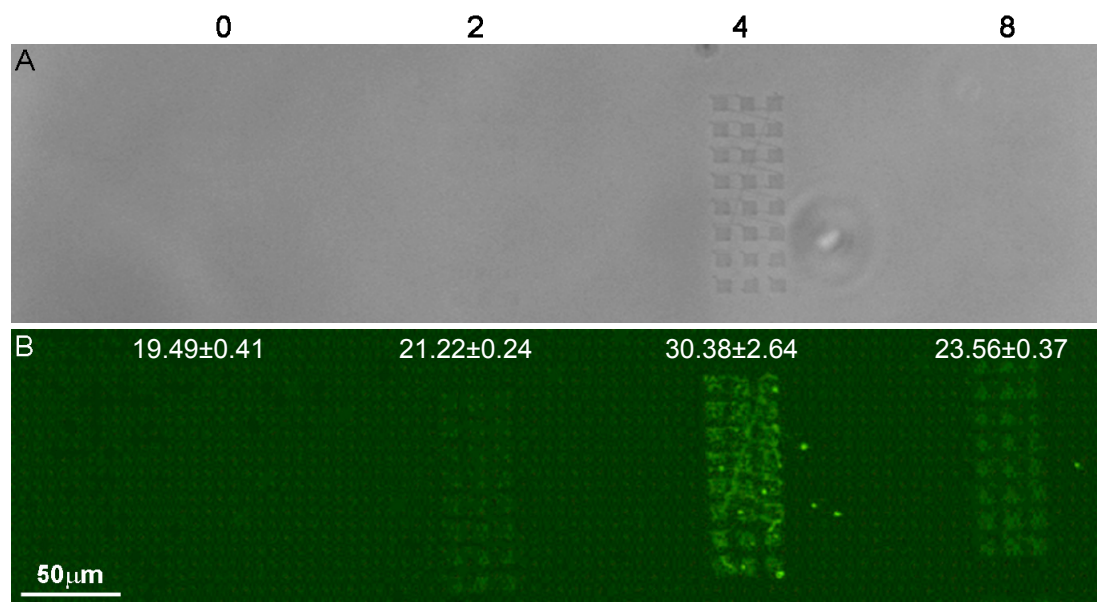


Figure 3.16. Immobilization of *E. coli* expressed ShhN-GFP-His-Biotin on biotinylated phospholipid patterns with streptavidin as the linker between the lipids and the protein. Phospholipid patterns were deposited on PEG treated glass surfaces to form supported lipid multilayers. Phospholipids were admixed with 2, 4, and 8 mol% biotinylated lipids. Bright field image indicated the DPN patterns of the biotinylated lipids (A). The surfaces with the biotinylated patterns were incubated in 5 μg/ml streptavidin at room temperature for 30 minutes, rinsed twice with PBS and incubated in 1 μM ShhN-GFP-His-Biotin at room temperature for 30 minutes. The fluorescence image shows the highest green intensity when ShhN-GFP-His-Biotin was immobilized on 4 mol% biotinylated lipids (B), indicating that the maximal amount of ShhN-GFP-His-Biotin was immobilized. The numbers above the figure represent the mol% of biotinylated lipids admixed in DOPC.

Since biotin/streptavidin binding is restricted to the C terminus of ShhN-GFP-His-Biotin, the orientation of immobilized ShhN-GFP-His-Biotin was controlled. This biotin/streptavidin immobilization system also ensures the availability of the pseudo-active site of ShhN-GFP-His-Biotin for Ptc binding.

Despite the strength of biotin/streptavidin interaction, immobilization of ShhN-GFP-His-Biotin is based on the affinity between biotin and streptavidin, and is non-covalent. To irreversibly immobilize ShhN on functionalized surfaces, the SNAPTM system was employed.

3.3.2.3. ShhN immobilization via benzylguanine/SNAPTM covalent reaction on the benzylguanine functionalized phospholipids

The SNAPTM system relies on the adaptation of the alkylguanine transferase (SNAPTM), which was tagged to ShhN resulting in ShhN-GFP-His-SNAP (sequence information in table 2.1). To immobilize this SNAPTM tagged ShhN-GFP-His-SNAP via the BG/SNAPTM interaction, the BG terminated lipids were first mixed with DOPC at the ratio of 1:1. The mixed lipids were then delivered by DPN on the polystyrene surfaces in 10 μ m \times 10 μ m square patterns. The modified surfaces were then exposed to 1 μ M ShhN-GFP-His-SNAP solution at room temperature for 30 minutes. It would finally lead to covalent immobilization of the protein onto the patterns of BG terminated lipids. Figure 3.17 shows specific binding of ShhN-GFP-His-SNAP to the BG terminated lipid printed areas on native polystyrene surfaces. No protein adsorption was detected on the polystyrene surfaces where no BG functionalized lipids were deposited, since the surfaces were not made hydrophilic and protein attractive by UV irradiation as what was mentioned in section 3.3.1.

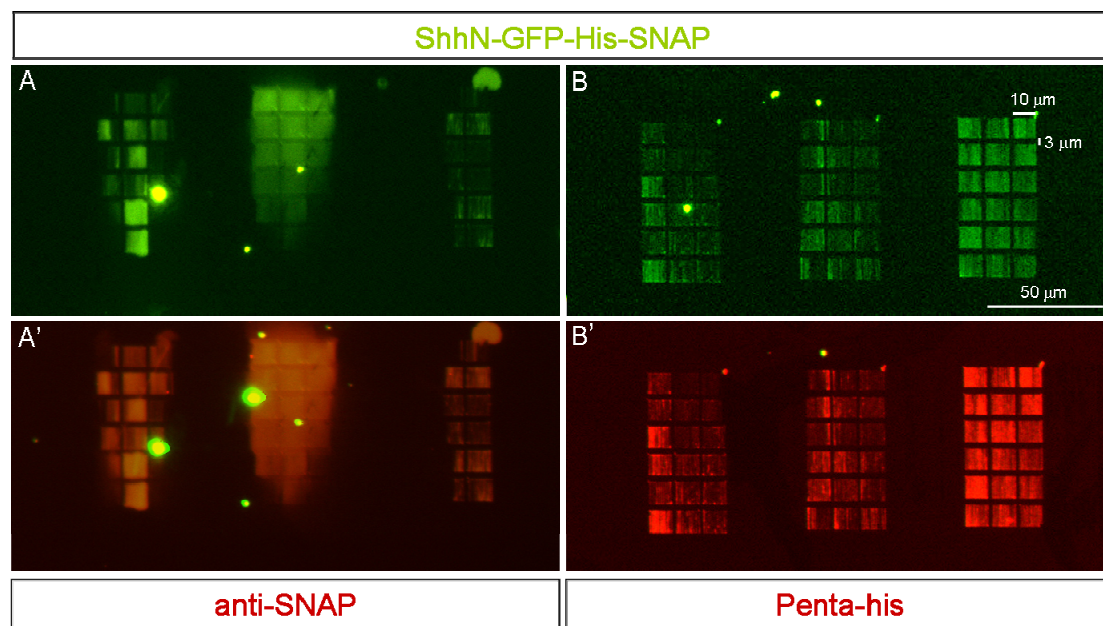


Figure 3.17. Immobilization of ShhN-GFP-His-SNAP on the biotin functionalized lipids via covalent binding between the BG and the SNAPTM tag fused at the C-terminus of ShhN-GFP-His-SNAP. BG terminated DOPE lipid was mixed with DOPC at the ratio of 1:1. Binding of ShhN-GFP-His-SNAP to BG was visualized by the green fluorescence signal (A, B), and detected by immunofluorescence using anti-SNAP and Penta-his antibodies (in red) (A', B').

Similar to the biotin tag, the SNAPTM tag was introduced at the C terminus of ShhN-GFP-His-SNAP, hence the BG/SNAPTM immobilization reaction should not interfere with the binding between the pseudo-active site of ShhN-GFP-His-SNAP and the Shh receptor Ptc.

3.3.3. Immobilization of ShhN-GFP-His-SNAP on gold surfaces via benzylguanine thiol/SNAPTM covalent binding

3.3.3.1. Microcontact printing of benzylguanine terminated thiol on gold surfaces

Microcontact printing (μ Cp) was used to introduce a monolayer of benzylguanine thiol (BGT) on gold surfaces for covalent immobilization of ShhN-GFP-His-SNAP.

The immobilization was started by mixing the BGT and the passivating thiol EG6OH with $\chi_{\text{BGT}}=0.1$. χ_{BGT} represents the molar fraction or ratio of BGT concentration to the total concentration of BGT and EG6OH. A solution of 0.1mM BGT/EG6OH was formed. The solution was coated onto the PDMS stamp with $50\mu\text{m}\times 50\mu\text{m}$ square patterns, which would then be used to deliver the BGT/EG6OH in patterns onto gold surfaces. Next, patterned gold surfaces were backfilled with 0.1mM pure EG6OH solution at room temperature for 1 hour and exposed to 500nM ShhN-GFP-His-SNAP at room temperature for 1 hour for BG/SNAPTM specific covalent binding. The thiol groups have a strong affinity to the gold surface and the bond formed between the BGT and the SNAPTM tag fused to ShhN-GFP-His-SNAP was covalent. Therefore the protein was irreversibly attached to the gold substrate (Figure 3.18).

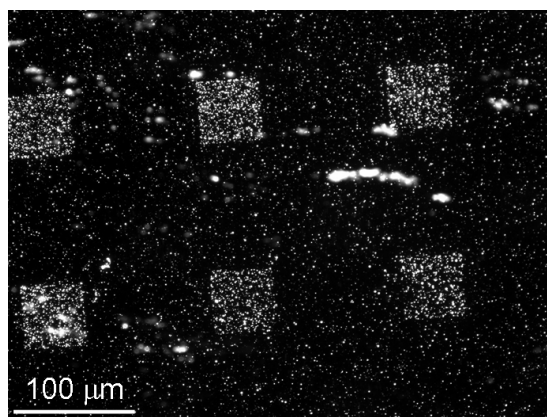


Figure 3.18. Immobilization of ShhN-GFP-His-SNAP on gold surface. The gold surface was stamped with a mixture of BGT and EG6OH by μ Cp. The immobilized ShhN-GFP-His-SNAP in squares was observed via fluorescence microscopy.

Though ShhN-GFP-His-SNAP was immobilized on the BGT stamped area on the gold surface, aggregate formation of the protein was noticed (Figure 3.18). It was discovered that SNAPTM tagged proteins have the tendency of forming aggregates because the SNAPTM binding domain is poor in resisting extreme temperature and pH, and the presence of denaturant (Chivers et al., 2010). Even the immobilized protein would remain attached under these harsh conditions, the protein may unfold, aggregate and promote unspecific binding (Chivers et al., 2010). However, in this experiment, immobilization of ShhN-GFP-His-SNAP was done at room conditions using PBS as the buffer. Rather, GFP tends to oligomerize and form aggregates, and therefore contributes to massive clustering of ShhN-GFP-His-SNAP through crosslinking (Miyawaki, 2005; Yanushevich et al., 2002). Moreover, precipitation of BGT on the stamp surface upon drying prior to stamping onto the gold substrate could result in disordered BGT containing SAMs on the stamped gold areas. These disordered SAMs increase unspecific protein adsorption and affect specific BG/SNAPTM binding adversely.

To minimize aggregation of ShhN-GFP-His-SNAP, 0.5mM DTT was added to the protein buffer. ShhN-GFP-His-SNAP was produced fresh for every experiment and used within a week. UV photolithography instead of μCp was employed for patterning on gold surfaces to avoid disorganization of BGT upon drying since BGT would be used in a solution form to backfill the UV photopatterned area.

3.3.3.2. UV photopatterning and ToF-SIMS analysis of BGT SAM, and immobilization of ShhN-GFP-His-SNAP on gold surfaces

To form a uniform SAM on gold surface 0.1mM EG6OH solution was applied at room temperature for 16 hours. Selected areas of the EG6OH SAM were decomposed by deep UV light for 100 minutes, resulting in formation of $50\mu\text{m}\times 50\mu\text{m}$ square patterns. Backfilling with BGT containing solution was then performed by incubating the surface in 0.1mM BGT/EG6OH solution with $\chi_{\text{BGT}}=0.1$ at room temperature for 1 hour.

By comparing the negative secondary ion spectra of both pristine thiols, gold surfaces coated with EG6OH or BGT could be distinguished using ToF-SIMS. As shown in Figure 3.19, EG6OH contains 6 ethylene glycol ($-\text{CH}_2\text{CH}_2\text{O}-$) repeat units at the tail, which can be identified by their corresponding fragments in ToF-SIMS. BGT contains several nitrogen containing moieties which in turn result in e.g. strong CN^- and CNO^- secondary ions. In addition, it was possible to detect also the intact guanine fragment of BGT in ToF-SIMS providing direct evidence for the successful formation of a BGT SAM.

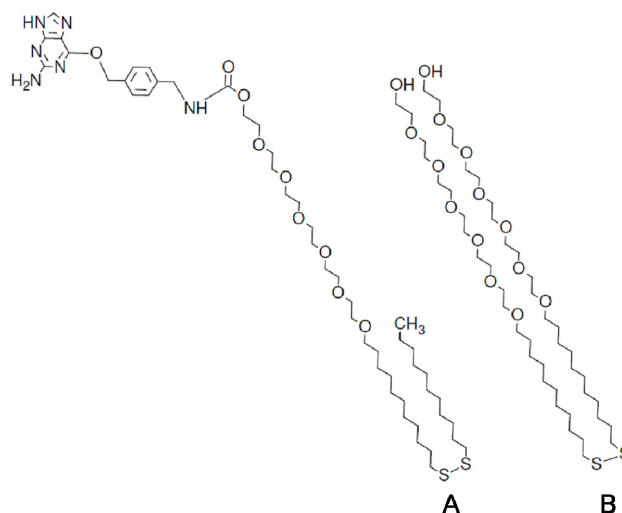
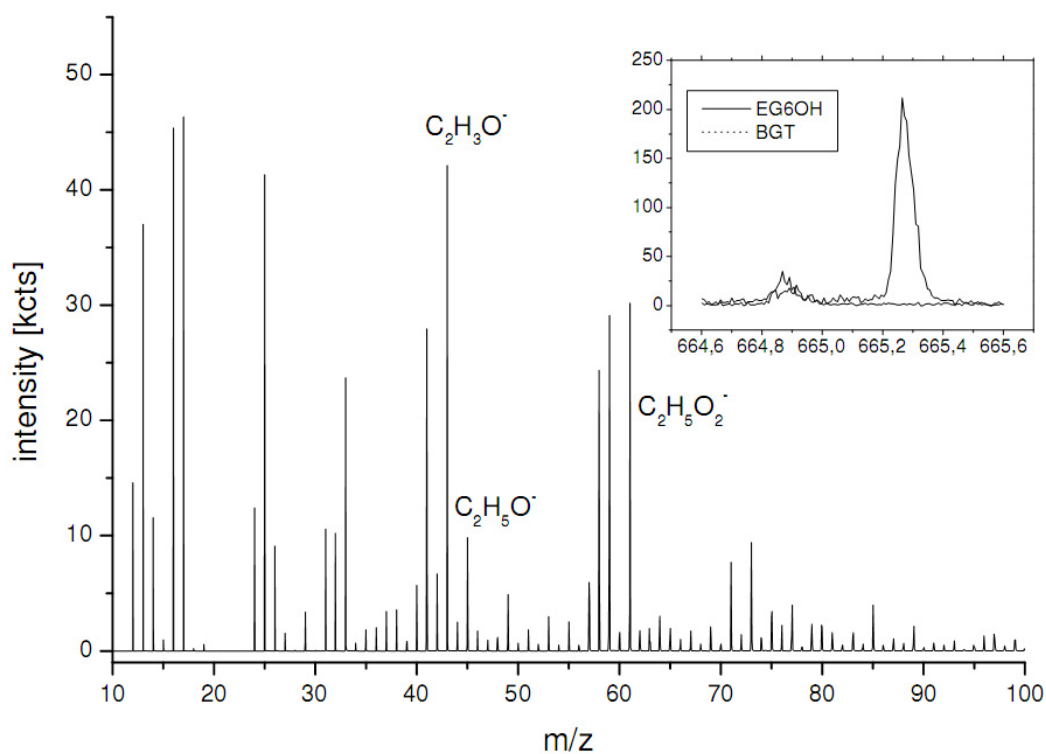


Figure 3.19. Molecular structures of the applied disulfides that form a self-assembled monolayer on gold surfaces for the immobilization ShhN-GFP-His-SNAP. (A) Benzylguanine terminated disulfide (BGT). (B) Passivating thiol EG6OH.

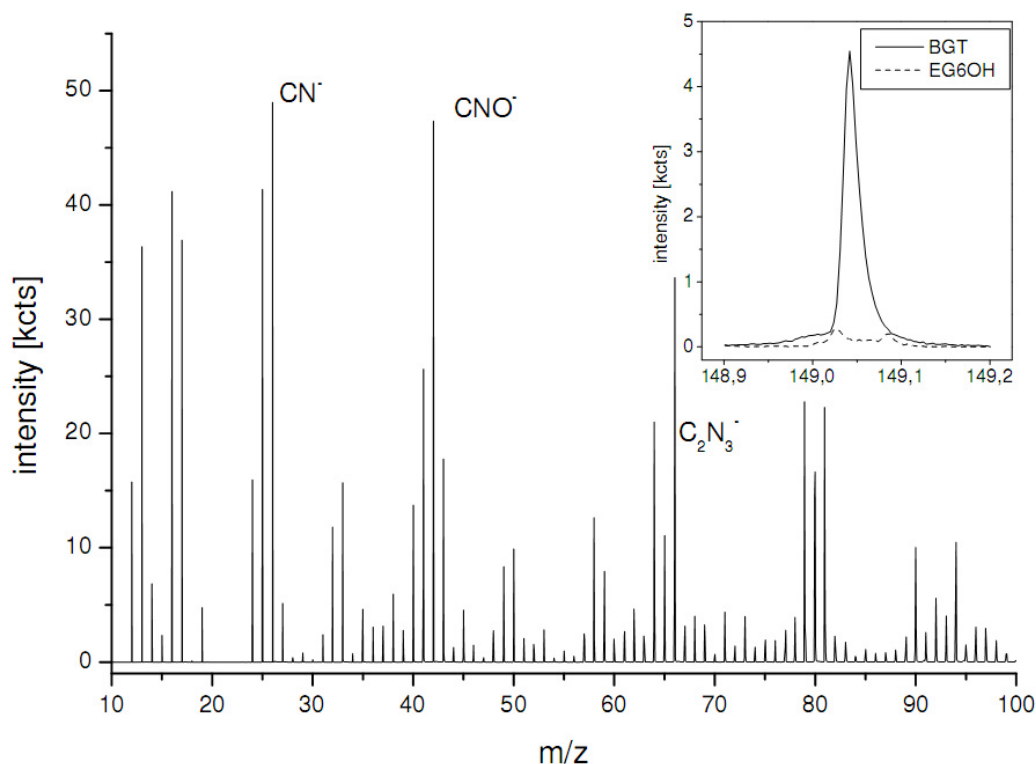
Graphs 3.9 and 3.10 are negative secondary ion spectra of pristine EG6OH and BGT SAMs.

Signals of the ethylene glycol repeat units $C_2H_3O^-$, and the $C_2H_5O_2^-$ head group indicate the presence of EG6OH (Graph 3.9). The intensity for oxidized species such as CHO_2^- is low. Also no significant CN^- and CNO^- signals were detected.



Graph 3.9. Negative secondary ion spectrum from a pristine EG6OH self assembled monolayer. Spectra recorded in bunched mode with high mass resolution, total counts: 1.8×10^6 . Insert: Detail spectrum around 665amu, 5 points binning of original data, for two different SAMs: EG6OH (solid line), and BGT (dotted line). Spectra scaled by total intensity.

In the negative secondary ion spectrum of BGT (Graph 3.10), characteristic CN^- and CNO^- signals for BGT were detectable. Like the spectrum of EG6OH, weak signal was detected for CHO_2^- in pristine BGT SAM in the absence of photo degradation.



Graph 3.10. Negative secondary ion spectrum from a pristine BGT self assembled monolayer. Spectra recorded in bunched mode with high mass resolution. Insert: Detail spectrum around 149amu, 5 points binning of original data. The CN^- , CNO^- and guanine signals indicated the presence of BGT, which contained amine and amide groups at the tail of the thiol.

Images of time-of-flight secondary ion mass spectroscopy (ToF-SIMS), shown in Figures 3.20 and 3.21 illustrated EG6OH and BGT assembling on gold surface with UV photopatterning and backfilling. Signals of $\text{C}_2\text{H}_3\text{O}^-$ and $\text{C}_2\text{H}_5\text{O}_2^-$ from EG6OH were recorded from the area where there was no UV degradation of the SAM (Figure 3.35). Localized degradation of EG6OH by masked UV exposure led to formation of oxidized species resulting in CHO_2^- and SO_4H^- signals in the square areas exposed to UV light. Prior to the BGT backfilling, the CN^- and CNO^- signals remained weak.

Results

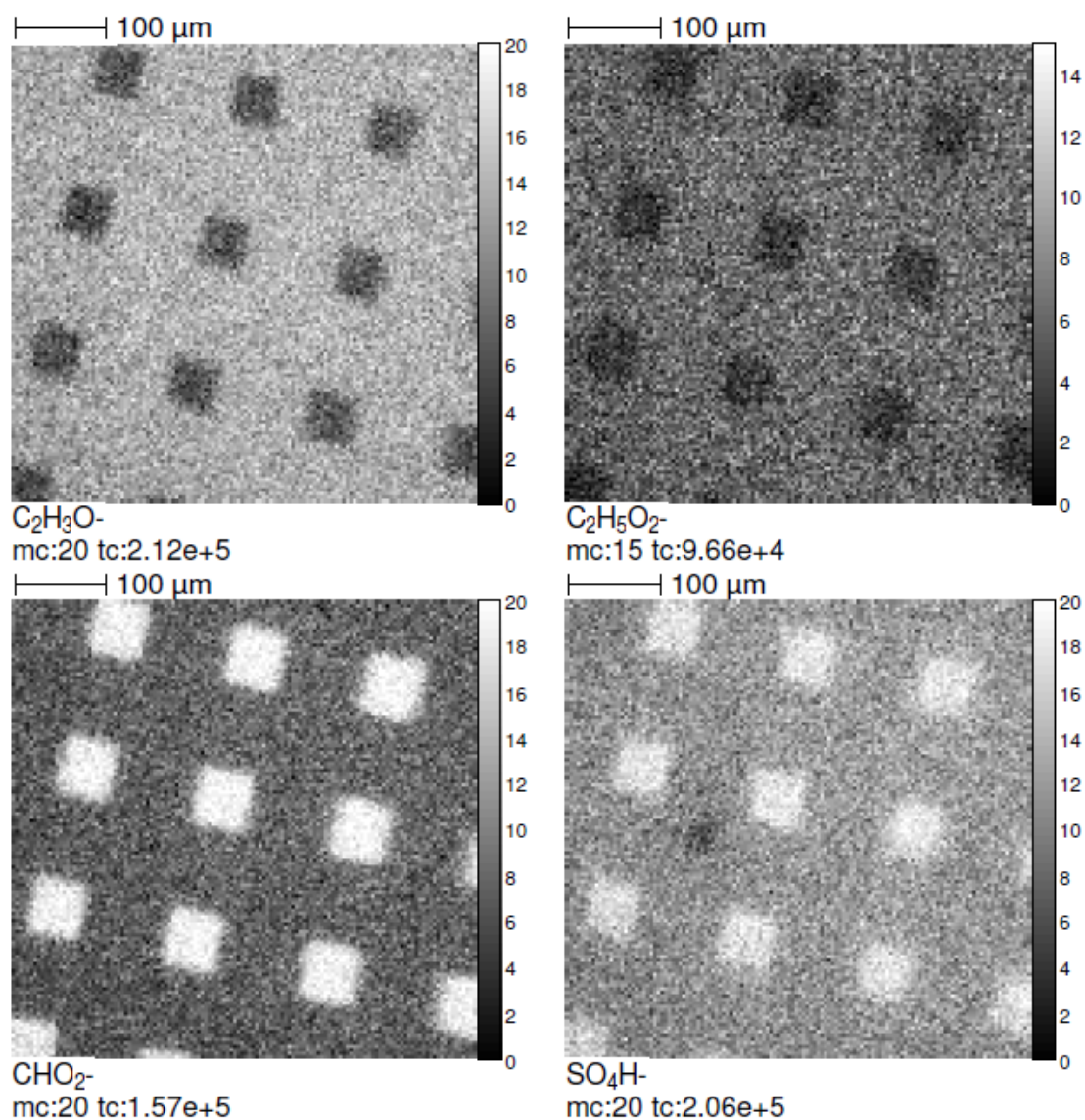


Figure 3.20. ToF-SIMS images of photo patterned EG6OH SAM. 100min UV exposure. Data recorded in bunched mode with high mass resolution. $C_2H_3O^-$ and $C_2H_5O_2^-$, which composed of the tail of EG6OH, were detected in the non-irradiated area. UV degradation of the EG6OH SAM led to formation of oxidation species, which resulted in signals of CHO_2^- and SO_4H^- in the squares exposed to UV.

When BGT, mixed with EG6OH at the ratio of 1:5, was backfilled on the photopatterned EG6OH coated surface, the CN^- , and CNO^- , and guanine signals became clearly detectable (Figure 3.21), indicating the adsorption of BGT in the regions of photo damaged EG6OH, since the gold surface, previously occupied by the EG6OH, was available again for deposition of BGT. In summary, a patterned SAM of

BGT and EG6OH was obtained and could be used to selectively bind the ShhN-GFP-His-SNAP protein.

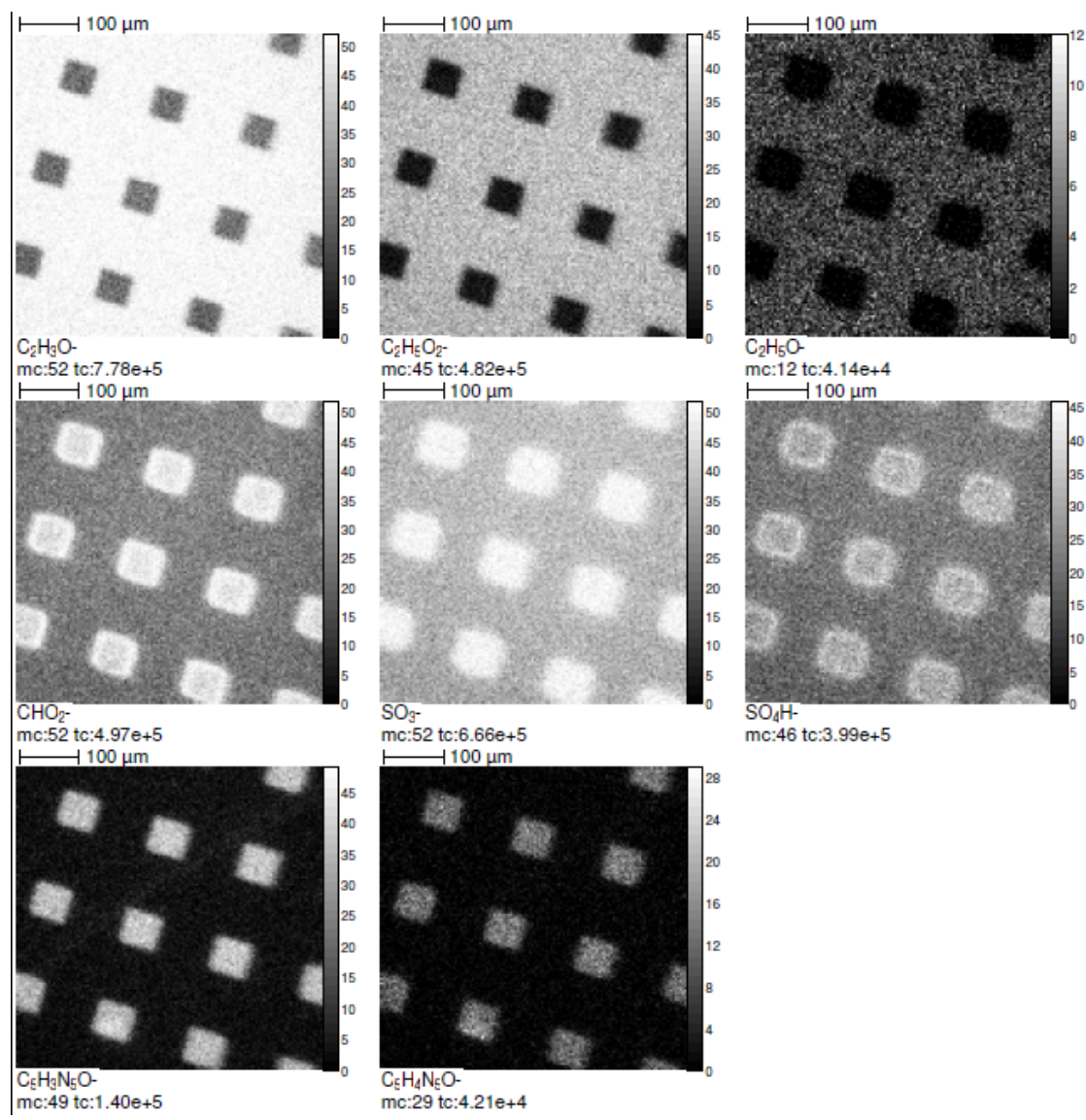


Figure 3.21. ToF-SIMS images of photo patterned EG6OH sample with 60min UV exposure after backfill with BGT/EG6OH 1:5. $C_2H_3O^-$ and $C_2H_5O_2^-$ signals from EG6OH were still detected in the non-irradiated area. Strong signals of CN^- and CNO^- in the patterned squares indicated the presence of BGT, which occupied the space where photo degradation of the EG6OH SAM was carried out.

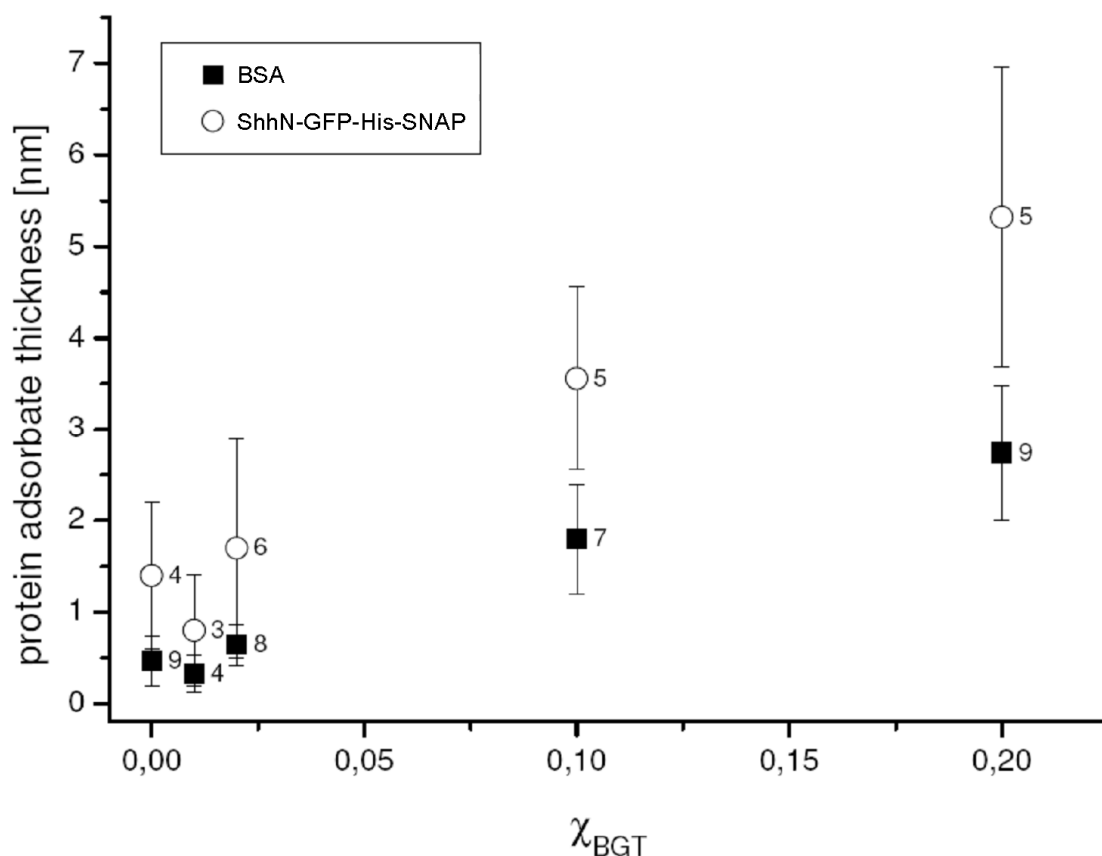
3.3.3.3. QCM-D analysis of BGT/ShhN-GFP-His-SNAP binding on gold surfaces

Because of the presence of the SNAPTM tag, ShhN-GFP-His-SNAP could covalently bind to the BG terminated molecules with high specificity. Even so, background interference by unspecific protein adsorption should be taken into account.

To determine the immobilization efficiency of ShhN-GFP-His-SNAP on the BGT SAM on gold surface, quartz crystal microbalance with dissipation monitoring (QCM-D) was employed. QCM-D is a method used for measuring molecular adsorption/desorption and binding kinetics to various types of surfaces. It is useful for determining molecular interactions with surfaces as well as between molecules.

Crystals with golden electrodes were exposed to 0.1mM BGT/EG6OH solution with different molar ratio of BGT concentration to the total concentration of BGT and EG6OH (χ_{BGT}) at room temperature for 1 hour. 1mg/ml BSA and 500nM ShhN-GFP-His-SNAP solutions were subsequently applied on the same surfaces. The thicknesses of the proteins deposited were calculated from the changes of the resonance frequencies.

From Graph 3.11, it could be noticed that as the χ_{BGT} increased, the thickness (i.e. amount) of ShhN-GFP-His-SNAP increased accordingly. At the same time, more BSA was also adsorbed on the surface, indicating that BGT could introduce unspecific protein binding when its ratio to the passivating thiol was high enough.



Graph 3.11. QCM-D measurement of adsorption of BSA and ShhN-GFP-Hi-SNAP on BGT modified gold surfaces with different χ_{BGT} . The thickness (i.e. amount) of the both BSA and ShhN-GFP-His-SNAP increased with an increasing χ_{BGT} applied to the gold surface. A χ_{BGT} of 0.10 was found to be the optimal for immobilizing ShhN-GFP-His-SNAP specifically on BGT while unspecific protein binding, as revealed by BSA, is bearable.

After several replicates of measurement by QCM-D, it was concluded that a $\chi_{\text{BGT}} = 0.1$ could compromise the background effect and allowed an acceptable amount of ShhN-GFP-His-SNAP to be specifically immobilized on gold surfaces via BGT.

3.3.3.4. Immobilization and immunodetection of the HEK293 cell expressed ShhN-GFP-His-SNAP on gold surfaces

After optimizing the immobilization condition on gold surfaces via BGT using the *E. coli* expressed ShhN-GFP-His-SNAP, the ShhN-GFP-His-SNAP was immobilized directly from the conditioned media of transfected HEK293 cells. Since the protein amount is under the detection limit of Western blotting, it was detected by immunofluorescence using the anti-Shh antibody 5E1, which recognizes the pseudo-active site of Shh for Ptc binding, and a green fluorescence labeled secondary antibody.

Figure 3.22 shows the immunofluorescence images of immobilized ShhN-GFP-His-SNAP (from the conditioned medium of HEK293 cells transfected with ShhN-GFP-His-SNAP construct). 0.1mM of the passivating thiol EG6OH was applied to gold surfaces for 16 hours to ensure thorough coverage with EG6OH. The modified surfaces were placed underneath a patterned mask and exposed to UV irradiation for 1 hour, resulting in square patterns with decomposed EG6OH. The surfaces were then backfilled with 1:10 BGT/EG6OH solution for 1 hour to fill up the areas where EG6OH had been decomposed. The collected conditioned medium of ShhN-GFP-His-SNAP from HEK293 cells was filtered with a 0.22 μ m syringe filter to get rid of any cell debris and was applied to the BGT/EG6OH functionalized gold surfaces without dilution at room temperature for 2 hours. The surfaces were immunostained with the anti-Shh monoclonal antibody 5E1, which recognizes and binds to the Ptc binding pseudo-active site, and a GFP labeled secondary antibody for the detection of ShhN-GFP-His-SNAP.

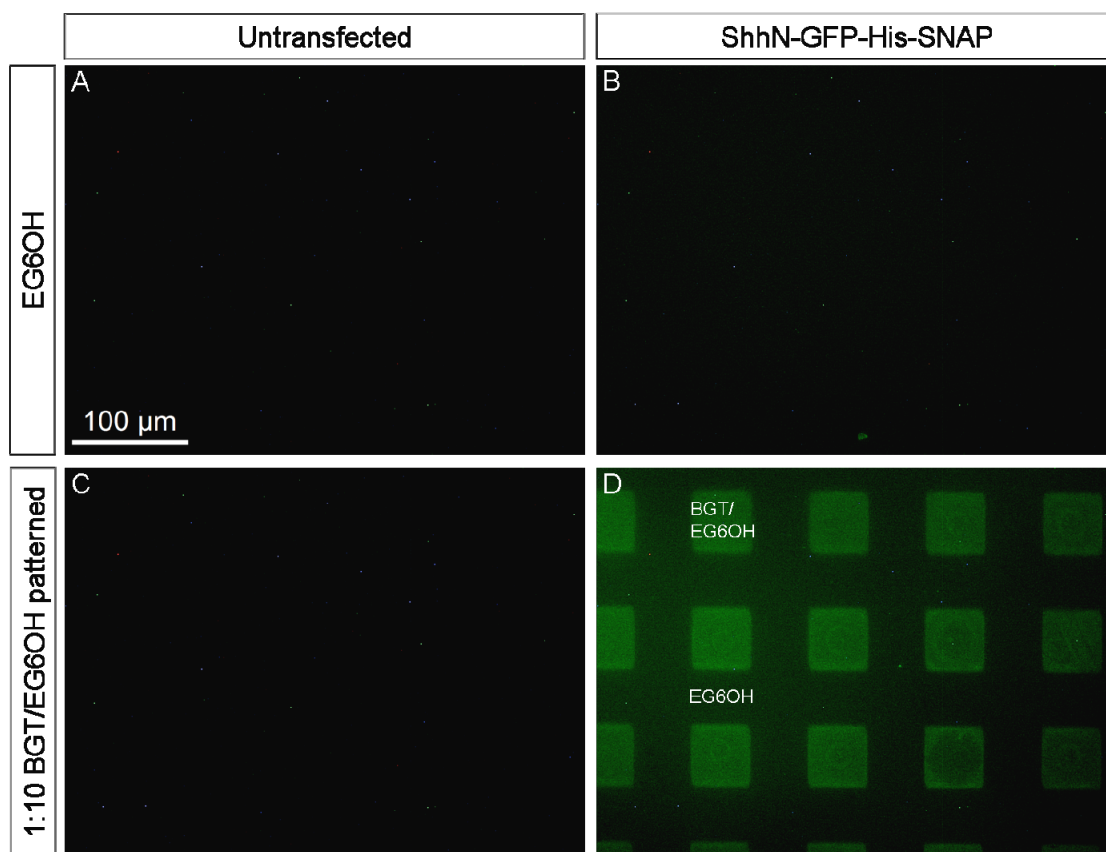


Figure 3.22. Immunofluorescence of the HEK293 cell expressed ShhN-GFP-His-SNAP on 1:10 BGT/EG6OH functionalized gold surfaces. Gold surfaces were exposed to 0.1mM EG6OH for 16 hours. UV irradiation was employed to decompose selective areas of the EG6OH SAM in $50\mu\text{m}\times 50\mu\text{m}$ square patterns. An 1:10 BGT/EG6OH solution as used to functionalize the irradiated surfaces for 1 hour. The anti-Shh antibody 5E1 was used to detect the immobilized ShhN-GFP-His-SNAP. The green fluorescence signals indicate the ShhN-GFP-His-SNAP immobilized and the availability of the pseudo-active site of ShhN for Ptc binding (D). Conditioned medium from untransfected HEK293 cells and pure EG6OH surfaces were the negative controls of SNAP protein binding (A to C).

The green fluorescence signal detected in the square patterns, where there was a SAM of BGT/EG6OH, indicates the presence of ShhN-GFP-His-SNAP. Binding of the 5E1 antibody and the GFP labeled secondary antibody indicated the availability of the pseudo-active site of ShhN. It suggests that the protein immobilization via BGT does not block the binding of ShhN-GFP-His-SNAP to its receptor Ptc.

3.3.4. Adsorption of ShhN-His and ShhN-GFP-His on surfaces coated with the extracellular matrix components collagen and fibronectin

Collagen and fibronectin were expected to have similar abilities in retaining ShhN in their networks, since both of them are extracellular matrix (ECM) substances involved in morphogen distribution. Collagen or fibronectin were applied from 25 to 240 μ g/ml solutions in H₂O onto glass surfaces at room temperature for 1 hour. The collagen or fibronectin coated surfaces were then exposed to 500nM solution of ShhN-His or ShhN-GFP-His at room temperature for 1 hour. Adsorption of ShhN-His or ShhN-GFP-His was analyzed by immunofluorescence, enzyme linked immunosorbent assay (ELISA), quartz crystal gravimetry (QCM), and fluorescence recovery after photobleaching (FRAP).

3.3.4.1. Detection and quantification of adsorbed ShhN-His and ShhN-GFP-His on collagen and fibronectin coated glass surfaces

From Figure 3.23, it can be seen that both ShhN-His and ShhN-GFP-His were adsorbed in collagen, regardless if the protein was fused merely with a poly(6)histidine tag or with an additional GFP. The absence of fluorescence and immunodetection signals from GFP-His indicated that there was no GFP-His adsorbed on the collagen coated surfaces, indicating that collagen shows no affinity to GFP-His. The adsorption of ShhN-His and ShhN-GFP-His by collagen was not contributed by any interaction between collagen and GFP or poly(6)histidine but between collagen and ShhN. The findings suggested that collagen is a good substrate for label free adsorbed of ShhN-His and ShhN-GFP-His.

	GFP channel	RFP channel	5E1	Shh (N-19)	Penta-his
Collagen only	A 100 μ m 0.80 \pm 0.38	B 5.96 \pm 1.20	C 6.85 \pm 0.40	D 5.33 \pm 0.22	E 4.53 \pm 0.40
Collagen + ShhN-His	A' 6.49 \pm 0.46	B' 6.53 \pm 0.25	C' 98.92 \pm 5.02	D' 136.21 \pm 23.61	E' 82.12 \pm 7.54
	GFP channel	RFP channel	5E1	Shh (N-19)	Penta-his
Collagen only	F 0.80 \pm 0.38	G 5.96 \pm 1.20	H 4.89 \pm 0.59	I 5.33 \pm 0.22	J 7.95 \pm 1.52
Collagen + ShhN-GFP-His	F' 188.79 \pm 11.18	G' 6.66 \pm 0.11	H' 126.81 \pm 11.79	I' 110.53 \pm 9.37	J' 122.07 \pm 12.09
Collagen + GFP-His	F'' 5.29 \pm 0.29	G'' 4.96 \pm 0.20	H'' 5.47 \pm 0.52	I'' 5.01 \pm 0.24	J'' 5.07 \pm 0.37

Figure 3.23. Immunofluorescence detection of ShhN-His and ShhN-GFP-His adsorption on collagen coated surfaces from a 240 μ g/ml collagen solution. The anti-Shh antibodies 5E1 and Shh (N-19):sc1194, and Penta-his antibody were used to detect ShhN-His and ShhN-GFP-His. Collagen surfaces without any protein served as negative controls for fluorescence and immunodetection (A to E, F to J). Green fluorescence signal was observed from ShhN-GFP-His on collagen surfaces (F'). Positive immunofluorescence signals were noticed from application of ShhN-His and ShhN-GFP-His on collagen surfaces, indicating adsorption of the proteins (C' to E', H' to J'). Very weak green fluorescence and immunofluorescence signals were seen when GFP-His was applied on collagen surfaces (F'' to J''). The antibodies 5E1, Shh (N-19):sc1194, and Penta-his are written in colors, which represent the fluorescence of the secondary antibodies used for the detection of the antibodies. The numbers at the right hand lower corners are arbitrary units of green fluorescence intensity \pm standard deviation. Abbr.: GFP, green fluorescence protein; RFP, red fluorescence protein.

Results

Adsorption of ShhN-His and ShhN-GFP-His on collagen surfaces was label free and yet selective comparing to GFP-His. The adsorbed proteins could be detected by antibodies, indicating the availability of the Ptc binding site. The potential drawback of collagen adsorption of ShhN was possible random adsorption, imposing binding between collagen and ShhN may block a certain ratio of the pseudo-active site, though it is not necessarily the case. Collagen allowed migration of ShhN in the matrix. Motility of ShhN was not hindered while the advantage of controlling the spatial and concentration distributions of the protein could be taken.

On the contrary, no satisfactory result was obtained from the fibronectin adsorption setups for ShhN-His and ShhN-GFP-His. Immunofluorescence signals revealed from the Shh specific and histidine antibodies were weak, indicating poor adsorption of ShhN-GFP-His on fibronectin coated surfaces (Figure 3.24).

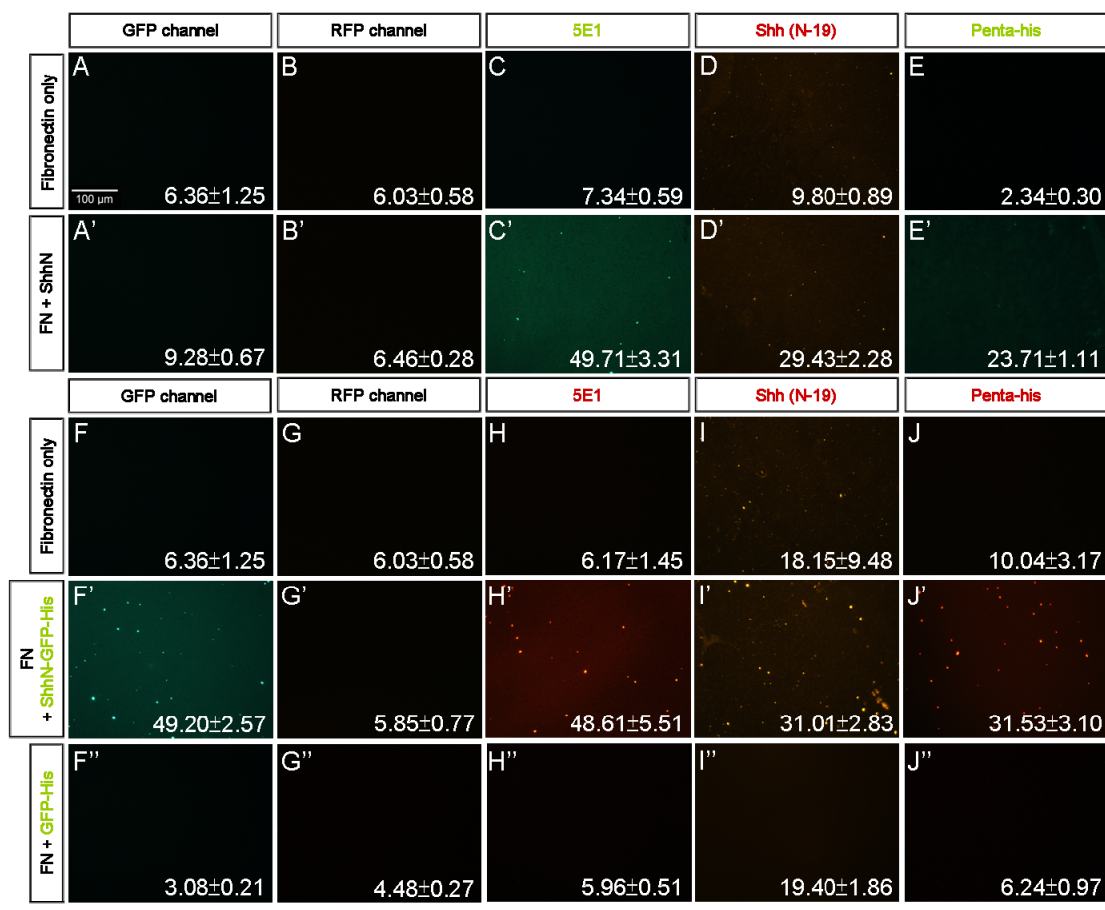


Figure 3.24. Immunofluorescence detection for adsorption of ShhN-His and ShhN-GFP-His on fibronectin coated surfaces from a 240 μ g/ml fibronectin solution. The anti-Shh antibodies 5E1 and Shh (N-19):sc1194, and Penta-his antibody were used to detect ShhN-His and ShhN-GFP-His. Fibronectin surfaces without any protein served as negative controls for fluorescence and immunodetection (A to E, F to J). Very weak green fluorescence signals were observed from ShhN-GFP-His on FN surfaces (F'). Application of ShhN-His and ShhN-GFP-His on fibronectin surfaces demonstrated poor IF signals (C' to E', H' to J', H'' to J''), indicating that ShhN-His and ShhN-GFP-His were as badly adsorbed on fibronectin coated surfaces. No signal was shown by GFP-His on fibronectin (F''). Fibronectin did not promote protein adsorption. The antibodies 5E1, Shh (N-19):sc1194, and Penta-his were written in colors, which represent the fluorescence of the secondary antibodies used for the detection of the antibodies. The numbers at the right hand lower corners were arbitrary units of green fluorescence intensity \pm standard deviation. Abbr.: GFP, green fluorescence protein; RFP, red fluorescence protein.

Results

Although both collagen and fibronectin were ECM substances, they possess different capabilities in adsorption of ShhN-His and ShhN-GFP-His. Fibronectin does not allow for efficient adsorption of ShhN proteins.

To analyze the effects of different collagen amounts deposited on a substrate for ShhN-GFP-His binding, a concentration series of 25 to 240 μ g/ml of collagen was tested. A minimal concentration of 25 μ g/ml of collagen is suggested for surface coating (Roche, Mannheim, Germany). The collagen coated surfaces were exposed to a fixed concentration of ShhN-GFP-His (500nM). As seen in Figure 3.25 (E – H), concentrations of collagen between 25 and 240 μ g/ml had comparable ability in adsorbing ShhN-GFP-His, as they showed similar intensities of GFP fluorescence. Increase in collagen concentration within the tested range did not contribute to the surface's capacity for further protein adsorption.

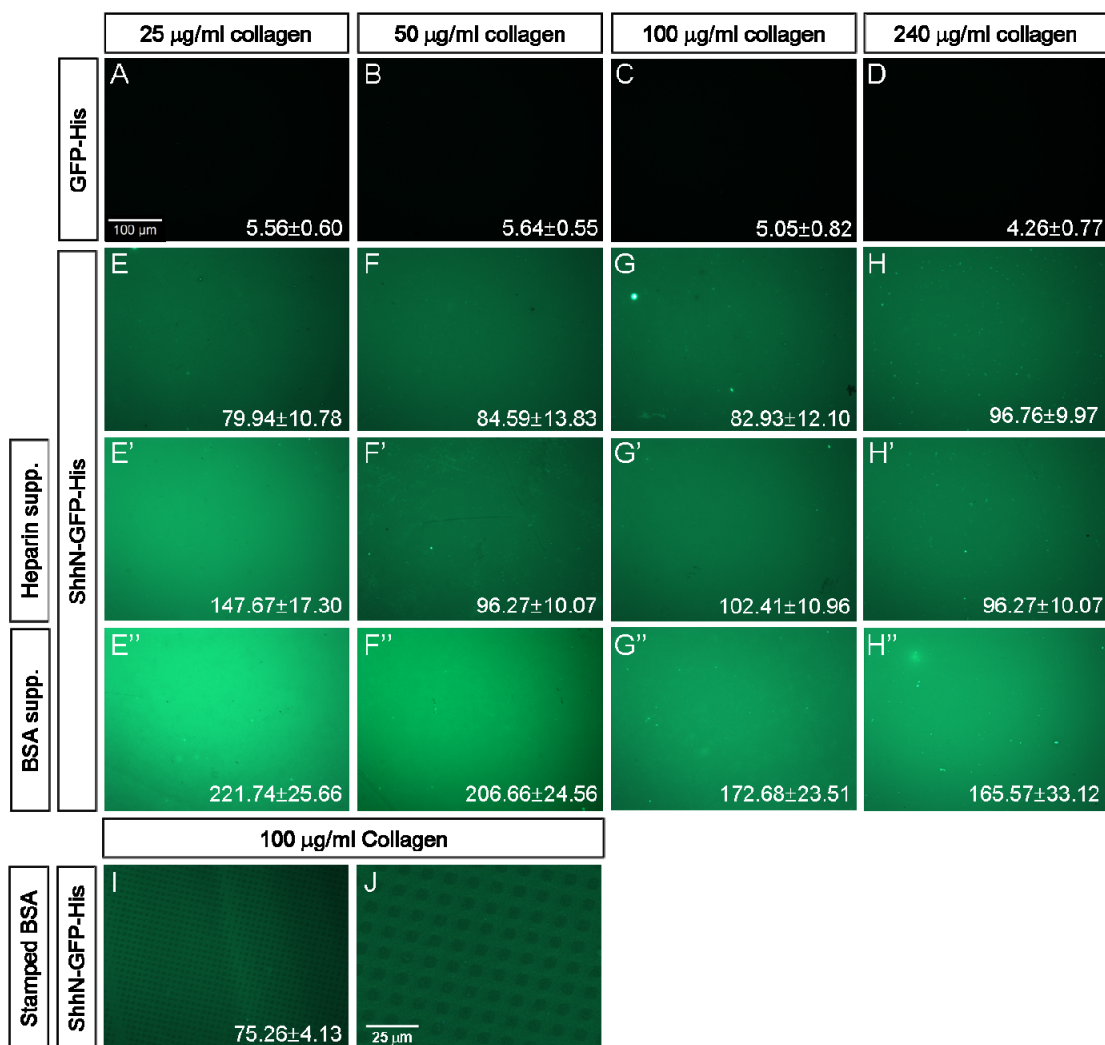
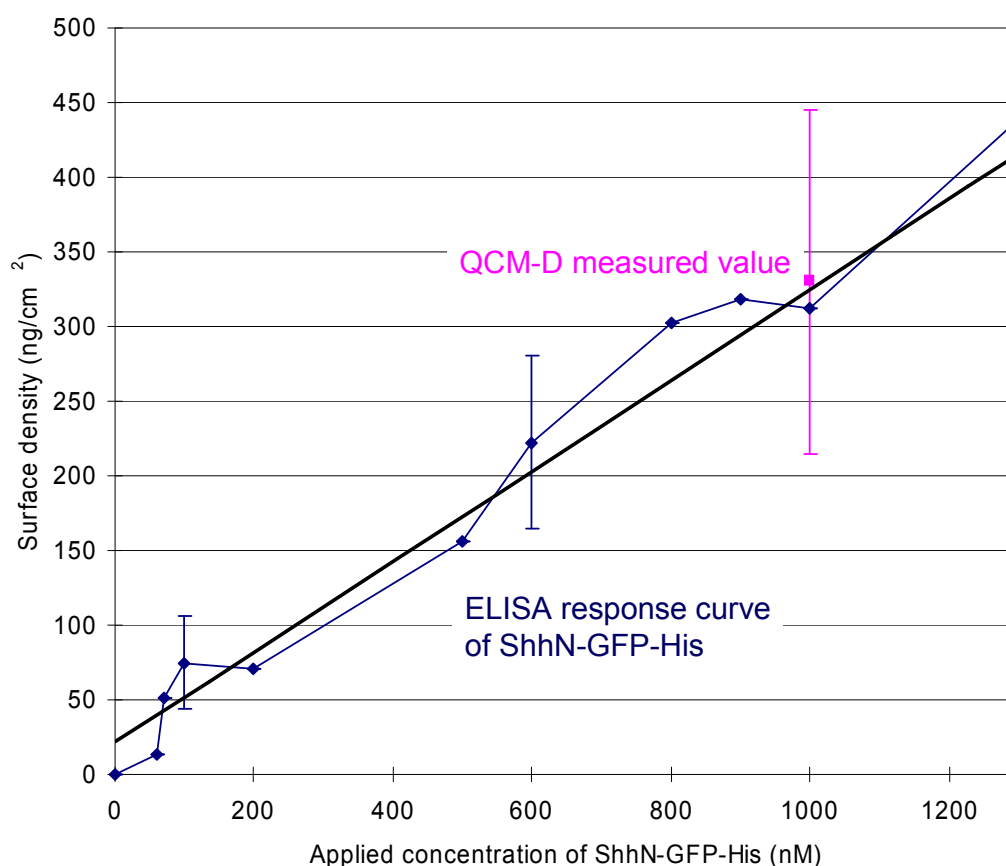


Figure 3.25. ShhN-GFP-His adsorption on collagen coated surfaces. (A – D) GFP-His was the negative control that is not adsorbed on collagen. (E – H) Collagen with a series of concentrations (from 25 to 240 $\mu\text{g/ml}$) was used to adsorb ShhN-GFP-His from a 100nM solution on glass surfaces. (E' – H') Supplement of 1 μM heparin resulted in slight increase of green fluorescence intensity from ShhN-GFP-His. (E'' – H'') Supplement of 1mg/ml BSA resulted in dramatic increase of green fluorescence intensity from ShhN-GFP-His. (I, J) Blockage of adsorption of ShhN-GFP-His with microcontact printed BSA in selected areas of collagen coated surfaces. BSA was stamped on collagen functionalized surfaces in square patterns by μCp . The unstamped areas were not influenced and showed comparable green fluorescence intensity to the image (G) that no μCp was conducted. The numbers at the right hand lower corners were arbitrary units of green fluorescence intensity \pm standard deviation.

Results

In Graph 3.12, it can be seen that an ELISA response curve was obtained by depositing collagen from a 100 μ g/ml solution and ShhN-GFP-His from solutions with different concentrations on glass surfaces. ELISA was carried out with Shh (N-19):sc1194 antibody conjugated with anti-goat IgG peroxidase conjugate. The amount of ShhN-GFP-His adsorbed on a given area on the collagen coated glass surfaces was found to be dependent on the ShhN-GFP-His concentration. Since there was only one band detected by the Shh (N-19):sc1194 antibody in the Western blot (Figure 3.2), the ELISA quantification of ShhN-GFP-His was protein-antibody specific. The amount of protein measured on the surfaces could only come from the ShhN-GFP-His but not any other proteins possibly adsorbed on the surfaces. Quartz crystal microbalance with dissipation monitoring (QCM-D) was used to quantify the deposited mass of ShhN-GFP-His on collagen surfaces with an input ShhN-GFP-His concentration of 1 μ M.



Graph 3.12. ELISA response curve showing the surface densities (ng/cm^2) of ShhN-GFP-His deposited on collagen coated surfaces. The surface density of ShhN-GFP-His on collagen surfaces was proportional to the concentration of ShhN-GFP-His applied for deposition. The pink data point indicates the surface density of ShhN-GFP-His resulting from ShhN-GFP-His adsorption from $1\mu\text{M}$ ShhN-GFP-His solution on collagen coated QCM-D sensors. The average surface density of ShhN-GFP-His deposited measured by QCM-D was comparable to the value shown from the ELISA response curve.

QCM is a methodology based on the masses of the substances adsorbed on the surface but has no selectivity on any particulars. It provides an overall information of the masses of all input molecules deposited. On the other hand, ELISA is a selective method of detecting target proteins using specific antibodies. Though being two independent methods for determination of the amount of ShhN-GFP-His deposited on collagen functionalized surfaces, the measurements by QCM-D and ELISA were found to be comparable. Although multiple bands were detected in the Western blot

Results

using Penta-his antibody (Figure 3.5), the QCM-D quantification demonstrated that the amount of other non-ShhN proteins adsorbed on collagen was insignificant. Further, it was found from ELISA that for a constant concentration of collagen, the amount of ShhN-GFP-His adsorbed on the collagen surfaces was dependent on the applied concentration of ShhN-GFP-His.

Heparin is a component of the ECM and is capable of binding to the Cardin-Weintraub sequence of ShhN (Cardin and Weintraub, 1989). Therefore 1 μ M heparin was mixed with the collagen solutions prior to exposure of the surfaces to substrate and adsorption of ShhN-GFP-His. This was to test if supplementation by heparin could enhance the adsorption of ShhN-GFP-His in the collagen matrix. Figure 3.25 (E' – H') demonstrates that exposure of collagen coated surfaces to ShhN-GFP-His with 1 μ M heparin supplement in the collagen. results in an increase of green fluorescence intensity suggesting an increase of amount of ShhN-GFP-His adsorbed onto the modified surfaces. This effect is most pronounced at low collagen concentrations.

Apart from heparin, supplement of 1mg/ml BSA to the collagen matrix was observed to have similar effect on facilitating adsorption of ShhN-GFP-His on collagen functionalized surfaces. It can be seen from Figure 3.25 (E'' – H'') that a mixture of collagen and BSA almost doubled the green fluorescence intensity measured, and hence the amount of ShhN-GFP-His adsorbed. Again this effect is the most prominent for low collagen concentration solutions applied for collagen deposition.

While supplement of BSA in the collagen matrix resulted in enhancement of the adsorption of ShhN-GFP-His in collagen, microcontact printing (μ Cp) of BSA on the

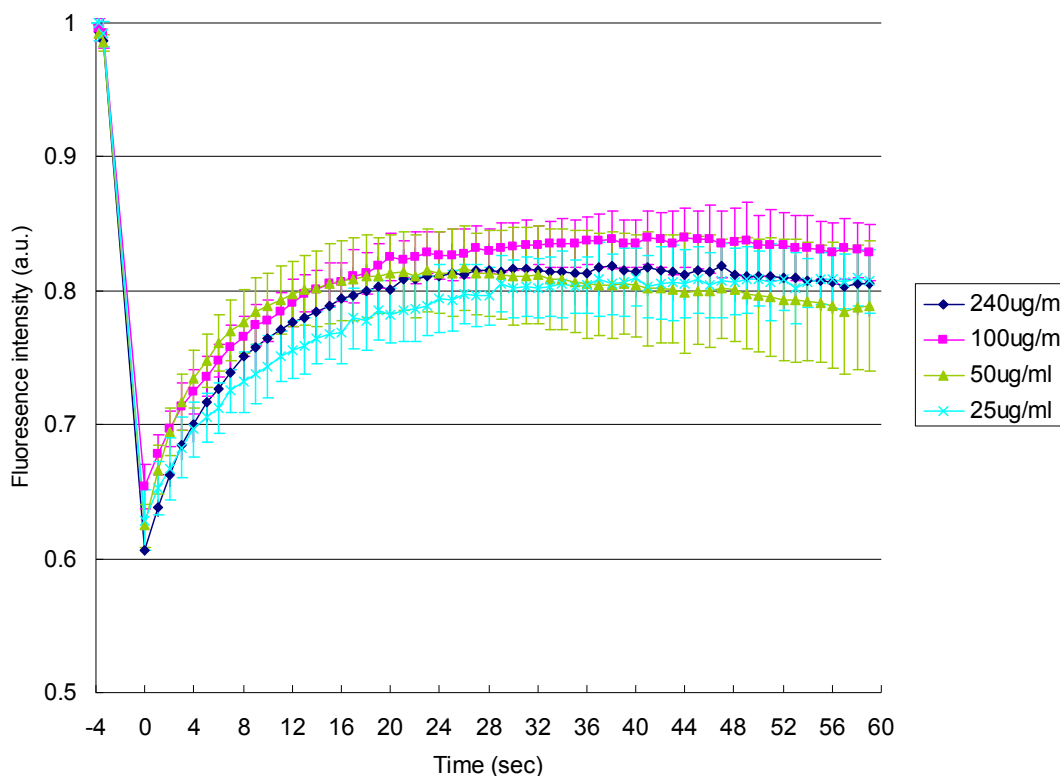
collagen functionalized surfaces was observed to block ShhN-GFP-His adsorption on the printed areas (Figure 3.25 (I, J)). In this experiment, glass surfaces were exposed to 100 μ g/ml collagen at room temperature for 1 hour and blown dry with nitrogen stream. A square patterned PDMS stamp was soaked in a 1mg/ml BSA solution at room temperature for 15 minutes and dried in a stream of nitrogen. The BSA from the stamp was then transferred onto the collagen coated surfaces by μ Cp for 1 minute. Finally these layers were exposed to ShhN-GFP-His at room temperature for 1 hour. In the square patterned areas where BSA was stamped, there was no green fluorescence signal observed from ShhN-GFP-His, suggesting that the stamped BSA formed a layer in the middle isolating collagen and ShhN-GFP-His and thereby inhibited the adsorption of ShhN-GFP-His in the collagen matrix. While BSA blocked the stamped area, the unstamped area showed comparable green fluorescence intensity, indicating that adsorption of ShhN-GFP-His on unstamped collagen was unaffected.

3.3.4.2. Analysis of the motility of ShhN-GFP-His on collagen coated glass surfaces by fluorescence recovery after photobleaching

Fluorescence recovery after photobleaching (FRAP) denotes an optical technique capable of quantifying lateral molecule diffusion or protein binding. The molecules or proteins under investigation are fluorescence labeled. By exposure to a strong laser light under a confocal microscope, a selected area of the sample is photobleached. Fluorescence intensity of the bleached area is then recorded in set time intervals to monitor a fluorescence recovery. The time and extent of recovery of fluorescence intensity in a photobleached area is dependent on the migration of the target molecules or proteins from the surrounding non-bleached areas into the bleached area.

FRAP was employed to measure the motility of adsorbed ShhN-GFP-His in the collagen network. To do so, surfaces with different collagen layers (deposited from concentrations of 25 to 240 μ g/ml) were exposed to solutions of the same concentration (500nM) of ShhN-GFP-His, and washed twice in PBS. An area was selected randomly and bleached by a laser beam under the confocal microscope. GFP intensity in the photobleached area was measured against time.

Graph 3.13 shows that after photobleaching, the green fluorescence intensity in the bleached area of ShhN-GFP-His loaded collagen increased gradually, indicating a fluorescence recovery of the bleached area by migration of the ShhN-GFP-His from the surrounding non-bleached area. Such migration of ShhN-GFP-His in the collagen matrix suggested a reversible adsorption of ShhN-GFP-His on collagen, which provides a dynamic environment that allows movement of ShhN-GFP-His in the matrix.



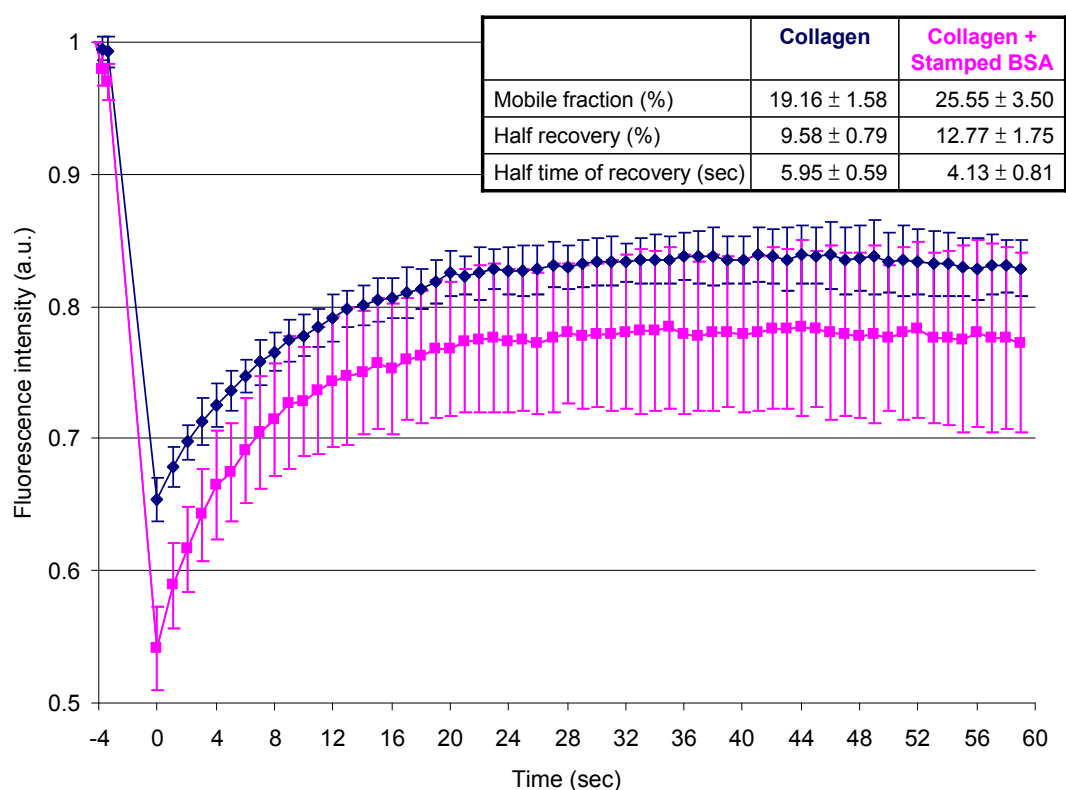
Graph 3.13. Comparison of ShhN-GFP-His motility on surfaces coated with different concentrations of collagen. Similar FRAP profiles shown by ShhN-GFP-His (from 500nM solution) adsorbed on surfaces coated with different collagen concentrations (from 25 to 240 μ g/ml solutions). A circle with diameter of 30 μ m was bleached by a laser irradiation at $\lambda=488$ nm under the confocal microscope for 3 seconds. The green fluorescence intensity in photobleached area was measured in 1 second intervals after bleaching for 1 minute. Initial signals were scaled to 1.

Consistent with the protein intensity measurements, same input concentration of ShhN-GFP-His on surfaces coated with different concentrations of collagen gave rise to very similar FRAP profiles, indicating that there was no direct relationship of fluorescence recovery and the collagen concentrations used.

Stamping of BSA on collagen coated surfaces by microcontact printing (μ Cp) resulted in blockage of ShhN-GFP-His adsorption in collagen. However, it did not affect the overall movement of ShhN-GFP-His within the unstamped collagen matrix as demonstrated by the FRAP profile (Graph 3.14). The paths for ShhN-GFP-His

Results

movement were still connected by the matrix in the unstamped regions. The microcontact printed area can be adjusted by using BSA coated stamps of different sizes and patterns. In other words, ShhN with a variety of local spatial distributions, and hence local concentrations, can be adsorbed on a single collagen coated surface with freedom of movement in the matrix.



Graph 3.14. Comparison of the motility of ShhN-GFP-His adsorbed on collagen functionalized surfaces. Similar FRAP profiles obtained for adsorption of ShhN-GFP-His on collagen coated glass surfaces (blue line) and on unstamped area after the collagen coated glass surfaces were subjected to μ Cp with BSA (pink line). Initial signals were scaled to 1.

Concluding from the results of immunofluorescence and FRAP, collagen is a good substrate for adsorbing ShhN and yet allows the protein to diffuse within the matrix.

3.3.4.3. Adsorption and biological activity analysis of the HEK293 cell expressed ShhN-GFP-His on collagen coated glass surfaces

Comparing to other surfaces, preparation of collagen coated glasses was simple and required no sophisticated equipment. The surfaces provide a convenient platform for preliminary studies of biological activity of adsorbed ShhN-GFP-His.

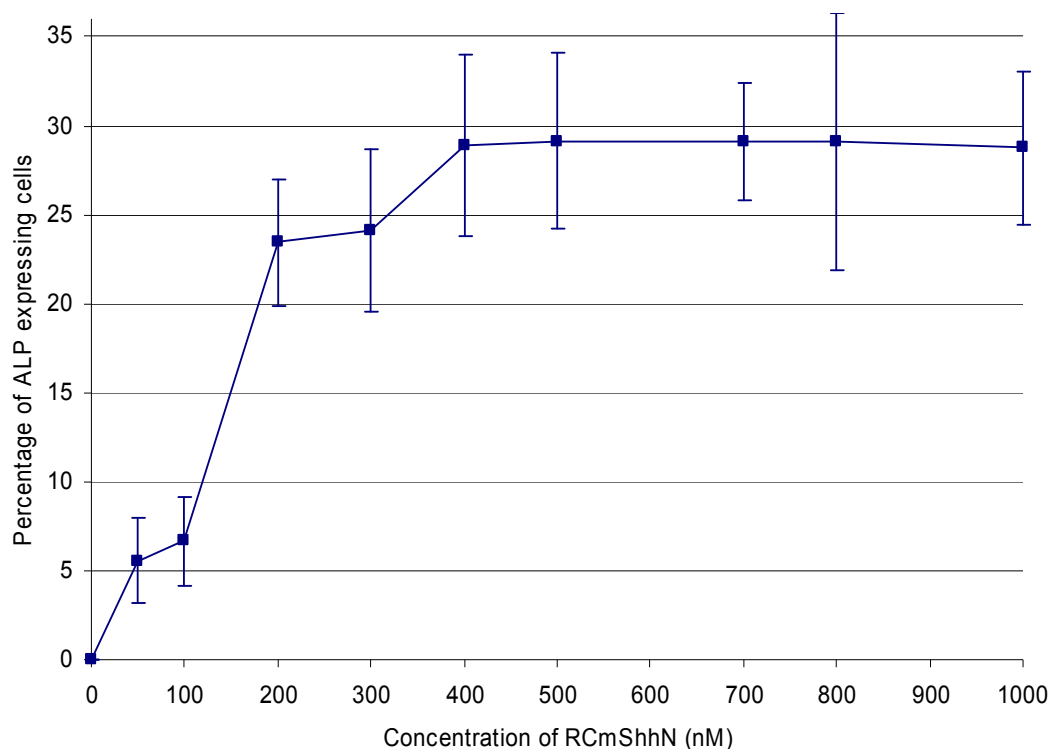
Since the HEK293 cell expressed ShhN-GFP-His, as shown previously in section 3.2.6, was biologically active in soluble form, it was selected to adsorb on collagen coated glass surfaces to investigate the biological activity of adsorbed ShhN-GFP-His. The *E. coli* expressed RCmShhN purchased from Neuromics (Edina, MN, USA) served as positive controls.

100 μ g/ml collagen was used to functionalize the glass surfaces. The collagen surfaces were then exposed to RCmShhN solutions with different concentrations. The modified surfaces were washed twice in PBS to remove any unbound RCmShhN proteins. C3H10T1/2 clone 8 cells, which can express ALP in response to Shh signaling, was cultured on the surfaces at 37°C with 5% CO₂ for 5 days. Expressed ALP was detected with BCIP/NBT substrates in ALP staining solution.

Concentration dependent ALP expression in the C3H10T1/2 clone 8 cells was detected, indicating that RCmShhN was adsorbed on the collagen matrix and capable of triggering Shh signal transduction (Graph 3.15). The biological activity of the adsorbed RCmShhN on collagen surfaces was the highest when 400nM RCmShhN were applied. Concentrations of RCmShhN higher than 400nM did not induce ALP expression any further, resulting in a level off of the percentage of ALP expressing

Results

cells. ShhN-GFP-His adsorption in collagen may have reached the threshold. Increase in the input concentration of RCmShhN would not improve the amount of RCmShhN adsorbed and thus the cellular responses.



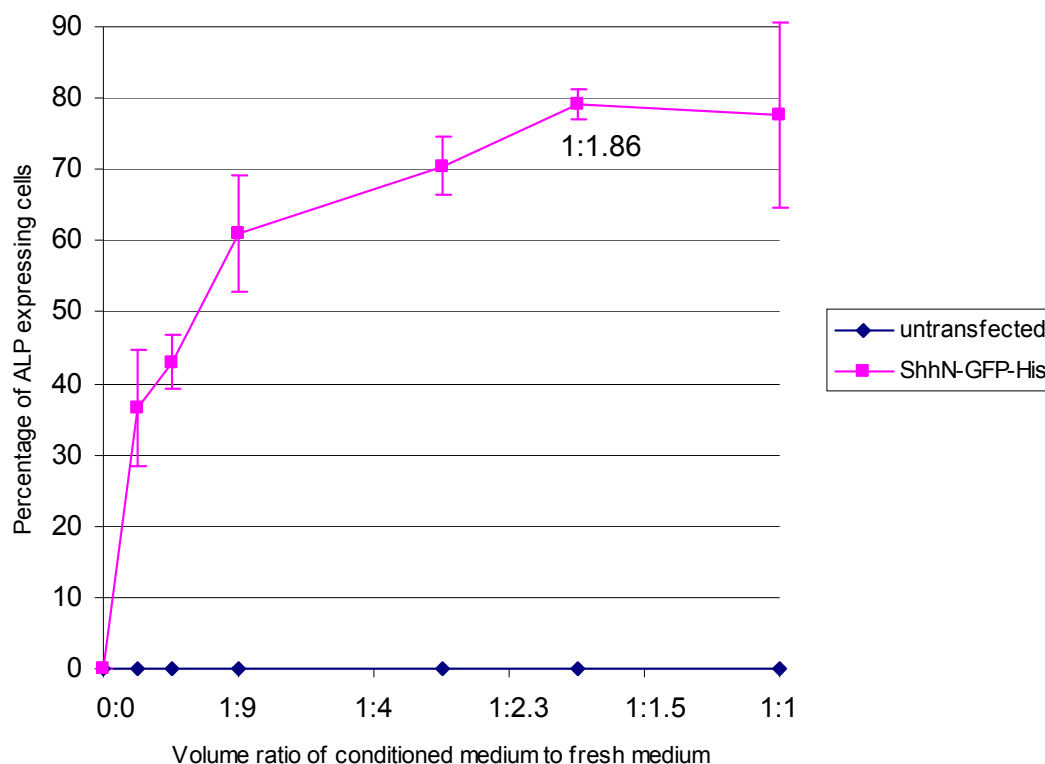
Graph 3.15. ALP expression induction in C3H10T1/2 clone 8 cells RCmShhN adsorbed on collagen coated surfaces. The percentage of ALP expressing C3H10T1/2 clone 8 cells increased with an increasing concentration of RCmShhN until a maximum was reached with 400nM RCmShhN. After then RCmShhN showed a level off in inducing further C3H10T1/2 clone 8 cells to express ALP.

After confirming the biological activity of the adsorbed ShhN in collagen matrix using RCmShhN, the HEK293 cell expressed ShhN-GFP-His was tested. After coating the glass surfaces with the 100 μ g/ml collagen solution, conditioned medium containing ShhN-GFP-His (from HEK293 cells transfected with the ShhN-GFP-His construct) in different volume ratios to fresh medium (containing DMEM and 0.5% FBS) was added to the surfaces. C3H10T1/2 clone 8 cells were seeded on the surfaces

and were incubated at 37°C with 5% CO₂ for 5 days. ALP expressing cells were counted. Conditioned medium from untransfected HEK293 cells was used as the negative control of biological activity analysis. The soluble form of the ShhN-GFP-His served as the positive control. This was done by incubating the C3H10T1/2 clone 8 cells in the ShhN-GFP-His conditioned medium.

The biological activity of the soluble form of the HEK293 cell expressed ShhN-GFP-His is shown in Graph 3.16. The percentage of ALP expressing C3H10T1/2 clone 8 cells increased when an increasing volume ratio of the applied ShhN-GFP-His conditioned medium was applied. The highest percentage (about 80%) of ALP expressing cells was noticed when a conditioned to fresh medium ratio of 1:1.86 was used.

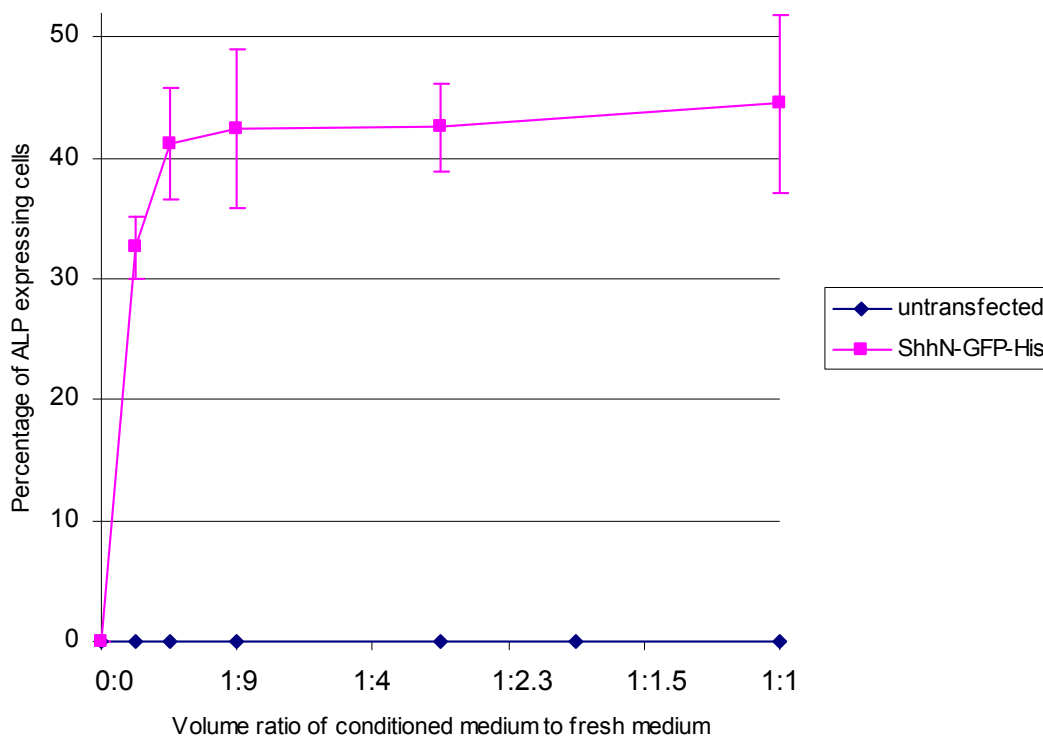
Results



Graph 3.16. Induction of ALP expression in C3H10T1/2 clone 8 cells by the HEK293 cell expressed ShhN-GFP-His. The C3H10T1/2 clone 8 cells showed specific ALP expression to the soluble form of ShhN-GFP-His (from the conditioned medium collected from HEK293 cells transfected with the construct of ShhN-GFP-His). Conditioned medium from untransfected HEK293 cells served as the negative control.

Graph 3.17 illustrated the biological activity of adsorbed ShhN-GFP-His on collagen surfaces. The conditioned medium from HEK293 cells transfected with the construct of ShhN-GFP-His with volume ratio to the fresh medium was used for the adsorption of the HEK293 cell expressed ShhN-GFP-His in collagen. Any unbound ShhN-GFP-His was removed by washing the surfaces twice in PBS. C3H10T1/2 clone 8 cells were then cultivated on the modified surfaces. Any ALP expressing cells were counted. The response curve shown in Graph 3.17 demonstrates the collagen adsorbed ShhN-GFP-His was able to induce ALP expressing C3H10T1/2 clone 8 cells even with small volume ratios. With the conditioned medium to fresh medium ratio of 1:9, there was about 43% C3H10T1/2 clone 8 cells expressing ALP. Higher

ratios of the ShhN-GFP-His conditioned medium applied did not result in more ALP expressing cells, suggesting that there is a threshold of the amount of ShhN-GFP-His adsorbed in collagen matrix, so as the number of cells responding to the protein and expressing ALP.



Graph 3.17. Induction of ALP expression in C3H10T1/2 clone 8 cells by the HEK293 cell expressed ShhN-GFP-His adsorbed on collagen surfaces. The BCIP/NBT staining for ALP expression showed that C3H10T1/2 clone 8 cells were specifically responsive to the ShhN-GFP-His adsorbed on collagen surfaces. The percentage of ALP expressing cells increased in a concentration dependent manner up to about 43% with the volume ratio of conditioned medium to fresh medium equals 1:9 and leveled for higher ratios. Conditioned medium from untransfected HEK293 cells served as negative control, indicating the ALP expression detected was induced by Shh signaling.

Results

Though the amount of ShhN-GFP-His in the conditioned medium was under the detection limit of Western blot, it did not mean that there was inadequate ShhN-GFP-His for biological activity. An undetectable amount of HEK293 cell expressed ShhN-GFP-His could still be able to trigger prominent Shh signal transduction.

The most significant difference between applications of the soluble and the adsorbed form of ShhN-GFP-His was the amount of the protein available for Ptc binding and the subsequent cellular response. For the soluble ShhN-GFP-His, the conditioned medium concentration applied to the responding cell culture remains constant throughout the treatment of cells. In the case of adsorbed ShhN-GFP-His, the available amount of the protein depends on the adsorption threshold of the substrate. Excess protein molecules in the conditioned medium applied could no longer be adsorbed above the threshold. Further increase of the volume ratio of ShhN-GFP-His conditioned medium to fresh medium beyond 1:9 did not improve the activity level, for 1:9 is the threshold of 100 μ g/ml collagen for ShhN-GFP-His adsorption.

Figure 3.26 showed a positive control image of ALP expression after applying the HEK293 cell expressed ShhN-GFP-His to the C3H10T1/2 clone 8 cells. C3H10T1/2 clone 8 cells were grown on glass chambered slides. The ShhN-GFP-His conditioned medium was applied to the cells with the volume ratio of 1:1 to fresh medium. ALP expression in response to Shh signaling was detected after 5 days of treatment, indicating the biological activity of ShhN-GFP-His.

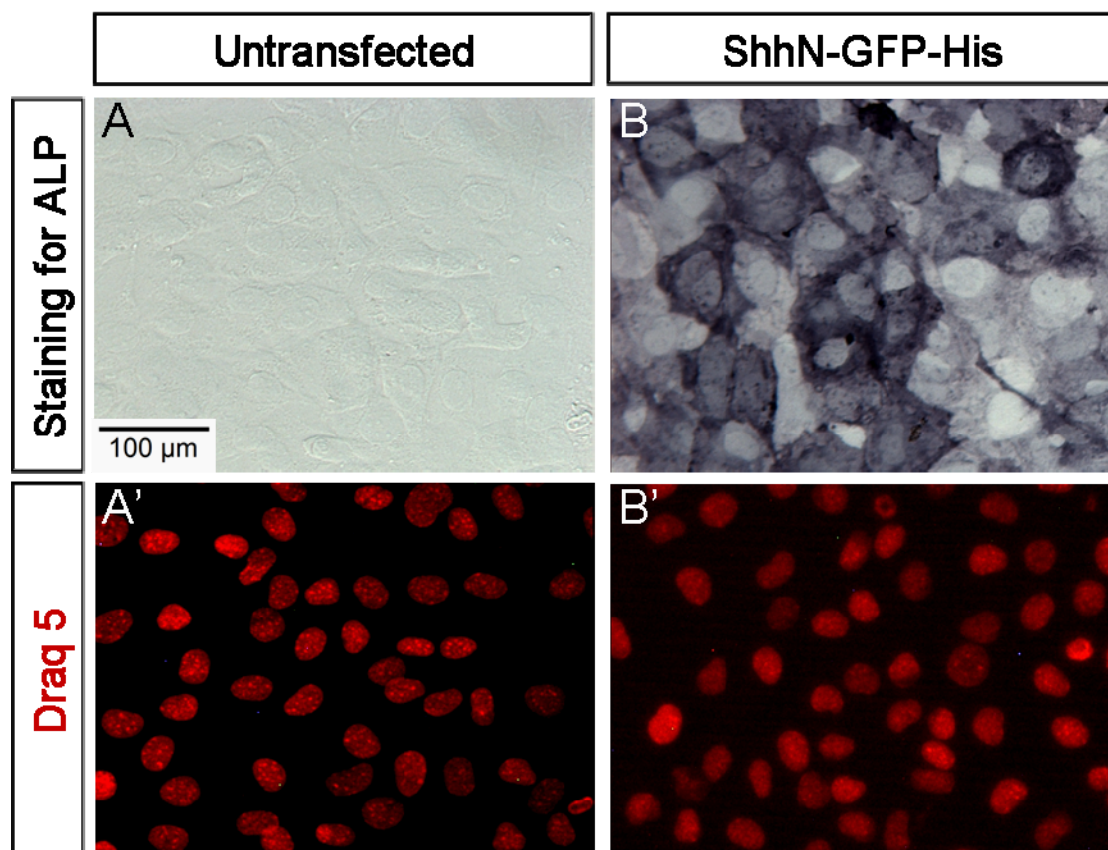


Figure 3.26. Induction of Shh signaling specific ALP expression in C3H10T1/2 clone 8 cells by the HEK293 expressed ShhN-GFP-His. ShhN-GFP-His conditioned medium with the volume ratio of 1:1 to fresh medium was added to C3H10T1/2 clone 8 cells. ALP expression was detected by BCIP/NBT substrate after 5 days. In the negative controls with conditioned medium from untransfected HEK293 cells, no ALP expression was detected (A). Soluble form of ShhN-GFP-His activated Shh signal transduction and induced ALP expression in C3H10T1/2 clone 8 cells (B). Nuclei were stained with Draq 5 (A' and B').

When ShhN-GFP-His (from the conditioned medium with the volume ratio of 1:1 to fresh medium) was adsorbed on collagen coated surfaces, ALP expression was induced in C3H10T1/3 clone 8 cells, demonstrating the biological activity of the protein (Figure 3.27).

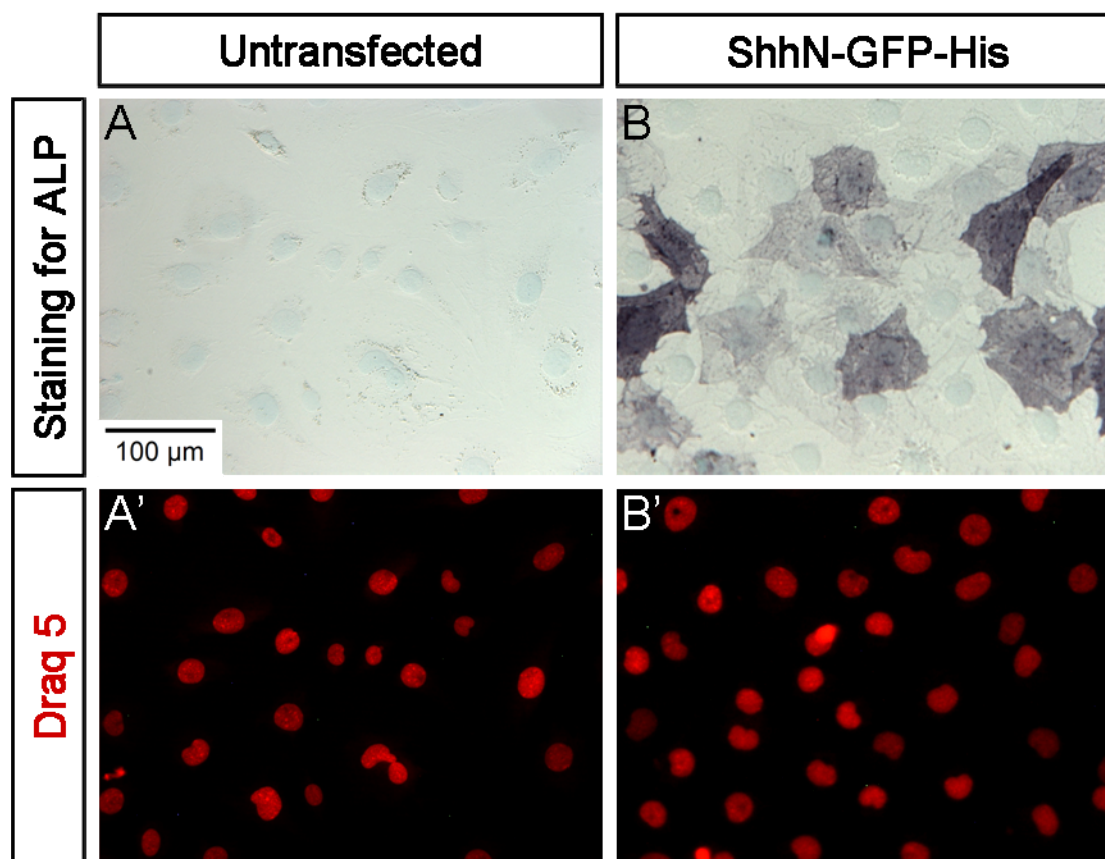


Figure 3.27. Induction of ALP expression in C3H10T1/2 clone 8 cells by the HEK293 cell expressed ShhN-GFP-His adsorbed on collagen coated surface. BCIP/NBT staining for Shh signaling induced ALP was done after a 5-day ShhN-GFP-His treatment of the C3H10T1/2 clone 8 cells on collagen functionalized surfaces. Glass surfaces were first exposed to 100μg/ml collagen solution. ShhN-GFP-His conditioned medium with the volume ratio of 1:1 to fresh medium was then added to the collagen coated surfaces. The modified surfaces were incubated with C3H10T1/2 clone 8 cells for 5 days. ALP expression was detected by BCIP/NBT substrate. In the negative controls with conditioned medium from untransfected HEK293 cells, no ALP expression was detected (A). Adsorbed ShhN-GFP-His activated Shh signal transduction and induced ALP expression in C3H10T1/2 clone 8 cells (B). Nuclei were stained with Draq 5 (A' and B').

Collagen served as a good substrate for adsorbing ShhN-GFP-His. Collagen not only allowed freedom of ShhN-GFP-His migration in the matrix, as demonstrated by FRAP experiment, but also retained the biological activity of the protein, which was shown by the ALP expression detection and cell counting assay. Though the same amount of ShhN-GFP-His (from a ShhN-GFP-His containing conditioned medium

with the volume ratio of 1:1 to fresh medium) was used in both setups shown in figures 3.26 and 3.27, it appears that there were fewer cells expressing ALP in response to the Shh signaling. It may be due to the saturation of protein adsorption in the collagen matrix, resulting in a limited supply of the protein comparing to the soluble one even the same amount of the protein is supplied initially. This argument is supported by the findings in graphs 3.16 and 3.17. It can be seen that when the ShhN-GFP-His containing medium to fresh medium ration was increased beyond 1:9, there was a continuous increase of cellular response when ShhN-GFP-His was applied in a soluble form; while a level off of cellular response was observed when the same amount of protein was used for surface adsorption.

4. Discussion

The project presented the establishment of different immobilization approaches for *in vitro* studies of Shh protein/morphogen. The *E. coli* expression systems were applied for robust expression of ShhN variants with selected modifications for protein immobilization and surface analysis; while the eukaryotic HEK293 cells were employed for the production of ShhN that was used for biological activity determination. The biological activity of the ShhN variants expressed in the two systems was found to be dependent on the analytical assays used. For Shh is an important signaling molecule, but the protein activity is complicated to study *in vivo*, the data shown in the thesis may provide a reference for future *in vitro* assay development for the investigation of Shh morphogen function, as well as proteins that share similar physicochemical properties.

4.1. Expression and detection systems of ShhN variants

The ALP expression and Gli-luciferase reporter assays are classical analytical methods of evaluating the biological activity of Shh in *in vitro* cell culture systems. In this project, it was found that both of these assays were only capable of evaluating the biological activity of the HEK293 expressed but not the *E. coli* expressed ShhN variants. By using the chondrocyte differentiation assay, the biological activity of the *E. coli* expressed ShhN variants were detected, indicating the importance of the selection of a valid /appropriate system for protein activity analysis. The chondrocyte differentiation assay, however, is time consuming and therefore plays a minor role in Shh activity detection.

Establishment and optimization of protein adsorption or immobilization conditions require a rather large amount of the target fusion protein. Therefore the *E. coli* expression system was chosen to guarantee a robust production of the ShhN variants for surface analysis; while the HEK293 system was used to produce ShhN variants, the biological activity of which was readily detectable with the ALP expression and Gli-luciferase reporter assays.

4.2. Immobilization of ShhN on different substrates for various *in vitro* studies of protein activities

There are various substrates and techniques available for *in vitro* protein adsorption or immobilization depending on the applications.

Earlier in 2003, Jarov and colleagues used bovine plasma fibronectin and mouse laminin-1 to adsorb different variants and mutants of Shh, and illustrated an example of *in vitro* study of Shh in adsorbed or immobilized conditions. In their work, they observed that the extracellular matrix (ECM) adsorbed Shh resembled the Shh expressed by neuroepithelial cells. The adsorbed Shh promotes ventral cell type differentiation in the neural plate explant from Japanese quail embryos, though not as efficiently as the soluble Shh. It was also discovered to profoundly reduce cell-substrate adhesion by inactivating the β 1-integrins at the cell surface, and in turn inhibits cell spreading. Apart from preventing cell-substrate adhesion, the protein further modifies N-cadherin mediated cell-cell adhesion and therefore led to cell compaction. With reference to the work of Jarov and his group, adsorption of ShhN was performed using fibronectin and the other ECM substrate collagen.

Recently in 2010, Amadi and colleagues developed a Resistor-Capacitor (RC) device and successfully monitored neuronal differentiation of the mouse embryonic stem cells by applying a graded concentration of Shh in the hydrogel mimicking the architecture of ECM. At the same time, Angeloni et al. (2010) published their findings of using peptide amphiphile (PA) nanofibers to encapsulate Shh and deliver the protein to the injured cavernous nerves in rats. Regeneration of the penis was detected in the treated rats. The erectile function was also found improved. The work of Angeloni and colleagues demonstrated that adsorption or immobilization of Shh not only is useful in addressing fundamental scientific questions but also has its value in clinical practice.

While the above mentioned projects focused on investigating the protein activity directly without characterizing the substrate and protein conditions; the adsorption efficiency of the substrates, motility and quantity of the adsorbed ShhN were considered important and therefore were first evaluated in this project. Any change of these parameters can heavily influence the performance of the protein as well as the subsequent cellular responses.

The presented project showed that ShhN could be immobilized on functionalized surfaces via physisorption on collagen, affinity binding between poly(6)histidine and nickel, biotin and streptavidin, and covalent bonding between SNAPTM tag and benzylguanine (BG). The immobilization systems tested offered distinct protein adsorption strengths, from the weakest: physisorption to the strongest: covalent binding. These different immobilization approaches affect the motility of the ShhN variants on the surface and the availability of the protein to the responsive cells.

4.2.1. Collagen matrix allows motility and availability of ShhN

Collagen differs from other extracellular matrix (ECM) substrates by its ability to self-assemble and aggregate to form compact and tough bundle networks. It provided an excellent substrate for ShhN adsorption. Adsorption of ShhN-GFP-His on the collagen matrix was found to be dependent on the applied protein concentration, and a saturated loading of the protein can be reached for possible maximal cellular responses (compare graphs 3.16 and 3.17). Collagen coated surface therefore is a convenient system for ShhN immobilization.

Previous studies demonstrated a relationship between internalization of morphogens, including Shh, and cellular response to the morphogen signals (Gallet and Therond, 2004; Torroja et al., 2004; Incardona et al., 2000). A number of investigations on the subcellular length scale support the idea that ShhN is incorporated in vesicles together with its receptor Patched (Ptc) and endocytosed into the cell (Gallet and Therond, 2004). The collagen/ShhN interactions led to adsorption of ShhN in the matrix, while the absence of covalent bonds allowed ShhN to diffuse within the matrix, bind to the receptor and be endocytosed (Graphs 3.15, 3.17; Figure 3.27). Collagen would therefore be a material of choice for the adsorption of ShhN, and maybe other morphogens or signal molecules with similar properties.

4.2.2. Supplement of heparin or BSA in the collagen matrix further resembles the *in vivo* extracellular environment

ShhN possesses a Cardin-Weintraub sequence at the N terminus that can be recognized by and is capable of binding to heparin and heparin sulfate proteoglycan

(HSPG). Such interaction is critical in extracellular transportation and controlling the concentration gradient of ShhN *in vivo*. In the project, more ShhN-GFP-His was found to be adsorbed on the heparin supplemented collagen surface as compared to the non-supplemented collagen surface (Figure 3.25).

Similarly, BSA was observed to facilitate ShhN-GFP-His adsorption on the collagen matrix (Figure 3.25). BSA did not block but largely promoted ShhN adsorption in collagen. In the *in vivo* system, Shh is expressed and transported in the microenvironment of ECM. Since there could be a long distance for Shh to travel from its source of secretion to the recipient cells, protection of the protein from degradation is necessary. BSA is commonly used to protect commercially supplied protein containing reagents. It protects other proteins against denaturation and digestion (Williams et al., 1996). The presence of BSA in collagen matrix may thus favor the protection of ShhN-GFP-His from degradation and offer an advantage of facilitating adsorption of ShhN-GFP-His on collagen surfaces.

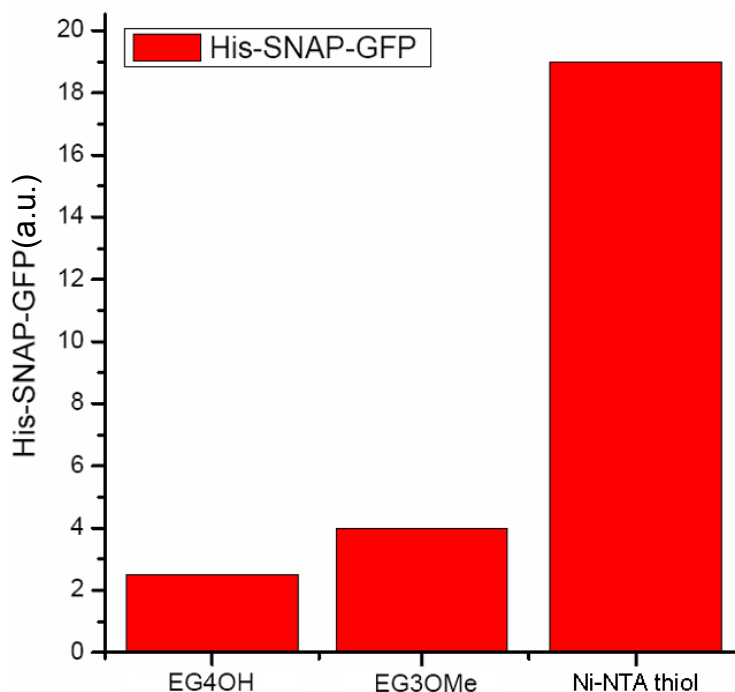
Taken together, the finding from the supplementation of heparin to the collagen matrix went along with the observations by Dierker and colleagues (2009a) that heparin contributes to retaining Shh in the ECM. Supplement of BSA prevents degradation of Shh before it finally arrives at the responsive cells. The example of heparin and BSA also encouraged the use of *in vitro* systems for studying *in vivo* biomolecule activities by simple modifications.

4.2.3. UV irradiated polystyrene surfaces presenting nickel adsorb histidine tagged proteins but provide no sufficient selectivity

The increased hydrophilicity of UV irradiated polystyrene advances its usage in cell culture and protein adsorption (Welle et al., 2002, 2005). As shown in figure 3.13, UV irradiation and nickel functionalization provided a surface modification for the immobilization of histidine tagged ShhN. ShhN-GFP-His was bound on the UV irradiated and nickel modified regions but not on the remaining non-irradiated areas. Additionally, surface sterilization can be achieved by the UV irradiation. High degree of surface organization by UV lithography with masks of different patterns favors studying ShhN and other morphogens with graded concentrations on a single surface.

Though the nickel head group is selective to the histidine tagged protein, the UV irradiated polystyrene surface favors adsorption of all kinds of proteins. The resulting UV irradiated and nickel functionalized surface is insufficient to support protein immobilization with selectivity. To facilitate immobilization of a specifically tagged protein, it is essential to develop substrates with high selectivity to this tagged protein and repellent to other proteins. Application of pure passivating thiol EG6OH on gold surfaces appeared to be efficient in preventing unspecific adsorption or immobilization of proteins (Graph 3.11, Figure 3.22). Combined usage of passivating thiols and Ni-NTA head groups can therefore be a solution for the unspecific adsorption problem. Indeed, the work of Dr. S. Engin (KIT, Karlsruhe, Germany) has demonstrated that EG4OH and EG3OMe are another two alternative passivating thiols in minimizing protein adsorption (Graph 4.1; communication with Dr. S. Engin); while Ni-NTA thiol was found to selectively immobilize polyhistidine tagged

proteins on gold surfaces (Graph 4.1; communication with Dr. S. Engin; Hainfeld et al., 1999).



Graph 4.1. Immobilization of His-SNAP-GFP on gold surface via the Ni-NTA thiol. The polyhistidine-tagged GFP protein is selectively bound to the Ni-NTA head group. EG4OH and EG3OMe are passivating thiols that have no selectivity to any protein and acted as the negative controls of protein adsorption. (Courtesy of Dr. S. Engin)

4.2.4. ShhN immobilization by dip-pen nanolithography retains the motility of the immobilized protein

Similar to UV photolithography, DPN lithography is capable of delivering biomaterials with designated patterns of restricted sizes and spacing on a surface. Modified phospholipids were deposited on selected surfaces by DPN. The ShhN variants were then immobilized via nickel/poly(6)histidine, biotin/streptavidin, and BG/SNAPTM interactions with respect to the modifications made to the phospholipids (Figures 3.14 – 3.17). Like the collagen matrix and UV irradiated polystyrene,

phospholipids are unselective and can non-specifically absorb other proteins (Nair et al., 2011). Blocking of the phospholipid patterns with BSA before the protein binding step to the head groups is necessary (Nair et al, 2011). In addition to the flexibility of interactions offered for protein immobilization, the phospholipids, being the primary component of cell membrane in nature, provide an excellent interface between the cell membrane and the adsorbed protein. Even when the protein is immobilized via strong bondings between the tags or linkers fused to the peptide and the head groups in the phospholipids, it is still mobile and can be endocytosed in the form of a lipid complex into the cell body once it is in touch with the cell membrane.

However, because of the lateral diffusibility within the printed lipids, it is impossible to generate continuous gradients of the immobilized protein as there is an equilibrium formation. DPN can only generate step gradients based on individual spots or areas for the immobilized protein, and it would hinder *in vitro* concentration gradient analysis of morphogens, which work in a continuous gradient *in vivo*. Patterns of different protein concentration are therefore compactly organized down to the nano scale in order to compensate the need of continuous protein gradient and to minimize the possibility of equilibrium formation. As demonstrated in the presented project, different amounts of ShhN variants could be adsorbed and organized in subcellular scale on the functionalized surfaces (Figures 3.14, 3.16). The remaining limitation is the protein binding capacity of the head groups in the phospholipids. Both nickel chelating and biotinylated lipids showed a maximum of binding of the ShhN variants at certain molar ratios of active and inert lipids in the ink (Figures 3.14, 3.16). The saturation was probably due to crowding effect of the head groups printed on the surface, leading to ligand structure disruption (Nelson et al., 2001). In addition, a mixture of 4% biotinylated lipids in DOPC appeared to show the most conspicuous

DPN printed pattern even before the addition of streptavidin and immobilization of ShhN-GFP-His-Biotin (Figure 3.16). It indicated that the molar ratio of the lipids is another governing factor for biotin head group delivery on a substrate.

Apart from the properties of the phospholipids and technique applied, the substrates also play a critical role in effective protein immobilization as well as cell adhesion. Both the PEG-g-PLL and polystyrene surfaces used in this project showed good performance in phospholipid adsorption (Figures 3.14 – 3.17) but did not support cell adhesion (VandeVondele et al., 2002). VandeVondele and colleagues (2002) found that pendant functionalization of the PLL grafted PEG by covalent conjugation to the peptide motif RGD was an alternative in inducing cell binding, at the same time blocking unspecific protein adsorption. Therefore the next step for immobilizing ShhN variants via modified phospholipids could be the preparation of surfaces with RGD conjugated PEG coating and nanoscaled features produced via DPN allowing ShhN binding. The specificity of protein binding to the nickel, biotin and BG head groups in the phospholipids would not be interfered; while adhesion of the Shh responsive cells could be achieved for biological activity analysis of the protein.

4.2.5. The benzylguanine/SNAPTM system allows for highly selective ShhN immobilization

The high selectivity of the BG/SNAPTM system enabled a specific adsorption of ShhN-GFP-His-SNAP on patterned BGT SAM on gold surfaces (Figure 3.25). Preliminary cell culture tests demonstrated that a variety of cell types showed predominant adhesion on the UV modified surfaces where BGT would be used for backfilling (data not shown). Taken together, the UV irradiated gold/BGT/SNAPTM

system appeared to be good for studying specific protein-cell interactions. In this project, the strong protein binding property of the gold/BGT/SNAPTM system offers an additional advantage for the investigation of ShhN. The thiol/gold binding is semi-covalent and the BG/SNAPTM interaction is covalent. The ShhN adhered strictly on the surface. Diffusion of the ShhN protein immobilized in the gold/BGT/SNAPTM setup is therefore prohibited compared to the SNAPTM tagged ShhN immobilized via the BG terminated lipids deposited by DPN. By comparing with the soluble ShhN, the BGT SAM system may give new information for the elucidation of the modes of action of Shh.

Apart from covalent binding, the BGT/SNAPTM system can provide a platform for immobilizing ShhN with continuous gradient on a single plain. It was demonstrated that UV irradiation could effectively introduce patterns on an EG6OH modified gold surfaces (Figures 3.21, 3.22). Therefore different amounts of ShhN-GFP-His-SNAP could be immobilized via binding with BGT on the UV irradiated EG6OH modified gold surface. Because the BGT/gold interaction is semi-covalent and BGT/SNAPTM binding is covalent, there is no motility of protein on the surface. A graded pattern of ShhN can therefore be established in a highly controlled manner.

4.3. Immobilization of ShhN with the flexibility for controlled protein motility

Though there are pros and cons for each of the systems developed in this work, information needed for establishing an ideal surface for ShhN immobilization was obtained. So far, the BGT/SNAPTM system showed the highest potential for further investigation.

It has been widely observed that ShhN is internalized together with Ptc after receptor binding (Gallet and Therond; 2004; Varjosalo and Taipale, 2007, 2008). Therefore it is worth to establish a system to study ShhN as a morphogen by stringently immobilizing the protein on a single surface mimicking the *in vivo* microenvironment, and yet allowing the release of the ligand simultaneously after the cells settle down on the surface.

Glutathione S transferase (GST) and polyhistidine are commonly used for protein purification (Hosfield and Lu, 1999). To remove the tags after purification and obtain pure proteins of interest, enteropeptidase can be employed, provided that a (Asp)₄-Lys site is introduced between the polyhistidine tag and the protein. Therefore, if a (Asp)₄-Lys site is inserted between the C-terminus of ShhN and the SNAPTM tag, immobilized ShhN on BGT SAM could be released from the surface by enteropeptidase. In other words, the concentration gradient of ShhN could be established and strictly controlled, while endocytosis of the ligand, if needed, is permitted for proper signal transduction. The resulting immobilization system would mimic the *in vivo* environment to the closest extent.

4.4. Alternative analytical strategies for determination of the biological activity of immobilized ShhN

In this project, cellular responses to the ShhN proteins were investigated by ALP colorimetric and Gli-luciferase reporter assays, which require cell lysis. While these assays are sensitive and accurate enough in reporting the cell behaviors, the positional and morphological information from individual cells on the surface cannot be recorded. If ShhN is to be studied as a morphogen and the activity of the protein with

graded concentrations on one single surface is to be compared, it is necessary to look into individual cells or small populations of cells at different locations on the surface. The following methods are introduced to compensate the loss of cell location and morphological information from the ALP and luciferase assays.

4.4.1. Investigation of cell migration by time lapse imaging

It has been reported in previous studies that Shh restricted cell migration and played a role in cell fate determination in neural tube development (Ericson et al., 1996). It is therefore worth to employ the Shh responsive multipotent neuronal stem cell line MNS70 (Nakagawa et al., 1996) to look into the migration and behaviors of the stem cells in the presence of immobilized Shh. Would the cells show affinity to higher Shh concentration, and be able to sense and migrate actively to Shh if the morphogen is restricted to certain position instead of diffusing or being transported to the cells? This cell migration assay not only helps understand the function of Shh on neuronal development but also indicates the requirement of extracellular control in governing the availability and concentration of Shh to the responsive cells.

Time lapse imaging could be conducted following the seeding of Shh responsive cells on the ShhN protein functionalized surfaces. The speed and direction of cell migration would give information for the interaction between the morphogen and the cells.

4.4.2. Localized study of signal transduction induced by immobilized ShhN with fluorescence labeled Gli reporter cell line

Gli is a targeting transcription factor in the Shh pathway. In order to determine Shh signal transduction, the Shh LIGHT II cells, which had been stably transfected with the Gli responsive firefly luciferase reporter (Sasaki et al., 1997) and respond by producing firefly luciferase in the presence of Shh signaling, were employed. Nevertheless, the cells should be lysed for assay. Schwend and colleagues (2010) have generated the Gli-d mcherry reporter construct, which was used as a hedgehog pathway reporter to visualize Gli activity in the craniofacial tissues in transgenic zebrafish. The sequence structure of the Gli-d mcherry reporter construct is the same as the Gli responsive firefly luciferase reporter, except that the firefly luciferase reporter sequence is replaced by mcherry. The availability of the Gli-d mcherry reporter construct and hence the establishment of a stable transfected cell line would be constructive in studying the cellular response of Shh responsive cells *in situ* at the gene transcription level.

4.4.3. Establishment of specific reporter cell lines for investigation of the role of Shh in neural cell fate determination

Shh is a renowned modulator of cell differentiation in the developing embryonic neural tube (Jarov et al., 2003). The secreting locations and concentrations of the morphogen are critical for cell fate determination (Cayuso et al., 2005; Fuccillo et al., 2006; Monuki, 2007). In *in vivo* system, the influence of morphogen concentration on different gene or protein expressions in specific tissues can be manipulated, for

example, via conditional gene knockdown or overexpression,. Nevertheless, information obtained *in vivo* is inadequate to elucidate the significance of localized concentrations on individual cells. Establishment of reporter cell lines would therefore be essential for investigation of the concentration effects of a morphogen, such as Shh, at the subcellular level.

Nakagawa and colleagues (1996) showed that the multipotent neural stem (MNS) cell lines from rat were induced by SHH to differentiate into microtubule-associated protein 2 (MAP2) and Pax-6 positive neurons, gene glial fibrillary acidic protein (GFAP) positive astrocytes and microtubule-associated protein 2 (MAP2), glial fibrillary acidic protein (GFAP) and galactocerebroside (GC) positive oligodendrocytes. SHH treated MNS-70 was also found to express the ventral cell-specific transcription factors *Isl-1*, *Nkx-2.1* and *Nkx-2.2*, which play crucial roles in specification of the ventral phenotype of neuroepithelial cells (Echelard et al., 1993; Roelink et al., 1994; Martí et al., 1995; Ericson et al., 1995; Barth and Wilson, 1995). With reference to the work of Nakagawa et al. (1996), by cultivating the MNS cells on the immobilized biologically active ShhN with different spatial organization and concentration gradient, the parameters for the function of Shh on neural cell fate determination could be estimated.

The transgenic zebrafish with different Shh responsive neural markers in the KIT fish facilities provide a wide source of reporter cell lines for Shh function analysis. They offer an alternative for the determination of the capability of Shh to facilitate differentiation of certain types of neurons or glial astrocytes.

4.5. Conclusions

The immobilization systems for ShhN variants established in the presented project offer a variety of choice for studying the biological activity and modes of action of Shh. Though there is still room for optimization of each of the methodologies for the investigation of specific aspects, however the information obtained from the current work provided massive information for surface and assay development. For instance, the supplement of heparin and BSA on collagen coated surfaces suggested the possibility of including any extracellular substrates in the immobilization system. This would be helpful in studying the protein diffusion from a simple to sophisticated level, as well as the contribution of each factor in controlling the diffusion of the protein. To take a close observation at the Shh-cell interaction at subcellular length scales, deposition of modified phospholipids by DPN and immobilization of ShhN ligands can be conducted. A combination of UV lithography and BGT SAMs on gold surfaces enabled ordered covalent adsorption of highly selective SNAPTM tagged proteins. Table 4.1 summarizes the findings about the different protein immobilization approaches obtained in this project.

The above mentioned systems of course are not merely applicable for Shh immobilization, the concepts can also be applied for proteins or biomolecules with properties comparable to those of Shh. Wnt, transforming growth factor beta (TGF β), epidermal growth factor (EGF) and fibroblast growth factors (FGFs) are morphogens like Shh and function with similar mechanisms. They are secreted from a localized source and bind as a ligand to the corresponding receptors at the cell membrane, thereby activating subsequent signaling pathways.

Discussion

The findings obtained in this project are therefore essential not only in *in vitro* investigating ShhN as a signaling molecule but also in developing suitable platforms to control the extracellular spatial distribution of other morphogens of interest.

	Collagen, without patterning	μ Cp		Ni-NTA on UV irradiated PS	DPN of functionalized lipids			BGT& MT SAM on gold, lithographic patterning
		BSA on collagen	BGT& MT SAM on gold		Ni head group on PEG	Biotin head group on PEG	BG on PS	
ShhN variant binding	Yes, label free	Yes, label free	Yes, SNAP TM tag. Aggregates due to drying of BGT	Yes, His tag	Yes, His tag	Yes, biotinylated	Yes, SNAP TM tag	Yes, SNAP TM tag
Unspecific adsorption of other proteins	Yes, by physisorption	Yes, by physisorption by collagen	No, passivation by EG6OH	Yes, physisorption on UV irradiated PS	Yes, due to non-selectivity of phospholipids	Yes, due to non-selectivity of phospholipids	Yes, due to non-selectivity of phospholipids	No, passivation by EG6OH
Methods for reduction of unspecific protein adsorption	Not available, dependent on high purity of protein solution	Not available, dependent on high purity of protein solution	Not necessary	Not available, dependent on high purity of protein solution	Dependent on high purity of protein solution, and BSA blocking	Dependent on high purity of protein solution, and BSA blocking	Dependent on high purity of protein solution, and BSA blocking	Not necessary
Cell adhesion	Yes	Yes	No, passivation by EG6OH	Yes	No, passivation by PEG	No, passivation by PEG	No, self passivation (BSA) of native PS	No, passivation by EG6OH
Possible functionalization for cell controlled adhesion	Not applicable	Not applicable	Application of RGD in BGT/EG6OH solution	Not applicable	Application of RGD conjugated PEG or lipids	Application of RGD conjugated PEG or lipids	Application of RGD conjugated lipids	Application of RGD in BGT/EG6OH solution
Continuous gradient	No, Shh is diffusive	No, but step gradient with stamp of different feature and pitch sizes		Yes, dependent on proximity gap and irradiation time	No, but step gradient with lipid patterns with different amount of head groups, and pattern and pitch sizes			No, but step gradient
ShhN motility	Yes, Shh physisorption	Yes, on the unstamped collagen surface	No, BG/SNAP TM binding is covalent	Possible, Ni-ShhN binding strong but not covalent	Yes, within each individual lipid deposit due to the diffusive property of phospholipids			No, BG/SNAP TM binding is covalent

ShhN internalization	Yes, Shh physisorption	No, BG/SNAP TM binding is covalent	Possible, Ni-protein binding due to strong affinity but not covalent	Yes, due to the dynamicity property of phospholipids. However, internalization is strongly affected in case of BGT lipid/SNAP TM -ShhN system.	No, BG/SNAP TM binding is covalent			
Lateral resolution	Not applicable	μm	μm	μm	nm	nm	nm	μm
Diversity of application	No	Yes, direct stamping or backfilling of protein	Yes, direct stamping or backfilling of BGT	No	Yes, dependent on the head group conjugated phospholipids	Yes, dependent on the head group conjugated phospholipids	Yes, dependent on the head group conjugated phospholipids	No
Sterility	No, aseptic precaution needed	No, aseptic precaution needed	No, aseptic precaution needed	Yes, due to UV irradiation and sterile substrates	No, aseptic precaution needed	No, aseptic precaution needed	No, aseptic precaution needed	No, aseptic precaution needed
Transparency	Yes	Yes	No	Yes	Yes	Yes	Yes	No
Time	Short	Short	Short	Moderate	Long	Long	Long	Long, upscaling possible
New pattern layout	Not applicable	Slow (master for stamp casting)		Slow (lithography mask)	Fast, no master needed			Slow (lithography mask)
Instrumentation / Cost	Cheap	Moderate (masters, stamps)		Moderate (masks, lamp)	Expensive (DPN setup)			Moderate (masks, lamp)

Table 4.1. Summary of different approaches used for ShhN immobilization. The substrate properties and characteristics of each immobilization system are listed and compared. Immobilization of ShhN and other proteins can be achieved by specific approach according to the investigation aspect.

References

- Agarwal et al. (2003). Immobilization of histidine-tagged proteins on nickel by electrochemical dip pen nanolithography. *J. Am. Chem. Soc.* 125, 7408-7412.
- Ågren et al. (2004). Expression of the PTCH1 tumor suppressor gene is regulated by alternative promoters and a single functional Gli-binding site. *Gene* 330, 101-114.
- Amadi et al. (2010). A low resistance microfluidic system for the creation of stable concentration gradients in a defined 3D microenvironment. *Biomed. Microdevices* 12(6), 1027-1041.
- Ashe and Briscoe (2006). The interpretation of morphogen gradients. *Development* 133, 385-394.
- Axelrod et al. (1976). Mobility measurement by analysis of fluorescence. *Biophys. J.* 1055-1069.
- Ayers and Théron (2010). Evaluating Soothened as a G-protein-coupled receptor for Hedgehog signaling. *Trends Cell Biol.* 20(5), 287-298.
- Barth and Wilson (1995). Expression of zebrafish nk2.2 is influenced by sonic hedgehog/vertebrate hedgehog-1 and demarcates a zone of neural differentiation in the embryonic forebrain. *Development* 121, 1755-1768.
- Belu et al. (2003). Time-of-flight secondary ion mass spectrometry: techniques and applications for the characterization of biomaterial surfaces. *Biomaterials* 24, 3635-3653.
- Bosanac et al. (2009). The structure of SHH in complex with HHIP reveals a recognition role for the Shh pseudo active site in signaling. *Nat. Struct. Mol. Biol.* 16(7), 691-698.
- Cardin and Weintraub (1989). Molecular modelling of protein-glycosaminoglycan interactions. *Arterioscler. Thromb. Vasc. Biol.* 9, 21-32.
- Cayuso et al. (2005). The Sonic hedgehog pathway independently controls the patterning, proliferation and survival of neuroepithelial cells by regulating Gli activity. *Development* 133, 517-528.
- Chang and Zhao (2008). Quartz crystal microbalance study of DNA immobilization and hybridization for DNA sensor development. Michigan State University, Department of Civil and Environmental Engineering.

References

- Chang et al. (1994). Products, genetic linkage, and limb patterning activity of a mouse hedgehog gene. *Development* 120, 3339-3353.
- Chaudhuri et al. (1999). Effect of the extra N-terminal methionine residue on the stability and folding of recombinant α -lactalbumin expressed in *Escherichia coli*. *J. Mol. Biol.* 285, 1179-1194.
- Chen et al. (1998). Micropatterned surfaces for control of cell shape, position and function. *Biotechnol. Prog.* 14, 356-363.
- Chen et al. (2004). Palmitoylation is required for the production of a soluble multimeric Hedgehog protein complex and long-range signaling in vertebrates. *Genes Dev.* 18, 641-659.
- Chiang et al. (1996). Cyclopia and defective axial patterning in mice lacking Sonic Hedgehog gene function. *Nature* 383, 407-413.
- Chivers et al. (2010). A streptavidin variant with slower biotin dissociation and increased mechanostability. *Nat. Methods* 7(5), 391-393.
- Corbit et al. (2005). Vertebrate Smoothed functions at the primary cilium. *Nature* 437, 1018-1021.
- Deglau et al. (2006). Targeting microspheres and cells to polyethylene glycol-modified biological surfaces. *J. Biomed. Mater. Res. Part A*. DOI:10.1002/jbm.a.31092.
- Dessaud et al. (2008). Pattern formation in the vertebrate neural tube: a sonic hedgehog morphogen-regulated transcriptional network. *Development* 135, 2489-2503.
- Dierker et al. (2009a). Heparan sulphate and transglutaminase activity are required for the formation of covalently cross-linked Hedgehog oligomers. *J. Biol. Chem.* 284, 32562-32571.
- Dierker et al. (2009b). Heparan sulfate-modulated, metalloprotease-mediated Sonic hedgehog release from producing cells. *J. Biol. Chem.* 284, 8013-8022.
- Dillon et al. (2003). Short- and long-range effects of Sonic hedgehog in limb development. *Proc. Natl. Acad. Sci. USA* 100, 10152-10157.
- Dreier et al. (2008). Terminal differentiation of chick embryo chondrocytes requires shedding of a cell surface protein that binds 1,25-dihydroxyvitamin D₃. *J. Biol. Chem.* 283, 1104-1112.
- Echelard et al. (1993). Sonic hedgehog, a member of a family of putative signaling molecules, is implicated in the regulation of CNS polarity. *Cell* 75, 1417-1430.

- Ekblad and Liedberg (2010). Protein adsorption and surface patterning. *Curr. Opin. Cell. Interf. Sci.* 15, 499-509.
- Ericson et al. (1996). Two critical periods of Sonic Hedgehog signaling required for the specification of motor neuron identity. *Cell* 87, 661-673.
- Fuccillo et al. (2006). Morphogen to mitogen: the multiple roles of hedgehog signaling in vertebrate neural development. *Nat. Rev. Neurosci.* 7(10), 772-783.
- Gallet and Therond (2004). Temporal modulation of the Hedgehog morphogen gradient by a patched-dependent targeting to lysosomal compartment. *Dev. Biol.* 277, 51-62.
- Ginger et al. (2004). The evolution of dip-pen nanolithography. *Angew. Chem. Int. Ed.* 43, 30-45.
- Goetz et al. (2002). Sonic Hedgehog as a mediator of long-range signaling. *BioEssays* 24, 157-165.
- Guerrero and Chiang (2006). A conserved mechanism of Hedgehog gradient formation by lipid modifications. *TRENDS Cell Biol.* 17(1), 1-5.
- Gulacsi and Lillien (2003). Sonic hedgehog and bone morphogenetic protein regulate interneuron development from dorsal telencephalic progenitors *in vitro*. *J. Neurosci.* 23(30), 9862-9872.
- Hainfeld et al. (1999). Ni-NTA-gold clusters target His-tagged proteins. *J. Struct. Biol.* 127, 185-198.
- Han et al. (2004). *Drosophila* glypicans controls the cell-to-cell movement of Hedgehog by a dynamin-independent process. *Development* 131, 601-611.
- Heemskerk and DiNardo (1994). *Drosophila* hedgehog acts as a morphogen in cellular patterning. *Cell* 76, 449-460.
- Heussler and Suri (2003). Sonic hedgehog. *J. Clin. Pathol.: Mol. Pathol.* 56, 129-131.
- Hidalgo (1991). Interactions between segment polarity genes and the generation of the segmental pattern in *Drosophila*. *Mech. Develop.* 35, 77-87.
- Hochman et al. (2006). Molecular pathways regulating pro-migratory effects of hedgehog signaling. *J. Biol. Chem.* 281(45), 33860-33870.
- Hochuli (1988). Large-scale chromatography of recombinant proteins. *J. Chromatogr.* 444, 293-302.

References

- Holmberg et al. (2005). The biotin-streptavidin interaction can be reversibly broken using water at elevated temperatures. *Electrophoresis* 26, 501-510.
- Huang et al. (2001). Poly(L-lysine)-g-poly(ethylene glycol) layers on metal oxide surfaces: surface-analytical characterization and resistance to serum and fibrinogen adsorption. *Langmuir* 17, 489-498.
- Incardona et al. (2000). Receptor-mediated endocytosis of soluble and membrane-tethered Sonic hedgehog by Patched-1. *Proc. Natl. Acad. Sci. USA* 97(22), 12044-12049.
- Hosfield and Lu (1999). Influence of the amino acid residue downstream of (Asp)₄Lys on enterokinase cleavage of a fusion protein. *Anal. Biochem.* 269, 10-16.
- Ingham (1993). Localized hedgehog activity controls spatial limits of wingless transcription in the *Drosophila* embryo. *Nature* 366, 560-562.
- Ingham (1995). Signaling by hedgehog family proteins in *Drosophila* and vertebrate development. *Curr. Opin. Genet. Dev.* 5, 492-498.
- Jarov et al. (2003). A dual role for Sonic hedgehog in regulating adhesion and differentiation of neuroepithelial cells. *Dev. Biol.* 261(2), 520-536.
- Johnson and Tabin (1995). The long and short of hedgehog signaling. *Cell* 81, 313-316.
- Kang et al. (2007). Hedgehog signalling: cooking with Gas1. *Sci. STKE* 403, 1-3.
- Karpen et al. (2001). The Sonic hedgehog receptor Patched associates with Caveolin-1 in cholesterol-rich microdomains of the plasma membrane. *J. Biol. Chem.* 276(22), 19503-19511.
- Kellner et al. (2002). Effects of hedgehog proteins on tissue engineering of cartilage *in vitro*. *Tissue Eng.* 8(4), 561-572.
- Keppler et al. (2003). A general method for the covalent labelling of fusion proteins with small molecules *in vivo*. *Nat. Biotechnol.* 21, 86-89.
- Kim et al. (2008). Analysis of direct immobilized recombinant protein G on a gold surface. *Ultramicroscopy* 108, 1152-1156.
- Kindermann et al. (2003). Covalent and selective immobilization of fusion proteins. *J. Am. Chem. Soc.* 125, 7810-7811.
- Kinto et al. (1997). Fibroblasts expressing Sonic hedgehog induce osteoblast differentiation and ectopic bone formation. *FEBS Lett.* 404, 319-323.

- Koppel et al. (1979). Fluorescence redistribution after photobleaching a new multipoint analysis of membrane translational dynamics. *Biophys. J.* 28, 281-292.
- Krauss et al. (1993). A functionally conserved homolog of the *Drosophila* segment polarity gene *hedgehog* is expressed in tissues with polarizing activity in zebrafish embryos. *Cell* 75, 1431-1444.
- Kreszberg and Wolpert (2007). Specifying positional information in the embryo: looking beyond morphogens. *Cell* 130, 205-209.
- Lee et al. (1992). Secretion and localized transcription suggest a role in positional signaling for products of the segmentation gene *hedgehog*. *Cell* 71, 33-50.
- Lefers et al. (2001). Genetic dissection of the *Drosophila* *Cubitus interruptus* signaling complex. *Dev. Biol.* 236(2), 411-420.
- Lenhert et al. (2007). Massively parallel dip-pen nanolithography of heterogeneous supported phospholipid multilayer patterns. *Small* 3(1), 71-75.
- Lequin (2005). Enzyme immunoassay (EIA)/enzyme-linked immunosorbent assay (ELISA). *Clin. Chem.* 51(12), 2415-2418.
- Lin (2004). Functions of heparin sulphate proteoglycans in cell signalling during development. *Development* 131, 6009-6021.
- Livnah et al. (1993). Three-dimensional structures of avidin and the avidin-biotin complex. *Proc. Natl. Acad. Sci. USA* 90, 5076-5080.
- Love et al. (2005). Self-assembled monolayers of thiolates on metals as a form of nanotechnology. *Chem. Rev.* 105(4), 1103-1169.
- Malaquin et al. (2003). Using PDMS as thermocurable resist for a mold assisted imprint process. *Alternative Lithography "unleashing the potentials of nanotechnology"* Volume Chapter 8. Edited by Clivia M Sotomayer Torres. Kluwer Academic Publishers Boston/Dordrecht/London, 169-199.
- Martí et al. (1995). Requirement of 19K form of Sonic hedgehog for induction of distinct ventral cell types in CNS explants. *Nature* 375, 322-325.
- Martín et al. (2001). The sterol-sensing domain of Patched protein seems to control Smoothed activity through Patched vesicular trafficking. *Curr. Biol.* 11, 601-607.
- Maun et al. (2010a). The hedgehog pathway antagonist 5E1 binds hedgehog at the pseudo-active site. *J. Biol. Chem.* Epub ahead of print; DOI: 10.1074/ibc.M110.112284.

References

- Maun et al. (2010b). Pseudo-active site of protease domains: HGF/Met and Sonic hedgehog signaling in cancer. *Biol. Chem.* 391, 881-892.
- Mehlen et al. (2005). Morphogens and cell survival during development. *J. Neurobiol.* 64(4), 357-366.
- Michel et al. (2001). Printing meets lithography: soft approaches to high-resolution patterning. *IBM J. Res. & Dev.* 45(5), 697-719.
- Miura and Treisman (2006). Lipid modification of secreted signaling proteins. *Cell Cycle* 5(11), 1184-1188.
- Miyawaki (2005). Innovations in the imaging of brain functions using fluorescent proteins. *Neuron* 48, 189-199.
- Mohler (1998). Requirements of hedgehog, a segment polarity gene, in patterning larval and adult cuticle of *Drosophila*. *Genetics* 120, 1061-1072.
- Monnier et al. (2002). Hedgehog signal transduction proteins: contacts of the Fused kinase and Ci transduction factor with the Kinesin-related protein Costal2. *BMC Dev. Biol.* 2, 4.
- Monuki (2007). The morphogen signaling network in forebrain development and holoprosencephaly. *J. Neuropathol. Exp. Neurol.* 66(7), 566-575.
- Morales et al. (2006). Epithelial trafficking of Sonic hedgehog by megalin. *J. Histochem. Cytochem.* 54(10), 1115-1127.
- Mrksich and Whitesides (1996). Using self-assembled monolayers to understand the interactions of man-made surfaces with proteins and cells. *Annu. Rev. Biophys. Biomol. Struct.* 25, 55-78.
- Nair et al. (2011). Using patterned supported lipid membranes to investigate the role of receptor organization in intercellular signaling. *Nat. Protocols* 6(4), 523-539.
- Nakagawa et al. (1996). Roles of cell-autonomous mechanisms for differential expression of region-specific transcription factors in neuroepithelial cells. *Development* 122, 2449-2464.
- Nelson et al. (2001). Surface characterization of mixed self-assembled monolayers designed for streptavidin immobilization. *Langmuir* 17, 2807-2816.
- Ostuni et al. (2009). Using self-assembled monolayers to pattern ECM proteins and cells on substrates. *Methods Mol. Biol. Extracellular Matrix Protocols* 522, 183-194.
- Pegg (2000). Repair of O(6)-alkylguanine by alkyltransferase. *Mutat. Res.* 462, 83-100.

- Peters et al. (2004). The cholesterol membrane anchor of the Hedgehog protein confers stable membrane association to lipid-modified proteins. *Proc. Natl. Acad. Sci. USA* 101(23), 8531-8536.
- Renault et al. (2003). Fabricating arrays of single molecules on glass using microcontact printing. *J. Phy. Chem. B.* 107, 703-711.
- Ribes and Briscoe (2009). Establishing and interpreting graded Sonic hedgehog signaling during vertebrate neural tube patterning: the role of negative feedback. *Cold Spring Harb. Perspect. Biol.* 1, 1-16.
- Riddle et al. (1993). Sonic hedgehog mediates the polarizing activity of the ZPA. *Cell* 75, 1401-1418.
- Robbins et al. (1997). Hedgehog elicits signal transduction by means of a large complex containing the kinesin-related protein costal-2. *Cell* 90, 225-234.
- Robinson et al. (2009). Immunofluorescence. *IHC guidebook*, 5th ed. Chapter 10, 62-65.
- Roelink et al. (1994). Floor plate and motor neuron induction by vhh-1, a vertebrate homolog of hedgehog expressed by the notochord. *Cell* 76, 761-775.
- Saha and Schaffer (2005). Signal dynamics in Sonic hedgehog tissue patterning. *Development* 133, 889-900.
- Sasaki et al. (1997). Two-dimensional arrangement of a functional protein by cysteine-gold interaction: enzyme activity and characterization of a protein monolayer on a gold substrate. *Biophysical J.* 72, 1842-1848.
- Schmitt et al. (1993). Affinity purification of histidine-tagged proteins, *Mol. Biol. Rep.* 18, 223-230.
- Schwend et al. (2010). Visualization of Gli activity in craniofacial tissues of hedgehog-pathway receptor transgenic zebrafish. *PLoS ONE* 5(12), e14396.
- Sekula et al. (2008). Multiplexed lipid dip-pen nanolithography on subcellular scales for the templating of functional proteins and cell cultures. *Small* 4(10), 1785-1793.
- Sigal et al. (1996). A self-assembled monolayer for the binding and study of histidine-tagged proteins by surface plasmon resonance. *Anal. Chem.* 68, 490-497.
- Sisson et al. (1997). Costal2, a novel kinesin-related protein in the hedgehog signaling pathway. *Cell* 90, 235-245.
- Soumpasis et al. (1983). Theoretical analysis of fluorescence photobleaching recovery

References

- experiments. *Biophys. J.* 41, 95-97.
- Spetz (2006). Chemical sensor technologies, Tutorial 2006. Michigan State University, Department of Civil and Environmental Engineering.
- Staszczak (2007). An in vitro method for selective detection of free monomeric ubiquitin by using a C-terminally biotinylated form of ubiquitin. *Intl. J. Biochem. Cell Biol.* 39, 319-326.
- Tabata et al. (1992). The *Drosophila* hedgehog gene is expressed specifically in posterior compartment cells and is a target of engrailed regulation. *Genes Dev.* 6, 2635-2645.
- Tessmar and Göpferich (2007). Customized PEG-derived copolymers for tissue-engineering applications. *Macromol. Biosci.* 7, 23-39.
- Thibault et al. (2005). Direct microcontact printing of oligonucleotides for biochip applications. *J. Nanobiotechnol.* 3(7), 1-12.
- Thorne et al. (2008). In vivo diffusion of lactoferrin in brain extracellular space is regulated by interactions with heparin sulfate. *Proc. Natl. Acad. Sci. USA* 105(24), 8416-8421.
- Torroja et al. (2004). Patched controls the Hedgehog gradient by endocytosis in a dynamin-dependent manner, but this internalization does not play a major role in signal transduction. *Development* 131, 2395-2408.
- VandeVondele et al. (2002). RGD-grafted poly-L-lysine-graft-(polyethylene glycol) copolymers block non-specific protein adsorption while promoting cell adhesion. *Biotechnol. Bioeng.* 82(7), 784-790.
- Varjosalo and Taipale (2007). Hedgehog signaling. *J. Cell Sci.* 120(1), 3-6.
- Varjosalo and Taipale (2008). Hedgehog: functions and mechanisms. *Genes Dev.* 22(18), 2454-2472.
- von Philipsborn et al. (2006). Growth cone navigation in substrate-bound ephrin gradients. *Development* 133, 2487-2495.
- Wang and Holmgren (2000). Nuclear import of *Cubitus interruptus* is regulated by Hedgehog via a mechanism distinct from Ci stabilization and Ci activation. *Development* 127, 3131-3139.
- Wang et al. (2007). Shifting paradigms in Hedgehog signaling. *Curr. Opin. Cell Biol.* 19, 159-165.
- Welle et al. (2002). Patterned polymer surfaces for cell culture applications. *Biomed.*

- Tech. (Berl.) 47 Suppl. 1 Pt. 1, 401-403.
- Welle et al. (2005). Photo-chemically patterned polymer surfaces for controlled PC-12 adhesion and neurite guidance. *J Neurosci. Methods* 142, 243-250.
- White, et al. (2007). Complex regulation of *cyp26a1* creates a robust retinoic acid gradient in the zebrafish embryo. *PLoS Biology* 5, e304.
- Williams et al. (1996). BSA and restriction enzyme digestions. *Promega Notes* 59, 46-48.
- Williams et al. (1999). Functional antagonists of sonic hedgehog reveal the importance of the N terminus for activity. *J. Cell Sci.* 112, 4405-4414.
- Willumeit et al. (2007). Phospholipids as implant coatings. *J. Mater. Sci.: Mater. Med.* 18, 367-380.
- Wilson and Chuang (2010). Mechanism and evolution of cytosolic Hedgehog signal transduction. *Development* 137, 2079-2094.
- Wong et al. (2009). Selective covalent protein immobilization: strategies and applications. *Chem. Rev.* 109, 4025-4053.
- Yanushevich et al. (2002). A strategy for the generation of non-aggregating mutants of Anthozoa fluorescent proteins. *FEBS Lett.* 511, 11-14.
- You et al. (2009). Affinity capturing for targeting proteins into micro and nanostructures. *Anal. Bioanal. Chem.* 393, 1563-1570.
- Zhu and Scott (2004). Incredible journey: how do developmental signals travel through tissue? *Genes Dev.* 18, 2985-2997.